



THE UNIVERSITY *of* EDINBURGH

This thesis has been submitted in fulfilment of the requirements for a postgraduate degree (e.g. PhD, MPhil, DClinPsychol) at the University of Edinburgh. Please note the following terms and conditions of use:

- This work is protected by copyright and other intellectual property rights, which are retained by the thesis author, unless otherwise stated.
- A copy can be downloaded for personal non-commercial research or study, without prior permission or charge.
- This thesis cannot be reproduced or quoted extensively from without first obtaining permission in writing from the author.
- The content must not be changed in any way or sold commercially in any format or medium without the formal permission of the author.
- When referring to this work, full bibliographic details including the author, title, awarding institution and date of the thesis must be given.

A Closed-Loop Prosthetic Hand: Understanding Sensorimotor and Multisensory Integration under Uncertainty.

Ian Saunders



Doctor of Philosophy
Institute of Perception, Action and Behaviour
School of Informatics
University of Edinburgh
2011

(Graduation date: 25th June 2012)

Abstract

To make sense of our unpredictable world, humans use sensory information streaming through billions of peripheral neurons. Uncertainty and ambiguity plague each sensory stream, yet remarkably our perception of the world is seamless, robust and often “optimal” in the sense of minimising perceptual variability. Moreover, humans have a remarkable capacity for dexterous manipulation. Initiation of precise motor actions under uncertainty requires awareness of not only the statistics of our environment but also the reliability of our sensory and motor apparatus.

What happens when our sensory and motor systems are disrupted? Upper-limb amputees fitted with a state-of-the-art prostheses must learn to both control and make sense of their robotic replacement limb. Tactile feedback is not a standard feature of these open-loop limbs, fundamentally limiting the degree of rehabilitation. This thesis introduces a modular closed-loop upper-limb prosthesis, a modified Touch Bionics iLIMB hand with a custom-built linear vibrotactile feedback array. To understand the utility of the feedback system in the presence of multisensory and sensorimotor influences, three fundamental open questions were addressed: (i) What are the mechanisms by which subjects compute sensory uncertainty? (ii) Do subjects integrate an artificial modality with visual feedback as a function of sensory uncertainty? (iii) What are the influences of open-loop and closed-loop uncertainty on prosthesis control?

To optimally handle uncertainty in the environment people must acquire estimates of the mean and uncertainty of sensory cues over time. A novel visual tracking experiment was developed in order to explore the processes by which people acquire these statistical estimators. Subjects were required to simultaneously report their evolving estimate of the mean and uncertainty of visual stimuli over time. This revealed that subjects could accumulate noisy evidence over the course of a trial to form an optimal continuous estimate of the mean, hindered only by natural kinematic constraints. Although subjects had explicit access to a measure of their continuous objective uncertainty, acquired from sensory information available within a trial, this was limited by a conservative margin for error.

In the Bayesian framework, sensory evidence (from multiple sensory cues) and prior beliefs (knowledge of the statistics of sensory cues) are combined to form a posterior estimate of the state of the world. Multiple studies have revealed that humans behave as optimal Bayesian observers when making binary decisions in forced-choice tasks. In this thesis these results were extended to a continuous spatial localisation task. Subjects could rapidly accumulate evidence presented via vibrotactile feedback (an “artificial modality”), and integrate it with visual feedback. The weight attributed to each sensory modality was chosen so as to minimise the overall objective uncertainty.

Since subjects were able to combine multiple sources of sensory information with respect to their sensory uncertainties, it was hypothesised that vibrotactile feedback would benefit prosthesis wearers in the presence of either sensory or motor uncertainty. The closed-loop prosthesis served as a novel manipulandum to examine the role of feed-forward and feed-back mechanisms for prosthesis control, known to be required for successful object manipulation in healthy humans. Subjects formed economical grasps in idealised (noise-free) conditions and this was maintained even when visual, tactile and both sources of feedback were removed. However, when uncertainty was introduced into the hand controller, performance degraded significantly in the absence of visual or tactile feedback. These results reveal the complementary nature of feed-forward and feed-back processes in simulated prosthesis wearers, and highlight the importance of tactile feedback for control of a prosthesis.

Acknowledgements

First and foremost I offer my sincerest gratitude to my supervisor, Prof. Sethu Vijayakumar. His patience and understanding allowed me freedom to explore and discover the wonders of science, his encouragement and support ensured I did not get disheartened along the way, and his wisdom and knowledge inspired me from start to finish.

I would like to thank my M.Sc. student Eduardo Moraud for helping to run one of my experiments, I would like to thank the team at Touch Bionics for their help and advice, and I would like to thank the numerous experimental subjects who have generously volunteered their time to become points on graphs.

I am indebted to my many student colleagues for providing a brilliant environment in which to learn and discover new things. There are too many of you to mention, but thank you all for your energy and passion which have made this such a fun and fulfilling experience. I am especially grateful to my good friend Stuart Wilson for his encouragement and enthusiasm in helping me turn my ideas into reality.

I wish to thank my wonderful girlfriend Oyinlola Oyeboode for helping me through the tough times, for her tolerance and patience when I was in “work mode” and for her unconditional love and devotion which has provided a light at the end of the tunnel.

For all the emotional support, camaraderie and entertainment my amazing friends have provided, I wish to thank you too. Whether it be running mountain marathons, playing football in “The Cage”, movie-making at Firbush, or our hilarious Come Dine With Me competitions, there has never once been a dull moment. A special mention goes to Ginny Hunter, whose delicious cooking has rescued the Informatics Forum from stale sandwiches and greasy pizza — and completely revolutionised the Edinburgh catering scene.

Most importantly of all, I can not express in words how grateful I am to have such a wonderful family. I would like to thank to my brother Mark for being my role model as a scientist, and my special sister Helen, who has always deserved a special mention because she is wonderful.

Finally, there are two people without whom this entire thesis would not exist: the two most caring, kind and loving people I know; my parents Pauline Walker and John Saunders. Everything I am, everything I have and everything I will one day be, I owe to you. I proudly dedicate this thesis to you with the whole of my heart.

Declaration

I declare that this thesis was composed by myself, that the work contained herein is my own except where explicitly stated otherwise in the text, and that this work has not been submitted for any other degree or professional qualification except as specified.

(Ian Saunders)

Contents

1	Introduction	1
1.1	Motivation	2
1.2	Aims	2
1.3	Overview of this Thesis	3
2	Background	9
2.1	Probabilistic Models in Human Sensorimotor Control	10
2.1.1	Introduction	10
2.1.2	Multisensory Integration	11
2.1.2.1	Ideal Observer Behaviour	11
2.1.2.2	A-Priori Integration	14
2.1.2.3	Maximum Likelihood	15
2.1.2.4	Maximum A-Posteriori and Bayes	17
2.1.2.5	Criticisms	17
2.1.3	Bayes in the Brain	20
2.1.3.1	Neural Implementation	20
2.1.3.2	Population Codes	21
2.2	Decision-Making over Time	24
2.2.1	Introduction	24
2.2.2	Continuous Tracking and Pointing Tasks	24
2.2.2.1	Traditional Tracking Tasks	24
2.2.2.2	Pointing and Reaching Tasks	29
2.2.3	Temporally-Evolving Decisions	33
2.2.3.1	Continuous Optimal Decisions	33
2.2.3.2	Changing one's Mind	35
2.2.4	Continuous-Time Decision Mechanisms	36
2.2.4.1	Attention and Cognitive Phenomena	36
2.2.4.2	Maximising Expected Gain	37
2.2.4.3	Acquisition of Sensory Integration	37

2.2.4.4	Acquisition of Sensory Uncertainty	38
2.3	Human Grasping	40
2.3.1	Introduction	40
2.3.2	Motor Control and Somatosensation	40
2.3.2.1	Physiology	40
2.3.2.2	Sensory Perception	42
2.3.2.3	Ownership of the Hand	43
2.3.3	Experimental Perspectives	44
2.3.3.1	Healthy Human Grasping	44
2.3.3.2	Sensory Deprivation	46
2.3.3.3	Robotic Manipulandum	47
2.3.4	The Role of Internal Models	49
2.4	Prosthetic Systems	52
2.4.1	Introduction	52
2.4.2	Feedback	52
2.4.2.1	Sensory Augmentation	52
2.4.2.2	Sensors	55
2.4.2.3	Vibrotactile Feedback	56
2.4.2.4	Electrotactile Feedback	58
2.4.3	Control	59
2.4.3.1	Target Muscle Reinnervation (TMR)	59
2.4.3.2	EMG control	60
2.4.3.3	Direct Neural Control	60
2.4.3.4	Actuation Strategies	61
2.4.4	A Closed-Loop Prosthetic Hand	62
2.4.4.1	Historical Attempts to Close the Loop	62
2.4.4.2	Measuring Success	62
2.4.4.3	21st Century Closed-Loop Prostheses	64
3	System Design	67
3.1	Motivation	68
3.1.1	Introduction	68
3.1.2	Debugging the closed-loop	68
3.1.2.1	Combinatorial Explosion	68
3.1.2.2	Idealised Manipulandum	69
3.1.2.3	Modularity	70
3.1.2.4	The Gold Standard	70
3.2	Methods and Results	73

3.2.1	Introduction	73
3.2.2	Robotic Hand Actuation	73
3.2.2.1	Introduction	73
3.2.2.2	Differential Control	74
3.2.2.3	Responsive Stall Control	74
3.2.2.4	Pulsing Linear Force Control	76
3.2.3	Control Signal	77
3.2.3.1	Surface Electromyography	77
3.2.3.2	Simulating an Amputation	78
3.2.3.3	Noise-Free Simulated Amputation	78
3.2.3.4	Idealised Control and Cursor Control	79
3.2.4	Sensation and Sensors	79
3.2.5	Vibrotactile Feedback System	80
3.2.5.1	Introduction	80
3.2.5.2	Hardware	80
3.2.5.3	Firmware	81
3.2.5.4	Software	89
3.2.5.5	Alternative Feedback Systems	89
3.2.6	Task: Vibrotactile Discrimination	91
3.2.6.1	Motivation	91
3.2.6.2	Methods	91
3.2.6.3	Results	92
3.2.7	Advanced Tasks	93
3.2.7.1	Vibrotactile Localisation	93
3.2.7.2	Vibrotactile Integration	94
3.2.7.3	Grasp, Lift, Move and Hold	94
3.2.7.4	Activities of Daily Living	95
3.3	Discussion	96
4	Estimating Sensory Uncertainty Over Time	99
4.1	Motivation	100
4.2	Methods	102
4.2.1	The Butterfly-Catching Paradigm	102
4.2.1.1	Overview	102
4.2.1.2	Task Manipulations	104
4.2.2	Experimental Methodology	105
4.2.2.1	Subjects	105
4.2.2.2	Structure	105

4.2.2.3	Mean Estimation Task	105
4.2.2.4	Confidence Estimation Task	106
4.2.2.5	Performance Feedback	106
4.2.2.6	Apparatus and Data Collection	107
4.2.2.7	Visual Stimuli	108
4.2.3	Data Analysis	110
4.2.3.1	The Ideal Observer	110
4.2.3.2	Sensorimotor Delay Model	111
4.2.3.3	Weight Regression	113
4.2.3.4	Model Parameter Learning	114
4.3	Results	116
4.3.1	Mean estimation performance	116
4.3.2	The effect of perturbations on mean estimation trajectories	117
4.3.3	Mean estimation performance across subjects	119
4.3.4	Optimal mean estimation model	120
4.3.5	Optimal weight evolution for mean estimation	122
4.3.6	Uncertainty estimation performance	124
4.3.7	Near-optimal model for uncertainty estimation	126
4.4	Discussion	131
4.4.1	Overview	131
4.4.2	Implications	131
4.4.2.1	Objective Uncertainty Acquisition	131
4.4.2.2	Optimal Perception	132
4.4.2.3	Cognitive Mechanisms	135
4.4.3	Conclusion	136
5	Optimal Multisensory Integration	137
5.1	Motivation	138
5.1.1	Pilot Experiment	139
5.1.2	Main Experiment	139
5.2	Methods	141
5.2.1	Pilot Experiment	141
5.2.1.1	Overview	141
5.2.1.2	Stimuli	141
5.2.1.3	Control	143
5.2.1.4	Analysis	143
5.2.1.5	Training	144
5.2.1.6	Hypotheses	144

5.2.2	Main Experiment	144
5.2.2.1	Task	144
5.2.2.2	Experiment Structure	146
5.2.2.3	Cursor Control	147
5.2.2.4	Success/Failure Feedback	147
5.2.2.5	Subjects	147
5.2.2.6	Stimuli	148
5.2.2.7	Analysis	148
5.2.2.8	Simulation	150
5.3	Results	153
5.3.1	Notation	153
5.3.2	Pilot Results	153
5.3.2.1	Position Control Group	153
5.3.2.2	Velocity Control Group	159
5.3.3	Main Experiment Results	161
5.3.3.1	Sensory Substitution	161
5.3.3.2	Sensory Integration	162
5.3.3.3	Optimal multisensory integration	168
5.4	Discussion	170
5.4.1	Pilot Experiment	170
5.4.2	Main Experiment	171
5.4.3	Conclusion	173
6	Feedforward and Feedback processes during Closed-Loop Prosthesis	
	Control	175
6.1	Motivation	176
6.2	Methods	179
6.2.1	Subjects	179
6.2.2	Hardware Setup	179
6.2.2.1	Closed Loop Hand	179
6.2.2.2	Vibrotactile Feedback Array	179
6.2.2.3	Differential Force Control	179
6.2.2.4	Sensor Recording Equipment	180
6.2.3	Experiments	182
6.2.3.1	Preliminary Experiment: ‘Just noticeable difference’ measurement	182
6.2.3.2	Overview: Economical Grasping Paradigm	182
6.2.3.3	Experiment 1: Grasp, lift and move task	182

6.2.3.4	Experiment 2: Grasp and lift task with feed-back deprivation	184
6.2.3.5	Experiment 3: Grasp and lift task with feed-back deprivation and feed-forward deprivation	185
6.2.4	Performance measures and statistical analysis	186
6.2.4.1	Automatic Segmentation	186
6.2.4.2	Grasp Force	186
6.2.4.3	Ramp Duration	186
6.2.4.4	Trial Duration	187
6.2.4.5	Number of errors	187
6.2.4.6	Grasp Score	188
6.2.4.7	Analyses	188
6.3	Results	189
6.3.1	Preliminary Experiment: Grasp forces are effectively communicated to patients using artificial feedback	189
6.3.2	Experiment 1: In ideal conditions, ‘simulated amputees’ perform economical grasps regardless of feedback	189
6.3.3	Experiment 2: When deprived of additional sensory cues, trained subjects still show no significant deficit in grasp economy	191
6.3.4	Experiment 3: When feed-forward uncertainty is increased, trained subjects show significant performance deficits when deprived of either visual or tactile feedback	193
6.4	Discussion	196
6.4.1	Overview	196
6.4.2	Justification of Methods	197
6.4.2.1	Feedback Choice	197
6.4.2.2	“Ideal” Conditions	197
6.4.2.3	Temporal Delays	198
6.4.2.4	Task and performance measurement	199
6.4.3	Implications	199
6.4.3.1	Recommendations	199
6.4.3.2	Reactive behaviour	200
6.4.3.3	Control Strategy	200
6.4.3.4	Generalisability	200
6.4.3.5	Closing Remarks	201
7	General Discussion	203
7.1	Summary of Results	204

7.2	Critical Evaluation	206
7.2.1	High Dimensionality	206
7.2.2	Feedback Encoding	206
7.2.3	Sensorimotor Task Design	207
7.2.4	The Benefits of Feedback	208
7.2.5	Uncertain Uncertainty	208
7.2.6	Healthy grasping	209
7.2.7	Achievement of Aims	210
7.3	Future Perspectives	212
7.3.1	Multisensory Confidence Estimation	212
7.3.2	Remaining Dimensions	215
A	Uncertainty in Sample Standard Deviation	217
A.0.3	Computing the uncertainty in our estimate of the mean	218
A.0.3.1	Butterfly Catching	218
A.0.3.2	Cochran's Theorem	219
A.0.3.3	Derivation of deviate distributions	219
A.0.3.4	The distribution of mean estimator	220
A.0.3.5	Student's t distribution	221
A.0.3.6	Estimating the distribution of the mean estimator	222
A.0.3.7	Application	223
A.0.3.8	Conclusion	224
A.0.4	Score functions	224
A.0.4.1	Motivation	224
A.0.4.2	Score Functions	224
A.0.4.3	Levels of Uncertainty	225
	Bibliography	227

Chapter 1

Introduction

1.1 Motivation

The state-of-the-art in prosthetic hands for transradial amputees is an underactuated open-loop robotic device with few degrees of control (e.g. Cipriani et al., 2008, Otr et al., 2010). For many decades researchers have considered the possibility of ‘closing the loop’ for upper-limb prosthesis wearers by incorporating an *artificial* channel of feedback to restore the missing sense of touch, dating as far back as Beeker et al. (1967). Feedback has been shown to improve prosthesis acceptance (Shannon, 1979b) and reduce the demand on visual feedback (Pylatiuk et al., 2004), but this success is not universal (Chatterjee et al., 2008) and the state-of-the-art have been described as clumsy (see Zhou et al., 2007). Commercially available prostheses remain open-loop, but as robotic devices become cheaper and information processing capabilities continue to advance it is more important than ever that we find effective ways of delivering feedback to amputees. In this thesis I hypothesise that a fundamentally limiting aspect of prosthesis control is the lack of sensory feedback.

The incorporation of an artificial sense relies on the development of a feedback system that can become an integral part of our healthy sensory system. This may rely on technological breakthroughs in sensor technology (e.g. Edin et al., 2006), neural control (e.g. Dhillon and Horch, 2005) and surgical procedures (e.g. Kuiken et al., 2004), as well as a deeper understanding of the cognitive phenomena underlying sensorimotor control (e.g. Körding and Wolpert, 2004a). In this thesis I focus specifically on the role of uncertain sensory feedback and uncertain feed-forward control in the context of closed-loop sensorimotor tasks. By developing novel psychophysical and experimental approaches I address fundamental questions regarding the integration of sensory feedback with visual feedback and with feedforward control.

In developing closed-loop tasks and a closed-loop prosthesis I am able to create an artificial sensorimotor circuit. This system can be seen as a novel manipulandum in which the plant control and the arrival of sensory feedback can be experimentally manipulated. This provides a window into human sensorimotor control that would be impossible with healthy individuals, useful for understanding current theories of sensorimotor control. This may help to bridge the gap from the state-of-the-art in prostheses to the gold standard of the healthy human hand.

1.2 Aims

This thesis has two primary aims:

- **Aim 1:** To quantify the benefits of sensory feedback for the control of closed-loop sensorimotor systems, such as a prosthetic hand, in the presence of different

sources of uncertainty.

- **Aim 2:** To further understand the mechanisms by which sensory uncertainty influences perception and influences control of closed-loop sensorimotor systems.

To achieve these aims I address the following questions:

- **1: Sensory Communication:** Can I establish a high-bandwidth sensory feedback channel that people are able to detect and decode?
- **2: Sensory Augmentation:** If I can establish a sensory feedback channel with sufficient bandwidth, will a person be able to use it to do a task, such as estimating forces, or positions? Can it adequately *augment* or *substitute* for information presented in another modality, such as vision?
- **3: Sensory Integration:** If I can establish a sensory feedback channel with sufficient bandwidth, and the person can use it, will a person also *integrate* this information with their existing senses? Will it *complement* existing modalities, and add additional benefits?
- **4: Optimal Sensory Integration:** Will a successfully integrated artificial modality be combined with existing senses in a manner which is *optimal* with respect to the reliability of the sensory information it provides? Are optimal weights *learned* or *innate*?
- **5: Sensory Uncertainty Acquisition:** Optimal sensory integration assumes an ability of subjects to *acquire* statistical information from the world. How is such information (such as the mean and uncertainty of sensory evidence) computed? To what extent can this explain multisensory perception?
- **6: Sensorimotor Integration:** If I can establish an optimally integrated sensory feedback channel, does this scale to real world sensorimotor tasks such as grasping and lifting objects? To what extent is present prosthesis-control suboptimality governed by sensory uncertainty versus motor uncertainty?

1.3 Overview of this Thesis

In this thesis I focus on the integration of multiple sensory signals for sensorimotor control in the presence of uncertainty or noise. The thesis is split into chapters spanning engineering, psychophysical experiments, practical deployment and evaluation of a closed-loop prosthetic hand.

In **Chapter 2: Background** I present a review of models of probabilistic perception and sensory processing; a summary of the state-of-the-art in closed-loop prosthetics; and a survey of the mechanics of the healthy human hand and grasping behaviour. This chapter provides a comprehensive summary of the literature relevant to the topics addressed in this thesis, and introduces the key ideas that have motivated the present research questions.

In **Chapter 3: System Design** I present the practical considerations and engineering accomplishments that were necessary to design and build a prototype closed-loop system, addressing **Question 1** of section 1.2. This chapter is largely based on a technical report and conference paper. Much of this technical work was done in collaboration with Touch Bionics, a leading prosthetics company, which has resulted in a product license and patent application.

- Ian Saunders, Sethu Vijayakumar. (2009). **A Closed-Loop Prosthetic Hand: The Development of a Novel Manipulandum for Understanding Sensorimotor Learning**. *Technical Report EDI-INF-RR-1321*.
 - Introduces the major components of the closed-loop prosthetic hand, and motivates the utility of a closed-loop prosthesis as a manipulandum;
 - Provides a number of potential experiment designs, ranging from cursor tracking to real-world grasping tasks, outlining their theoretical motivation;
 - Presents technical details (in appendix) of electrotactile and vibrotactile feedback hardware;
- Ian Saunders, Sethu Vijayakumar (2009a). **A Closed-Loop Prosthetic Hand**. *Proc. Key Issues in Sensory Augmentation*.
 - Presents a cursor navigation task for quantitative evaluation of the benefits of a vibrotactile feedback system, asking “Do humans optimally integrate sensory information, regardless of the modality it is presented in?”;
 - Presents a simulation of human grasp-aperture control using the optimal feedback control framework, asking “Is human motor control ‘optimal’ with respect to available sensory feedback?”.
- Ian Saunders, Sethu Vijayakumar, Hugh Gill. (2011b) The University Court of the University of Edinburgh/Touch Emas Ltd., **Improvements in or relating to Prosthetics and Orthotics**, *GB Patent Application - Category P120168.GB.01*.
 - Details a novel approach for control and receiving feedback from a prosthesis. Further information can not be disclosed due to licensing restrictions.

Chapter 4: Estimating Sensory Uncertainty Over Time is the first of three experimental results chapters. I focus on **Question 5** of section 1.2, to address the fundamental question of *how are the statistics of uncertain sensory information acquired*. I have developed a continuous target localisation task to evaluate the mechanisms of mean and uncertainty estimation over time. This chapter is based on a conference paper, a journal paper under peer review and an unpublished work.

- Ian Saunders, Sethu Vijayakumar, (2011c) **Continuous Estimation of Mean and Uncertainty**, *Proc. The 21st Annual Conference of the Japanese Neural Network Society*.
 - Introduces a novel experiment design (the *butterfly catching task*) for simultaneous measurement of subjective mean and uncertainty estimates;
 - Presents experimental findings, revealing that subjects assign equal weight to each cue presented over time when estimating the mean. Confidence-estimate trajectories increase as a function of cue-uncertainty and in the presence of cue-perturbations, but overestimate the true uncertainty.
- Ian Saunders, Sethu Vijayakumar. (2011a). **Continuous Evolution of Statistical Estimators for Optimal Decision-Making**. *PLoS ONE (Under Peer Review)*
 - Presents the butterfly catching task in greater detail, motivating the key experimental manipulations that were required to observe the results above;
 - Compares experimental findings in the butterfly catching task to those of a simulated ideal observer parametrised with sensorimotor delays, speed and acceleration constraints. Empirical and model cue-weights are computed over time.
 - Subjective estimation of the mean has striking similarity to the model: (i) equal weights are assigned to all observed cues (prior to a sensorimotor delay); (ii) cue weighting adapts as further cues arrive; and (iii) average trajectories and endpoint errors are quantitatively indistinguishable from the model. It is concluded that mean estimation performance is optimal with respect to the sensory cues and natural kinematic constraints.
 - Subjective estimation of the uncertainty is similar to the model in that: (i) increasing the cue-variance causes increases in the average uncertainty estimate; (ii) cue-perturbations result in predictable uncertainty-trajectory increases (in onset and magnitude); (iii) the magnitude of average endpoint

confidence estimates are predictable when a conservative margin for error is allowed. It is concluded that either uncertainty estimation or gain maximisation is less than ideal and although subjects are able to reliably discriminate different levels of sensory uncertainty they do so with a suboptimal overestimate.

In **Chapter 5: Optimal Multisensory Integration** I develop a tracking paradigm to understand the processes of continuous *integration* of *multiple* uncertain sensory cues. This allows me to quantify the degree of integration of the artificial sensory channel, as well as address the mechanisms by which multiple sensory signals are integrated in the presence of uncertain sensory feedback, addressing **Questions 3 and 4** of section 1.2. This chapter is based on a conference paper and unpublished work.

- Ian Saunders, Sethu Vijayakumar. (2009b). **A Closed-Loop Prosthetic Hand as a Model Sensorimotor Circuit.** *Proc. International Workshop on Computational Principles of Sensorimotor Learning.*
 - Introduces a continuous multimodal tracking experiment whereby subjects are required to navigate a cursor (presented in both tactile and visual modalities) towards a target location.
 - Behaviour of subjects is compared to a Bayes-optimal ideal-observer model, as well as a range of alternative suboptimal hypotheses. The alternative hypotheses are inconsistent with empirical observations and so are rejected.
 - On average, subjects are found to favour the more reliable modality on a given trial, and moreover allocate weight in a manner which is quantitatively indistinguishable from a Bayes-optimal observer.

In **Chapter 6: Feedforward and Feedback processes during Closed-Loop Prosthesis Control** I present results of three behavioural experiments in which the developed closed-loop prosthesis was tested for the task of grasping and lifting objects. These experiments examined the role of feedback in the presence of feedback and feedforward uncertainty, addressing **Question 6** of section 1.2. This chapter is based on a journal paper (in press) and unpublished work.

- Ian Saunders, Sethu Vijayakumar. (2011). **The Role of Feed-forward and Feedback Processes for Closed-Loop Prosthesis Control.** *Journal of Neuroengineering and Rehabilitation (In Press)*
 - This paper introduces the *grasp and lift* paradigm for evaluating performance of prosthesis functionality. Healthy individuals are known to grasp *econom-*

- ically* (assigning greater grip force to heavier objects), and this phenomenon is explored using the prosthesis as a sensorimotor manipulandum.
- Three manipulations are applied to the task: increasing tactile uncertainty, visual uncertainty and feedforward uncertainty.
 - In “ideal” feedforward conditions subjects show preservation of economical grasping even in the complete absence of tactile and visual feedback. However, as feedforward uncertainty is increased the benefits of tactile and visual feedback on task performance are observed.

Finally **Chapter 7: General Discussion** summarises and discusses the main achievements of the thesis as highlighted above, and presents potential directions for future research.

Appendix A: Uncertainty in Sample Standard Deviation, provides a summary of mathematical derivations relevant to uncertainty estimation in Chapter 4.

Chapter 2

Background

In this chapter I review the literature surrounding closed-loop sensorimotor behaviour. Firstly, I address probabilistic theories of sensory perception, providing a theoretical framework with which to describe the role of sensory uncertainty in behaviour. Secondly, I review the temporal aspects of perception, motivating the need for continuous-time sensorimotor tasks in understanding the role of uncertainty in the real world. Thirdly, I examine current theories about human hand control and tactile sensation, providing a gold standard which a closed-loop system may aim to replicate. Finally, I review the state of the art in closed-loop prostheses.

2.1 Probabilistic Models in Human Sensorimotor Control

2.1.1 Introduction

Every decision we make involves some degree of uncertainty. The human brain has a remarkable capacity to combine the masses of information that continually stream through our multiple sensory organs, tunnelling down tactile fingertip fibres, retinal receptors and auditory afferents. Nevertheless, our perception of the world is generally robust, stable and free from ambiguity. How the brain achieves this is a primary focus of much research in neuroscience and neuroinformatics.

Much of the inspiration behind this research stems from perceptual illusions. Alais and Burr (2004) discuss the “ancient art of making one’s voice appear to come from elsewhere”. The so-called *Ventriloquist Effect* (Jack and Thurlow, 1973, Thurlow and Rosenthal, 1976) essentially describes the phenomenon of visual stimuli (the movement of a puppets mouth) “capturing” auditory stimuli (the sounds emerging from the pupeteers mouth). The brain chooses to resolve the correlated sensory information into a unified percept, which favours the spatially-reliable visual stimulus and so the sounds appear to originate from the puppet. Intriguingly, this phenomenon is reversed when audition is the more reliable modality (for example, in temporal judgements) and auditory stimuli can “capture” visual stimuli (Burr et al., 2009).

Many other illusions rely on the ability of the brain to seamlessly integrate multiple sensory cues. In the *McGurk Effect* (McGurk and MacDonald, 1976) it was shown that spoken phoneme perception is governed by both auditory and visual cues: The syllable “Ba” when dubbed on to lip movements for “Ga”, is perceived as “Da”. In the *Parchment-Skin Illusion* a sound that is played synchronous to us rubbing our hands together strongly modifies the perception of dryness and friction (Jousmäki and Hari, 1998). These illusions touch on the fundamental issue of the roles and interdependencies of different sensory systems on our seamless perception of the world.

One key hypothesis is that the brain employs probabilistic models to achieve robust perception. This hypothesis is observed electrophysiologically at the single-neuron level, described computationally through population-code neural networks and measured behaviourally with psychophysical studies. In this section I will briefly review this evidence and discuss some key questions that remain to be answered.

A central principle of probabilistic theories of perception is Bayesian Decision Theory (see Yuille and Bulthoff, 1996). Bayesian Decision Theory is a statistical approach in which the costs of decisions are quantified and combined with their probabilities to enable statistically-optimal decisions. Evidence for Bayesian mechanisms in the brain are based on a great number of key psychophysical results. In the phenomenon of “multi-

sensory integration” (also known as bimodal, multimodal and cross-modal integration), subjects are shown to merge information from multiple sensory modalities according to an optimal Bayesian approach. In the following sections I will review these studies.

2.1.2 Multisensory Integration

Rock and Victor (1964) conducted a classic experiment in which subjects were asked to grasp a visually-distorted object, then draw it. Unaware of the distortion, vision dominated perception, and so the phenomenon was dubbed “visual capture”. Subsequently, Welch et al. (1979) found that visual capture over proprioception was compromised during active movement, but not during passive movement, arguing that visual dominance was due to its reliability. According to their “Modality Appropriateness” hypothesis, discrepancies were resolved in favour of the more *precise* or more *appropriate* modality. For a temporal estimation task in which audition was more reliable Welch et al. (1986) showed that vision does not always dominate. Young et al. (1993), among others, showed that the respective weighting of a sensory cue changes as signal *reliability* is manipulated. This has led to statistical models of cue integration, which I will review here.

2.1.2.1 Ideal Observer Behaviour

Bayesian Statistics Consider the task of localising a stimulus x . Suppose that a number of sensory estimates, x_i , arise from the stimulus, indexed by i . Each estimate may be from a different sensory modality, such as vision or audition, or perhaps from a number of cues within a modality.

Under the Bayesian framework one aims to compute the probability distribution of the true location x , given sensory evidence x_i for $i = 1, \dots, n$.

$$\underbrace{\Pr(x | x_1, \dots, x_n)}_{\text{posterior}} = \frac{\underbrace{\Pr(x_1, \dots, x_n | x)}_{\text{likelihood}} \cdot \underbrace{\Pr(x)}_{\text{prior}}}{\underbrace{\Pr(x_1, \dots, x_n)}_{\text{marginal likelihood}}} \quad (2.1)$$

Equation 2.1 is an example of Bayes’ rule. It explains how to optimally update our beliefs under multiple sources of sensory information. $\Pr(x)$ reflects our *prior belief* in x , i.e. our belief in a particular state of the world before sensory input is received. In the presence of multiple sources of sensory information one can compute the overall *likelihood* of the evidence, i.e. the probability of observing this evidence given all possible x . From the normalised product of the likelihood and prior one can then estimate the evidence-based probability distribution of the state, termed the *posterior*.

It is often assumed that the variability or the noise in the different sensory streams is independent. Therefore, under the condition that the sensory estimates are *conditionally independent* given the true stimulus we see that

$$\Pr(x|x_1, \dots, x_n) \propto \Pr(x_1|x) \cdot \Pr(x_2|x) \cdots \Pr(x_n|x) \cdot \Pr(x) \quad (2.2)$$

Maximum Likelihood (ML) If the prior term in equation 2.2 is ignored, we can compute the *maximum likelihood* estimator of x . This is the value of x that maximises

$$\mathcal{L} = \prod_i \Pr(x_i|x)$$

Assuming that the noise affecting each modality i is Normal with mean x_i and variance is σ_i^2 , i.e.

$$\Pr(x_i|x) = \frac{1}{\sqrt{2\pi} \sigma_i} \exp\left(-\frac{(x - x_i)^2}{2\sigma_i^2}\right)$$

then the minimum variance estimator of the stimulus location is easily computed by taking the logarithm of the likelihood and differentiating with respect to x .

$$\frac{\partial}{\partial x} \log \mathcal{L} = \sum_i \frac{\partial}{\partial x} \log \Pr(x_i|x) = 0$$

In doing this we find that:

$$x_{ML} = \sum_i \left(x_i \cdot \frac{\sigma_i^{-2}}{\sum_j \sigma_j^{-2}} \right) \quad (2.3)$$

Thus, the maximum likelihood multimodal estimate is simply the average of the unimodal sensory estimates each weighted by its relative inverse variance, i.e. its relative *reliability* (see Ernst and Bühlhoff, 2004).

Maximum A Posteriori (MAP) The *maximum a posteriori* approach is identical to the above, except that it also accounts for the prior term in equation 2.2. If the prior is treated as uniform (each location equiprobable) then the MAP estimate is identical to the ML estimate.

Alternatively if the prior is considered to be Normally distributed with mean x_{prior} and variance σ_{prior}^2 , the MAP estimate is identical to the ML estimate where the prior becomes an additional piece of weighted sensory evidence.

Of course, it is not necessary to make assumptions about the nature of the prior. As shall soon be revealed, a number of studies have chosen prior distributions that allow the properties of probability distribution perception to be inferred.

Suboptimal Models There is no reason to expect perception to be statistically optimal. According to the visual capture hypothesis (Rock and Victor, 1964), one modality or cue solely determines our observations.

$$x_{UNI} = x_k$$

An alternative equal-weighting hypothesis may average all available sensory cues, regardless of their reliability.

$$x_{AVG} = \frac{1}{N} \sum_i x_i$$

However, these *uncertainty-independent* strategies seem unlikely, not least because they are inconsistent with empirical observations (see later). Alternative *uncertainty-dependent* models of integration seem more plausible.

The *winner-takes-all* approach (Gahahramani et al., 1997) is an extension of the modality appropriateness hypothesis to *cues* rather than modalities (see Welch et al., 1979), in which a sensory signal dominates if it is the most reliable:

$$x_{WTA} = x_i \iff \forall j. \sigma_i^2 \leq \sigma_j^2$$

A *stochastic* integration model has also been proposed (Gahahramani et al., 1997), in which the observer adopts a single cue with a given *probability*. i.e.

$$x_{STO} = \begin{cases} x_1 & \text{with probability } p_1 \\ \vdots \\ x_n & \text{with probability } p_n \end{cases}$$

If p_i is a function of the *reliability* of the cue, this approach would result in average behaviour (over many trials) identical to the ML model. Furthermore, this behaviour may arise *passively*. For example, a low contrast stimulus may be observed less often than a high contrast stimulus, with probability inversely proportional to its uncertainty.

Alternatively, subjects could perform *cue switching* rapidly throughout a trial (Ernst and Bühlhoff, 2004). If the switch was determined by the cue reliability, this would also result in behaviour identical to ML.

A multitude of alternative possible models exist, and it has been a primary focus of research into multimodal integration to determine the model deployed by the nervous system (e.g. Ernst and Banks, 2002). In Chapter 5 I introduce a multisensory integration task which allows me to compare human behaviour to the predictions of the above models.

2.1.2.2 A-Priori Integration

No one sensory signal can provide reliable information about the world in all circumstances. One could attempt to resolve this by collecting more sensory information but this would result in intolerable delays for most tasks. It is argued that a central function served by the perceptual system is to make decisions needed to interact with the environment by relying on the *anticipated* consequences of actions (Ernst and Bühlhoff, 2004). These are captured by *prior beliefs* in the Bayesian framework.

Körding and Wolpert (2004a) present evidence for the influence of prior distributions in a reaching task. Subjects received momentary visual feedback of hand position midway through a reach and made online corrections based on this sensory information. The visual feedback comprised clouds of blobs, which were made more or less reliable by adjusting their distribution. Also, the feedback location was distorted laterally by noise from trial to trial according to a probability distribution which defined a *prior*, which subjects learned to estimate over 1,000 training trials. As predicted quantitatively by the Bayesian framework, movements with reliable feedback rejected the prior, but when feedback was degraded the estimate was biased towards the prior as a function of its reliability. This phenomenon also applied to a bimodal prior. It is argued that this shows that the brain *internally represents* both the prior statistics of the environment and the uncertainty in its sensors, combining these sources of information optimally (Bays and Wolpert, 2007) .

To explain their findings, Körding and Wolpert (2004a) discuss three potential models of integration: (i) Subjects obey the prior distribution and disregard the visual evidence; (ii) Subjects disregard the prior and compensate fully for the visual feedback; and (iii) subjects combine prior and evidence in a Bayesian manner. Their results are incompatible with suboptimal models (i) and (ii). They also discuss the possibility of an additional model in which subjects learn a *mapping* from visual feedback to lateral shift, which would result in the same outcome as (iii) without subjects explicitly representing the prior or uncertainty. In order for subjects to learn this mapping they would need knowledge of the error at the end of each trial, which they are not given. From this it is concluded that subjects must *explicitly* represent prior and sensory uncertainty. However, it is also possible that visual uncertainty is *implicitly* encoded in perceptual signals, which may result in the same empirical observations. Although the precise mechanisms are debatable, it is clear that subjects are capable of combining prior information and sensory evidence.

Important questions still remain to be answered. In a review Körding and Wolpert (2006) ask “How is prior information encoded in the central nervous system? How is it combined with new evidence to generate estimates?” More generally, it is not known

how *sensory evidence* is acquired by the nervous system, how it is encoded, nor how it is combined. In this thesis I examine these questions in more detail from novel experimental perspectives.

2.1.2.3 Maximum Likelihood

Numerous studies have provided evidence for maximum likelihood multisensory integration. These studies typically involve two noisy sensory cues to a stimulus property (often in different modalities), presumed to arise from the same underlying source. Subjects are required to report the stimulus property based on either a single cue or both cues. The maximum likelihood multisensory estimate of the stimulus property is proportional to the weighted sum of unimodal estimates with the weights determined by the cue reliabilities (see equation 2.3).

Jacobs (1999) provided the first psychophysical evidence of this phenomenon. Subjects were required to use depth cues to estimate the curvature of cylinders. This could be achieved using texture cues (the shape of circles projected onto a simulated cylindrical surface), from motion cues (the position of fixed-size circles moving over the simulated surface), or from both cues together (the position and shape of circles moving over the simulated surface). In the combined task, subjects were shown to integrate the cues according to a Bayesian model, based on the reliabilities as determined from the unimodal tasks. However, it should be noted that in unimodal trials the model accommodated a bias parameter that made the assumption that the ellipse was perceived as “more circular” than it actually was. Also, although motion cues actually contain curvature information in the density of the blobs it was argued that this third cue is weak due to the spacing between blobs. However, under these assumptions they demonstrated a very good fit of human behaviour to the model.

Ernst and Banks (2002) showed that the maximum likelihood principle applies to humans integrating information from multiple modalities. They asked subjects to judge the relative height of a bar, presented unimodally (haptically or visually) and multimodally. Visual cues were distorted by differing degrees of noise. In the unimodal trials subjects were presented with two stimuli, one of standard height and one of unknown height, in random order, and asked to choose which was taller. Discrimination thresholds were used to compute the *reliability* of the unimodal cues, which in turn were used to compute the maximum likelihood *weights* which should be allocated to each cue in the multimodal task. In the multimodal task the standard stimulus had constant haptic height but had a range of visual heights *discrepant* to the haptic height, which allowed measurement of the empirical weights. For increasing visual uncertainty they observed increasing dominance to the haptic cue, in accordance with maximum likelihood integ-

ration. This finding also holds for alternative sources of visual uncertainty (e.g. viewing angle, Gepshtein and Banks, 2003; and blur Helbig and Ernst, 2007).

In a similar study for audio-visual integration, Alais and Burr (2004) asked subjects to localise “blobs” (low-contrast Gaussians of varying widths) or “clicks” (location determined by inter-aural time differences). Again, psychometric curves were used to measure subject’s decision as a function of audio-visual conflict. When visual localization is good, vision dominates sound, as per the ventriloquism effect. For blurred visual stimuli the reverse holds: sound dominates vision. For different degrees of blur a continuum exists in which perceptual weight follows the maximum likelihood integral. A key further observation is that bimodal performance exceeds unimodal performance, indicative of utilising both sources of information together to maximise reliability (and minimise uncertainty). These results therefore argue against the “visual capture” and “auditory capture” hypotheses in favour of optimal integration.

Furthermore, humans have been shown to combine proprioceptive information about the location of our hand with visual information of the hand itself (van Beers et al., 1999), and from the configuration of our joints (Sober and Sabes, 2005). The phenomenon of multisensory integration applies not only to per-modality weightings but also within-modality directional sensitivity (van Beers et al., 1999). Further, within-modality studies have shown that people combine visual texture, motion and stereo cues into a single depth estimate (Jacobs, 1999, Knill and Saunders, 2003, Hillis et al., 2004), and visual cues of relative contrast, frequency and orientation of textures allow us to discriminate edges (Landy and Kojima, 2001).

However, Helbig and Ernst (2007) argue that the above results may be measuring indirect behaviour. Firstly, the above approaches use two-interval and two-alternative forced-choice (2-IFC and 2-AFC) designs above rely on memory, and this may be affected indirectly by uncertainty. They choose to use a 1-IFC approach (subjects make a decision based on simultaneous stimuli). Secondly, they tested whether statistical optimality holds for *real* (rather than simulated) visual and haptic shape information, since multimodal integration may depend on spatial alignment of sensory cues (Gepshtein et al., 2005). Helbig and Ernst (2007) used mirrors to separate visual and haptic information for oriented ellipses, asking subjects to feel the ellipse while observing it in a (blurry) aperture. Nevertheless, despite these modifications they observed optimal behaviour consistent with Ernst and Banks (2002).

Over a wide range of phenomena and with different experimental approaches, it is clear from these studies that we can combine multiple sensory signals in a manner quantitatively consistent with statistically-optimal integration (Wolpert, 2007). Moreover, it has been argued that Bayesian processes may be a fundamental element of sensory

processing in the nervous system (Körding and Wolpert, 2006).

2.1.2.4 Maximum A-Posteriori and Bayes

The ML framework maximises the probability of observing some state of the world given the parameters of a probabilistic model describing the consequences of our actions. We have seen that much behaviour is quantitatively accounted for by this model in which precision is naturally maximised by minimising variability. However, evidence is not unanimous, and a number of studies have found suboptimal biases (e.g. Burr et al., 2009, Knill and Saunders, 2003) which we will discuss later. An obvious weakness of the ML model is that it does not account for *a priori* influences on behaviour.

If we have knowledge about the parameters of the world — a prior — then the Bayesian approach allows us to estimate the posterior, the most probable explanation of our observations given the evidence available.

Previously I discussed a study by Körding and Wolpert (2004a), in which subjects were trained to learn a *prior probability distribution*. In this study subjects were biased towards the prior as predicted quantitatively by the maximum a-posteriori (MAP) estimation model. Subjects optimally combined the available evidence with respect to the uncertainty of the visual cues and the uncertainty of the prior. Similar MAP-optimal behaviour was also seen in a force estimation task (Körding et al., 2004) and a pointing task (Tassinari et al., 2006). These results together suggest that when people learn new tasks they learn not only the underlying statistics of the *task* but also the underlying statistics of their own *sensory apparatus* — and combine the two in a Bayesian manner (Wolpert, 2007).

2.1.2.5 Criticisms

Despite the evidence reported above, a number of studies have demonstrated discrepancies in optimality of integration. Battaglia et al. (2003) provided evidence for both visual capture and maximum likelihood theories, since the relative reliability of cues affected spatial localisation but these judgements included an overall visual bias. Similarly, Burr et al. (2009) showed that audition dominated vision for perception of interval, but quantitatively the weights were “less than optimal”. Likewise, Knill and Saunders (2003) computed slant discrimination thresholds based on stereo and texture cues and found that texture information was under-weighted. What could be the explanation for this suboptimality?

Inaccurate Sensory Estimates Rosas et al. (2005) studied visual-haptic cue combination for slant-discrimination. Visual cue (texture) reliability was varied and performance

measured in comparison to the maximum likelihood prediction. They found that subjects performed *worse* in the multimodal condition than in the texture-only condition for all but one of the subjects in one condition. More than 80% of their data were inconsistent with maximum likelihood. They conclude that, while the visual system is sensitive to the cue reliabilities, integration weights are not statistically optimal. Oruç et al. (2003) studied slant estimation from the combination of linear perspective cues and texture gradient cues. For three out of eight subjects they found evidence in favour of optimal cue combination, for three they observed data consistent with optimal combination with the assumption that internal cue estimates were correlated, and for two the cue combination strategy was sub-optimal. Clearly “flexible mechanisms” (Sober and Sabes, 2005) underlie multisensory integration. Rosas et al. (2005) concede that subjects may have attempted to combine cues optimally but “did not have an accurate estimate of the variance of the individual cues”.

It is not clear how reliability is perceived by the nervous system, nor is it clear what reliability signal is used. Sober and Sabes (2005) argue that *objective uncertainty*, the empirical variability in the task, does not necessarily define integration weights. They showed that sensory integration weights are not solely statistically-determined, but also that the *nature of use* of the multimodal estimate resulted in a “diversity of weightings”. Subjects’ inaccurate estimates (Rosas et al., 2005) define their *subjective uncertainty*, which ought also be considered when evaluating the mechanisms of integration.

Implicit Encoding and Recall As discussed previously, Helbig and Ernst (2007) argue that forced-choice paradigms may induce apprehension, especially with increased uncertainty. This apprehension may indirectly provide a measure of stimulus uncertainty that does not require an explicit conscious representation. Experimental manipulations to increase uncertainty, such as decreasing stimulus contrast or adding uncorrelated noise, may increase the latency with which subjects can react to stimuli. In this way, much research on statistical optimality includes situations in which the mechanisms of perception may *implicitly* encode uncertainty, and so optimal integration may be a by-product of these phenomena.

Cue Conflicts To capture explicit, active decision-making, Boulinguez and Rouhana (2008) used a “delayed recall task”. This (i) avoided the use of multisensory conflicts; and (ii) required subjects to make active decisions. They argue that the incongruency of sensory cues in typical integration studies may bias behaviour. They instead used a novel task in which subjects were asked to memorise a trajectory applied proprioceptively (moving the right hand with pulleys), visually (a dot on a screen) or both together. They then asked subjects to reproduce the trajectory using proprioception (moving the

right hand), vision (controlling the dot with the left-hand) or both (controlling the dot with their right-hand motion). By randomising encoding and recall configurations this arrangement allowed them to examine how the trajectory was recalled under expected visual and proprioceptive dominance. They found that the weighting of each modality was based on its relative precision at encoding but the integrated response was inconsistent with optimal integration.

Wallace et al. (2004) also raised concerns that discordant stimuli may indirectly alter perception and integration. Subjects were asked whether they believed auditory and visual stimuli to be unified in an auditory localisation task. When stimuli were perceived as unified their perception was biased towards the visual stimulus but when not unified it was biased against. They describe this perceptual phenomenon as multisensory “attraction” and “repulsion”. However, it is not possible to rule out the possibility that the nature of the task biased subjects towards making binary decisions, causing the attraction and repulsion observation. Nevertheless, their results demonstrate that people can judge unity and discrepancy well, a factor which is often overlooked in multisensory studies.

The Bayesian approach and the weak fusion model require that subjects are able to determine cue reliabilities which they can then combine linearly. However, Maximum Likelihood models break down when it is not clear whether two observations are derived from the same underlying cause (Hospedales and Vijayakumar, 2009), and so one must consider the possibility that subjects discount a discrepant stimulus when performing multisensory integration. For example, Johnston et al. (1994) presented subjects with conflicting stereo and motion depth-cues and found that a *linear combination* rule was insufficient to describe the data. However, this may be because discrepancies induce nonlinearities (Körding et al., 2007). Nonlinearities are still integrated in a way that can be reliably predicted by Bayesian Model Selection (Körding et al., 2007).

Mechanisms of Integration As discussed previously, Ernst and Bühlhoff (2004) argue that cue weighting studies do not rule out the possibility of a ‘cue switching’ strategy in which an observer uses one cue at a time but switches between cues in proportion to the cue reliability. This may appear optimal on average. Within-trial analyses may help to resolve this. For example, the per-trial perception of discrepancy reported above argues for the presence of active, conscious multisensory decision-making processes (Wallace et al., 2004).

In an attempt to resolve issues of integration mechanism, Landy et al. (1995) distinguish strong and weak integration, capturing cue-agnostic behaviour versus linear integration in a common reference frame. The Bayesian approach is neither strong nor

weak, and says nothing about the mechanisms available to the nervous system. Strong and weak models may provide one useful distinction. In general, in order to understand the mechanisms of cue combination it is important to distinguish the processing steps in dynamic integration.

Attention Helbig and Ernst (2008) examined visual-haptic integration in the presence of a distractor. It was hypothesised that, since the distraction should increase the uncertainty of a reliable stimulus more than an unreliable stimulus (the principle of *inverse effectiveness*, see Meredith and Stein, 1983, Anastasio et al., 2000), then the resultant modality weighting would indicate whether or not the distraction was integrated early or late into the integration process. It was found that subjects integrated the cues prior to the effects of the distraction, suggesting the presence of an automatic (attention-independent) integration mechanism.

An alternative explanation of this result is that the cue weights are learned under conditions of low attentional load and that the weights are applied under conditions of high attentional load. However, if the weights were learned, how would the system decide which set of weights to apply in which situation? This argues against the growing body of evidence in favour of an online estimation of the weights from the variances of the current stimuli (e.g. Alais and Burr (2004), Ernst and Banks (2002), Hillis et al. (2002)). However, such a possibility can not be ruled out without directly addressing the mechanisms of uncertainty estimation.

It is also important to note that Helbig and Ernst (2008) measure an increase in task-level performance by the Just Noticeable Difference (JND) in perception. This is a measure of the *objective* reliability, and is *not* the same as the *true* reliability of the stimulus, or indeed subject's *perception* of the true reliability.

In summary, Helbig and Ernst (2008) expose a number of fundamental questions: (i) can subjects distinguish different sources of uncertainty? (ii) to what extent are subjects consciously aware of this uncertainty? (iii) by what mechanisms is this information acquired? and (iv) is the consciously acquired information used to determine multisensory integration weights, or is this mediated by a separate, innate process?

It is not obvious how these questions can be addressed through the classical forced-choice approach.

2.1.3 Bayes in the Brain

2.1.3.1 Neural Implementation

The case for Bayesian mechanisms in the brain is evidenced by both neurophysiology and computational models.

Morgan et al. (2008) measured neural activity in macaque visual cortex as the animal was passively moved, with visual and vestibular cues indicating the motion while the animal was required to fixate on a dot. They found that when the reliability of the visual cue was degraded its influence on the bimodal neural response reduced while the influence of the vestibular cue increased. The fact that single neurons adjust the weighting of their inputs to reflect the relative reliabilities of stimuli suggests an innate capacity of the brain to handle probabilistic information.

The *superior colliculi* are the mammalian midbrain areas which receive visual, auditory and somatosensory information, controlling orienting behaviour and head and eye movements in the presence of multisensory stimuli. Meredith and Stein (1983) showed that superior colliculus neurons respond more vigorously to multimodal rather than unimodal stimuli. Cells in the upper layers of the superior colliculi are primarily visual, while deeper layers respond to combinations of visual, tactile and auditory stimuli (reviewed in Holmes and Spence, 2005). The main properties of these multisensory cells are:

1. **Multisensory enhancement:** By the *spatial rule*, stimuli in different senses that arrive from the same location (i.e. have the same *receptive field*) are enhanced. According to the *temporal rule*, stimuli in different senses that arrive at the same time are enhanced;
2. **Inverse effectiveness:** According to the *inverse effectiveness rule*, when enhanced, weak responses increase by a greater proportion than strong responses;
3. **Within- and cross-modality suppression:** Neural responses are *suppressed* when within- or cross-modal stimuli are discrepant (i.e. they occur simultaneously in the separate receptive fields; or in the same receptive field at different times).

These phenomena can, in fact, be modelled by Bayes rule. Anastasio et al. (2000) demonstrate how the principles of inverse effectiveness and cross-modality suppression emerge naturally as a consequence of combining probability distributions. Further, Barber et al. (2003) present a mathematical formulation of how neurons might perform Bayesian computations. Hoyer and Hyvärinen (2002) demonstrate that Poisson noise empirically observed in neural recordings may, in fact, be a bi-product of an implementation of Bayes in the brain.

2.1.3.2 Population Codes

Kepecs et al. (2008) showed that firing rates of neurons in rat orbitofrontal cortex respond to stimulus uncertainty. In an olfactory discrimination task rats were trained

to choose one of two odours when cued with a mixture. The odour with the higher proportion defined the “correct” choice, and the animal was rewarded. After training, the response of cortical neural populations could predict both the chosen decision as well as the amount of time the animal would wait for a reward, suggesting that confidence information is encoded in population code activity.

Deneve et al. (1999) asked how neural networks might implement maximum likelihood. This can be achieved with a biologically plausible recurrent network of non-linear neurons with Poisson-distributed noise. Deneve et al. (2001) generalise the model and show how it remains optimal when the reliability of cues changes from trial to trial. While most studies of multisensory integration assume that modalities are remapped into a common reference frame, Deneve and Pouget (2004) argue that multisensory integration occurs via a “cross-modal dialogue”, not a supra-modal common reference frame. In their model, uncertainty is encoded in the *gain* of the neural responses, not in the distribution of population activity. The latter theory would be unable to capture contrast-induced reliability and does not easily handle the presence of different reference frames. Of course, it would also be possible to describe a model which included additional layers to perform these coordinate transformations prior to multisensory layers, which would result in conceptually the same model.

Crucially, for populations of neurons encoding stimuli with Poisson-like neural responses, with gains tuned to the reciprocal variance, Bayesian inference reduces to a linear combination of the unimodal neural responses (Deneve et al., 2001). In such a system, cortical neural variability allows neurons to *automatically* encode probability distributions. However, this does not explain how prior information may be encoded. If one assumes a topological arrangement of input layers (Magosso et al., 2008) a population-distribution model can encode priors by potentiating network connections with the arrival of sensory inputs. It is not immediately obvious how gain-encoded uncertainty allows for this. It is possible that the presence of neural noise can enhance weak signals by “stochastic resonance” to transform gains into distributions (Goodwin and Wheat, 2004).

An important difference between alternative population code models of multisensory integration is whether or not subjects learn to *explicitly* represent the statistical information about stimuli across a population of neurons, or if subjects sample from random variables that represent the statistical information about the stimuli (an *implicit* encoding). In forced-choice psychophysical experiments, these two methods are difficult to reliably distinguish, since the experimenter is *sampling* behavioural responses. Indirect measures such as measuring response variability can be of some use, but to directly tease apart these different approaches we stress the importance of continuous decision-making

tasks and within-trial analyses.

2.2 Decision-Making over Time

2.2.1 Introduction

In the previous section I have reviewed evidence that the brain employs Bayes-optimal multisensory integration for a range of binary decision tasks (e.g. Ernst and Banks, 2002). This growing empirical consensus is based on psychophysical studies, computational models, and neurophysiological recordings.

A key assumption of the Bayesian approach is that people are somehow capable of *acquiring* sensory evidence and using it to form *probability distributions*. Neural recordings reveal the presence of statistical signals in the brain (Kepecs et al., 2008) and population code models can explain many behavioural results (Deneve and Pouget, 2004), but in order to understand how sensory information is used to establish cue reliabilities it is necessary to look at within-trial behaviour.

It is not known what measure of “confidence” people use to make optimal decisions. In numerous studies cue weighting is shown to be optimally based on objective uncertainty, but in other cases this may be inadequate (Sober and Sabes, 2005), perhaps because subjects may not be able to estimate this quantity accurately (Rosas et al., 2005). To understand the mechanisms of confidence estimation a direct approach may be more suitable.

Forced-choice binary decisions may not reliably discriminate optimality from the passive effects of uncertainty (Helbig and Ernst, 2007). We can ask subjects to make active decisions (e.g. Boulinguez and Rouhana, 2008), but the best way to distinguish active cue integration from emergent optimality in average behaviour (e.g. for a cue-switching approach, Ernst and Bühlhoff, 2004) is, again, to record within-trial decisions.

A number of studies have shown that optimal integration occasionally fails (e.g. Knill and Saunders, 2003, Burr et al., 2009), motivating the need for a better understanding of the underlying processes. Further insight about the underlying processes could be gained by examining the evolution of decision-making process and by observing cue integration on a finer temporal granularity.

In this section I review *continuous* sensorimotor tasks. These could provide a valuable tool for identifying the underlying processes of multisensory integration.

2.2.2 Continuous Tracking and Pointing Tasks

2.2.2.1 Traditional Tracking Tasks

A classic paradigm for assessing motor control is that of tracking a target on a screen. The task has several variants:

- *pursuit tracking* requires the subject to follow a randomly displaced target dot with a cursor.
- *compensatory tracking* requires the subject to maintain a cursor in a fixed position while it is randomly perturbed.
- *preview tracking* provides the subject with a preview of where the target will be in the future, adding the element of planning to the task.
- *step tracking* is a pursuit tracking task in which the target may be randomly displaced for a brief interval. This step is spatially unpredictable, but the return step is not. Temporal unpredictability can also be added by randomising the step onset time and duration.
- *predictable target tracking* involves a predictable target pattern that is temporarily occluded.

Within these tracking categories, the nature of the visual feedback can be varied (i.e. delays added, noise added, occlusions etc.) to examine different elements of the subjects sensorimotor behaviour.

The paradigm has proven useful for quantifying impairment in a number of neurological disorders. For example, it has been shown that patients with Parkinson's Disease have difficulty in initiating rather than executing pre-programmed movements (Day et al., 1984, Bloxham et al., 1984), and that patients with cerebellar ataxia show irregular modulation of pursuit velocity when tracking a predictable constant-velocity target (Beppu et al., 1987). The visuomotor tracking paradigm is related to many real-world sensorimotor tasks as it involves feedback, prediction, planning, reacting, motor initiation and motor execution. Sensitive to quantifiable subtleties of behaviour such as latency, magnitude and frequency of motor responses under different experimental conditions, it is unsurprising that such a paradigm has been used to pick apart the relative contributions of different aspects of sensorimotor control. Fig. 2.1 illustrates a range of variants to the tracking task for understanding aspects of human sensorimotor function.

Responding to Perturbations Jones and Donaldson (1986) designed three tasks to allow quantitative assessment of different aspects of sensorimotor function. As has already been seen (i) *preview tracking* measures ability at planning and execution; and (ii) *step tracking* measures ability at reaction and anticipation (by including both predictable and unpredictable target 'jumps'); Jones and Donaldson (1986) also introduce (iii) a *combined* task (Fig. 2.1B). Since their conception, these basic tracking tasks

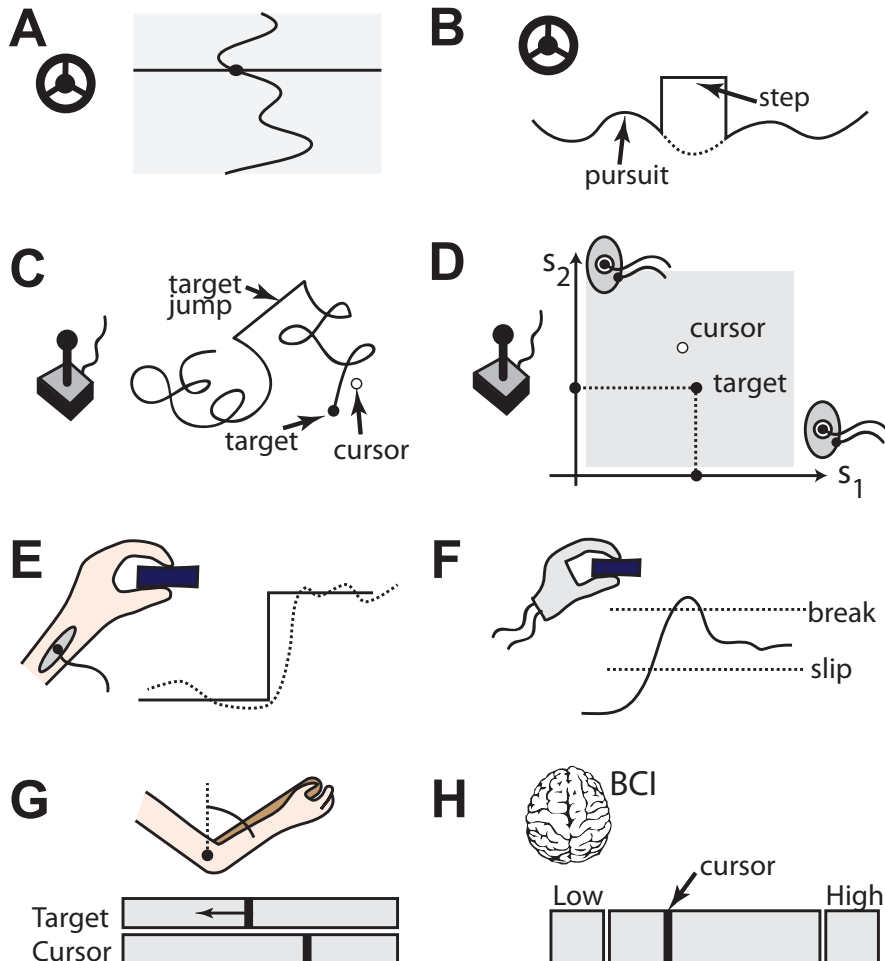


Figure 2.1: **Tracking Tasks.** (A) Tracking a 1-D cursor (e.g. using steering wheel Davidson et al. (2002)). (B) Pursuit tracking and step tracking to distinguish predictive and reactive behaviour (e.g. Jones and Donaldson (1986)). (C) 2-D cursor tracking (with target jumps, Foulkes and Miall, 2000; with time-delayed cursor Miall and Jackson, 2006). (D) Multimodal tracking, with electro-tactile representation of 2-D position (Szeto and Chung, 1986). (E) Controlling the grip force of a neuroprosthesis (amplification of muscle signals in quadriplegic patients), e.g. shoulder-position-controlled (Hines et al., 1992). (F) Robotic prosthesis control of grip force (e.g. Zafar and Doren, 2000). (G) Joint-controlled cursor tracking (e.g. Beppu et al., 1984, 1987). (H) Brain-controlled (EEG) cursor tracking (e.g. Chatterjee et al., 2008)

have proven very useful due to their low cost and high value in assessing motor function. For example, Allen et al. (2007) demonstrate their use for discriminating between patients with different levels of bradykinesia. Their findings demonstrate the value of tracking tasks for separating predictive and reactive aspects of control. On this theme, Davidson et al. (2000) and Davidson et al. (2002) present subjects with a ‘driving’ task, requiring subjects to learn a “novel visuomotor relationship” when *preview tracking*. Subjects track a moving sinusoidal target using a steering wheel (Davidson et al., 2002) or joystick (Davidson et al., 2000) with unusual dynamics (Fig. 2.1A).

On alternating trials the cursor is periodically hidden, requiring subjects to rely on open-loop control. Over a sequence of many trials there is a progressive transfer of learning from closed- to open-loop control, which is attributed to feed-forward learning. Interestingly, once performance has reached a peak, it appears the feedforward controller continues to learn and adapt to feedback even though it can not further reduce errors in the with-feedback condition. The effects of this learning are immediately obvious when feedback is removed. Davidson et al. (2000) argue that this indicates the presence of a combined feed-forward and feedback controller. The results are explained by a model featuring an adaptive feed-forward process, feedback-driven error-correction and feedback-driven feedforward adaptation (Davidson et al., 2002).

Tactile Tracking With vibrotactile and electrotactile stimulation (see later sections 2.4.2.3 and 2.4.2.4), one can create a tactile sensations using vibratory or electrical stimuli on the skin. This can be used to create a tactile analogue to the visuomotor tracking paradigm.

Szeto et al. (1979) compared ten electrotactile feedback stimuli in an electrotactile tracking task. Subjects were trained to use the feedback, then they used a joystick to track a target presented in the tactile modality and visually on an oscilloscope screen (Fig. 2.1D). It was found that spatial modulation codes were significantly superior to single-electrode codes modulating frequency modulation, since single-electrode codes were prone to sensory adaptation. Further codes were explored by Szeto (1982), who found that frequency modulation had the fastest learning-rate, but a linear array of simulators resulted in greatest performance. Monophasic stimulation proved more effective than biphasic stimulation, and the ventral forearm was shown to be more sensitive than the dorsal. Szeto and Farrenkopf (1992) examined the perceptual response to frequency-modulated electrocutaneous signals and Szeto and Saunders (1982) reviewed stimulus parameters and coding formats to recommend procedures for implementing safe, reliable, high-bandwidth, low-adaptation electrotactile displays.

A more complex paradigm relevant to prosthesis feedback requires subjects to in-

terpret data presented in two dimensions simultaneously. Szeto and Chung (1986) introduced a dual-channel 2-dimensional (2D) electrocutaneous tracking task. Previous attempts at a similar task resulted in high inter-subject variability and low inter-group variability (Szeto and Lyman, 1977), making it difficult to reliably discriminate performance differences due to different tactile codes. Using an elaborate and time-consuming training protocol to achieve the necessary level of performance (9 daily training sessions, each lasting 2-3 hours), they were able to train subjects at the task, though they reported that the task required significant mental effort. Such a lengthy training process suggests that multidimensional tracking is cognitively demanding.

Sensorimotor Delays When sensory information is made unreliable by a delay, how do we deal with it in tracking tasks? In the Smith predictor hypothesis (Miall et al., 1993) it is supposed that prediction and control are combined into a common framework that parametrically accounts for these delays. To test this, Foulkes and Miall (2000) required subjects to track unpredictable, continuously moving 2D targets using a hand-held joystick (Fig. 2.1C) while visual feedback of the joystick position was delayed (by 0 ms, 200 ms or 300 ms). Subjects adapted to the delay, with a significant drop in tracking error. Foulkes and Miall (2000) argue that subjects learn an adaptive delay that is added to the forward model to compensate for delays in external feedback, consistent with the Smith predictor hypothesis. Likewise, Miall and Jackson (2006) showed that introduction of visual feedback delays disrupt tracking performance, with an increase in errors and a reduction in the magnitude of corrective movements. However, in the presence of delays subjects should increase the frequency of corrective movements. Instead they improved the feed-forward control of their corrective movements so that they were more accurate. This indicates that prediction and control are separate processes, and argues against the Smith predictor hypothesis.

Force Tracking We have seen that the tracking paradigm can be used to study both visual and electrotactile perception. It also extends naturally to force perception and control. Hines et al. (1992) evaluated the force-control ability of a functional stimulation neuroprosthesis. Shoulder-position signals were used to electrically stimulate the arm-muscles of patients with spinal cord injury to initiate grasps. Hines et al. (1992) used a visual pursuit tracking task analogous to control of grasp force or grasp aperture (Fig. 2.1E). Using this same setup, Adamczyk and Crago (1996) assessed the effect of non-linearities and time delays on performance. They reported that, for force control, neuroprostheses with with linear, low latency controllers are preferred.

On the theme of force estimation in prostheses, Zafar and Doren (2000) used a video-based simulated prosthesis to determine whether grasp-force feedback can improve

control in the presence of realistic visual information. Subjects had to achieve and maintain the (simulated) grasp force within a target window. It was found that force feedback improved force control as well as error detection.

However, the same was not found in a study by Chatterjee et al. (2008) using a force-matching grasping task for EMG prosthesis wearers (Fig. 2.1F). Vibrotactile grip-force feedback improved performance for experienced subjects in only one out three force conditions. Naive subjects performed worse in the presence of feedback. These unexpected results suggest either that: (i) subjects can not utilise feedback until they have learned feed-forward control the hand. This may be due to the noisy EMG interface; (ii) learning to use feedback can take considerable time, owing to its “unfamiliar nature”; or (iii) Feedback offers limited utility (and potentially hindrance) in the presence of other factors suitable for learning (such as vision, audition, tactile sensation at the stump/arm and feed-forward prediction).

Tracking tasks are relevant to prosthesis control because they provide a systematic, controlled and rapidly executed sensorimotor assay.

More Elaborate Control Finally we consider that tracking tasks can be extended to the assessment of controlling more elaborate signals. Beppu et al. (1984) and Beppu et al. (1987) used a visuomotor task controlled by elbow movements. Amongst other findings they showed that cerebellar disorders increased action initiation latency, impaired velocity control and a higher frequency of corrective moments (Fig. 2.1G).

Recently, Chatterjee et al. (2007) fitted subjects with an electroencephalogram (EEG) brain-computer interface. Mu-rhythms were used to control a virtual cursor, presented visually and via vibrotactile feedback. After training, subjects could control the cursor with either feedback modality (Fig. 2.1H).

In summary, tracking tasks show versatility, flexibility and discriminatory power for (i) understanding a range of sensory disorders; (ii) developing control interfaces relevant to prosthesis design; and (iii) developing feedback interfaces relevant to prosthesis design.

2.2.2.2 Pointing and Reaching Tasks

Response to Perturbations We have previously discussed a study by Körding and Wolpert (2004a), where subjects made online corrections to momentary visual feedback of hand position during a reach (Fig. 2.2A). This approach lends itself readily to static manipulations, such as cue variance and prior cue distributions.

In contrast, Saunders and Knill (2004) present continuous feedback of the fingertip location. This allows for testing of dynamic manipulations, e.g. to decouple the role

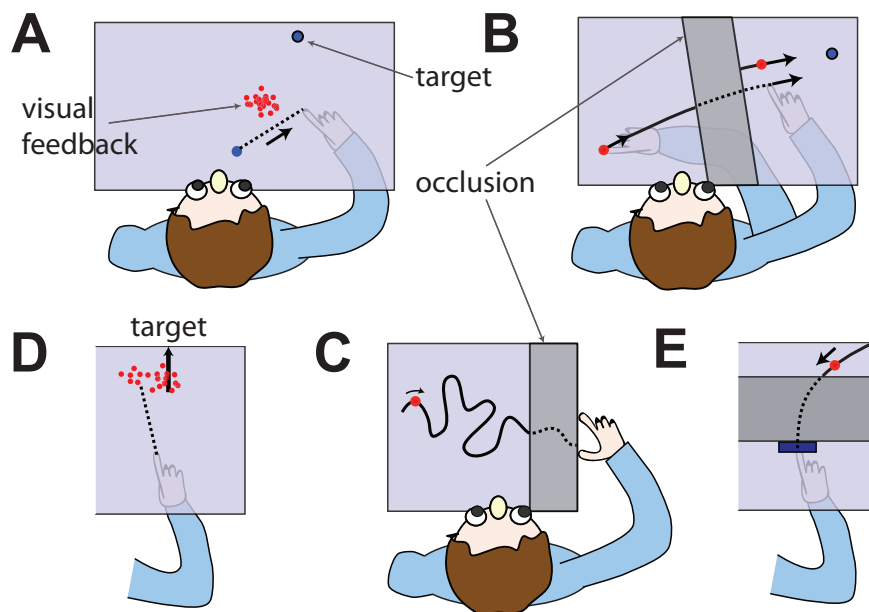


Figure 2.2: **Pointing and Reaching Tasks.** **(A)** Subjects reach for a target with a hand hidden by an opaque mirror. Instantaneous feedback (noisy and perturbed) is given mid-way through movement (Körding and Wolpert, 2004a). **(B)** Feedback is continuous except for an occluded region in which a perturbation may occur (Saunders and Knill, 2004). **(C)** Subjects control a “pea-shooter” to align the average of a distribution to a target (Körding and Wolpert, 2004b). **(D)** Subjects estimate the emergent position of randomly-walking visual feedback that passes behind an occluder (Graf et al., 2005). **(E)** Subjects estimate the final position of a falling ball. On movement initiation the ball is occluded (Faisal and Wolpert, 2009).

of *motion information* and *position information* in reaching. As subjects move past an occluder, fingertip position feedback may be randomly perturbed (Fig. 2.2B). By varying the relative position and/or direction of the perturbation, they discovered that subjects are able to correct their internal model based on both sources of information.

Together, these studies provide evidence that subjects update their decision as information arrives, relying on instantaneous evidence (Körding and Wolpert, 2004a) or motion evidence (Saunders and Knill, 2004). By what mechanisms may this be achieved?

Izawa and Shadmehr (2008) changed the properties of a target stimulus during a trial: its location and/or its uncertainty (blur). They found that the response to the changing stimulus was a *weighted combination* of the old and new stimulus, and the speed of adjustment depended on the relative uncertainties, accurately modelled by a Kalman filter. Hence it appears that continuous confidence estimation and multisensory integration are fundamental features of human sensorimotor function — and not limited to the perceptual examples discussed previously.

The above studies focus on per-trial optimal behaviour. Burge et al. (2008) show that learning and adaptation behaviour over many trials is also in accordance with optimality principles. In three sequential blocks of reaching trials subjects were (i) given correct fingertip feedback; (ii) given feedback displaced by a constant amount in a fixed direction; and (iii) given correct fingertip feedback again. Subjects' *rate of adaptation* to the step between phases (i)→(ii) and (ii)→(iii), was a function of feedback uncertainty, as modelled precisely by an optimal Kalman filter model.

In the above examples, uncertainty can be added to visual stimuli by adjusting the distribution of clouds of dots (Körding and Wolpert, 2004a), through periodic occlusion (Saunders and Knill, 2004), or by adjusting the blurriness or relative contrast of the stimulus (Izawa and Shadmehr, 2008). All of these methods increase the probability of task errors, but do not provide us with insight of the mechanisms by which this probability of error is perceived (and hence used for optimal decision making). To address this, Körding and Wolpert (2004b) provide *skewed* feedback information. In a “pea-shooter” task, subjects received samples from an asymmetrical bimodal distribution centred relative to the direction of their fingertip. They received frequent samples from the distribution, allowing them to adjust their fingertip to ensure that the peas were “on average as close to the target as possible”. It was assumed that subjects were optimising a *loss function* (i.e. minimising some internal measure of task-error). By adjusting the spread and skewness of the distribution it was possible to infer from their decisions the form of the loss function, revealing that small deviations were penalised with squared error but larger deviations were between squared error and absolute error (Fig. 2.2C).

This study is an important step in understanding how people utilise sensory evidence for decision making.

Estimation over Time The tasks of reaching and grasping are fundamental to human behaviour, and lend themselves readily to understanding the mechanisms of sensorimotor control. A particularly interesting problem is in understanding how sensorimotor decision-making evolves over time.

In a novel reaching task, Graf et al. (2005) presented subjects with a stimulus that travels across a screen, changing direction randomly at brief regular intervals (“random walk”). For different levels of directional variability subjects were asked to estimate the location of the stimulus as it emerged from behind an *occluder*. They do this in two ways: (i) they report the most likely location estimate with a fixed marker; and (ii) they report a “capture region” in which they are certain the stimulus lies (Fig. 2.2D). Interestingly, they found that the capture region chosen was a function of the stimulus variability and occluder width. In asking subjects to explicitly report this capture region they make the important observation that subjects must be explicitly aware of stimulus variability. However, they do not provide a model to explain their findings.

In a second experiment, Graf et al. (2005) changed the reliability of the stimulus at random points in the trial. They observed symmetrical capture regions for *low*→*high* and *high*→*low* reliability transitions. This suggests that subjects may be able to accumulate visual evidence over the full range of the trial.

Recently, Faisal and Wolpert (2009) examined the trade-off between allocating time to perception and time to action. Subjects reached with a paddle under a table when anticipating the trajectory of a falling ball (2.2E). However, on movement initiation, the ball was occluded. Hence, subjects were required to allocate time to forming a reliable estimate and time for executing reliable movement. In preliminary experiments it was found that later-onset and larger-distance movements increased movement variability, whilst earlier movements increased sensory variability. In the main experiment each subject timed their decisions in an optimal fashion so as to minimise the overall variability, apparently accommodating knowledge of their own sensorimotor uncertainty.

Multisensory and Sensorimotor Behaviour We have seen that reaching and pointing tasks can inform us about spatio-temporal aspects of perception. I argue that, just as tracking tasks can provide us with a window into sensorimotor behaviour, pointing tasks can provide similar insights specific to the dynamical system of a healthy limb. For example, Bhushan and Shadmehr (1999) examined reaching movements in novel force-fields to understand the role of internal models in arm control.

Sober and Sabes (2005) studied the role of vision and proprioception for reaching behaviour. Subjects placed their right hand on a table under a mirror so that visual feedback could be presented in the location of the hand, and they placed their left hand under the table so that a proprioceptive ‘alignment’ signal could also be utilised. They were asked to reach for visual and/or proprioceptive targets with displaced visual feedback of their fingertip or whole-arm, finding that the modality of the target and the nature of the feedback both affected errors in reach planning.

The above reaching tasks expose the fact that the planning, execution and maintenance of reaching movements relies on diverse and flexible internal mechanisms. In designing an artificial sensorimotor circuit we must consider the nature and availability of multiple sensory signals and the degree to which these signals can be integrated seamlessly and continuously to achieve successful sensorimotor behaviour.

2.2.3 Temporally-Evolving Decisions

2.2.3.1 Continuous Optimal Decisions

We have seen that Bayesian Decision Theory provides a coherent way of describing discrete sensorimotor decisions (Körding and Wolpert, 2006) but in general a continuous trajectory of movement arises in response to a stream of sensory input. This can be modelled with a Kalman filter (Kalman, 1960), a Bayesian estimator for time varying systems (Wolpert, 2007). The Kalman filter is an efficient (minimum mean-square error) algorithm to estimate the state of discretised linear dynamic system.

We assume that, at each time step, the system is linearly derived from the current state and a motor action. Let us assume at time t a stimulus is located at position x_t . In general we describe x_t as the *state* of the system. The Kalman filter addresses the general problem of trying to estimate an *evolving state* given noisy *observations*, comparable to Hidden Markov Model (HMM) inference. The Kalman algorithm provides an estimate, \hat{x}_t , of the true state, x_t , by combining a feedforward prediction with feedback-based evidence, according to the schematic in Fig. 2.3.

The power of the model comes from the choice of a *gain* term, which controls the relative weighting allocated to feedforward and feedback information. In the classic Kalman algorithm (Kalman, 1960) this is modulated so as to achieve an *optimal estimate* of the system state, that is, it minimises the covariance of the error between the current estimate and the true state of the system. This is essentially achieved by using the observation error covariance (i.e. the observation noise) and the feedforward error covariance (i.e. the prediction noise), to appropriately weight each stream. For a mathematical review see Brown and Hwang (1992).

The Kalman filter model provides a mathematically principled continuous extension

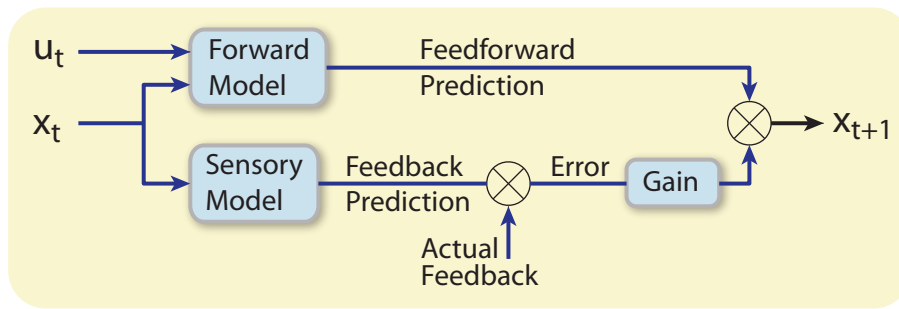


Figure 2.3: Schematic illustration of Kalman Filter estimation (adapted from Wolpert et al. (1995)). To obtain an up-to-date sensory estimate x_{t+1} , feedforward and feedback processes are combined weighted by a *gain* term. The feedforward prediction is based on the current estimate x_t and the current action u_t ; The feedback correction is based on a feedback estimate and the actual feedback observed.

of Bayesian estimation. The key features of this optimal model are the presence of complementary (and appropriately weighted) feedforward and feedback processes, and again the assumption that the statistical properties of the system being estimated are known to the observer. This model has been supported by empirical studies examining estimation of hand position (Wolpert et al., 1995), posture (Kuo, 1995) and head orientation (Merfeld et al., 1999), describing adaptation within trials (Izawa and Shadmehr, 2008) and learning across trials (Burge et al., 2008).

Reaching and pointing tasks provide valuable insights into the underlying mechanisms of continuous estimation in humans. Baddeley et al. (2003) applied random walk perturbations to visual feedback of hand position during a pointing task. It was found that subjects achieved efficient performance by “exponentially weighting recent errors” as a function of the random walk variability. Though the model lacked a proprioceptive component it is apparent that subjects were able to accumulate the statistics of the randomly walking trajectory over time, a key assumption of the Kalman model.

As discussed earlier, Izawa and Shadmehr (2008) changed the properties of a target stimulus during a trial: its location and/or its uncertainty. According to the Kalman model, the rate of reach-adaptation for transitions between each of these conditions depends on the uncertainty of the previous state estimate and the updated state estimate. Indeed, empirical data supported this finding.

Over a longer time scale, Burge et al. (2008) provided evidence for cognitive Kalman processes in adaptation across trials. Firstly, they demonstrated that the rate of adaptation to changing stimuli depends on feedback uncertainty. This is likened to the modulation of the *Kalman gain* to favour the more reliable stream, as discussed above. Secondly, they showed that if measurement uncertainty is greater in one dimension over

another (using anisotropic visual stimuli) the Kalman observer adapts more slowly in the uncertain direction, again confirmed empirically. Thirdly, they had subjects follow random-walking trajectories. When random walk variability was increased, adaptation rate increased, simply because subjects became more certain about the stimulus uncertainty. However, they found that subjects were not Kalman-like in response to random perturbations. They did not adapt optimally to perturbations, attributed to a lower rate of learning environmental statistics than was expected.

The results of [Izawa and Shadmehr \(2008\)](#) and [Burge et al. \(2008\)](#) provide convincing evidence that the key components of Kalman estimation govern perception, adaptation and learning, in particular for the magnitude of adaptation rate under uncertainty and the relative weighting of feedforward and feedback signals. These continuous-time computations must be formed rapidly, and flexibly updated over time as evidence arrives. However, it seems that some aspects of continuous decision-making are not optimal. It is difficult to reconcile the observed discrepancies as the mechanisms underlying statistical estimation are largely unknown ([Burge et al., 2008](#)).

2.2.3.2 Changing one's Mind

When do we decide to make a decision? [Gold and Shadlen \(2007\)](#) review a possible neural mechanism that may underlie decision-making processes. Using sequential estimation based on noisy evidence, they show how evidence in favour of a hypothesis accumulates in the form of a random walk. This model, closely linked to neural firing rate, can explain the onset and timing of discrete decisions. However, in making these decisions, subjects must also make a trade-off between allocating time to perception, and time to action (see [Faisal and Wolpert, 2009](#), discussed previously). Since there is a considerable time delay between sensing the world and initiating motor actions, subjects often make decisions while sensory information is arriving, and it has been shown that certain decisions made under these conditions, in particular *changes of mind*, reflect the properties of this processing pipeline. In a vision-based reaching task [Resulaj et al. \(2009\)](#) are able to predict these discrete events based on the time-delayed accumulation of evidence.

Previously I described a “pea-shooter” task ([Körding and Wolpert, 2004b](#)), in which subjects accumulated information from samples (“peas”) to estimate the mean. Continuous tasks in which evidence accumulates have potential to tell us about how sensory estimates are formed and utilised.

2.2.4 Continuous-Time Decision Mechanisms

Continuous-time tasks may prove valuable in understanding multisensory integration phenomena. Such tasks have the potential to explain the cognitive processes underlying integration over time, but due to the added attentional and motor demands may also prove difficult to interpret.

2.2.4.1 Attention and Cognitive Phenomena

To further understand the cognitive functions discussed thus far one must be aware of conflicting processes which may confound or provide alternative interpretations to empirical observations.

Jack and Thurlow (1973) showed that the ventriloquism effect is only successful in the presence of spatial and temporal constraints. Although the illusion is robust to some degree of spatial misalignment (Kennedy et al., 2009), temporal alignment between sound and lip movement is crucial for the success of the illusion (Jack and Thurlow, 1973). This could be due to the accuracy of visual and auditory temporal judgement, but the reduced accuracy of auditory localisation judgement. In cue integration experiments the effect of discrepancies between sensory modalities may create unwanted attentional modulations that could otherwise explain the effect of sensory uncertainty on decisions (Helbig and Ernst, 2007).

Gepshtein et al. (2005) found that size-estimation uncertainty increased by changing the spatial offset between visual and haptic stimuli. This confirms the importance of visual-haptic congruence for integration. Spence et al. (2004) showed that vibrotactile targets presented to the thumb or the index finger of either hand with visual distractors resulted in slower and less accurate performance during incongruent stimuli. However, when using mirrors to create spatial offset, Helbig and Ernst (2007) showed optimal integration, perhaps indicating that while uncertainty may change with spatial incongruence, the integration mechanism remains robust. However, it should be noted that although mirror-adjusted stimuli were spatially discrepant from their tactile counterparts they arose from the same true source. Therefore it seems that to preserve integration the stimuli should at least be attributed to the same source if not perceived in the same location.

Sensory conflicts provide a useful means to calculate per-modality weighting. Warren et al. (1983) show that moderate degrees of inter-cue discrepancy (between vision and audition for spatial localisation) does *not* modify sensory integration, and it is argued that adaptation to sensory conflict is separate to sensory integration processes (Welch et al., 1979). However, considerable cue conflicts may result in sensory fission (see previously), where one modality is rejected. Also, incongruence of noise in stimuli

can cause a visual “distraction” that indirectly influences performance. This has been shown for vibrotactile perception at the fingertip (Spence et al., 2004), as well as for electrocutaneous stimulation of the earlobes (Tajadura-Jiménez et al., 2009). Reaction times may be improved with congruent stimuli, and perceptual errors reduced. To avoid these confounding possibilities in multisensory integration studies conflicts must be counterbalanced in direction and magnitude as well as go unnoticed by the subject.

2.2.4.2 Maximising Expected Gain

What motivates people to form optimal decisions? Recall again the “pea shooter” experiment (Körding and Wolpert, 2004b) which was used to infer the loss function for combining samples over time. It was shown that samples are fused according to loss function that lies somewhere between square error and absolute error. One could argue that people are acting to maximise some mathematically defined reward.

Indeed, this hypothesis was addressed by Trommershäuser et al. (2003), who asked subjects to point to a target where certain locations near to the target were marked with a numerical penalty. This revealed that subjects are able to choose an average pointing location so as to maximise the expected gain with respect to the variability of their own pointing movements.

Rewards and point-scoring provides a valuable method of encouraging certain behaviour from subjects. By designing a task with a simple reward function subjects may be more likely to behave predictably and consistently. With an accurate model of the reward function, behaviour can be compared to an “ideal” observer, optimised to maximise the specified reward.

2.2.4.3 Acquisition of Sensory Integration

Previously it was described how Helbig and Ernst (2008) examined early- versus late-integration of visual-haptic information, which posed some interesting questions surrounding *learning* of multisensory integration uncertainties.

Gori et al. (2008) showed that optimal multisensory integration only develops in middle childhood. Children less than 8 years of age did not integrate visual and haptic stimuli for judging orientation or size, instead relying on a single modality. For size discrimination, haptic information dominated, whereas for orientation discrimination, vision dominated. However, for children aged between 8 and 10 years the integration was statistically optimal, consistent with Ernst and Banks (2002). Ernst (2008) raise the issue of a correspondence problem between modalities: during early-childhood sensory organs are constantly growing and reorganising. It is also likely that one sense is used to calibrate the other during development, and so multisensory integration must come

later (Gori et al., 2008). These results indicate that there is a trade-off between sensory integration and plasticity.

Is our ability to fuse stimuli learned? Or is our ability to estimate sensory uncertainty learned? This can be tested in a number of ways: (i) by introducing a novel modality (i.e. one in which we the relationship between cues and their objective reliability are unknown); or (ii) examine within-trial behaviour, and examine if subjects can acquire sensory evidence over the time course of a single trial. Sensory evidence could include evidence pertaining to an estimate of the mean of the visual stimuli, or indeed evidence pertaining to an estimate of the uncertainty of visual stimuli.

2.2.4.4 Acquisition of Sensory Uncertainty

Earlier I presented a large number of psychophysical experiments that support the proposition that perception is statistically-optimal. The theory of statistical optimality in the brain relies crucially on the fact that humans must somehow accumulate statistical information from unpredictable stimuli.

Humans are not only able to predict the position of objects moving along random or noisy trajectories, but they are also able to report a level of confidence in this prediction (Graf et al., 2005). This is not a uniquely human capacity: rats are also capable of uncertainty-based decisions (Kepecs et al., 2008), and in monkeys it was shown that the degree of decision-confidence is encoded in parietal cortex neurons (Mulliken et al., 2008). Perhaps, then, sensory uncertainty is naturally encoded by the visual system, perhaps even independently of perceptual awareness.

Jacobs (2002) reviews evidence for two hypotheses relating to how visual cue reliability is formed: (i) the estimated reliability of a cue is related to the ambiguity of the cue, i.e. the Bayesian and Kalman approaches discussed previously; and (ii) cue correlations are used to estimate cue reliabilities, i.e. a cue that is correlated with other cues in the environment is regarded as reliable. Resolution of these hypotheses may be achieved by further understanding the mechanism(s) for estimating cue reliabilities.

Graf et al. (2005) showed that subjects estimate the emergent position of randomly-walking visual feedback that passes behind an occluder. Subjects' report a capture region, which requires them to explicitly acknowledge the uncertainty in the stimuli. As the capture region size is altered in proportion with the random walk variability, subjects are clearly aware of the stimulus uncertainty.

There are a number of possible "reliability signals" that people could use to form such uncertainty estimates in order to make uncertainty-based decisions (Jacobs, 2002). For example, we distinguish *true* uncertainty from *objective* uncertainty and, moreover, from *subjective perception* of this uncertainty. Barthelmé and Mamassian (2009) asked

if people are aware of the uncertainty in their own actions. Subjects were asked: (i) to choose the less uncertain stimulus of two noisy oriented ellipses; then (ii) distinguish the orientation of the chosen stimulus. These two tasks allowed the experimenter to separate perception (subjective uncertainty) from behaviour (objective uncertainty).

Barthelmé and Mamassian (2010) present reservations regarding a Bayesian approach to understand uncertainty estimation, such as the presence of suboptimal underconfidence and overconfidence reported in the literature, and known suboptimal risk-aversion behaviour (versus loss-function optimisation). Nonetheless, their results remain consistent, at least qualitatively, with this approach (Barthelmé and Mamassian, 2009, 2010).

It is possible that unconscious neural mechanisms indirectly account for uncertainty judgements in a wide range of optimal integration studies presented here (Helbig and Ernst, 2007), but this is resolved by asking subjects to *directly* report a capture region (Graf et al., 2005), and explicitly provide a judgement of uncertainty (Barthelmé and Mamassian, 2009). By combining explicit confidence judgement with a cue integration task it may be easier to understand the mechanisms of statistical estimation for optimal decision-making.

2.3 Human Grasping

2.3.1 Introduction

Dexterous manipulation of objects is a skill which takes many years to refine. A typical daily task which healthy individuals take for granted is that of reaching, grasping and lifting an object. Each of these phases requires careful modulation of muscle forces, a difficult task for an open-loop control policy.

The healthy human hand is a closed-loop system, exploiting a vast array of sensory receptors to readily detect an object slipping from our grasp, react to the sudden sensation of heat, and dexterously control our fingers to tie a shoelace. These actions are all impaired in the absence of tactile sensibility. Visual feedback may be too slow and inaccurate for these purposes and would require us to deploy considerable conscious effort to achieve the same level of dexterity. This presumably contributes to the slow, sequential and unnatural hand control observed in amputees fitted with open-loop prostheses.

Aside from the sense of touch, another important sensory signal arises from muscles and joints. This proprioceptive feedback gives us knowledge of the position of our body in space. How does the nervous system integrate these percepts to provide dexterous, adaptive and dynamic interactions with the world?

This section reviews the sensory, motor and cognitive aspects of healthy human grasping that defines the gold standard for prosthesis design.

2.3.2 Motor Control and Somatosensation

2.3.2.1 Physiology

The Sense of Touch The tactile sense is capable of discriminating grip force (Johansson and Westling, 1984a), object roughness (Johansson and Westling, 1984a), surface patterns (Chapman et al., 2002), curvature and force direction (Johansson, 2002), object taper (Jenmalm et al., 2000), torque loads and mass distributions (Johansson, 2002), softness (Srinivasan and LaMotte, 1995), shape (Wheat and Goodwin, 2001) and orientation (Hsiao et al., 2002). While it is known that we *can* interpret these properties, it is not known which items of information *are* exploited by the nervous system to aid manipulating objects. This is made even more challenging due to the predominantly unconscious processing of the tactile modality. Understanding the role and function of different feedback sources is thus still an open question.

Each fingertip contains around 2000 tactile sensors, with different temporal and spatial characteristics. At the skin surface, rapidly-adapting RA-I (Merkel) neurons are suspected to inform the brain of ‘goal completion’, spiking on object contact, lift-off and slip (Johansson, 2002), with large receptive fields, while slowly-adapting SA-I

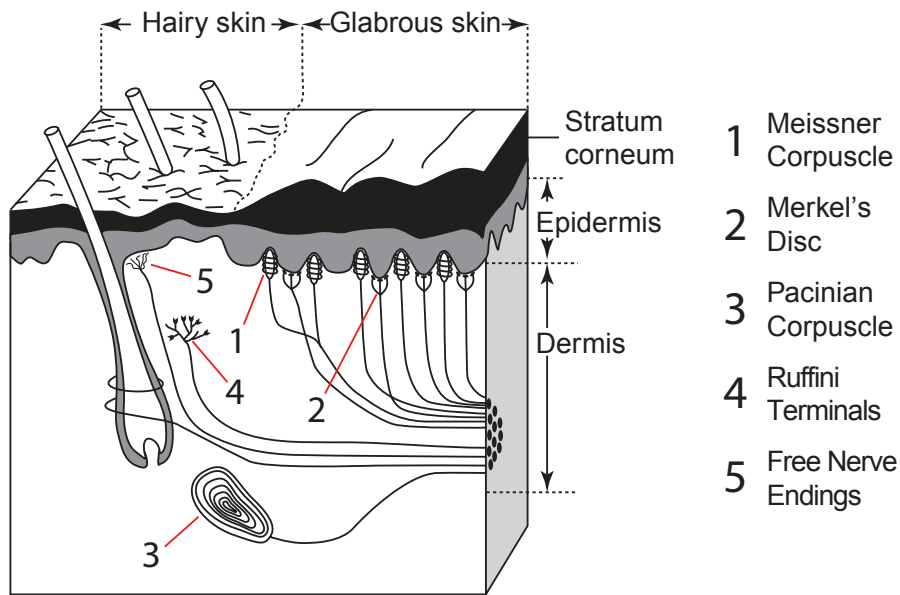


Figure 2.4: **Skin.** Schematic cross-section of human skin, illustrating the structure and location of numerous sensory receptors (adapted from [Witney et al., 2004](#)).

(Meissner) neurons are more responsive to perception of shape and edges ([Wheat and Goodwin, 2001](#)), and responsible for detection of the magnitude of forces at high spatial resolution. Deeper into the skin, rapidly-adapting RA-II (Pacinian) receptors have low spatial resolution but are sensitive to transient (high frequency) or vibratory stimuli, immune to low frequency activity due to their lamellar structure. Slowly-adapting SA-II (Ruffini) receptors detect skin stretch and deformations. Fig. 2.4 illustrates these key sensory receptors in human skin, which are summarised in [Johnson \(2001\)](#).

Muscles Muscle control related to grasping is complex, involving temporal parsimony and co-contractile synergy between different muscles in complementary roles as motors, moderators, restrainers, and antagonists (reviewed in [Flatt \(2000\)](#)). For the purposes of this thesis I take the simplified view that muscles are elastic, and induce torques around joints. Joints are equipped with antagonistic muscle pairs, and it is the combined contribution of these muscles that determines the final joint torque generated. Under no external load there is an approximate one-to-one mapping between a muscle activity and finger position.

[Long \(1968\)](#) used electromyographic recordings of hand and forearm muscles to classify finger control. Three major muscles were identified as critical for basic movements, namely the flexor digitorum profundus (FDP), extensor digitorum (ED) and the lumbricalis (LB). FDP and ED are located in the forearm, and LB in the palm. The fingers are at rest in a slightly curled posture under the elastic influence of FDP. When

ED is contracted alone the fingers ‘claw’, bending at only the distal joints. Simultaneous contraction of FDP with ED is sufficient to fully flex (close) the finger joints. LB extends the knuckle joint and simultaneously relaxes the elastic effect of FDP. In this configuration the ED serves to extend the fingers.

Proprioception Another important aspect of the somatosensory system is proprioception. Without vision monkeys can accurately point to targets, but proprioceptive deafferentation impairs this capacity (Taub et al., 1975).

There are two primary sensors which accomplish this proprioception: muscle spindles and Golgi tendon organs. The muscle spindle is composed of fibres within skeletal muscle which contract in parallel to the muscle. These sensors enable the detection of muscle length to establish the position of our limbs. Golgi tendon organs are located in the tendons of skeletal muscles. These sensors are activated in series to the muscle, indicating the force or strain exerted by the muscle.

Proprioception is a readily adapting sense (relying on visual feedback to maintain its calibration). In modulating grip aperture, for example, one can use a virtual reality set up to shift proprioceptive feedback. It is found that while we adapt readily to changes in offsets in aperture size we are less adaptive to changes in the slope Säfström and Edin (2005). In equipping amputees with prostheses we must be aware of the limitations of proprioceptive adaptation.

2.3.2.2 Sensory Perception

In a landmark result, Rock and Victor (1964) demonstrated the dominance of vision over tactile information for perception of shape. As we have previously seen, however, the visual capture hypothesis has been since replaced by more elaborate models of multisensory integration.

How does perception arise from sensory signals? Goodwin and Wheat (2004) review models of neural populations for tactile encoding. They conclude that interpreting neural responses to explain perception is inherently difficult owing to: (i) the fact that the whole finger deforms when contacting a simple object; (ii) the role of receptors with different spatial and temporal characteristics; (iii) the presence of high levels of noise. However, Dostmohamed and Hayward (2005) showed how the perception of smooth and continuous shape can be convincingly simulated simply using a flat surface that changes orientation to supply the appropriate tangential force. Using a similar setup, Robles-De-La-Torre and Hayward (2001) showed that, regardless of the geometry of the surface (i.e. the position of the finger), force cues were sufficient for subjects to locate shape features.

These studies reveal a remarkable redundancy within tactile and proprioceptive sensation. The nature of the feedback required to elicit convincing sensations indicates that shape and curvature perception may be mediated by higher-level processes, centrally rather than peripherally. The redundancy and multidimensional complexity of neural information may serve simply to allow a reduction to much simpler internal representations to provide us with robust tactile perception. Srinivasan and LaMotte (1995) compared the differential role of tactile and proprioceptive information for discriminating the softness (compliance) of objects. Tactile, but not proprioceptive information was sufficient for softness discrimination of objects with a compliant surface (where finger deformations would provide softness cues), but both tactile and proprioceptive feedback were needed for discriminating rigid-surfaced objects. This again reveals the level of redundancy between sensory systems.

Sensory perception is hugely complex and the role of different sensory signals in creating this perception is largely unknown, making the design of an artificial sensorimotor system especially challenging. Fortunately, however, perception is inherently plastic. For example, In the size-weight illusion, a subject comparing two objects of equal weight but different size typically perceive the smaller object as heavier. Flanagan et al. (2008) showed that this relationship can be reversed with practice. Later I will discuss further examples of perceptual plasticity that may provide some hope for prosthesis wearers.

2.3.2.3 Ownership of the Hand

In this thesis I focus on the functional benefits of feedback for prosthesis control. However, as well as being of functional importance, proprioceptive and tactile feedback are linked to the feeling of body *ownership* and therefore prosthesis acceptance. Marasco et al. (2011) indicate that tactile sensation may help amputees regain an “intact self-image”, accepting the prosthesis as part of their own body.

Botvinick and Cohen (1998) discovered the “rubber hand illusion”, in which subject’s hands were hidden but then stroked synchronously with a fake (rubber) hand. This created the bizarre illusion that the rubber hand belonged to the subject. A sense of ownership arose due to the correlation between visual and tactile stimulation, and consequently the proprioceptively perceived location of the subjects hand adapted (Costantini and Haggard, 2007). The illusion requires the stimulation to be consistent in hand coordinates (stimulation location), but not body coordinates (arm posture), owing perhaps to the strength of tactile priors over proprioceptive priors (Costantini and Haggard, 2007). The neural mechanisms underlying the rubber hand illusion depend on three brain areas: multisensory integration in the cerebellum, proprioceptive recalibration in motor cortex, and “self-attribution” in premotor cortex (Ehrsson et al.,

2008).

This fascinating illusion exploits the latent plasticity in the nervous system. Remarkably, Ehrsson et al. (2004) showed that the illusion can also be used to induce the perception of a rubber hand in amputees. They provide a simple method to transfer tactile perception from the stump to a prosthesis. Further, Rosén et al. (2009) demonstrated that sensation transfer is not limited to a rubber hand but also a robotic prosthesis. For practical reasons Mulvey et al. (2009) showed that this illusion can be achieved using electrical nerve stimulation to the stump as a surrogate for true tactile sensations. The illusion requires good temporal asynchrony between visually and haptically evoked sensations (Shimada et al., 2009), but spatial asynchrony may be tolerable to some degree (White et al., 2010). It seems that the nervous system may be sufficiently plastic to defer taction to alternative body regions.

2.3.3 Experimental Perspectives

2.3.3.1 Healthy Human Grasping

A large body of evidence has been accumulated over the past two decades pertaining to the *precision grip*. Healthy individuals adjust grip force to an amount just greater than is sufficient to avoid object slip, setting a “safety margin” that is a function of friction at the skin-object interface and object weight (Westling and Johansson, 1984). Fig. 2.5 illustrates these observations. Rarely do healthy subjects over-grip objects, a mechanism which serves to avoid muscle fatigue and object breakage. This is impaired by digital anaesthesia (reviewed in Johansson, 2002) and also observed in amputees.

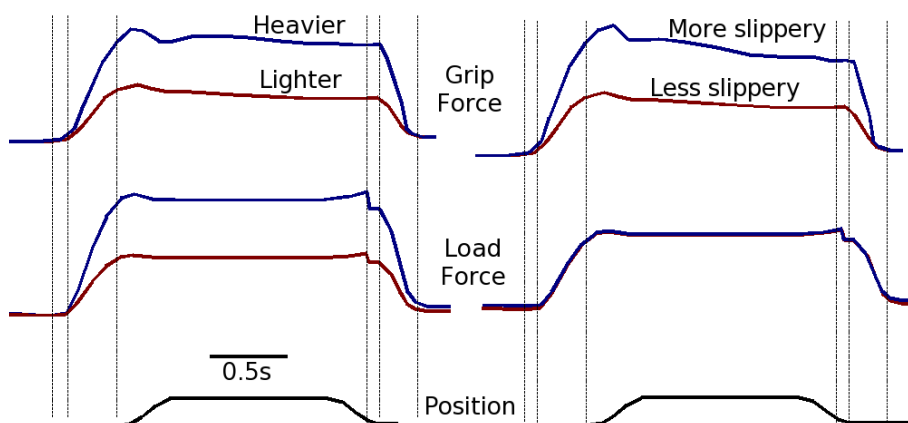


Figure 2.5: **Grip force control.** Anticipatory scaling of grip force in parallel with load force for objects of different surface properties (from Johansson and Westling, 1984a)

When lifting an object healthy people predictively increase the grip force in parallel with the lifting (or load) force (Fig. 2.5). The slope of the increase depends on the

frictional properties of the surface; a higher “grip-to-load-ratio” (Johansson and Westling, 1984). By ramping the grip in parallel with the load one needs only to accurately predict the grip-to-load ratio in order to lift the object, not the final mass. Amputees do not appear to gauge these forces, and tend to over-grip (e.g. Weeks et al., 2000).

Not only do predictably economical grip forces accommodate loads of varying weight and friction, load changes during acceleration of objects are also anticipated (Hermsdörfer et al., 2004). For example, for cyclic movements grip forces are continuously increased and decreased with the upward and downward deceleration components of the motion respectively, even though it is simpler to maintain our grip force at the maximum expected. Interestingly, while digital anaesthesia impairs modulation of grip force magnitude, it does not impair the timing of these anticipatory grip force increases and decreases. The peak of grip force aligns temporally with the peak of load force in both healthy and anaesthetised subjects (Augurelle et al., 2003). In a study of stroke patients with severe sensory (but not motor) loss it was noted again that anticipation of grip increases was present, even in a patient with 23 years of peripheral sensory neuropathy (Hermsdörfer et al., 2004). Grip force magnitude scaling, on the other hand, is not preserved under anaesthesia. Under anaesthesia people tend to over-grip objects, presumably as a strategy to avoid slip under the added uncertainty. It is also difficult to maintain grip forces at a steady value (Augurelle et al., 2003). This suggests that cutaneous cues are required to allow people to maintain a forward model of grip force. In a study comparing the ability of patients with ALS versus stroke patients (corresponding to motor versus sensory deficits respectively), it was suggested that neither the sensory nor the motor component could be held solely responsible for these observed impairments (Hermsdörfer et al., 2004).

Visual feedback contributes to the perception of object properties and therefore modulates grasping behaviour. Jenmalm et al. (2000) examined subjects ability to maintain the position of a torsional load and their ability to twist the load. The grip surface was a curved sphere. Under anaesthesia, blindfolding and both, it was found that prior visual feedback of the sphere was sufficient to allow the scaling of grip force, and visual feedback of the object during motion was sufficient to allow scaling of force for the twist. It was also found that tactile feedback was alone sufficient for both aspects, but in the absence of both vision and tactile feedback, performance was severely impaired. It appears that feedback allows for the parametrisation of grasping behaviour, but this relies heavily on memory for objects. Flanagan et al. (2001) showed that subjects retained memory of the size-weight relationship of novel objects, accurately recalling the appropriate fingertip forces even 24 hours after training.

However, these observations may have been biased by the absence of vision. Buck-

ingham et al. (2011) showed that anaesthetised individuals are unable to skilfully scale their grip and load force rates over repeated lifts without vision, but remarkably, even if the visual information provided is task-irrelevant (by occluding the object) successful grip scaling is still achieved. It appears that the availability of vision “triggers a shift into a more skilful, feedback-based mode of control”.

2.3.3.2 Sensory Deprivation

The role of sensory information for healthy grasping is clearly demonstrated in studies involving sensory loss.

Anaesthesia Anaesthesia impairs adaptation to different frictional conditions (Johansson and Westling, 1984), and impairs the scaling of the magnitude of grip forces, applying an excessive safety margin in the absence of tactile sensibility (Westling and Johansson, 1984). Monzée et al. (2003) showed that subjects significantly increased grip force after digital anaesthesia and found that tactile feedback was necessary to precisely align the finger and thumb, even with vision available. The increased torque due to misalignment could, in part, explain the increased forces observed for anaesthetised subjects.

However, some aspects of grip force control are not impaired. Nowak et al. (2001) examined the task of lifting an object up and down repeatedly. In anticipation of acceleration and deceleration when changing the movement direction a healthy subject anticipated the change with an appropriately scaled and timed grip force increase. An anaesthetised patient over-gripped at a level higher than the overall minimum necessary, but still maintained the precise timing of anticipatory grip changes. This provides evidence for separate feed-forward and feedback driven mechanisms.

Similarly, Augurelle et al. (2003) asked subjects to grasp, lift, hold and oscillate objects, testing multiple aspects of prediction, reaction and maintenance of forces. They found that, under anaesthesia, loss of cutaneous sensation produced a significant increase in force, but this declined over the hold period, and again over the oscillation period, resulting in drops. They argue that tactile feedback is required to maintain the *internal model* of grip force.

Disorders Sensory disorders can give us some insight into the role of sensory and motor processes. Iyengar et al. (2009) found that both anticipatory temporal-judgement and force magnitude scaling were impaired in multiple sclerosis (MS) patients. In a load-oscillation task, Hermsdörfer et al. (2004) observed increased grip forces and selective impairments to feedforward control task for different degrees of sensorimotor

impairment. All patients had intact cerebellar function, purported to subserve internal model formation. Nevertheless, feedforward control was severely disrupted in a deafferented patient, moderately impaired in amyotrophic lateral sclerosis (ALS) patients, and preserved in stroke patients. From these results it seems that sensory feedback has a crucial role in modulating and maintaining various key aspects of motor control.

Nowak and Hermsdörfer (2003) examined grip force control for patients with demyelinating polyneuropathy, sensory axonal polyneuropathy and chronic median nerve compression. These impairments resulted in preserved anticipatory temporal coupling but impaired grip scaling during oscillatory movements, consistent with the effects of anaesthesia (Nowak et al., 2001). However, for two patients with complete chronic deafferentation of the trunk and limbs (Hermsdörfer et al., 2008), despite overall grip force increases, it was found that the grip force level was adjusted to accommodate the load magnitude. It was hypothesised that patients utilised “visual and vestibular cues and/or an efferent copy” of the motor command to achieve economical grip force scaling. Though tactile sensory information appear important for precise internal model maintenance, compensatory mechanisms may also exist.

Cole and Sedgwick (1992) discussed a patient lacking tactile and proprioceptive feedback below the neck. Remarkably, he was able to maintain a posture and repeat rhythmic motion in the absence of vision. Furthermore, the subject could use visual feedback to judge object weight (by observing the passive displacement of his own arm). Evidently, at the expense of additional effort, tactile and proprioceptive feedback can be compensated for. In another study it was found that observers could discriminate object weight simply by *observing* a similar patient (Fleury et al., 1995).

There is considerable evidence to suggest that feedback is essential for the acquisition of internal models and might also be necessary for its maintenance, but can not be fully understood in the absence of other sensory signals and feedforward contributions. To further understand grip force control, Witney et al. (2004) raise the question of how contributions from proprioception and vision are integrated with cutaneous feedback during object manipulation, and how feedback is integrated with prior predictions in grip force control. Multisensory cue integration studies and the probabilistic framework discussed previously (Ernst and Banks, 2002, Körding and Wolpert, 2004a) could help explain these aspects of grip force control.

2.3.3.3 Robotic Manipulandum

Healthy Control Restoration A primary aim of this thesis is to explore a robotic alternative to healthy human hand function. Thus far I have discussed healthy hand physiology and behavioural observations deriving from anaesthesia and disorders. Rep-

licating healthy human capabilities must accommodate these findings.

I previously discussed the role of antagonistic muscle pairs to achieve proportional position and force control. This could be replicated in a servo motor with a *position-control* policy. When the hand is in contact with a rigid load such as an object being grasped, there is an approximate one-to-one mapping between muscle activity and the force applied. This could be termed a *force-control* policy. These are both *absolute* control policies. Contrastingly, the iLIMB, a state-of-the-art robotic prosthetic hand, adopts a *relative* control policy, meaning that muscle activity sets the movement speed of the fingers (control signals determine the torque on per-digit worm gear motors, which is equivalent to a *speed-control* policy under no external load, or a *yank-control* policy for a rigid load). To set fingers to a desired position or force in a relative control policy one would need to integrate the control signal over time (a potentially challenging task), which may explain the demand for visual attention for users of similar state-of-the-art prostheses.

Doubler and Childress (1984) revealed the importance of proprioception and its role in control in 1-D and 2-D pursuit tracking tasks — analogous to limb control. It is evident that direct proprioceptive feedback of limb state results in superior control ability. One may therefore hypothesise that a position-controlled prosthesis controller would provide superior control to a speed-controlled prosthesis controller.

To replicate healthy control we must consider the importance of rehabilitating proprioceptive and feed-forward aspects of healthy human physiology.

Healthy Feedback Restoration Jiang et al. (2009) found that grip force control deficits in multiple sclerosis patients (e.g. Iyengar et al., 2009) can be partially resolved with artificial force feedback. Error-corrective and force magnitude feedback had selective benefits for different degrees of sensory loss. Likewise, Riso et al. (1991) found that a quadriplegic patient benefited from tactile feedback. Consistency of grasps, and grasp economy were both improved in the presence of each of the two tactile feedback methods.

Weeks et al. (2000) measured grip force adjustments during predictable and unpredictable load changes. Subjects held an object aloft with one hand, and then: (i) added the weight with their other hand; or (ii) an experimenter added the weight. Healthy subjects showed anticipatory increases in both conditions, while a subject with a prosthesis anticipated the load only in condition (i). Thus, it was concluded that the absence of tactile feedback in the prosthesis wearer impaired reaction to, but not anticipation of load changes, a similar conclusion to the effects of digital anaesthesia of healthy grasping.

In this thesis I experiment with an artificial tactile channel with an aim to restore

healthy grasping (functional) capabilities. Stepp and Matsuoka (2010) showed that vibrotactile feedback could improve performance in a virtual reality object dragging task. Indeed, subjects found the task much easier in the presence of feedback. However, the task duration was massively increased, owing to subjects taking a long time to interpret the feedback. In untrained patients tactile feedback may actually hinder control (Chatterjee et al., 2007) and vibrotactile proprioceptive feedback systems might not be exploited in the presence of vision (Cipriani et al., 2008). The benefits and limitations of tactile feedback for upper limb prosthetics is discussed later.

Summary As we have seen, the healthy human hand is remarkably dexterous, seemingly effortless to control and equipped with a vast sensory system. Replicating these features in a prosthetic hand is a central goal for rehabilitation research, yet the state of the art falls far from this target. In this thesis I describe the development of a modular prosthesis which serves as a manipulandum with which to address the limiting factors of present technology.

2.3.4 The Role of Internal Models

Internal Models Prediction turns motor commands into expected sensory consequences, while control turns desired consequences into motor commands (Flanagan et al., 2003). The neural processes underlying prediction and control are termed ‘forward’ and ‘inverse’ models respectively. The presence of these models allows us to both predict and act, refining our predictions and mapping them to refined actions. We are able to gather information and act simultaneously (avoiding delayed action). In order to understand human motor control, computational architectures that combine both forward and inverse models have been developed (Wolpert and Kawato, 1998, Bhushan and Shadmehr, 1999).

Sensorimotor processes can be broadly described as feedback loops for separate modules of prediction, observation and correction. With the aim of selecting the best action at a particular juncture to achieve higher goals one requires feedforward (predictive) and feedback (corrective) actions. Fig. 2.6 summarises this framework for the present application, showing both the high-level optimal controller and the low-level sensory and motor components.

The ‘optimality’ of motor control is defined with respect to a *cost function*, assigning a measure of value or reward to different actions. In the presence of delayed feedback from the world, motor output is optimised (i.e. the cost of action is minimised) based on an *estimate* of the current system state and the *predicted* sensory consequences of actions. This *internal model* is corrected when feedback eventually arrives from

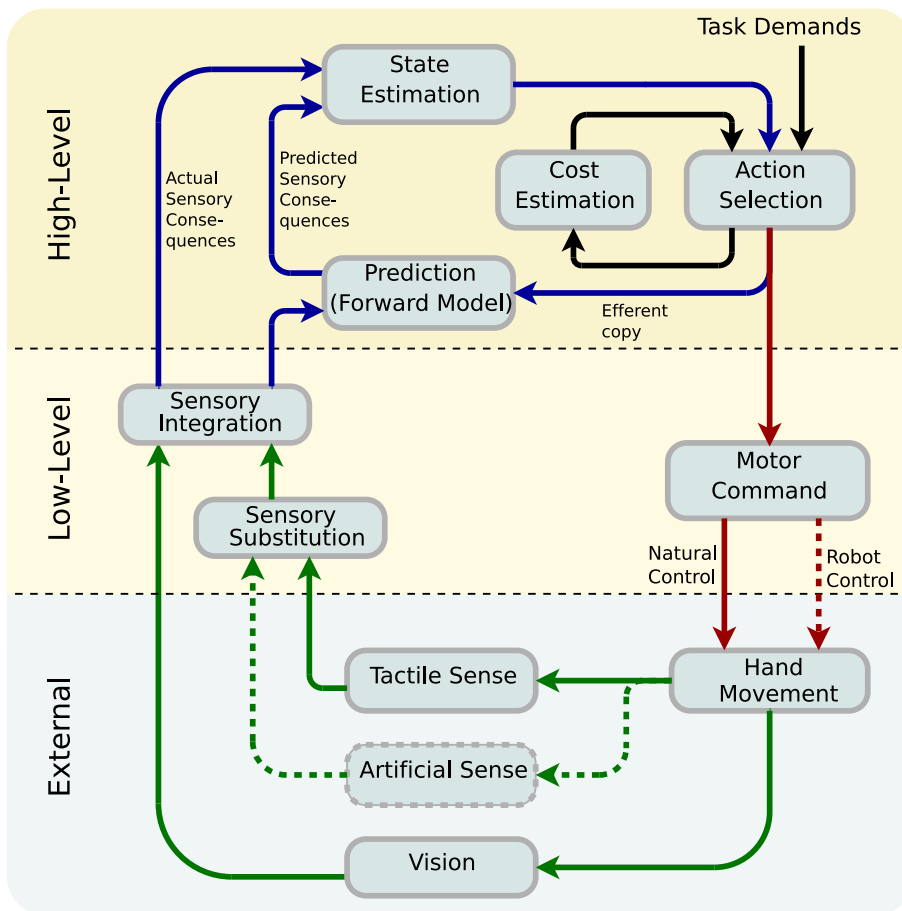


Figure 2.6: **Closed-Loop Control Schematic.** A schematic model for generating goal directed movements in a task involving visual and tactile processing. Unavoidable delays in feedback (indicated by the large sensory feedback loops) highlights the importance of an internal forward model, while feedback is necessary for correcting unavoidable errors in the forward model for state estimation and prediction (adapted from Fig. 2.3 and Shadmehr and Krakauer, 2008).

the world. This is a more elaborate formulation of the Kalman framework previously discussed (Fig. 2.3).

Take the example of picking up a cup. The cost function might be to minimise energy expended. Primarily one would wish to avoid dropping the cup, as this would cost the most effort. Secondly one might avoid over-grip as this wastes muscle energy. An emergent consequence of minimising a global cost function is the behaviour observed in healthy individuals, predictively applying a minimal necessary force with sufficient margin for error.

Evidence for Internal Models Flanagan et al. (2003) attached subjects to a manipulandum with novel dynamics and asked them to move the hand along a straight line

trajectory. In learning to control elbow position and grip force, subjects showed rapid learning of grip force (in around ten trials) but slower learning of arm control (around 70 trials), suggesting that there are separate internal models for grip force and arm position and a transfer from reactive (feedback) to predictive (feedforward) control. Flanagan et al. (2003) argue that this is evidence for separate complimentary forward and inverse processes, with prediction (grip) aiding the learning of control (arm movement).

Bhushan and Shadmehr (1999) examined reaching movements in novel force-fields: (i) a null field, i.e. with no force acting on the hand; and (ii) a viscous curl force field, i.e. proportional in strength to the instantaneous hand velocity and directed orthogonal to the instantaneous hand velocity. The resultant trajectory adaptation to a sudden change in the direction of the curl force field could only be explained by a model with both forward and inverse components. It is argued that both components are needed for successful control.

Flanagan and Wing (1997) argue that the nervous system is able to maintain various dynamic and kinematic models of objects being manipulated. Using a grasp manipulandum simulating a variety of dynamic load conditions (inertial, viscous, elastic and composite loads) it was shown that changes in the load due to arm movements were anticipated by the subject, who scaled their grip force by the appropriate magnitude. The presence of multiple complementary forward and inverse models for dexterous control is obviously computationally advantageous (Jordan and Wolpert, 1999) but makes distinguishing their contributions rather complex.

The above behavioural results are supported by brain lesion studies which suggest that state estimation, prediction, cost-estimation and action selection occur in parietal cortex, cerebellum, basal ganglia and motor cortex respectively (Shadmehr and Krakauer, 2008).

2.4 Prosthetic Systems

2.4.1 Introduction

We have seen above that healthy human control requires simultaneous feedforward and feedback processes. People act in a feed-forward manner when anticipating appropriate grip forces for object lifting or object movement. These forward mechanisms enable precise timing of control signals, even in the absence of feedback. However, feedback is needed for maintenance of forces (Augurelle et al., 2003), and possibly also for maintenance of forward models (see Hermsdörfer et al., 2008). Visual, tactile and proprioceptive feedback can each be utilised for determining object size, weight and shape, allowing selection of appropriate anticipatory grip forces. Tactile feedback is necessary for detecting object properties such as roughness, softness and curvature, as well for detecting unusual object dynamics. Feedback also allows people to refine their control policy when they receive evidence contrary to expectation. Evidently, in healthy individuals these processes are tightly coupled, supporting each other to enable successful control. How does this compare to an artificially-restored system, in which control is the responsibility of a robotic device, where feedback arises through artificial sensors and is fed back via novel sensory channels?

In this thesis we introduce an elementary closed-loop prosthetic hand, illustrated in Fig. 2.7. The key components of this system are control, actuation, sensation and feedback.

2.4.2 Feedback

2.4.2.1 Sensory Augmentation

Tactile Vision Substitution (TVS) y Rita et al. (1969) made an astonishing finding regarding the latent plasticity of the adult brain. Pioneering the first tactile vision substitution (TVS) system, he described a replacement for the visual system which provided video camera images to patient's lower back (Fig. 2.8A). Sighted and blind participants were presented with processed video information via a grid of 400 vibrating solenoid simulators. They reported near-immediate acquisition of basic skills such as orientation to light sources, tracking target objects and discriminating orientations. After this extensive training with with dots and oriented lines, subjects began learning to discriminate shapes, objects, multiple objects and even faces (Fig. 2.8B). Remarkably, after considerable training blind subjects could perform complex scene classifications (y Rita et al., 1969, y Rita and Kercel, 2003, y Rita, 2004).

Since this landmark work, portable systems have been developed using electrotactile tongue electrodes. Vision has been restored to the blind (Sampaio et al., 2001) and

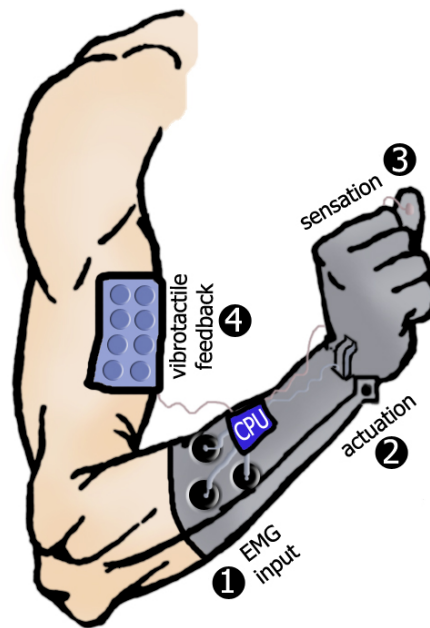


Figure 2.7: **Closed-Loop Prosthesis.** A closed-loop prosthetic hand for amputees, replacing four basic functions of the healthy human **(1) Control**. In healthy humans control signals arise from muscular activity. In amputees these can be recorded from residual muscles to provide a simplified control interface **(2) Actuation**. muscle activity drives tendons around joints, resulting in skeletal reconfiguration. This can be achieved with mechanical actuators based on the control signal. **(3) Sensation**. Healthy human somatosensation features vast and redundant arrays of sensory receptors. Lower-dimensional sensory information can be recorded with artificial sensors for forces and torques **(4) Feedback**. Post-amputation, many sensory nerves are no longer intact. Low-dimensional sensory information can be fed back to residual nerves, requiring sensory substitution to regain adequate sensibility.

balance to the vestibularly impaired (Tyler et al., 2003).

Limitations of Sensory Plasticity The amazing capacity of the nervous system to learn to control novel dynamical systems (see previously, e.g. Davidson et al., 2002) and make sense of artificial sensory data (e.g. y Rita et al., 1969) seems very promising from the perspective of restoring control to amputees. However, as we shall soon see, exploiting the *sensory substitution* phenomenon for practical use with prostheses has proven difficult, despite many attempts over the decades.

In the early days, sensory substitution systems may have been considered uncomfortable, or the devices impractical (Kaczmarek et al., 1991). However, despite improvements in these areas it is still not known how to most efficiently transfer useful information to the tactile sense. Some very basic questions are still to be answered.

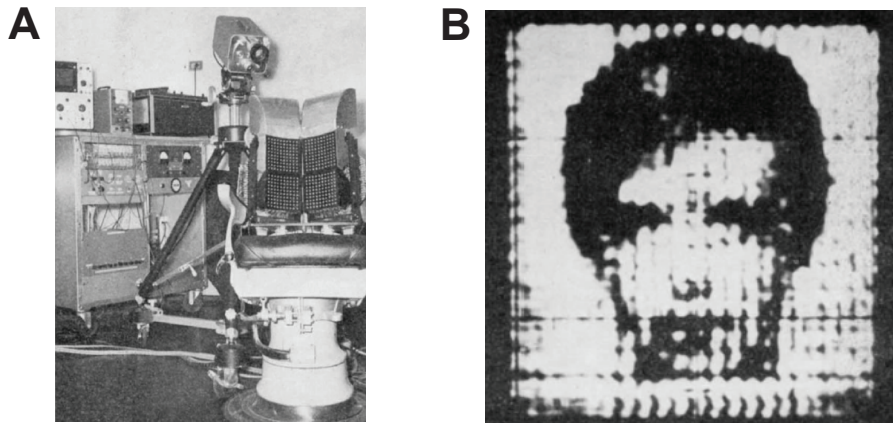


Figure 2.8: **Tactile Vision Substitution (TVS)**. The original TVS system (y Rita et al., 1969). **(A)** A digital video camera connected to 20x20 matrix of simulators mounted into a chair. **(B)** A typical stimulus which trained subjects are able to identify.

- (i) For restoration of hand sensibility we need to know *what* items of information are required as well as *how* to best communicate them to the subject.
- (ii) The potential bandwidth of the tactile channel is phenomenal (Kaczmarek et al., 1991), but to harness its full potential we must first understand how humans *acquire* and *integrate* sensory information to form robust perception of the world.
- (iii) To rehabilitate a complete sensorimotor system we must understand the complementary role of both sensory and motor components. It is interesting to note that in the TVS systems discussed above, learning is poor unless the subject is allowed to manipulate the camera themselves. This highlights the importance of a closed-loop for learning.

There may be fundamental limits on tactile plasticity. Säfström and Edin (2005) asked subjects to grasp objects where a fixed discrepancy was imposed between the observed and actual size of the object. Grip apertures adapted to these stimuli, and in addition generalised to new stimuli, demonstrating short-term plasticity of the sensorimotor system, but when the discrepancy was not flat but sloped, subjects were not able to generalise correctly.

Patterson and Katz (1992) argue that the nature of the feedback is important demonstrating the superiority of a pressure feedback signal to a substitution interface for reproducing pressure signals (Patterson and Katz, 1992). Likewise, force transducers can communicate force feedback (Meek et al., 1989). These interfaces exploit Extended Physiological Taction (EPT), the use of feedback stimuli which directly relate to the form of the actual stimuli. Natural and intuitive EPT schemes are potentially more

patient-friendly, but it is technologically more challenging to provide realistic feedback transduction, and arguably unnecessary on account of the brain's inherent plasticity as shown for TVS systems. Nevertheless, the limits of tactile plasticity may impose a fundamental constraint on success with sensory substitution interfaces.

Neural Plasticity Amputees often describe the sensation of having a *phantom limb*, the perception of a missing limb being still part of the body. Post-amputation the brain areas dedicated to limb control and sensation are still intact, resulting in this peculiar phenomenon and often painful sensations. Ramachandran et al. (1992) stimulated the stump of amputees in regions external to amputation and found that some stimuli were perceived as arising on the phantom limb. This is attributed to cortical reorganisation in the absence of sensory input from the amputated limb (Flor et al., 1995), indicative of the flexibility and plasticity of the nervous system. However, it is important to note that there are limits to cortical reorganisation. As well as being a slow process, some cortical areas adapt more readily than others (Jain et al., 2008), and it is not known why this is the case. This may be problematic for designing effective sensory substitution systems.

Poirier et al. (2007) review the neural processes during training to use a TVS system. One might expect (from the term *sensory substitution*) a successful TVS system for the blind would replace the dormant visual system in the brain, but instead artificial stimuli are associated with existing healthy senses as a form of “mental imagery” — which is in the auditory and haptic modalities for blind patients. This may seem worrying since we are aiming to achieve sensory restoration. However, though it is particularly difficult to elicit the perceptual nature of artificial visual perception in blind patients it should be noted that the nature of substitution perception may be entirely independent of the location in which it is processed. Therefore, one might instead aim to measure the degree of *sensory integration* as a more robust indicator of successful sensory rehabilitation. To date there are no examples of multisensory cue integration studies involving an artificial tactile channel.

2.4.2.2 Sensors

Feedback systems can encode any variety of sensory information. Rossi (1991) discuss the possibility of artificial haptic systems capable of surface texture discrimination, stable object grasping, fine-form detection, hardness evaluation and thermal sensing. Howe and Cutkosky (1993) present an electronic tactile sensor for high frequency tactile sensing for slip and texture detection. Recently, Edin et al. (2006) introduced a three-axis force sensor, capable of providing feedback of forces, force directions and sudden

force changes in the range of biological systems. The system can detect force fluctuations and reliably react to slips within 10ms (Edin et al., 2008). A low-cost alternative is to use computer optical mouse sensors to detect object slip (Romano et al., 2009).

In this thesis we focus mainly on position and force feedback, but clearly more elaborate signals and hardware exist.

2.4.2.3 Vibrotactile Feedback

Introduction Vibrotactile interfaces can be embedded into shoulder pads (Toney et al., 2003), or even applied to the toes (Panarese et al., 2009), making them discreet, non-invasive and appealing for feedback provision.

In this section we will discuss sensory-substitution based feedback systems. Firstly, note that Patterson and Katz (1992) provide an concise historical introduction to the key concepts for developing sensory feedback systems, including: signal bandwidth; logistics of integration; physiological-compatibility; stimulus generation; feedback modality; signal hardware and encoding; interference and cross-talk; extended physiology; adaptation; and learning rate.

Low-level feedback parameters To design an efficient vibrotactile display device there are a wide range of parameters to consider, ranging from amplitude, frequency, quantity and spacing of tactors (Yoon and Yu, 2008); the effects of place, space and age (Cholewiak and Collins, 2003); the effects of body site, space and time (Cholewiak, 1999); spatial patterns (Yoon and Yu, 2006); and pulse burst stimulus parameters (Perez et al., 2000) .

Approximately 5 distinguishable levels can be achieved for a single vibrotactile channel (Pongrac, 2006) and multiple channels should be spaced by at least 2 to 3 cm (van Erp, 2005). These parameters depend on location and body site (Cholewiak et al., 2004).

Feedback Encoding Using 48 vibrating motors in a 2-D array encoding sway and tilt, Sienko et al. (2008) showed significant improvements in all areas of postural performance in vestibular impaired patients. Asseman et al. (2008) used a similar topographic encoding (spatial encoding) to present vibrotactile stimuli to subjects' trunks in a gaze direction task. Subjects were presented with vibratory cues while saccade latencies and accuracies in the stimulus direction were measured. However, there was little improvement in latency and high variability in saccades, even after prolonged training, and the authors conclude that this vibrotactile representation was unintuitive for this task.

In contrast, Kadkade et al. (2003) found that a spatial encoding was superior to a

frequency-modulated code. In a task to stabilise a cursor presented in both visual and tactile modalities, with increasing amounts of cursor ‘instability’, they compared three different position configurations (for increasing numbers of tactors) and reported that the positional encoding was most effective at reducing errors. [Kadkade et al. \(2003\)](#) also compared different modes of delivering error signals (absolute and differential error feedback), and reported that a differential code was superior for their task.

An amplitude encoding can be implemented on a single tactor ([Bark et al., 2008](#)) by varying the amplitude of a sine wave sent to the tactor at a constant frequency. In doing this it was found that a logarithmic amplitude mapping was more effective than a linear one.

In a virtual aiming task with both visual and tactile feedback, a comparison of vibrotactile feedback and skin-stretch feedback showed that both resulted in improvements compared to a vision-only case ([Bark et al., 2008](#)). Skin-stretch, however, proved a more effective modality, perhaps owing to the depth and therefore lower spatial resolution of FA-II versus SA-II receptors mediating vibration and stretch perception respectively (see previously).

[Jiang et al. \(2009\)](#) report a technique for giving vibrotactile feedback to multiple sclerosis patients. This involves simultaneously varying the pulse-width and inter-pulse interval (period) of a vibrotactile stimulator. The simulators used are vibrating motors, and by varying the duty cycle of current to the motors (by increasing the pulse-width or reducing the inter-pulse interval) the intensity of the perceived sensation can be modified. [Jiang et al. \(2009\)](#) co-vary pulse width and period so that a larger range of sensations can be created. One could potentially pick a range of pulse-widths and periods which maximise the sensitive range of the subject and therefore increase the bandwidth of a single vibrotactile channel.

To achieve the perception of continuous movement of a tactile stimulus one can temporally vary the intensities of adjacent tactors ([Rahal et al., 2009](#), [Cha et al., 2008](#)). Two vibrating motors can be combined to create the perception of continuous sensation. This sensation is a function of relative location, relative amplitude and temporal order. For such moving stimuli, [Kohli et al. \(2006\)](#) found that subjects were good at recognising and distinguishing patterns of motion (a relative task), but were less good at speed recognition. Hence, the encoding of ‘absolute’ signals remains a challenge.

In summary, a wide range of feedback encodings have previously been considered and explored. A spatial (topographic) encoding appears to have been the most effective for maximising bandwidth and reducing adaptation, and is favourable as bandwidth is limited by the number of tactors.

2.4.2.4 Electrotactile Feedback

The merits of vibrotactile and electrotactile techniques have been reviewed in Saunders and Vijayakumar (2009). Electrotactile stimulator may require less power, deliver more “punctate” sensations (greater spatial resolution) and have reduced response latency.

In Saunders and Vijayakumar (2009) I discuss the major safety considerations for developing an electrotactile interface (see also Kaczmarek et al., 1991). a summary of the key safety concerns of electrotactile stimulation are:

- **Variable skin resistance:** The literature reports a wide range of skin resistances, (e.g. from $200\text{k}\Omega$ when dry down to $5\text{k}\Omega$ when vasodilated, see Szeto and Riso, 1990), and as a function of location, temperature, humidity, sweat, hair follicle location etc. It is difficult to deliver constant safe supply of current when the resistance is unpredictable and variable.
- **Charge Density:** The density of charge on the electrode increases with decreasing electrode size. With a 10mm^2 contact, the charge density could be around $0.14\mu\text{C}/\text{mm}^2$ in a typical stimulator (Szeto and Riso, 1990). An upper bound on safe charge density is reported as $0.4\mu\text{C}/\text{mm}^2$ (Szeto and Riso, 1990, shown to be safe for a coiled wire electrode). However, if an electrode is tilted up onto its edge, as may occur during movement of the subject, stings may occur due to sudden increase in charge density Szeto (1982).
- **Electrode Geometry:** While larger electrodes are desirable (lower charge density, less overall voltage required) delivered sensations will be harder to localise and may risk sudden stings if charge is not evenly distributed across the electrode Kaczmarek et al. (1991). Low-resistance conducting pathways under the skin are associated with hair follicles, sweat glands and breaks in the epithelial surface, and occur at a density of 1 per square mm (Szeto, 1982). The path of lowest resistance will receive the most current in a positive feedback manner (since skin resistance *decreases* with increasing intensity).
- **Direct Current Buildup:** *Monophasic* stimulation has a net direct current (DC) component, building up charge on the skin. One can use an output coupling capacitor to limit charge flowing into an electrode Kaczmarek et al. (1991a), and couple the output with a long time constant capacitor to prevent net accumulation of charge Szeto and Chung (1986). Use of *Biphasic* current stimulators (with no net DC component) can also avoid this problem.
- **Stimulation Waveform:** A number of parameters can be varied (such as pulse frequency, amplitude and duty cycle) each affecting the perceived sensation is a

variety of ways. See Saunders and Vijayakumar (2009) and also Szeto (1982), Buma et al. (2007), Arieta et al. (2005, 2006), Kim et al. (2005), Okada et al. (2007), Poletto and Doren (1999), Zafar and Doren (2000), Kaczmarek et al. (1991a), Solomonow and Lyman (1977), Szeto and Chung (1986), Szeto and Farrenkopf (1992).

- **Irreversible damage:** Fig. 2.9 illustrates some typical skin disorders that may arise from excessive electrical stimulation of the skin. To avoid damage, techniques used in the literature are optical isolation of different parts of the circuit (Poletto and Doren, 1999), capacitative coupling (to limit net charge transfer) (Szeto and Riso, 1990), and careful circuit design with redundancy (Poletto and Doren, 1999).



Figure 2.9: **Electrically-induced skin disorders.** (Dermatology.co.uk, Gomersall, 2008a,b).

In Saunders and Vijayakumar (2009) we present a biphasic constant-current stimulator based on modified TENS electrodes, which satisfies the above considerations. The design of the stimulator requires low currents and voltages, and limits these to specified maxima. However, the present thesis focuses entirely on a vibrotactile interface, which was preferred in the interest of safety, low cost and simple construction.

2.4.3 Control

2.4.3.1 Target Muscle Reinnervation (TMR)

Kuiken et al. (2004) surgically attached four nerve groups to chest muscle tissue in a bilateral amputee. The nerves innervated the muscle over a 5 month period, enabling voluntary contraction of chest muscle after this time. EMG signals on the chest muscle were used to control a robotic prosthetic arm in a technique that has become known as *targeted muscle reinnervation* (TMR).

Several years later the patient was fitted with a 6 degree of freedom prosthesis. Miller et al. (2008) showed that the patient could independently control shoulder flexion/extension, humeral rotation, elbow flexion/extension, wrist rotation, wrist flexion/extension, and digit flexion/extension. The authors claim he could operate up to four simultaneous control signals, although they acknowledge that this was rarely done

due to the “high cognitive demand” of the system owing to the lack of proprioceptive information.

This remarkable technique provides a great possibility for future amputees, but alleviating the cognitive demand will probably rely heavily on the ability to provide integrative feedback. Indeed, this may also be achieved by innervating chest tissue with sensory neurons.

However, one major criticism with this approach is that it relies on the residual neural capabilities of the amputee. This will often limit the degree of motor and sensory restoration, especially for severely injured patients. The technique is only really feasible in new amputees, and the invasiveness of the approach and the need for surgery may make the operation unappealing.

2.4.3.2 EMG control

Typical modern-day prostheses are controlled using surface electromyography (sEMG). The role of muscles in hand control is complex, involving temporal parsimony and synergistic co-contraction between different muscle groups (see section 2.3.2.1). Prosthetic systems may be controlled by EMG activity recorded at the Extensor Digitorum and Flexor Digitorum Profundus (Shannon and Agnew, 1979), but the activity of alternative muscles or even groups of muscles may be recorded to deal with wide variation in the nature and severity of the amputation. Moreover, the muscle(s) recorded do not operate as simple switches (Long, 1968, Flatt, 2000). Hence, most prosthetic systems require a considerable degree of re-learning to control the hand. Attempts to record ensemble activity have proven promising (Bitzer and van der Smagt, 2006), but nonetheless do not yet feature in state-of-the-art commercially available prostheses.

Since EMG signals used to initiate and control prosthesis movement fluctuate as a function of sweat, movement, muscle fatigue and skin-conductivity (Duchêne and Goubel, 1993) the most reliable EMG classifiers require 250-300ms of sampling time before accurate classification can be made (Lorrain et al., 2010). In the interest of responsiveness, controllability and expense, many commercially available prostheses use differential (“open/close”) controllers to defer the problem of EMG signal reliability to the temporal domain.

2.4.3.3 Direct Neural Control

A promising new possibility is for direct neural control. Dhillon and Horch (2005) demonstrated how intrafascicular electrodes could be used to record grip force and limb position signals from motor neurons, and provide feedback of grip force and position to sensory neurons. With strain gauge sensory feedback prosthesis users could discriminate

fingertip forces and with joint-angle sensory feedback prosthesis users could discriminate limb positions. With neural control of forces and angles, users could reliably attain target forces angles, in the absence of any feedback. The reliability with which users could control motor neuron activity and interpret sensory neuron stimulation provides promising possibilities for future neurally-controlled prostheses. Unfortunately the study did not explore the combination of control and feedback, which would offer valuable insight for closed-loop systems.

As well as intrafascicular recordings, animal studies have revealed the potential for cortical control. Mulliken et al. (2008) trained monkeys to control a visual cursor with a joystick. The experimenters were able to accurately predict the observed cursor trajectory in real-time from cortical recordings. Moreover, when using these predictions in place of the joystick, monkeys rapidly learned to control the cursor in its absence.

Gage et al. (2005) trained rats to control an auditory cursor without any prior training using a “co-adpating” controller connected to motor cortex: the rat brain and the Kalman-filter controller were learned in tandem. After training, the rats were able to reliably control the cursor to reach a target tone, and with further training learned to match the tone to one of several targets.

Invasive procedures are still under clinical testing since long term effects are unknown (Tenore et al., 2007). Non-invasive alternatives, such as electroencephalogram (EEG) mu-band readings from cortex violate the desire for a self-contained neuroprosthesis.

2.4.3.4 Actuation Strategies

Hines et al. (1992) fitted quadriplegic patients with shoulder-position controlled neuro-prostheses, controlling a “cursor” for both force and position. This presents a natural and intuitive scheme based on healthy hand control. Under unloaded conditions the task reduces to position-control and under loaded conditions it reduces to force-control.

The advantage of these strategies are that they adopt the concept of Extended Physiological Proprioception (EPP), the ability to use proprioceptive feedback to infer the state of the external “tool”. Shoulder-powered prostheses use the shoulder position to set the arm position, and grasp closure, and as such provide a direct mapping from signal to action that is superior to speed-controlled prostheses (Doubler and Childress, 1984).

In contrast, Otr et al. (2010) discuss the merits of the speed-controlled iLIMB hand against the DMC (dynamic mode control) hand. Though the speed-controlled hand offered reduced functionality, it provided more reliable grasps and was overall preferred by patients. In comparing the merits and limitations of prosthesis control methods Cipriani et al. (2008) show that to minimise effort, subjects prefer less interactive, more

automatic control of the prosthesis.

clearly the choice of actuation strategy is still open to debate, owing to the wide range of performance criteria to which one can assess prosthesis performance (see later).

2.4.4 A Closed-Loop Prosthetic Hand

2.4.4.1 Historical Attempts to Close the Loop

Shannon (1976) motivated the possibility of feedback systems for amputees with artificial limbs, reviewing attempts at closed-loop design (dating from as early as Beeker et al., 1967), arguing that electrical and mechanical skin stimulation could provide psychologically acceptable, physically feasible and functionally viable feedback. Following from this, Shannon (1979b) developed a closed-loop system in which finger strain was fed back to patients by electrotactile stimulation, reporting improved confidence in wearers. Almström et al. (1981) addressed the problem of interference control and feedback. Since these landmark results, many aspects of feedback provision have been discussed.

However, Scott et al. (1980) expressed reservations with performance evaluation, doubting the reliability of subjective opinion and the generalisability of task measures. Many prosthesis design criteria have since been discussed including functionality, dexterity, control and acceptance (Carrozza et al., 2006).

2.4.4.2 Measuring Success

In developing a prosthetic hand several crucial characteristics must be considered:

- **Functionality.** The hand should allow the user to perform vocational operations and activities of daily living (ADLs, Carrozza et al., 2006);
- **Control.** The amputee should feel like he/she is in control of the hand at all times (Carrozza et al., 2006);
- **Sensation.** The amputee should be able to sense the hand interacting with the world (see Dhillon and Horch, 2005);
- **Effort.** The amputee should not feel as though the hand is too much effort to control, both physically and mentally (Doubler and Childress, 1984);
- **Dexterity.** The hand should offer sufficient degrees of freedom, responsiveness and accuracy (Carrozza et al., 2006);

- **Cosmetics.** The prosthesis should have the size, shape and appearance of a human hand (see Carrozza et al., 2006, Wright et al., 2003) to maximise the illusion of ownership (Ehrsson et al., 2008);
- **Acceptance.** If all of the above criteria are satisfied the hand will not be a hindrance to the amputee, who should accept the prosthetic as though it were a real hand, both psychosocially and functionally (Wright et al., 2003). The alternative is rejection of the prosthesis and failed rehabilitation.

Performance Measures In line with these success criteria a range of assessment protocols have been developed. It is widely accepted that prosthesis functionality should be tested against the benchmark of Activities of Daily Living (ADLs). These include picking up coins, unfastening buttons, cutting food, turning pages in a book, removing lids from jars, pouring water from jug or carton, and moving tins, jars and cans from different locations (Light et al., 2002). However, these criteria are difficult to assess quantitatively.

The ABILHAND questionnaire assesses subjective perception of grip strength or dexterity, mental effort, fatigue and risk of breaking objects (Penta et al., 1998), providing a formalised subjective measure of success. To analyse objective functionality, the Southampton Hand Assessment Procedure (SHAP) protocol assigns scores depending on task-durations to complete a number of tasks equivalent to ADLs, each requiring use of different grasps (see Light et al., 2002). A similar Prosthetic Upper Extremity Functional Index (PUFI) considers a wider range of tasks relevant to children (Wright et al., 2003), and the Unilateral Below Elbow Test (UBET) provides an alternative objective assessment with good inter- and intra-observer consistency Bagley et al. (2006).

While the above protocols are valuable clinical assessment tools for assessing the whole range of prosthesis performance measures, I feel that for basic prosthesis evaluation the task of grasping and lifting objects sufficiently captures the key aspects of sensorimotor function (planning, acting, sensing and reacting). As discussed previously, the value of the grasp and lift task is that it is well characterised for both healthy and anaesthetised subjects, can be measured easily and consistently, and provides a robust objective benchmark for functional prosthesis control comparison.

Acceptance and Integration Acceptance of modern artificial limbs by amputees would be significantly enhanced by a system that provided sensations of touch and joint movement (Dhillon and Horch, 2005). The feeling of *ownership* (see section 2.3.2.3) is a requirement for successful prosthesis integration. A possible method to measure the acceptance of a new feedback system is by measuring the degree of integration with

other sensory modalities.

As discussed previously, cue integration studies provide a valuable method for measuring multisensory perception. In this thesis I develop a sensorimotor cue integration task which requires subjects to control a cursor in a manner analogous to prosthesis control. The degree of sensory integration provides a quantitative assessment of functional restoration.

2.4.4.3 21st Century Closed-Loop Prostheses

Cipriani et al. (2008) show that “reach, pick and lift” trials are improved in amputees with a single element of force feedback, and they report increased acceptance and usability. Similarly, amputees respond positively and rely less on visual control when picking up a soft ball (Pylatiuk et al., 2004). These subjective results highlight the importance of sensory feedback, motivating an objective quantification of performance, learning rates and degree of integration.

Cipriani et al. (2008) consider three rather elaborate hierarchical prosthesis control feedback schemes with differing amounts of feedback. Task accuracy increases with interactivity (more control and feedback). When vision is available for the tasks there is no quantifiable performance increase, though the presence of feedback is preferred by subjects nonetheless.

Vibrotactile feedback has been shown to be beneficial for brain-computer interface control, particularly when vision is compromised by distraction (Cincotti et al., 2007,a).

As discussed previously, using a video-based simulated prosthesis, Zafar and Doren (2000) found that tactile feedback improved qualitative reports and objective task performance in a grasp and hold task, even in the presence of vision. Pylatiuk et al. (2004) also integrated a force feedback factor into a prosthesis, making the prosthesis controllable without visual attention.

It is difficult to compare the studies above as they use different plants and feedback systems, but it appears that prosthesis control improvements due to feedback are inconclusive. To address this directly, Chatterjee et al. (2008) quantified prosthesis control improvements in the presence of vibrotactile force feedback in an EMG-controlled grasp-force matching task. This follows on from previous work in which a virtual cursor could be controlled (using a mouse) with performance aided by vibrotactile feedback, and reasonable performance in the complete absence of vision (Chatterjee et al., 2007). However, to their surprise, Chatterjee et al. (2008) found that feedback worsened overall performance for naive subjects, and only improved performance for experienced subjects in a subset of trials. They acknowledge that this could be due to (i) the difficulty of controlling EMG signals to drive the hand, which is “less intuitive” than healthy

hand control; (ii) increased muscular fatigue; and (iii) mechanical unreliability of the prosthesis. Such factors are, at present, unavoidable in state-of-the art prostheses. However, I would expect that such control difficulties would serve to exemplify the utility of artificial feedback, not reduce it.

Chapter 3

System Design

In this chapter I introduce an idealised experimental methodology with which I propose to address fundamental open questions facing the field of rehabilitation robotics. This methodology places healthy human performance as a gold standard. I present a closed-loop prosthetic hand as a novel sensorimotor manipulandum which, unlike in healthy individuals, can be readily manipulated and can therefore be used to decouple the respective roles of feedback, sensation and control. In this chapter I introduce the components of this system, and focus on the technological developments required to produce this novel plant. This system will be the focus of the experimental work documented in subsequent chapters and ultimately the target platform on which the research will be deployed.

Relevant Publications

- Ian Saunders, Sethu Vijayakumar. (2009). **A Closed-Loop Prosthetic Hand: The Development of a Novel Manipulandum for Understanding Sensorimotor Learning.** *Technical Report EDI-INF-RR-1321.*
- Ian Saunders and Sethu Vijayakumar, (2009a). **A Closed-Loop Prosthetic Hand.**, *Proc. Key Issues in Sensory Augmentation.*
- Ian Saunders, Sethu Vijayakumar, Hugh Gill. (2011a) The University Court of the University of Edinburgh/Touch Emas Ltd., **Improvements in or relating to Prosthetics and Orthotics**, *GB Patent Application - Category P120168.GB.01.*

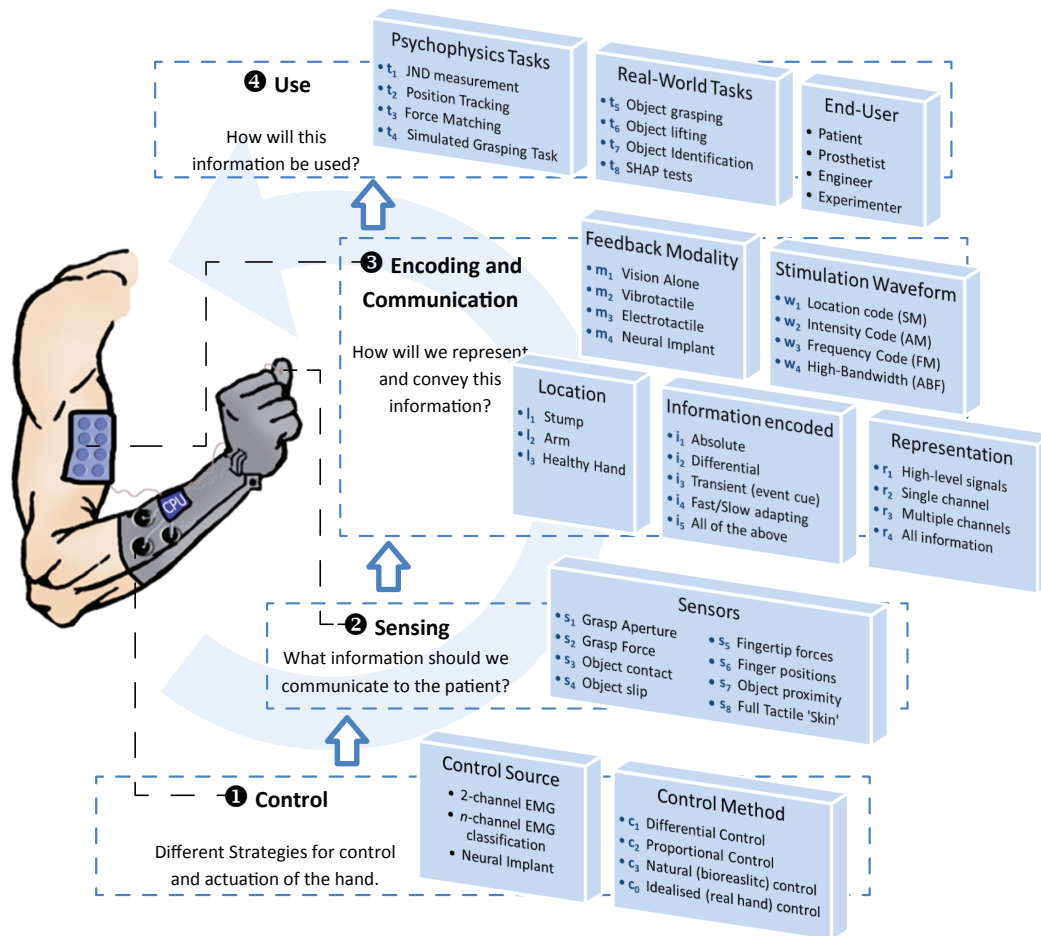


Figure 3.1: **Design of a Closed-Loop Prosthesis.** A closed loop prosthesis comprises design decisions in control, actuation, sensing, encoding, communication and use. These multiple dimensions make the task of prosthesis design a considerable challenge.

3.1 Motivation

3.1.1 Introduction

In this section I discuss the motivation for the system designed in this thesis. I also motivate the general methodology underpinning Chapters 4, 5 and 6.

3.1.2 Debugging the closed-loop

3.1.2.1 Combinatorial Explosion

Fig. 3.1 presents a scaffold for the general problem of closed-loop prosthesis design, summarising the many technological insights discussed in Chapter 2. Within each dimension one can imagine a path progressing from the practical and state-of-the-art, to the gold standard of healthy human performance. Researchers have addressed many

of the above dimensions in isolation (multiple channel EMG classification (Castellini et al., 2009); neural interfaces for control or feedback (Sachs and Loeb, 2007); tactile perception as a function of location, waveform and modality (Kaczmarek et al., 1991, Cholewiak and Collins, 2003; etc.). However, in order to engineer a complete solution we must understand the individual contributions of each design dimension to the complete system, including the role of the human user, under different task demands and constraints.

A feasible approach to systematically evaluate and compare the different design dimensions of Fig. 3.1 is to decouple them experimentally, then recombine them in a controlled manner.

3.1.2.2 Idealised Manipulandum

In this this chapter I will introduce a closed-loop prosthetic hand, combining the iLIMB, a state-of-the-art prosthetic hand, with a custom built vibrotactile feedback interface. In this thesis I aim to address the limiting factors of the closed-loop model by addressing the underlying sensorimotor processes from both neuroscientific and rehabilitative perspectives. Rather than attempting to engineer an entirely new closed-loop system (an approach which has achieved much technological success but has demonstrated limited rehabilitative benefit), I propose to use a state-of-the-art device and address more general questions regarding the nature of its use.

If one takes the healthy hand as the gold standard and strips it gradually of its tactile feedback components by means of anaesthesia, one will observe that certain aspects of control are lost while others are maintained, owing to the complementary influences of audition and vision, audition and feedforward control. Decoupling the multisensory and sensorimotor influences on control is a primary theme of this thesis.

I will present here a *simulated amputation*, allowing the attachment of a prosthesis to healthy individuals. This serves two purposes: (i) It is experimentally convenient to use healthy subjects; and (ii) Healthy individuals have intact end-effectors, allowing for a controlled comparison between healthy and amputee control. The present approach *idealises* the control of the closed-loop hand so that objective results can be obtained regarding the benefits of sensory feedback for amputees (independently of the difficulties inherent in prosthesis control).

This experimental platform provides a window into current theories about (i) sensory substitution; (ii) multisensory integration; and (iii) feedforward and feedback cognitive processes. The present chapter summarises the technological developments required to develop this novel manipulandum.

3.1.2.3 Modularity

Modularity it is a particularly important feature of the design, in the interest of generality, scalability and deployment. The modules considered are control, actuation, sensation and feedback (see Chapter 2). In this thesis a range of *end-effectors* or *plants* are considered. These are the environments in which the role of feedback is evaluated. The most obvious end-effector is the robotic manipulandum discussed above.

Having established a collaboration with the Edinburgh-based prosthetics company Touch Bionics, who in 2007 released the iLIMB, the world's first fully articulating commercially available bionic hand, I have investigated the current capabilities of users equipped with this device. Further, we have modified the hand to enable closed-loop control. An idealised implementation of this device allows control by healthy individuals.

In this thesis I also consider abstract end-effectors. I have developed a number of cursor-based tasks, where the subject controls a cursor and receives vibrotactile feedback relating to the cursor. In contrast to most tracking tasks discussed in Chapter 2 I replace the standard computer mouse or joystick with differential- and proportional-control interfaces. These can be considered analogous to modern prosthesis controllers, simulating the same dynamics in the absence of the physical plant.

The reason for making these abstractions is so that I can prototype suitable control and feedback methodologies in controlled conditions. before testing the scalability of the solution to the real world plant.

3.1.2.4 The Gold Standard

Healthy individuals provide a perfect example of how a closed-loop system should operate. For example, we have seen in Chapter 2 that in order to perceive and act in a robust fashion healthy individuals can combine multiple modalities in a way that is predictable and often statistically principled. If a sensory modality is removed (e.g. by amputation) or if a sensory modality is restored (e.g. by artificial means), we can begin to understand the learning mechanisms underlying these phenomena. The multi-sensory integration paradigm may provide a valuable experimental tool to evaluate the mechanisms of artificial cue integration and allow us to quantify the degree of sensory restoration.

Another crucial task of everyday living is that of reaching, grasping and lifting objects. This is an ideal task to study for three reasons: (i) it characterises the key aspects of sensorimotor control: sensing, planning, predicting and acting; (ii) it is well researched and understood in healthy and sensory-impaired individuals; and (iii) it is well known that humans behave in a 'stereotypical' or 'optimal' way in these simple

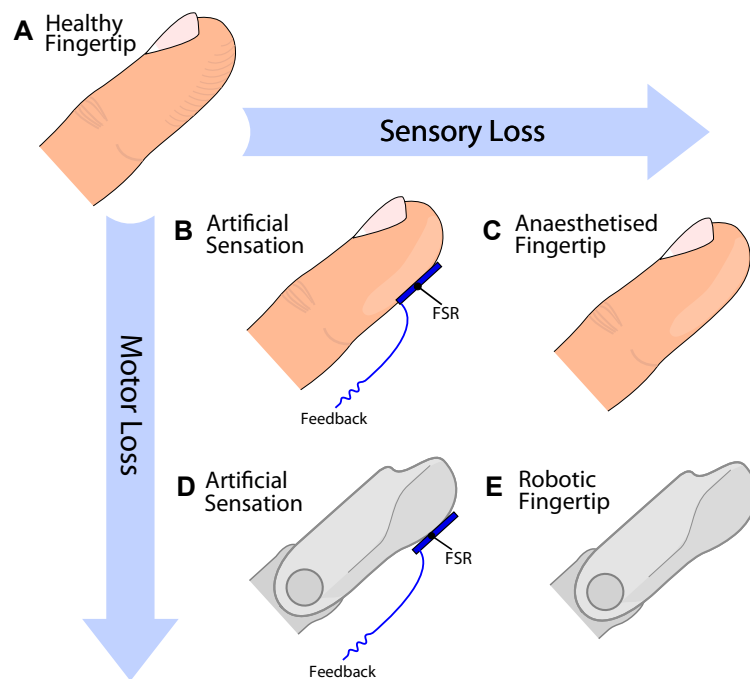


Figure 3.2: **Experimental Manipulations.** Five experimental conditions to elucidate the limiting factors in prosthesis functionality. **Condition A**, Those using their healthy hand have full control and full feedback. **Condition C**, Full anaesthesia of the fingertips eliminates tactile and force feedback. **Condition B**, Force feedback can be artificially restored to the natural control system using vibrotactile stimulation. **Condition E**, Full control can be removed by using a robotic hand (or an abstract end-effector such as an on-screen cursor). **Condition D**, Force feedback can be artificially restored to the artificial control system using vibrotactile stimulation.

tasks, allowing the quantification of prosthesis suboptimality. It is important to ask whether or not this suboptimality, either as measured by impaired performance in some task, or by comparison to statistical or computational models, can be explained by the lack of sensory feedback, or whether some other aspect of the closed-loop design is limiting performance.

The components of the closed-loop system can be decoupled, allowing one to establish which aspect is presently suboptimal. This can be visualised as starting with healthy human hand and gradually stripping it of its natural sensory components, to be replaced by an artificial (vibrotactile) sense. Likewise, replacing the healthy hand with a robotic or computer-based end-effector removes the natural control system. Together, this provides five experimental conditions, shown in Fig. 3.2.

The five exemplary conditions in Fig. 3.2 illustrate how control and feedback can be decoupled. Performance in **Condition C** demonstrates the effect of digital anaes-

thesia. Adding a source of artificial sensation to condition C results in **Condition B**, allowing the degree of *sensory restoration* provided by a particular feedback method to be quantified, independent of control of the hand. The ideal feedback method should be comparable to healthy performance, **Condition A**. Likewise, performance in **Condition E** demonstrates the effects of both sensory and motor deficits for amputees fitted with state-of-the-art prostheses. Comparing condition E to condition C allows for the degree of *control restoration* provided by a particular controller in the absence of feedback to be quantified. Finally, **Condition D** is the modified closed-loop prosthetic hand proposed here, providing simultaneously sensory and motor restoration. Comparing condition D to condition B allows the degree of control restoration for different feedback methods to be quantified. The holy grail in rehabilitation is to design condition D such that it is comparable to condition A.

This schematic defines the bigger picture of the present research, but in this thesis we use this framework to focus specifically on two key areas. Firstly, healthy individuals (condition A) combine sensory cues in a manner which is often statistically optimal. I ask if this phenomenon extends to the integration of an *artificial* feedback channel (condition B). In Chapter 5 I will show this is indeed the case. Secondly, in reviewing healthy human grasping tasks, I have described how certain aspects of economical grip-force scaling are impaired by digital anaesthesia (conditions A and C). Using the robotic hand as a model system, I compare grasping and lifting behaviour in a robotic system (conditions D and E) to quantify the effects of *artificial digital anaesthesia*, and modify the control system so as to minimise feedforward uncertainty (condition D) to quantify the effects of *artificial control*. In Chapter 6 I will show how impairments to economical grasping are minimised if the control system is designed in this way, implicating complimentary feedforward and feedback processes as is also observed in healthy individuals (condition A).

3.2 Methods and Results

3.2.1 Introduction

In this section I detail the hardware developed for this thesis. Owing to the modular approach discussed above (Fig. 3.1) and in Chapter 2 (Fig. 2.7), the main components of the system are *control*, *actuation*, *sensation*, *feedback* and *task*. Below I discuss the developments and design decisions in each of these areas, and present the results that have informed these decisions.

3.2.2 Robotic Hand Actuation

3.2.2.1 Introduction

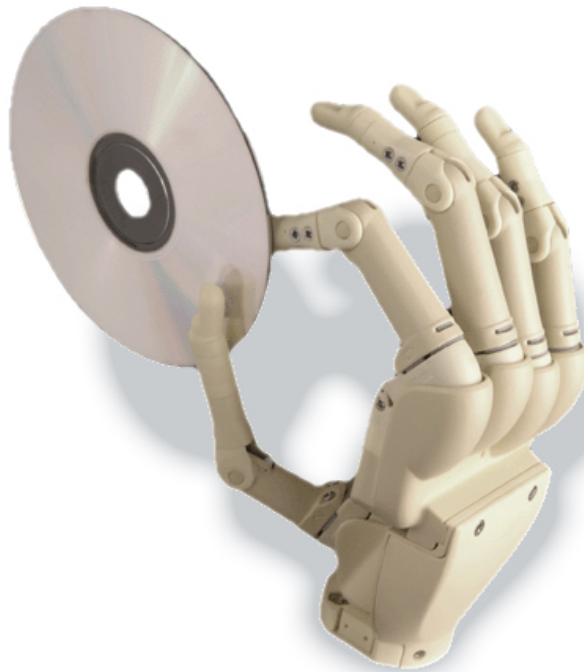


Figure 3.3: The Touch Bionics iLIMB

The iLIMB (Fig. 3.3) is a state-of-the-art prosthetic hand with two degrees of EMG control (for *open* and *close*). Using a miniature worm gear motor system, each finger of the iLIMB is individually powered, and “stalls” when the grip reaches a set threshold, enabling object-specific grasp shapes without user intervention. The iLIMB has scored highly in terms of patient satisfaction and reliability (Otr et al., 2010).

Different actuation strategies exist for prosthesis control. This translates to deciding how the control signal (typically EMG or FSRs) maps onto (for example) the end effector

positions, forces or velocities. The iLIMB presently deploys a *differential* (velocity) control strategy. However, the healthy human hand works on an *proportional* control method, whereby hand position and forces are governed by the relative viscoelastic contributions of opposing muscles (see Chapter 2). I have therefore implemented a differential force-control system and a proportional force control system for the iLIMB.

In this section I describe the existing iLIMB control algorithm. In its basic form, users can not easily control the force output of the hand. I highlight a number of alternative approaches I have developed to achieve signal-proportional force control and differential force control. Further details of the practical deployment of the above developed technology can not be divulged due to the terms of a license agreement between the University of Edinburgh and Touch Bionics and aspects of these methods form part of a patent application (Saunders et al., 2011a). Background intellectual property is documented in a published technical report (Saunders and Vijayakumar, 2009). Knowledge of the licensed technology is not necessary to reproduce the experiments in this thesis.

3.2.2.2 Differential Control

The iLIMB hand uses a differential control protocol. A simplified version of the algorithm is roughly described by the flowchart in Fig. 3.4.

The algorithm prescribes three main parameters per digit:

- **Activation threshold:** the threshold at which control inputs will begin to activate the hand
- **Speed:** a pulse-width-modulated speed parameter (PWM), proportional to the differential control signal input
- **Stall threshold:** the magnitude of current drawn by the motor at which the the motor will be turned off, or ‘stalled’.

By adjusting these parameters different types of grasp can be achieved. Users of the hand presently have control of the speed. I have considered a number of different control methods in this thesis.

3.2.2.3 Responsive Stall Control

The basic iLIMB control method expends more energy than necessary, due to high motor currents and long (100ms) delays after contact before the motors stall. By reducing this delay (by smoothing spikes from the current signal, and taking a briefer stall delay of just 5ms) a more responsive stall control routine is achieved. This allows grasps ranging

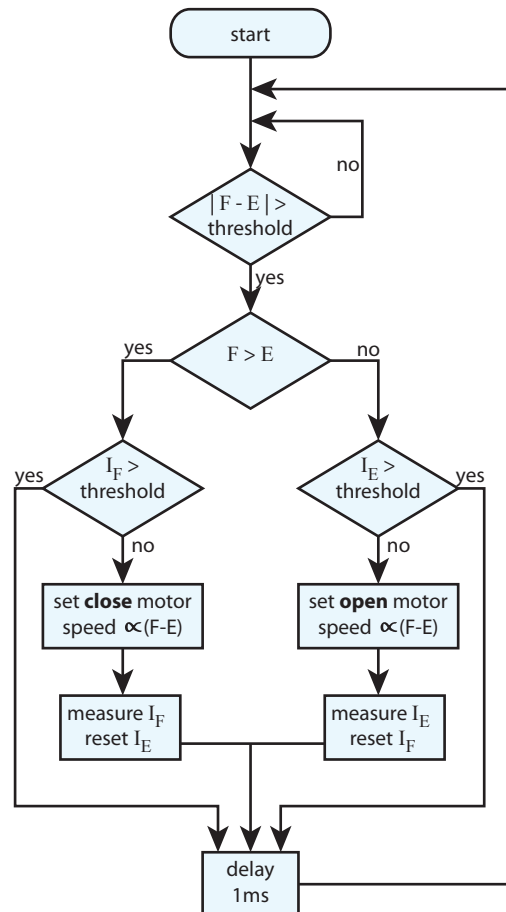


Figure 3.4: **The basic iLIMB control algorithm.** When the difference between the flexor (F) and extensor (E) signals reaches a threshold the prosthesis begins to open or close. The motor speed is set proportional to the signal. If during closing the flexor current (I_F) exceeds a threshold the hand stalls until extension is initiated, and vice versa a for the extensor current (I_E).

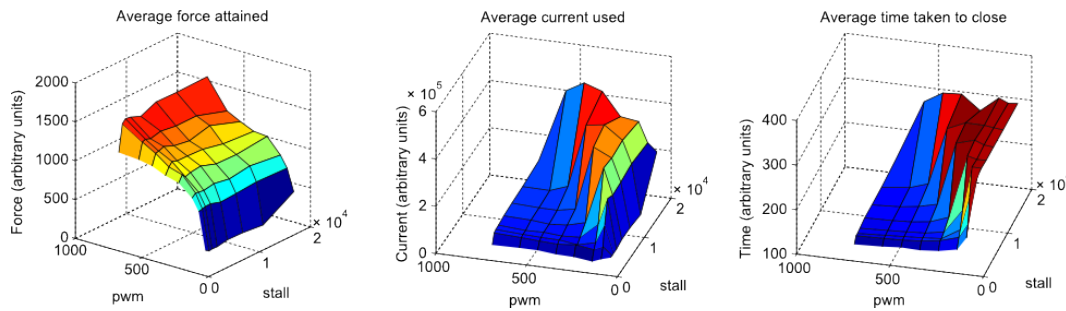


Figure 3.5: **Grasp force, current and duration.** Grasping with the iLIMB can be configured by adjusting the stall current and grip force. By gathering a large quantity of grasp data we can optimise these parameters to achieve efficient grasps and graded force control.

from 100g of load up to 1kg of load by adjusting the PWM (not the stall threshold). Data were collected from the hand for different values of PWM and stall threshold to measure the grip force attained, the current used, and the time taken for the hand to close.

The main findings of this were:

1. Stall threshold has very little effect on the final force output
2. PWM has a very strong effect of the final force output
3. High stalls can have the disadvantage that the hand fails to stall (consuming time and power)
4. Different values of PWM have only a marginal effect on the current consumed when the hand is unloaded

Therefore with responsive stall control as highlighted above, patients can use the proportional PWM controller to modulate their force output.

3.2.2.4 Pulsing Linear Force Control

I developed a method to control the hand that provides approximately linear force output over time. This is a significant development, as presently users do not have the facility to differentially-control the force output of the hand. This may be beneficial for fine control of grasps, avoidance of damage to delicate objects, and ultimately patient acceptance. The control algorithm for the flexor signal comprises two phases: (i) A ‘light touch’ grasp; and (ii) Linear force increase by a sequence of pulses of the thumb.

The light touch phase proceeds with a small “boost” (the motor is switched on for a duration of 50ms) to overcome ‘stiction’ (an inertial property of the motors). Each finger is then driven according to the standard algorithm (Fig. 3.4) with a low speed

(pulse-width modulated (PWM) at typically 150/700 when not using a cosmetic glove), with a high stall threshold. The thumb is driven at a low speed (PWM 200/700) and a low stall threshold. Resultantly the thumb stalls as soon as it is loaded. At this instant all other fingers are given a similarly low stall threshold and close until they make contact with an object or are closed. Consequently, the hand completes a very light grasp on the object (equivalent to approximately 300g). This ensures that: (i) a low overall squeezing force (opposing the thumb) is achieved; (ii) the fingers continue to move until the thumb is in opposition with them to wrap around the object; and (iii) fingers that do not contribute to the grasp are allowed to close completely, important for forming stable grasps.

The hand then instantly switches to thumb pulse mode. As all grasps are in opposition to the thumb it is both practical and economical to achieve the desired force range via only the thumb. In this mode the thumb is controlled by short pulses of current, of increasing PWM duty cycle. The magnitude is chosen so as to allow near-linear force increases with each successive pulse. This can allow for grasps ranging from very light (equivalent to 100g) to heavy (2kg), with the magnitude and duration of pulses tuned to achieve the desired rate of change of force.

3.2.3 Control Signal

3.2.3.1 Surface Electromyography

TMR- and EEG-controlled prostheses (Chapter 2) rely on existing neural activation and may therefore provide more ‘natural’ control. However these approaches may be presently impractical for the majority of prosthesis wearers, due respectively to the amputee’s desire to avoid further surgery and the need for cosmetic integration.

Most present-day prosthetic hands are controlled by Surface Electromyography (sEMG), the recording of electrical currents in contractile muscle tissue using surface-mounted (non-invasive) electrodes. EMG electrodes (an example shown Fig. 3.6) amplify these signals to control the so-called *myoelectric* prosthesis. Typical muscles exploited by prosthetists are the wrist flexor and extensor, and finger flexors and extensors (see Chapter 2). Typically just two electrodes are used to control open and close signals on the prosthesis. Alternatively a single electrode could be used to control closing of the hand (with the hand programmed to automatically reopen in the absence of a signal). In more elaborate systems a third electrode may be used to control thumb abduction, thumb rotation or wrist rotation. However, increasing the degrees of control increases the difficulty of learning to use the hand. In this thesis I focus only on 2-channel control.



Figure 3.6: Otto Bock EMG electrodes

3.2.3.2 Simulating an Amputation

For purposes of experimentation, healthy subjects can be given a *simulated amputation*, by anaesthetising and rigidly splinting the hand (see Fig. 3.7). Following amputation, partially amputated muscle heals onto remaining bone and tissue in the stump, which is simulated by locking the hand in place. The purpose of the anaesthetic is to avoid tactile cues from providing additional tactile or force feedback from the hand. EMG sensors can be applied to the simulated amputee in the normal way.

3.2.3.3 Noise-Free Simulated Amputation

Controlling the hand by recording EMG signals from the residual muscles of the amputee or simulated amputee has its limitations. A low signal to noise ratio means that considerable signal smoothing is needed, limiting the responsiveness and accuracy of the EMG signal. Learning to reliably decode EMG signals challenging, and it is likely that this limits effective prosthesis control. This can be avoided by replacing EMG electrodes on the muscle with force sensors on the end-effector. By recording muscle signals at the end effector of the muscle rather than at the muscle itself a much higher signal-to-noise ratio is achieved.

Rather than splinting a whole hand only single joint is necessary, such as the middle interphalangeal of the forefinger (Fig. 3.7). A prosthesis may be controlled by the FDP and ED muscles in the forearm, which are (essentially) an antagonistic muscle pair which control flexion and extension of the finger. This is simpler than rigid splinting of the whole hand, and in the same way is a noise-reduced alternative to EMG.

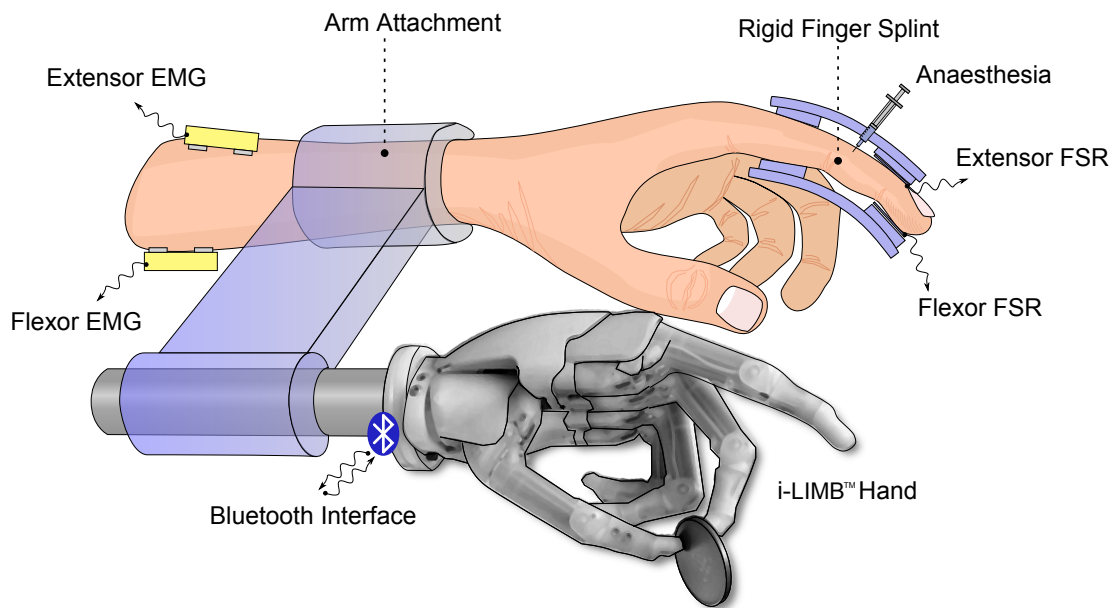


Figure 3.7: **Simulated Amputation.** For experimental convenience an amputation can be *simulated* by rigidly splinting an anaesthetised finger. Either EMG or force sensors can be used as control signals for an attached prosthetic device.

3.2.3.4 Idealised Control and Cursor Control

In the above design it may be unnecessary to anaesthetise or even bind the finger. In Chapter 2 it was noted that muscle-contraction proprioceptors and muscle length proprioceptors could provide suitable signals to allow reliable control of muscle activity. FSR force feedback at the fingertip may be considered an equivalent feedback signal (though it may be more reliable). An *idealised* control system is created by simply allowing the subject to press two force-sensitive buttons.

Such a system could be used to control a cursor on a screen. Conceptually equivalent to prosthesis control but practically simpler to implement, this idealised control scenario allows us to identify and isolate the obstacles facing successful rehabilitation independently of the limitations of control. This approach allows us to tackle fundamental questions the field of rehabilitation prosthetics outwith the capabilities of current technology.

3.2.4 Sensation and Sensors

Numerous tactile signals are available to healthy individuals, but may be of selective benefit depending on the task. In this thesis I focus on two elementary signals: position feedback and force feedback. The feedback modality may have an influence on the degree of perceptual rehabilitation (Patterson and Katz, 1992). However, the success of

TVS systems (y Rita et al., 1969) indicates that the information in an artificial feedback channel can be exploited regardless of its location or encoding.

3.2.5 Vibrotactile Feedback System

3.2.5.1 Introduction

The main considerations for developing a vibrotactile feedback system are discussed in Chapter 2. The system presented here is intended to achieve *sensory substitution* (y Rita et al., 1969) for the tactile sense.

Previous studies considering the most suitable design of a feedback system have found that, to maximise stimulus discriminability and bandwidth, one must take into account amplitude Bark et al. (2008), frequency Kadkade et al. (2003) quantity (Yoon and Yu, 2008) and spacing of tactors (van Erp, 2005) the effects of age (Cholewiak and Collins, 2003), body site (Cholewiak, 1999), separation of spatial patterns (Yoon and Yu, 2006) and pulse burst waveforms (Perez et al., 2000).

Based on these results I have developed an array of vibrotactile stimulation electrodes, or *vibrotactors*. This section describes the developed technology.

As mentioned in the previous section, the system is designed to provide position and force feedback. These signals were considered most relevant to the functional tasks considered in this thesis (Chapters 5 and 6).

3.2.5.2 Hardware

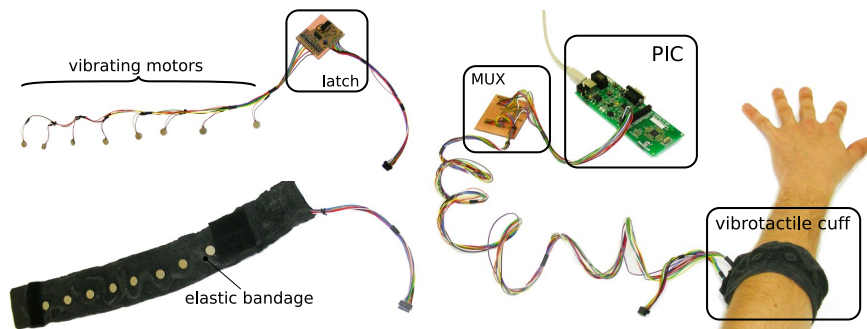


Figure 3.8: **Vibrotactile Feedback System**

Construction To satisfy the considerations of Chapter 2, I have developed and built a 32-channel vibrotactile feedback system. 32 vibrating motors (*tactors*) are controlled via a programmable microcontroller (PIC18F4550, Microchip, US, hereafter *PIC*) using a set of multiplexors (*MUX*) to independently adjust the vibration frequency and amplitude of each motor to deliver a wide range of sensations. The system connects to a personal computer (*PC*) by universal serial bus (*USB*) to allow simultaneous software

control of tactors and sensor data logging. Fig. 3.8 shows the main components of the system.

Circuit Diagram The vibrating motors are split into four groups of 8, and each motor is addressed by a combination of multiplexors and latches as shown in Fig. 3.9. Typically just 8 motors are used at any one time, stitched in an elasticated bandage and fastened with a fabric hook-and-loop fastener to make a wearable “cuff”.

Custom hardware also allows force and position sensors to be simultaneously sampled. This data is sent via a PC for purposes of temporal calibration and data logging, and can be used to update the vibratory stimulation at a rate of $>200\text{Hz}$ with latency $<1\text{ms}$. The lag time for the motor accelerating and decelerating to a given voltage is less than 40ms. Custom PC software can also be used to directly control the stimulation patterns, allowing flexibility of experimental design.

Motor Profile Each motor is a Precision Microdrives 310-101 10mm shaftless vibration motor. Its response function is shown in Fig. 3.10. Each motor is connected to a PNP transistor driven by 4V and gated by the output of a standard digital latch (Microchip, US) to allow persistent on and off signals to be sent to each motor.

Improved Efficacy I developed prototypes to improve the efficacy of the feedback by increasing the range of perceptual levels delivered by each vibrotactor.

The two methods devised were relatively simple: mounting the tactors on sponges (Fig. 3.11A), or mounting them on springs (Fig. 3.11B) embedded in a sponge casing (Fig. 3.11C). The latter method was effective at:

- (i) removing unwanted audibility of the tactors
- (ii) increasing the pressure of the tactor on the patient
- (iii) increasing the efficiency of the motors (so that the load of the motor is predominantly the patient, and not expended on the mounting surface or the spring)

3.2.5.3 Firmware

Hardware Communication interface The motors are controlled by a 9 wire connection from the PIC microcontroller (7 data bits plus power and ground lines). Data bits are multiplexor address bits (2), latch address bits (3), latch enable (1). and data (1).

The algorithm for hardware communication is as follows: (i) Disable the latch (so that it holds its current values on all outputs); (ii) Set the multiplexor address of the current array; (iii) Set the latch address of the current tactor; (iv) Set the data bit to

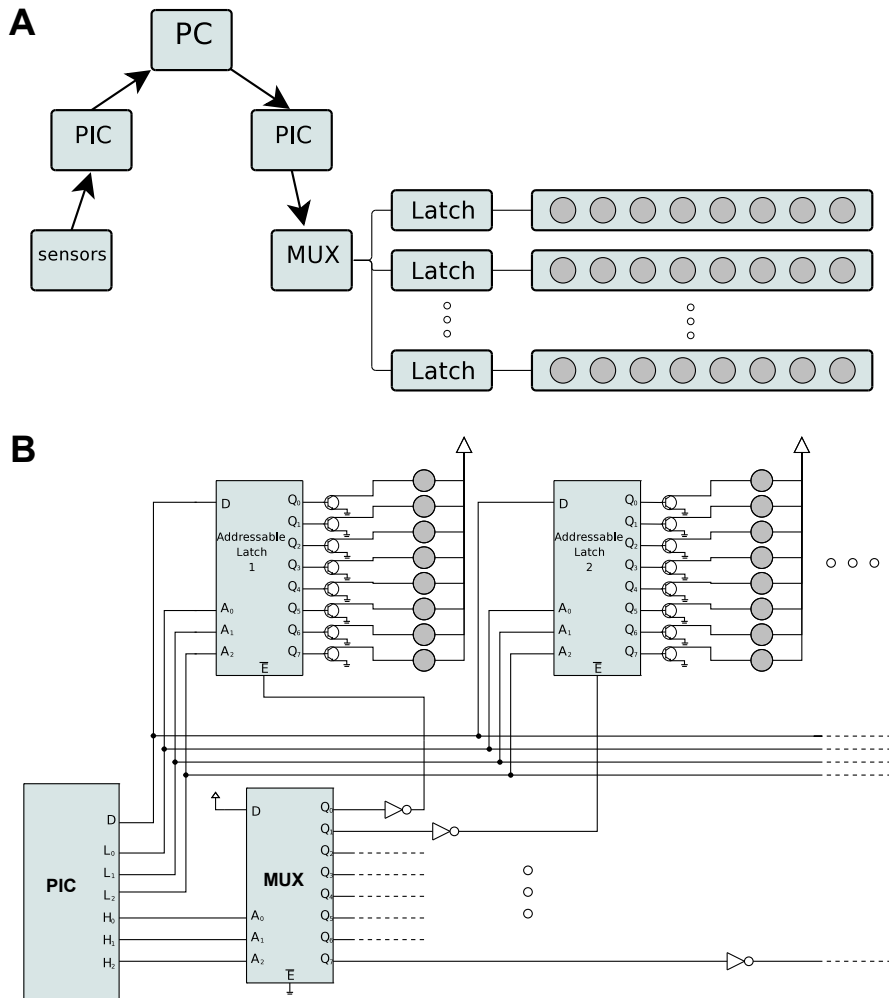


Figure 3.9: **Vibrotactile Feedback System Hardware Interface.** (A) Overview. (B) Connectivity Diagram.

1 or 0 according to its desired value; (v) Wait until the minimum data-ready time; (vi) Latch enable; (vii) Wait until the minimum latch time; and (viii) Latch disable.

In this thesis I use two different algorithms to control the motors. The first is a duty cycle encoding, the second is a combined pulse-width/frequency encoding.

Duty Cycle encoding The motors are updated by an on-chip algorithm cycling at 200Hz. Each cycle is discretised into 32 steps, each of duration $150\mu\text{s}$. Each motor is assigned a number m between 0 and 31 and is turned on for (m) time steps and off for the remaining ($31 - m$) steps. This allows discretised control of the duty cycle assigned to each motor.

Fig. 3.12 illustrates the microcontroller assembly language program to control the motors. The outer loop repeats at 200Hz making the system responsive to USB in-

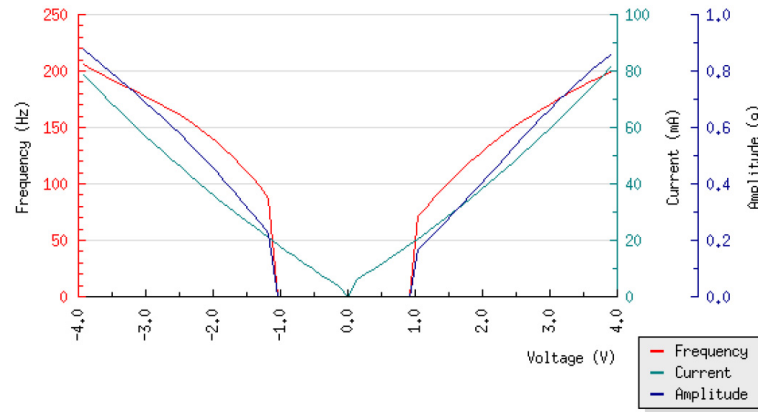


Figure 3.10: **Vibration Motor Performance.** [from data sheet for part 310-101 (Precision Microdrives, UK)]

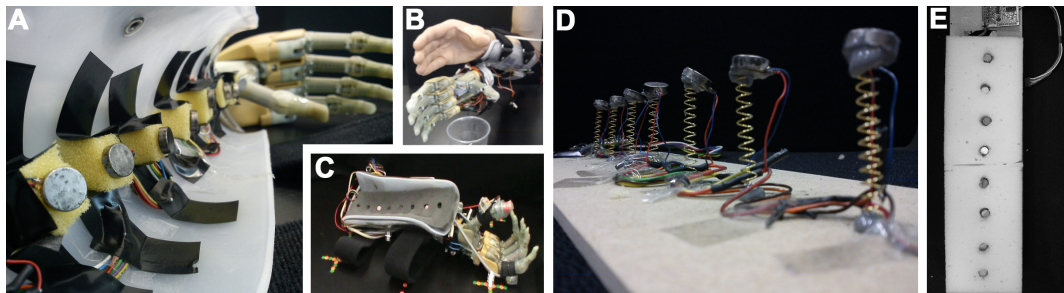


Figure 3.11: **Motor Mounting (A) Sponge-mounted vibrotactors.** A photograph of 8 vibrating motors mounted to the interior of the socket to provide tactile feedback to the subject. **(B)** A 'simulated amputation' subject is fitted with the robotic prosthesis via a custom made socket attached to the arm. **(C)** A finished socket with drilled sponge padding for comfort. **(D) Spring-mounted vibrotactors.** Photograph of 8 vibrating motors mounted on springs **(E)** The spring-mounted motors were housed in a drilled sponge casing to provide a surface sufficiently rigid on which to rest an arm, but soft enough that the spring-mounted motors could press firmly against the skin.

structions to change the motor amplitude. Fig. 3.13 shows the timing diagram for the microcontroller software.

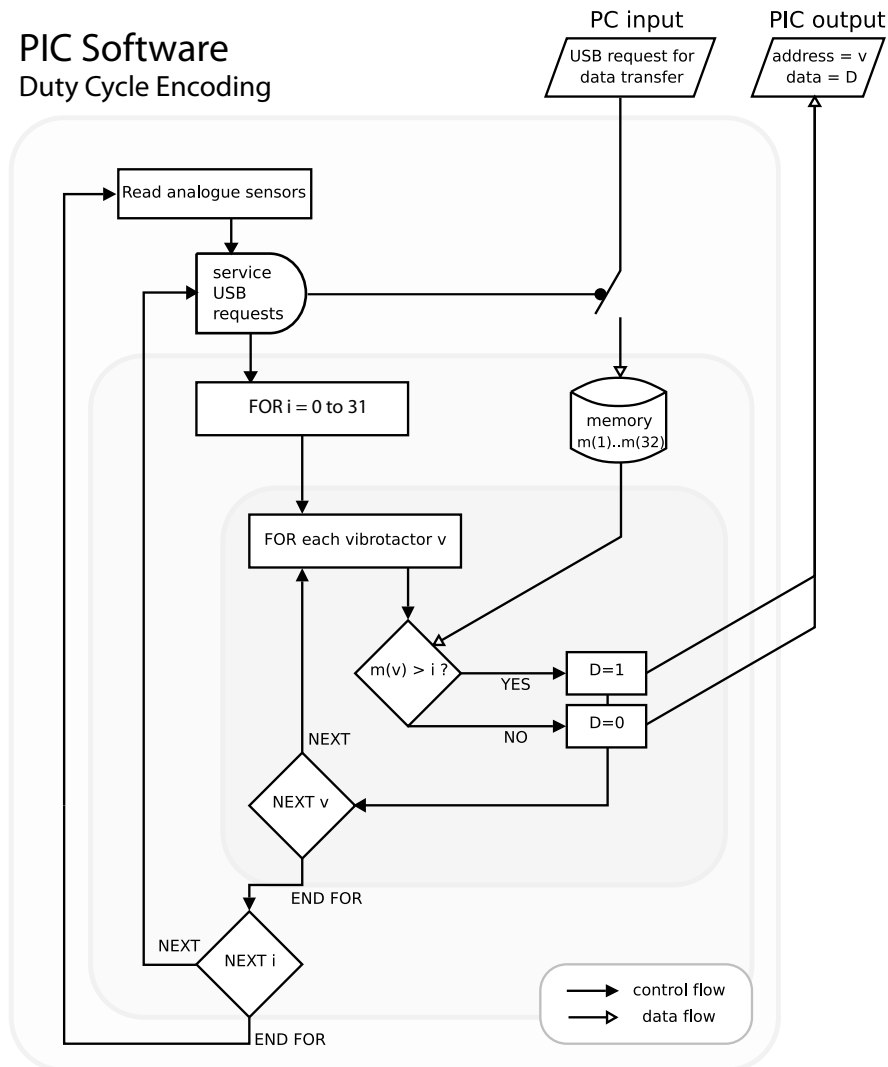


Figure 3.12: **Duty Cycle Encoding: Program.** The software services USB data transfer requests to update on-chip memory for each of the tactor channels. $m(v)$ is updated for each tactor v to sets its duty cycle and therefore vibration intensity.

Combined Frequency / Amplitude Encoding Jiang et al. (2009) recently showed that Multiple Sclerosis patients with different degrees of sensory loss were able to more accurately gauge grip forces with vibrotactile feedback. Their tactile code simultaneously modulated period and pulse width to increase the bandwidth of the channel. Based on this I implemented a system whereby pulse width and period can be independently modulated at a high temporal resolution, allowing for generation of a wide range of possible codes.

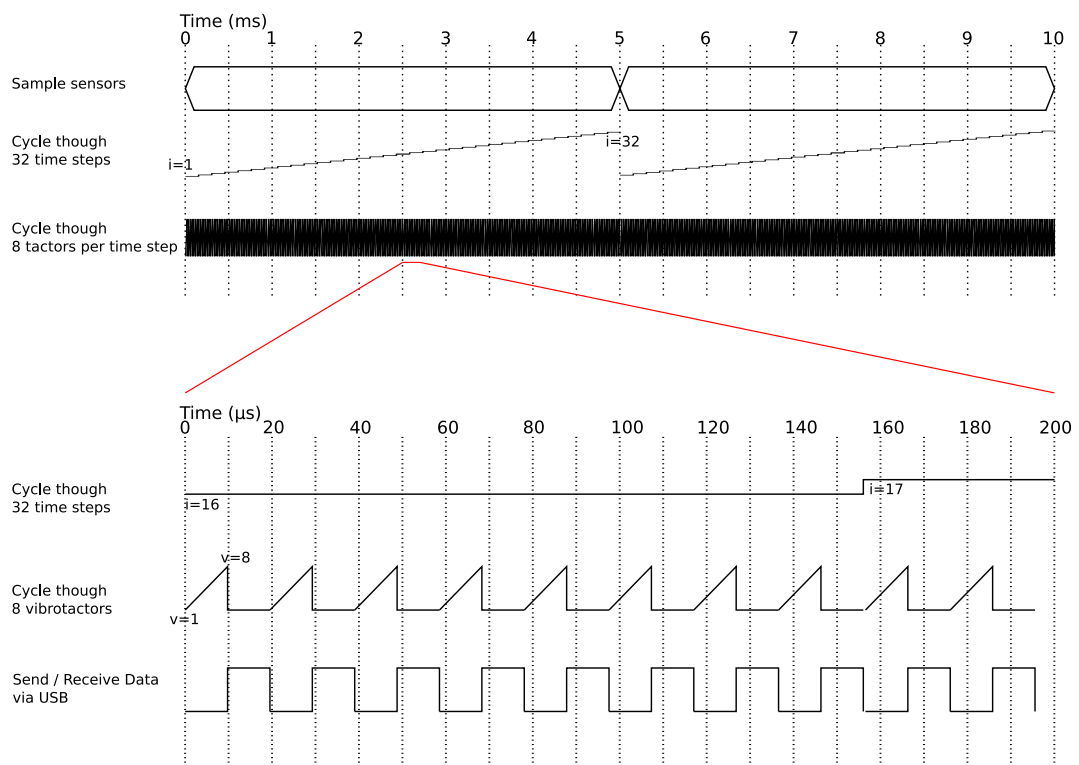


Figure 3.13: **Duty Cycle Encoding: Timing Diagram.** At a frequency of 200Hz the software reads analogue sensors, communicates with a PC via USB, and controls the vibration intensity of up to 32 factors

Cycling at a frequency of 2kHz, sensor values are streamed to the PC via USB and the motors are updated by USB requests. In the combined algorithm two values are set: the period, T , ranging from 0 to 255 (8 bits) and the pulse width, PW , ranging from 0 to 127 (7 bits). These values correspond to stimulation pulses occurring at a periods of 0ms to 1275ms in steps of 5ms, and lasting for 0ms to 63.5ms in steps of $500\mu\text{s}$. An additional bit is used to switch the multiplexor between different arrays to allow up to 16 channels, although in practice only 8 were used.

Fig. 3.12 illustrates the microcontroller assembly language program to control the motors.

A broader range of tactile stimuli can be encoded by this system in comparison to the duty cycle encoding. Indeed, the duty cycle method can be encoded by this system. Fig. 3.15 illustrates the modulation of pulse width, frequency and both simultaneously. By modulating both simultaneously it may be possible to exploit the skin's sensitivity to changes in amplitude at high frequency and changes in frequency at lower amplitude, providing a greater bandwidth of tactile information.

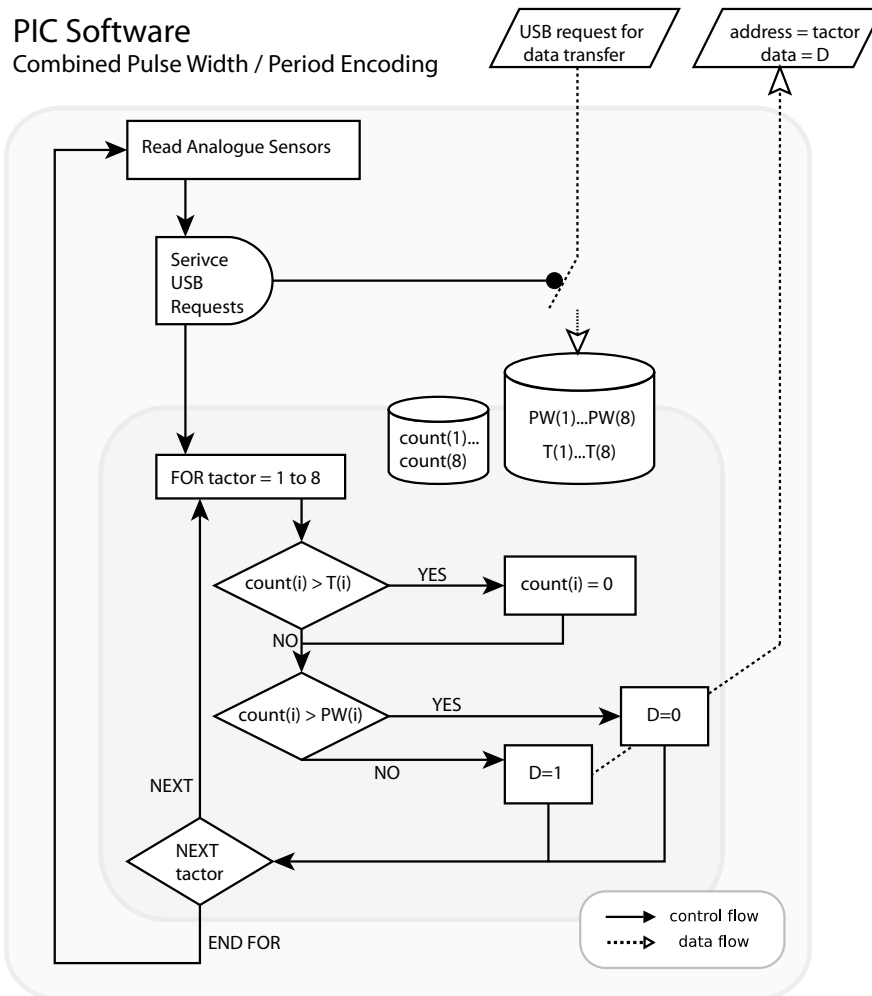


Figure 3.14: **Combined Encoding: Program.** The software services USB data transfer requests to update on-chip memory for each of the tactor channels. The number in memory location $m(v)$, sets to the duration to turn on the vibrating motor on output channel v , setting its duty cycle and therefore vibration intensity.

Feedback Encoding Reviewed in Chapter 2, Cholewiak and Collins (2003) investigated a number of parameters affecting vibrotactile localisation and perception. Body locus and tactor spacing are both significant factors in the successful interpretation of vibrotactile stimuli. I have explored a number of alternative encodings based on these findings.

Fig. 3.16 illustrates three typical encodings: (i) an *intensity* code, in which a single tactor may express a range of ‘intensities’ which defines a range of tactile percepts; (ii) a *spatial* code, in which the location of stimulation encodes the range of percepts; and (iii) an *interpolated* code, in which neighbouring tactors are co-simulated to create perceptual sensations localised between the tactors. It has been shown previously that

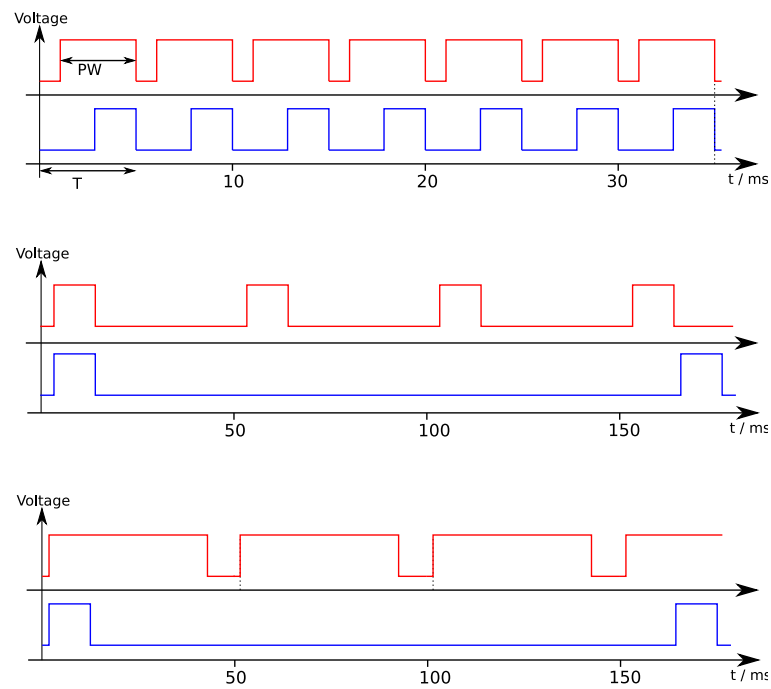


Figure 3.15: **Combined Encoding: Typical Waveforms.** An illustration of typical vibrotactile waveforms that can be produced with the hardware presented in this thesis; **(top)** Pulse Width Modulation (PWM): for the same period we can modulate the pulse width and thus the perception of changing intensity; **(middle)** Frequency Modulation (FM): for a fixed pulse width we can modulate the period of pulses and thus the perception of changing frequency; **(bottom)** Amplitude Based Feedback (ABF): based on the method employed by Jiang et al. (2009), pulse width and frequency are modulated together, providing a greater range of perceivable intensities.

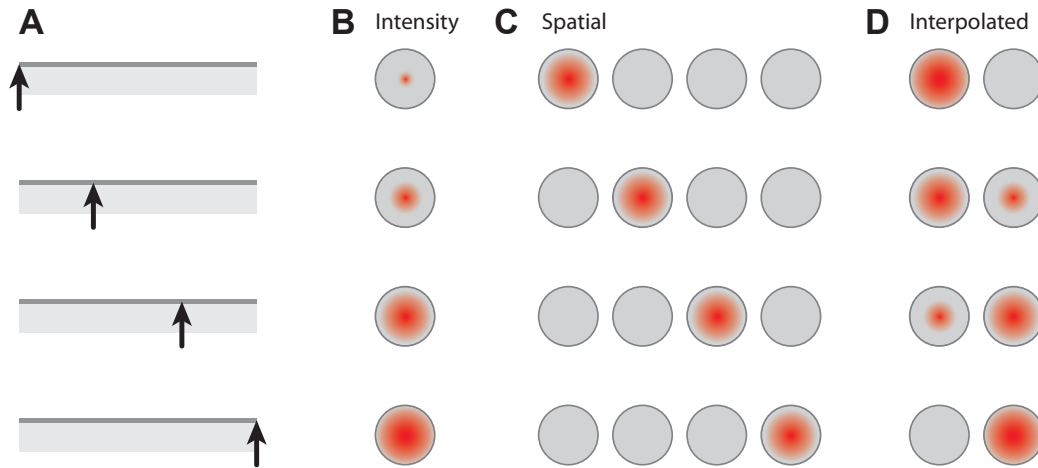


Figure 3.16: **Vibrotactile feedback encodings.** **(A)** Encoded signal **(B)** Intensity coding. Size of red blob indicates magnitude of stimulus ‘intensity’, for example duty cycle, frequency or amplitude. **(C)** Spatial encoding. The location of the activated factor encodes the signal. **(D)** Between-tactor sensations are created through co-stimulation of neighbouring factors.

spatial codes are particularly effective as they allow reliable encoding of signal magnitude (Kadkade et al., 2003), and may be less prone to adaptation compared to single tactor codes.

Encoding Methods ‘Intensity’ can itself be encoded in a number of ways. One could modify the duty cycle of stimulation, the frequency of stimulation, or the amplitude of stimulation.

Let us assume that we wish to encode a given signal x , ranging in intensity from 0 to $7a$ (for mathematical convenience). In the present hardware setup, a given tactor n is turned on with a pulse-width PW_n indexing into the range $[0\text{ms}, 0.5\text{ms}, \dots, 63.5\text{ms}]$, and a period T_n indexing into the range $[0\text{ms}, 5\text{ms}, \dots, 1275\text{ms}]$.

Three vibrotactile encodings are compared:

1. **Spatial Code** (equation 3.1, Fig. 3.17A)
2. **Duty-Cycle Code** (equation 3.2, Fig. 3.17B)
3. **Combined Pulse-Width / Period Code** (equation 3.3, Fig. 3.17C)

$$T_n = 40, \quad PW_n = \begin{cases} 0 & \text{if } x < (n-1)a \\ 0 & \text{if } x > (n+1)a \\ 40 * (1 - |\frac{x}{a} - n|) & \text{otherwise} \end{cases} \quad (3.1)$$

$$PW_n = 40 * (x/7a), \quad T_n = 80 \quad (3.2)$$

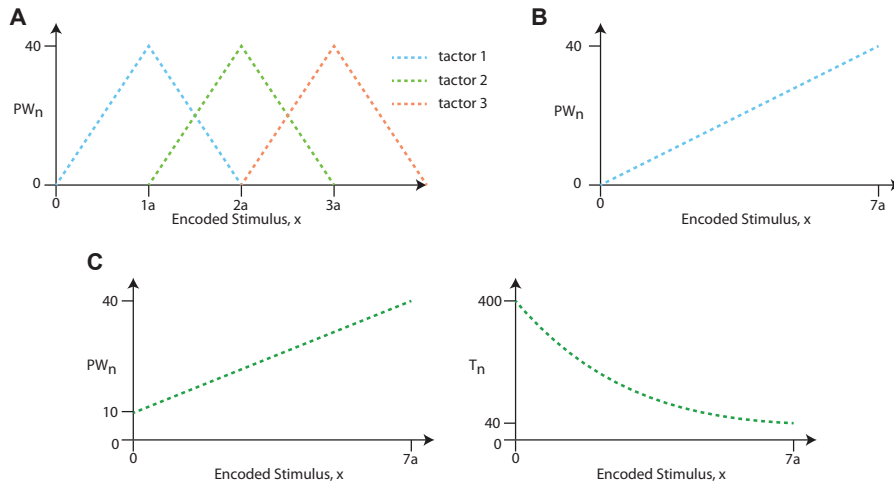


Figure 3.17: **Feedback parameters for different encodings. (A) Spatial Code, (B) Duty-Cycle Code, (C) Combined Pulse-Width / Period Code.**

$$PW_n = 10 + 30 * (x/7a), \quad T_n = 40 * [1/(1.1 - (x/7a))] \quad (3.3)$$

Note: equation 3.3 can be written in a parametric form, with parameters trained on subjective perception scores:

$$PW_n = b + c * (x/7a), \quad T_n = d * [1/(e - (x/7a))] \quad (3.4)$$

3.2.5.4 Software

A feedback encoding tool was developed to enable testing of different tactile encodings. This comprised a novel graphical user interface featuring a 2-D plot of pulse width and period. Users can ‘drag’ a stimulus through this space using the mouse whilst experiencing tactile stimuli on the arm. Fig. 3.18 provides a demonstration of this software tool.

The above software streams 16 bytes to the PIC microcontroller via a USB serial interface, corresponding to the period and pulse width of the 8 channels.

3.2.5.5 Alternative Feedback Systems

I also developed an electrotactile interface, which passes small safe levels of biphasic electric currents into the skin. The general principle involves passing small currents ($\sim 10\text{mA}$) for brief intervals ($\sim 100\mu\text{s}$) to the free nerve endings which reside in the dermis of the skin using surface-mounted electrodes. I have developed a low-cost electrode and a biphasic stimulator for this purpose, described in a separate report (Saunders

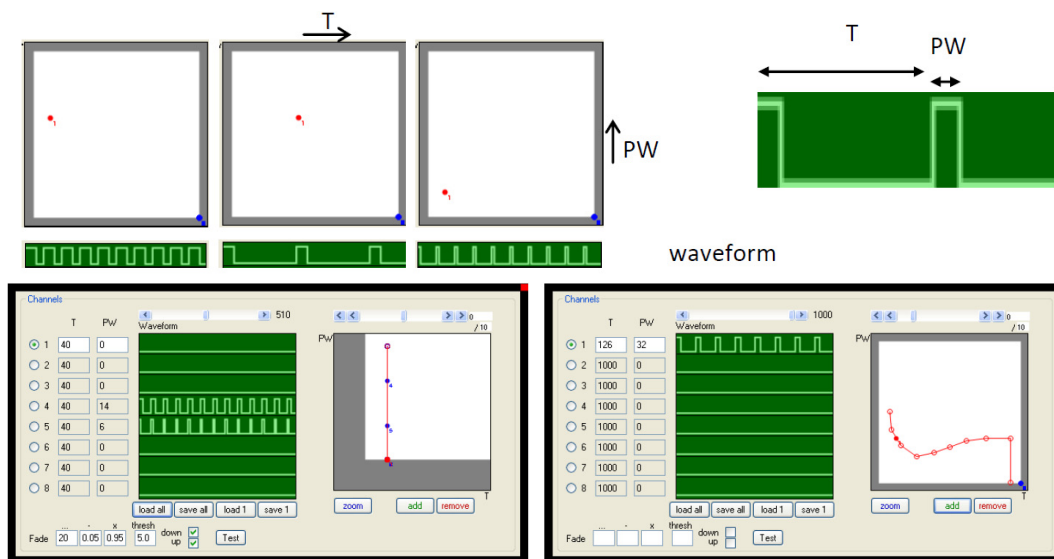


Figure 3.18: **Vibrotactile feedback encoding software.** Each motor can be assigned a different pulse width (PW) and period (T), creating a tactile waveforms modulated by these parameters (top right). This is represented by graphical interface in which stimuli can be dragged along these two dimensions (top left). A range of stimuli can be concatenated to form a feedback encoding. Multiple-tactor encodings, such as a spatial encoding (bottom left), allows for a greater perceptual range. An optimal single-tactor encoding can be created by simultaneously modulating the pulse-width and period (bottom right) to achieve greater bandwidth. Additional features such as 'fade' prevents the tactors from remaining on for too long – which can result in adaptation and decreased sensitivity.

and Vijayakumar, 2009). However, this thesis focuses on the vibrotactile stimulator described above.

3.2.6 Task: Vibrotactile Discrimination

3.2.6.1 Motivation

To choose the most appropriate tactile feedback code, a useful quantitative measure of the information content of different tactile codes is the channel bandwidth. The bandwidth of a perceptual property is often computed by measuring a subject’s discrimination ability when given two distinct stimuli. Reducing the distance between the stimuli decreases the perceptual discriminability, and the “75% just noticeable difference” (JND) threshold between two tactile stimuli measures the point perceptual discriminability at which stimuli are accurately distinguished 75% of the time. Such a measurement is made by asking subjects to choose one of two stimuli as satisfying some comparative perceptual property (such as which stimulus is more intense). JND thresholds vary as a function of tactile encoding (e.g. frequency, duty cycle, amplitude) as well as location and spacing of tactors (see Pongrac, 2006, Kohli et al., 2006, Kaczmarek et al., 1991, Szeto, 1982 reviewed in Chapter 2).

The results in this section are important for later experiments as they establish a baseline ‘quality’ of the tactile information, which may play a role in the degree to which subjects can utilise and integrate the information in the vibrotactile channel.

3.2.6.2 Methods

Overview I use a two-interval forced-choice (2-IFC) design to measure subjects discriminability of two stimuli. We use a “3 down, 1 up” *adaptive staircase* design to establish the 75% just-noticeable-difference (as recommended in García-Pérez, 1998). Subjects were presented with two successive vibrotactile stimuli (10ms duration, 3ms separation) and asked to report if the second stimulus was (a) located to the right or to the left of the first; or (b) more or less intense than the first, as appropriate.

Experiment 1 (N=1) In Pilot Experiment 1 I compared 3 tactile codes introduced previously: Pulse Width Modulation (PWM), Amplitude Based Feedback (ABF) and an interpolated spatial code (SM). One (trained) subject completed this pilot. A number of stimulus reference points were chosen for each encoding (5, 4 and 6 respectively), and 3 blocks of 20 comparisons were conducted for each reference stimulus, chosen according to the adaptive-staircase design. Further subjects were tested in an MSc project under my supervision (see Moraud, 2009).

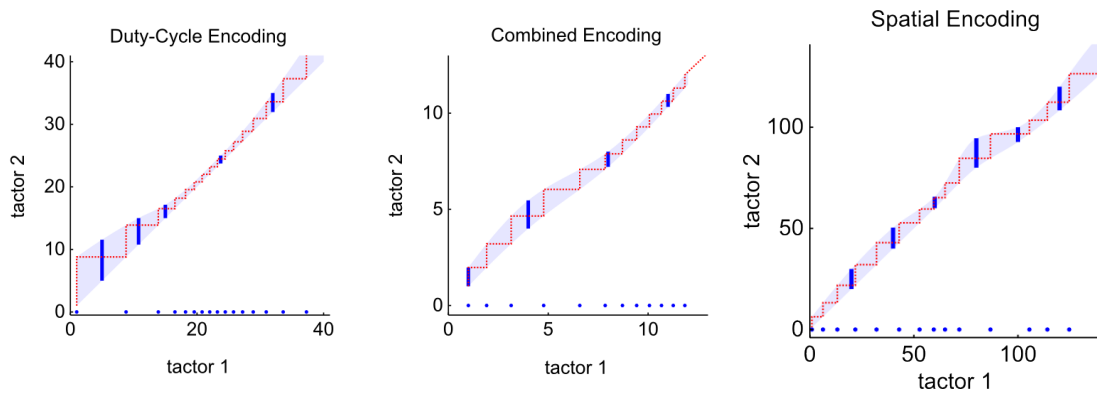


Figure 3.19: **JND performance for three encoding methods** Results of the vibrotactile discrimination experiment for three encoding methods. **(left)** duty cycle encoding, **(middle)** combined period/pulse-width, **(right)** spatial encoding

Experiment 2 (N=6) In Pilot Experiment 2 I tested the interpolated spatial code (SM) in 6 naive subjects. This was done at 6 reference locations along the forearm. Probe locations were chosen, as per the adaptive-staircase design, to converge on the 75% just-noticeable-difference (JND) threshold. This is the threshold at which subjects correctly determine the location on 75% of the trials, where chance is at 50%. Subjects received 20 pairs of stimuli for each location, which was sufficient to establish a per-subject psychometric curve and a per-location psychometric curve (across subjects).

3.2.6.3 Results

Experiment 1: spatial encoding provides greatest detectable range 75% JND thresholds is measured for three tactile encodings across a range of stimuli (see *methods*). These JND thresholds (indicated by dark blue bars in Fig. 3.19) are plotted across the space of possible stimulus values. From these curves I compute the number of perceptual levels attainable by drawing a steps from the lowest stimulus to the highest stimulus bounded by an interpolated region of indiscrimination. This defines the bandwidth of the encoding.

The three different feedback encodings have different perceptual qualities. The spatial encoding and the combined duty-cycle / frequency encoding were more uniform across stimulus space. The greatest bandwidth is achieved from the spatial and duty-cycle encodings. Consequently I chose to focus on the spatial encoding for the experimental work in later chapters of this thesis. Further investigation was the subject of Moraud (2009).

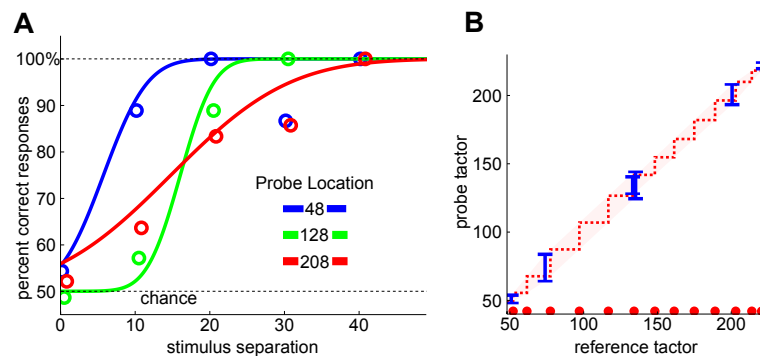


Figure 3.20: **Just Noticeable Difference (JND) experiment.** **(A)** Psychometric curves at three separate locations along the arm, starting from the wrist (location 0) to the elbow (location 255). The coloured circles correspond to average data when binned into groups of 10 data points. The psychometric curves are Cumulative Gaussians fit to the raw data over all subjects ($N=6$). **(B)** Sensitivity along the forearm can be plotted as a function of the success at distinguishing any two given factors. The 75% JND thresholds (blue bars) suggest a region of stimulus indistinguishability (red shaded region). From this region we calculate the number of just-distinguishable steps we can make. We plot a red blob at each step, showing that 12 just-distinguishable stimuli can be perceived along the forearm.

Experiment 2: spatial encoding is effective for naive subjects A cumulative Gaussian function was fit to the proportion of correct responses as a function of stimulus separation. Fig. 3.20A, shows curve fits at three locations along the arm. As the adaptive staircase method does not give evenly distributed points, I do not fit the curve to binned data (though it is shown for comparison). In Fig. 3.20B I plot the across-subject JND threshold as a function of location. The results indicate that at least 12 discriminable levels are attainable over the length of the forearm, and sensitivity increases near the wrist and elbow. These results are consistent with those previously reported in the literature (Cholewiak and Collins, 2003, Cholewiak et al., 2004). I was satisfied that this bandwidth of information was satisfactory for tasks in the present thesis.

3.2.7 Advanced Tasks

To extend the vibrotactile discrimination task discussed above, a battery of further experimental tasks to explore vibrotactile perception are covered in the following chapters of this thesis.

3.2.7.1 Vibrotactile Localisation

As a closed-loop alternative to passive vibrotactile discrimination, subjects can be asked to use feedback to perform a task (e.g. Szeto and Chung, 1986). In a simple arrangement

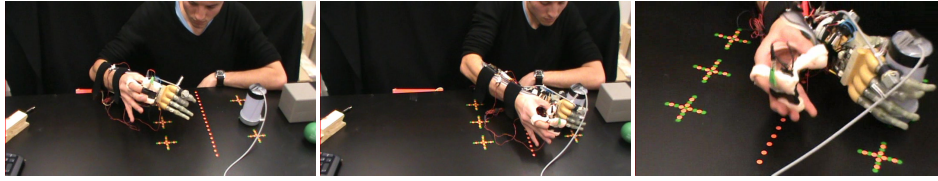


Figure 3.21: **Grasp, Lift and Move Task.**

a vibrotactile stimulus can be presented on the array and subjects are required to actively point to it. It may be moving continuously, requiring subjects to track it over time. In an alternative arrangement the vibrotactile stimulus is itself a cursor which subjects must move to a target location. Learning may be easier in this arrangement as subjects are in control of the cursor. These task variants are interactive and potentially more engaging and enjoyable for subjects to perform. Moreover, use of closed-loop tasks may facilitate greater learning (see Chapter 2), and are more relevant for understanding the role of feedback for sensorimotor control.

3.2.7.2 Vibrotactile Integration

The degree of sensory rehabilitation provided by a feedback system can be quantified by the level of integration with our existing healthy senses. Using the above discrimination and localisation tasks it is possible to measure vibrotactile localisation performance in the presence of a redundant modality. This task could be a cue integration task, requiring subjects to use both visual and tactile cues to localise a target. This has been well documented for healthy senses (e.g. Ernst and Banks, 2002, Alais and Burr, 2004) but for an artificial modality this has not been explored.

3.2.7.3 Grasp, Lift, Move and Hold

These tasks capture aspects of many ADLs, including planning, feedforward control and feedback control. These processes are well characterised in healthy and sensory-impaired individuals (e.g. Johansson and Westling, 1984, Nowak and Hermsdörfer, 2003, Hermsdörfer et al., 2008, discussed in Chapter 2). The task is illustrated in Fig. 3.21. Notably, healthy people scale grip and load force in parallel, grip economically (applying just enough force to avoid slip), and combine feedforward and feedback influences to coordinate such grasps. In the present thesis I extend the findings of this task to subjects fitted with a robotic prosthesis and artificial feedback of grip force.

3.2.7.4 Activities of Daily Living

Advanced ADLs are not covered in this thesis. Most of these tasks are particularly challenging for present day general purpose robotic prostheses, such as tying a shoelace; fastening a shirt button; writing with a pen; striking a match; and catching and throwing.

3.3 Discussion

In this chapter I have presented a number of key engineering developments necessary for the research which follows in Chapters 4, 5 and 6.

I have developed a responsive, 32-channel vibrotactile feedback system, incorporating original encoding methods: (i) an interpolated spatial code; and (ii) independent pulse-width/period encoding. I have evaluated these techniques using JND experiments and proven reasonable bandwidth with minimal training.

Further, I have written firmware for the iLIMB hand which has enabled: (i) differential force control; and (ii) proportional force control. This has involved novel engineering developments which are under license and patent application (Saunders et al., 2011a).

The control and feedback systems were incorporated into a modular design which may be seen as an experimental manipulandum for a range of tasks from basic tactile localisation through to ADLs. This has required the development of a ‘simulated amputation’ scenario. This is a novel approach to allow the decoupling of each component of the system to enable systematic evaluation and reduce the combinatorial complexity.

The focus of the remainder of the the thesis is experimental tasks involving the system described above. It is worthwhile to discuss the validity of the present approach and the potential limitations.

It should be noted that the spatially-encoded vibrotactile system offers reasonable bandwidth with minimal training. This is consistent with previous findings of the advantages of spatial codes. Kadkade et al. (2003) found that a spatial encoding was superior to a frequency-modulated code, and the above JND results reveal the superiority of a spatial encoding over a duty cycle encoding. Spatial codes are arguably better than single-factor codes for absolute judgement. However for detection of motion, Kohli et al. (2006) argue that spatial encodings are better suited to relative discrimination rather than absolute judgement of signal magnitude.

However, there are a number of limitations worth noting. There is a measurable 40ms lag time of motor accelerating to different speeds. This is same order of magnitude as healthy peripheral neural latency, and so may be tolerable. However, this is less responsive than (say) an electrotactile stimulator. For practical and safety reasons I argue that it is sufficient for the present purposes.

The use of JND experiments is suitable for measuring channel bandwidth but is less suited to measuring response latency or mental effort. These are parameters which may be tested by specific experimental investigation. However, tracking tasks (motivated by Kadkade et al., 2003, see Chapter 2), allows for high-level performance parameters such as sensory augmentation, integration and functional utility to be measured. The present system has sufficient bandwidth and is adequately responsive to study the questions of

sensorimotor and multisensory integration posed in Chapter 1.

Chapter 4

Estimating Sensory Uncertainty Over Time

Much research has exposed statistical-optimality in human perception and decision-making, suggesting indirectly that humans have explicit access to the uncertainty of both their senses and their decisions. In this chapter I introduce a novel visual tracking experiment that requires subjects to continuously report their evolving uncertainty over time. I show that subjects form an optimal continuous estimate of the mean, hindered only by natural kinematic constraints. Furthermore, I show that subjects have explicit access to a measure of their continuous objective uncertainty, rapidly acquired from sensory information available within a trial. However, this measure is limited by a conservative margin for error, suggesting that their reporting of uncertainty was less than optimal to achieve the goals of the task.

Relevant Publications

- Ian Saunders, Sethu Vijayakumar. (2012). **Continuous Evolution of Statistical Estimators for Optimal Decision-Making**. *PLoS ONE*
- Ian Saunders, Sethu Vijayakumar, (2011b) **Continuous Estimation of Mean and Uncertainty**, *Proc. The 21st Annual Conference of the Japanese Neural Network Society*.

4.1 Motivation

Uncertainty is present in every human action, and decisions are routinely made with incomplete knowledge of the world (Barthelmé and Mamassian, 2009). To handle uncertainty people make decisions based on previous experience as well as statistical information acquired directly from stimuli. The statistics of the environment govern our perceptions and our decision making processes when we reach for targets (Körding and Wolpert, 2004b, Tassinari et al., 2006, Faisal and Wolpert, 2009), interpret visual scenes (Jacobs, 1999, Hillis et al., 2004, Knill and Saunders, 2003) and combine multiple sensory modalities (Heron et al., 2004, Wallace et al., 2004, Ernst and Banks, 2002, Helbig and Ernst, 2008). This growing body of psychophysical experiments all support the proposition that many aspects of perception are statistically-optimal (Ernst, 2006, Ernst and Banks, 2002). That the human brain is optimised for statistical computations is perhaps unsurprising from an evolutionary viewpoint, but if true provides an elegant, mathematically principled model of perception. However, despite general agreement that it is of fundamental importance to the theory, the question of *how* humans gather the relevant statistical information to make their optimal decisions remains largely unexplored (Barthelmé and Mamassian, 2009).

The theory of statistical optimality in the brain relies crucially on the fact that humans must somehow accumulate statistical information from unpredictable stimuli. For example they may need to estimate not only the *mean*, but the expected variability in this estimate of the mean (or their *confidence*). Recently it was shown that humans are not only able to predict the position of objects moving along random or noisy trajectories, but also that they are able to report a level of confidence in this prediction (Graf et al., 2005). This is not a uniquely human capacity: rats are also capable of uncertainty-based decisions (Kepecs et al., 2008). Recently it was shown that subjective estimation of confidence is related to the *objective* uncertainty (Barthelmé and Mamassian, 2009), indicating that subjects may be acutely aware of the uncertainty in their decisions.

The forced-choice paradigm is classically used to compare decisions under uncertainty (e.g. Alais and Burr, 2004, Ernst and Banks, 2002). However, this method may be prone to bias (Helbig and Ernst, 2007), and does not *directly* capture the decision-making process (Graf et al., 2005). In this chapter I focus on a continuous decision-making task. In each trial, sensory evidence accumulates in the form of visual cues, with the mean and variance of these cues evolving as their number increases. With a continuous task we have the opportunity to look at the *process* of decision making, not just the outcome. By adding sensory uncertainty in the *temporal domain* I aim to characterise the role of *evolving* sensory evidence for *continuous* decision-making.

In this chapter I present a novel experimental paradigm that requires subjects to explicitly track the statistical properties of noise-perturbed visual cues over time. Two variants of the ‘butterfly catching’ task are devised to assess whether subjects can (i) track the *mean* of visual cues (*viz.* localising the butterfly); and (ii) indicate the *range* in which they believe the mean of the cues to lie (*viz.* choosing an appropriate size of net). From trial-to-trial the underlying spatiotemporal distribution of the cues is modulated, allowing observation of the evolution of mean and confidence estimates. This is coupled with a very simple model of sensorimotor latency to show the extent to which the observed trajectories are statistically-optimal with respect to the kinematic limitations of human motion. In addition, the evolving *weights* allocated to each cue over time are computed, to provide the first glimpse of the mechanisms underlying processes of continuous statistical estimation.

Phase	Task	Training	Structure			Configuration				Total No. of Trials
			No. of Sessions	Trials per Configuration	Pseudo-Random Cues	No. of Visual Uncertainties (σ)	No. of Perturbed Blocks (b)	No. of Perturbation Directions (p)	No. of Random-Length Trials	
1A	Mean	✓	3	15	✓	3	✗	✗	0	135
1B	Mean	✗	3	15	✓	3	✗	✗	0	135
2A	Conf.	✓	4	15	✓	3	✗	✗	0	180
2B	Conf	✗	1	15	✓	3	3	3	135	540

Table 4.1: **Experiment Structure.**

4.2 Methods

4.2.1 The Butterfly-Catching Paradigm

4.2.1.1 Overview

In this chapter I introduce the “butterfly catching” paradigm, illustrated in Fig. 4.1A. Visual stimuli are projected onto the line of subjects’ left forearm using a rear-projection screen and mirror as indicated. Subjects localise the stimuli with a variable sized “net”, indicated by lines projected from the forefinger and thumb of their right hand. They are successful in a given trial if the mean of the stimuli lies within the aperture of their net, and are awarded points for success. The stimuli are a sequence of blurry dot-clouds, which *jitter* (change location) randomly over the course of the trial. The trial duration is 3.75 seconds, in which time 15 visual cues are presented in locations $x_1 \dots x_{15}$ along the arm. Each cue x_i is selected from an approximate Normal distribution with mean μ and variance σ^2 (see Visual Stimuli).

I consider two task variants. In the *Mean Estimation* task I examine subjects’ ability to estimate the mean, μ , of the visual stimuli. In this variant the cursor has a *fixed aperture* (Fig. 4.1C, *left*), so that the separation of the subject’s finger and thumb does not change the size of the net. The maximum score is attained when subjects navigate to the true mean of the stimuli.

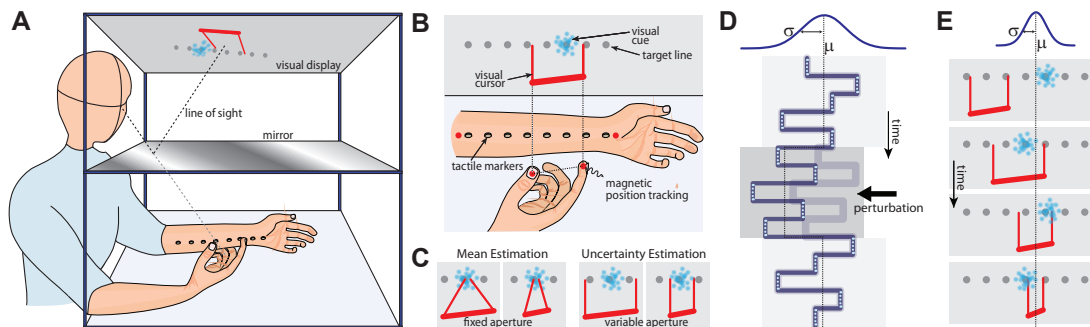


Figure 4.1: **Experiment Setup.** Illustration of the *butterfly catching experiment* setup. **(A) Projection Rig.** Subjects placed their left forearm under a mirror, and used their right hand to localise visual stimuli that appeared at random *target locations* along their arm. **(B) Cursor Control.** A 3D magnetic position tracking system is used to localise the arm and fingers, and an opaque mirror aligned with a rear-projection screen is used to presented visual feedback in the plane of the arm so that visual feedback of their arm and finger locations aligned veridically with the true finger and arm locations. **(C) Mean and Uncertainty Estimation.** Subjects performed two tasks: (i) In the mean estimation task they were asked to estimate the *mean* of the stimuli; (ii) in the confidence estimation task they were asked to indicate a *range* in which they believed the mean to lie. These two variants allowed us to establish (i) the objective uncertainty and (ii) subjective perception of the objective uncertainty. For the mean estimation task the aperture of the cursor was fixed for all trials, so that only the average position of the thumb and forefinger would determine the outcome. For the uncertainty estimation task subjects were able to control a *confidence window* using their thumb and forefinger. To penalise larger apertures, subjects were awarded a higher score for a narrower range. **(D) Task and Manipulations.** A total of 15 visual cues were presented in each trial. Each cue, lasting 250ms, was chosen from an underlying distribution with mean μ and variance σ^2 . On each trial σ was chosen at random to manipulate the uncertainty of the cue distribution. The sequence of cues was divided into the three blocks, and on catch trials one of these blocks was randomly perturbed in a given direction. The direction of the perturbation was either negative, zero, or positive, and the magnitude of perturbation was $0.3 \cdot \sigma$, a small fraction of the cue distribution. In the figure a negative perturbation of the second block is shown. **(E) Example.** Over the course of a trial, subjects should navigate the cursor towards the target, μ , which they can estimate from the cues. In the uncertainty estimation task they should decrease the aperture of the cursor as their confidence increases.

In the *Confidence Estimation* task subjects must instead indicate the *range of values* in which they believe the mean to lie, using a cursor with *variable aperture* (Fig. 4.1C, *right*), with width determined by the spacing between the thumb and forefinger. They are awarded more points for picking a narrower range, encouraging a trade-off between probability of success and point-scoring. The score function is designed such that the expected score is maximised when subjects choose a confidence range that spans 1 standard deviation of their *objective* performance distribution on either side of the mean. Hence, the maximum score is attained when subjects correctly compute the uncertainty in their estimate of the mean of the stimuli.

4.2.1.2 Task Manipulations

The purpose of this study is to understand the sensory processes involved in forming estimates of mean and uncertainty. By distributing the sensory evidence into a sequence of cues over time we can observe sensorimotor processes in action. In order that our data can inform us on the decision-making process the distributions of the stimuli are manipulated from trial-to-trial in two ways: (i) by modulating the variance of the visual cues; and (ii) by adding perturbations to subsets of the cues.

By manipulating the cue variance, σ^2 , randomly from trial to trial we can observe subjects' ability to localise the mean and report their uncertainty on a *per-trial* basis. Based on Barthelmé and Mamassian (2009) I hypothesised that subjects would be able to report the objective variability in their performance, and therefore an increase in cue variance should be reflected in both an increased distribution of errors in localising the mean and decreased confidence. σ is chosen from the range {50, 120, 200} pixels, hereafter *low*, *medium* and *high* uncertainty.

The sequence of cues on a given trial is divided into three subsets (*early*, *middle* and *late*). Perturbations are induced in a *negative* (leftward), *positive* (rightward) or *neutral* (no perturbation) direction to a chosen subset, randomly from trial-to-trial. For example, in 4.1C a negative perturbation of the middle subset is shown. By enumerating all nine possible combinations of perturbation onset and direction we can assess the role of cues at all stages of the trial. Note that there is no difference between trials with neutral perturbations, so these data are pooled in our analyses. The magnitude of non-zero perturbations is $0.3 \cdot \sigma$, a fraction of the spread of the cues.

In order to interpret the subtle effects of these manipulations robustly I designed a pseudo-random cue sequence that appears Normally distributed (see Visual Stimuli). Subjects completed 15 trials for each manipulation, and completed several sessions each with different sets of cue sequences. All trials and sessions were randomly intermixed. On every trial the target location μ was randomised.

Finally, trials of shorter duration were added into the sequence (of lengths 5, 10 and 15 cues). One-sixth of the trials were of this nature, but these trials did not contribute to the analysis. They were included to encourage *continuous behaviour* as subjects would not know when each trial was going to end. See Fig. 4.1 for further details on which manipulations were used for each part of the experiment.

4.2.2 Experimental Methodology

4.2.2.1 Subjects

Fourteen volunteers participated in this experimental study. All subjects were healthy, right-handed and aged between 21 and 30. All subjects had normal, or corrected-to-normal eyesight. All of the subjects were naive to the experimental manipulations and the experimental rig. Subjects gave written informed consent before participation in the study and received financial compensation for their time (approximately 90 minutes per subject).

4.2.2.2 Structure

Table 4.1 describes the structure of the experiment. Each subject performed 990 trials in total across four experimental phases. The first part of the experiment examined subjects' ability to estimate the *mean* of a jittering visual cursor, split into a training phase (*1A*) and a test phase (*1B*). The second part examined the subject's ability to report their *confidence* in this estimate, again with a training phase (*2A*) and a test phase (*2B*). Subjects performed several sessions in each phase to improve data integrity. On each trial stimulus uncertainty σ was varied (*low*, *medium* and *high*), to allow measurement of subjective perception of uncertainty. In the final phase (*2B*) a small random perturbation (0.3σ) was added to one third of the cues, varying the perturbed block b (*early*, *middle* and *late*) and direction of perturbation p (*negative*, *zero* and *positive*) from trial-to-trial. This would allow the effect of each cue in the decision making process to be measured. Occasional trials of random duration were included to encourage subjects to estimate continuously. All sessions and trials were randomly shuffled within a phase. There were 27 experimental configurations for phase *2B*, for each combination of $\sigma \times p \times b$. and 3 configurations for *1A*, *1B* and *2A*.

4.2.2.3 Mean Estimation Task

In the mean estimation phases the cursor had a small fixed-aperture, as shown in Fig. 4.1C, *left*. Subjects were instructed to place their left forearm under an opaque mirror onto an array of tactile markers (Fig. 4.1A and B). The markers served as a tactile ref-

erence frame, consistent and veridical with the visual display. Using the rear-projection mirror setup as illustrated in Fig. 4.1A, visual feedback was given in the plane of the arm so that feedback of the arm and finger locations aligned veridically with the true finger and arm locations, to ensure no confounding effects of visuo-spatial mismatch (as discussed in Gepshtein et al. (2005)).

Each subjects underwent an initial training period so that they could familiarise themselves with the task (phase 1A), followed by a large block of trials to assess their mean estimation performance, varying visual uncertainty, σ , from trial-to-trial (phase 1B).

4.2.2.4 Confidence Estimation Task

In the confidence estimation phases the role of visual cues for the estimation of mean and uncertainty were examined simultaneously. To succeed at the task subjects were required to accumulate sensory evidence over time to establish an estimate of these statistical properties.

Subjects were instructed to indicate the *range* in which they believed the mean to lie, using the variable aperture cursor controlled by their thumb and forefinger as shown in Fig. 4.1C, *right*, corresponding to the confidence in their mean estimate. In order to assess the ability of subjects to discriminate uncertainty the width of the distribution of jittering stimuli, σ , was varied from trial-to-trial (Fig. 4.1D). In order to assess the role of individual cues for decision making, blocks of trials were perturbed by small amounts ($\pm 0.3\sigma$) in random directions from trial-to-trial (see *Task Manipulations*).

Each subjects underwent an initial training period so that they could familiarise themselves with the task (phase 2A). Following this, each subject performed a large block of trials to assess their uncertainty estimation performance as visual uncertainty, perturbation block, perturbation magnitude and trial duration were varied from trial-to-trial (phase 2B).

Subjects were awarded a higher score for a narrower confidence interval (see *Performance Feedback*). It was intended that this would encourage subjects to aim for the interval that corresponded to the expected objective variability.

4.2.2.5 Performance Feedback

To motivate subjects in the confidence estimation task they were assigned a score on each trial. On completion of a trial it is assumed that subjects have positioned their right hand to indicate a confidence window of width d around their estimate of the mean, $\hat{\mu}$. The score function, $S(\hat{\mu}, d)$, assigns a per-trial score according to:

$$S(\hat{\mu}, d) = \begin{cases} R(d) & \text{if } |\hat{\mu} - \mu| \leq \frac{d}{2} \\ 0 & \text{if } |\hat{\mu} - \mu| > \frac{d}{2} \end{cases} \quad (4.1)$$

$$R(d) = \begin{cases} 10 & \text{if } d \leq \sigma_{target} \\ 10 \cdot \left(\frac{\sigma_{target}}{d}\right)^2 & \text{if } d > \sigma_{target} \end{cases} \quad (4.2)$$

Equation 4.1 captures success or failure to locate the true mean within the confidence window. If successful, equation 4.2 assigns a reward. The reward function penalises apertures larger than d_{target} . In our experiment, d_{target} is calculated for each subject based on the mean variability empirically observed in experiment phase 1B. For convenience, this is computed as the *objective error*, E_σ , the mean absolute endpoint deviation (error) for each σ in the mean estimation task:

$$E_\sigma = \frac{1}{N} \sum_n |x_n(T) - \mu_n| \quad (4.3)$$

In the confidence estimation task, d_{target} is set to twice the objective error, defining the target *objective error range*.

$$d_{target} = 2 \cdot E_\sigma \quad (4.4)$$

If subjects pick an aperture smaller than d_{target} this decreases the probability of success, while an aperture larger than d_{target} decreases the score. The reward function in equation 4.2 ensures that the overall maximum expected reward is achieved by choosing an aperture of exactly d_{target} . This method, therefore, encourages subjects to estimate their own *objective error range*. For more detail, see Appendix A.

In our task, if subjects are to maximise their expected gain (as in Trommershäuser et al., 2003) then they need explicit knowledge of their objective error. Subjects are adequately prepared to learn such a property (having performed 450 trials prior to the confidence estimation task). It has been recently shown that subjects have access to their objective uncertainty in a binary decision task of slant estimation (Barthelmé and Mamassian, 2009, 2010). The objective uncertainty in the task can only be estimated based on the stimuli observed within a trial, and therefore this task should expose the cue-driven mechanisms of acquiring this estimate.

4.2.2.6 Apparatus and Data Collection

Accurate three dimensional tracking of the arm and fingertips was achieved using a Polhemus Liberty 240Hz 8-sensor motion tracking system (POLHEMUS, USA). Arm and fingertip positions were sampled at a frequency of 20Hz (50ms) and logged data using custom personal computer (PC) software. The same PC software was responsible for

displaying and logging the stimuli, ensuring that our data and stimuli were temporally calibrated.

4.2.2.7 Visual Stimuli

15 Visual Cues are presented in each trial. For mathematical convenience let us describe the visual cues as a sequence defined by the locations x_1, \dots, x_{15} , where each x_i is drawn from an underlying pseudo-Normal distribution with mean μ and variance $\propto \sigma^2$. Each visual cue is presented for 250ms, described as “jittering” over time.

Each visual cue x_i comprises 5 frames. Each frame comprises a cloud of ten random blobs distributed with a standard deviation of 10 pixels in each direction, centred on the cue location x_i . Each of the blobs is a low-contrast 2-dimensional Gaussian of radius 8 pixels (see (Alais and Burr, 2004)). Using clouds of blobs adds uncertainty to a subject’s ability to localise a single cue and provides a way to modulate the underlying difficulty of the task. In this experiment the cloud parameters were not modulated.

Each visual cue x_i is chosen according to a pseudo-random sequence, using the algorithm illustrated in Fig. 4.2. The algorithm generates a block of 15 trials, where each trial contains a sequence of 15 cues. A matrix of cue indices C , with columns for trials and rows for cues for dictates the order cues on a trial, with each entry $c_{i,j} \in \{1, \dots, 15\}$. The algorithm is designed to maximise the unpredictability of each trial while maintaining the following constraints:

- (i) each cue index appears once and only once in each trial,

$$\forall i, n, j . i \neq j \implies c_{i,n} \neq c_{j,n} \quad (4.5)$$

- (ii) each cue appears at each time t once and only once across trials within the block,

$$\forall i, n, m . n \neq m \implies c_{i,n} \neq c_{i,m} \quad (4.6)$$

- (iii) The mean of each third of the trials, averaged over all trials, is exactly zero,

$$\sum_n \sum_{b=0}^2 \sum_{i=5b+1}^{5(b+1)} c_{i,n} = 0 \quad (4.7)$$

- (iv) the variance of each third of the trials, averaged over all trials, is constant,

$$\frac{1}{15} \sum_n \frac{1}{3} \sum_{b=0}^2 \frac{1}{5} \sum_{i=5b+1}^{5(b+1)} \left(c_{i,n} - \sum_{j=5b+1}^{5(b+1)} (c_{j,n}) \right)^2 = 1 \quad (4.8)$$

These constraints were designed to enable effective data analysis without imposing *uncontrolled* sources of uncertainty. By using this method each cue has equal weight and should contribute equally (on average) to subject’s decisions. *Controlled* uncertainty could then be introduced to the sequences as described below.

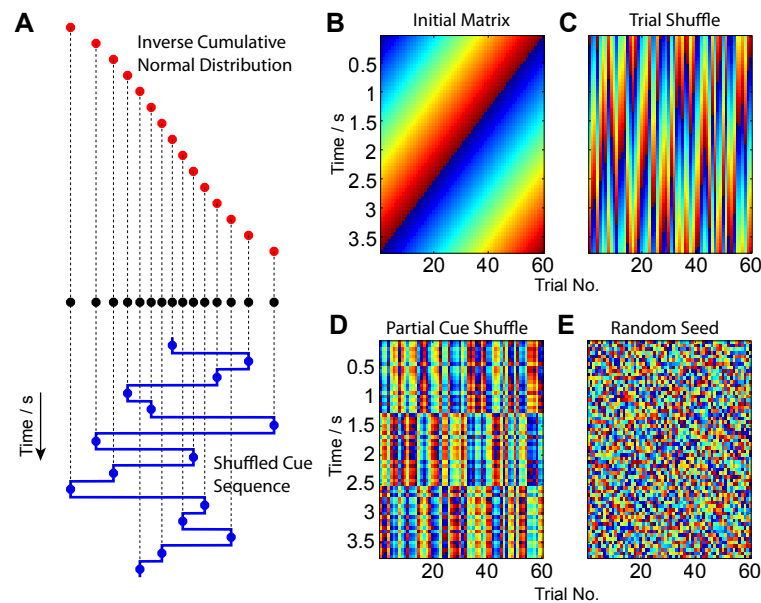


Figure 4.2: **Pseudo-Random Cue Sequence Generation.** This figure illustrates the Saundoku Algorithm for generating pseudo-random cue sequences. The purpose of this method is to ensure that cues are counterbalanced across trials so as to minimise systematic biases to the data, while at the same time presenting no additional information to subjects to aid their success at the task. **(A) Cue generation.** The sequence of cues to be used for a trial are generated from a pseudo-Normal distribution, created by sampling the Inverse cumulative Normal distribution function at equally spaced intervals (red blobs). The output (black blobs) is distributed *pseudo-Normally*, i.e. as the number of samples increases the histogram of the samples converges on the Normal probability density function. These samples are shuffled (blue blobs) to provide a cue sequence. The method of shuffling is illustrated in sub-plots B-E. **(B) Initial Cues.** A square *shuffle matrix* is created with rows for cue number (in time) and columns for trial number. Each matrix entry corresponds to a cue generated in sub-plot A. The matrix is initialised with diagonals to ensure that each cue appears only once in each trial, and once in every trial. In the figure for clarity I show 60 cues per trial and therefore 60 trials per condition, but in practice only 15 cues per trial and 15 trials per condition were presented. **(C) Trial Shuffle.** The order of trials was randomised to reduce the correlation between neighbouring trials. This does not violate the constraint that each cue appears only once in each sequence, and in every trial. **(D) Partial Cue shuffle.** The order of cues within each trial are randomised, but limited the first, second and final third of the sequence. This maintains the constraint that each cue appears only once in each sequence, and in every trial, and adds the additional constraint that each third contains all cues an equal number of times. **(E) Random Seed.** Finally, each entry of the matrix indexes into the shuffled pseudo-Normal sequence in sub-plot A. The resulting plot appears completely random, but the correlations between trials and the average mean and variance for the first, second and final third of trials are known across all trials.

To generate each x_i on a given trial j , $c_{i,j}$ is used as an index into a randomly shuffled pseudo-Normal sequence $N = n_1, \dots, n_{15}$ (generated by taking uniformly-spaced samples from the inverse cumulative Normal distribution, then shuffled randomly). Spatial uncertainty is added by multiplying by σ , and perturbations are added by shifting the mean of one third of the cues by $p \cdot 0.3\sigma$, where the direction of the perturbation $p \in \{-1, 0, 1\}$ and the block to perturb is $b \in \{0, 1, 2\}$. Each trial is also assigned a random target location, μ . Hence,

$$x_i = \mu + \sigma \cdot N_{c_{i,j}} + \begin{cases} p \cdot 0.3\sigma & \text{if } 5n + 1 \leq i \leq 5(n + 1) \\ 0 & \text{otherwise} \end{cases} \quad (4.9)$$

This was repeated using the same C and N for all experimental configurations. Subjects completed multiple sessions for each phase of the experiment (see Fig. 4.1) using some or all of the above manipulations. Each session used different instantiations of C and N , and all sessions within each phase of the experiment were shuffled randomly together. Each subject had different instantiations of C and N .

4.2.3 Data Analysis

4.2.3.1 The Ideal Observer

During a trial, as samples accumulate an *ideal observer* would accurately estimate the sample mean and sample variance of the cues thus far seen and make statistically-optimal decisions based on this available evidence. Given k cues x_1, \dots, x_k the maximum-likelihood unbiased estimates of the mean and variance are given by:

$$\hat{\mu}_k = \frac{1}{k} \sum_{i=1}^k x_i \quad (4.10)$$

$$\hat{\sigma}_k^2 = \frac{1}{k-1} \sum_{i=1}^k (x_i - \hat{\mu})^2 \quad (4.11)$$

In the *mean estimation* task the observer's ideal strategy is to select $\hat{\mu}_k$ at time k .

Subjects can optimally estimate the uncertainty of clusters of noisy visual samples as a function of k (Tassinari et al., 2006), although in this study the noisy clusters are distributed in *time* rather than *space*. One can show that the variance of the sample mean estimator is given by

$$\mathbb{V}[\hat{\mu}_k] = \mathbb{E}[(\hat{\mu}_k - \mu)^2] = \frac{\sigma_k^2}{k} \quad (4.12)$$

Thus, in the *confidence estimation* task the ideal observer strategy at time k is to select a confidence interval equal to $2 \cdot \sqrt{\frac{2}{\pi k}} \cdot \sigma_k$, which is equal to the objective error

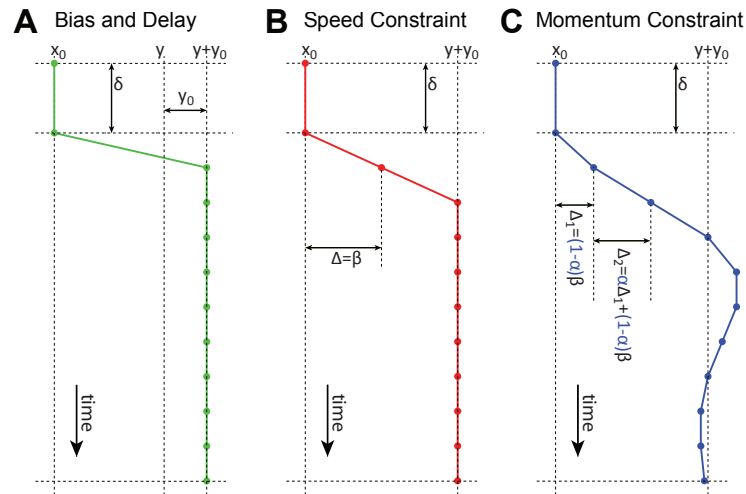


Figure 4.3: **Model of Sensorimotor Kinematics.** In order to explain subject's evolving trajectories over time, the inevitable kinematic constraints on movement are modelled. In the model it is assumed that, other than these limitations, subjects will behave as ideal observers. At time t , let an observer be in position x_t . To reach a target y they make a displacement of Δ_t . This figure illustrates the components of the model. **(A) Bias and Delay.** The model assumes that there is some delay, δ , before subjects initiate their movement. This captures sensory, processing and motor delays. Subjects may have some inherent bias in one direction or another, due to the configuration of the experiment or otherwise, captured by an (optional) bias parameter y_0 **(B) Speed Constraint.** A maximum speed, β , limits the speed at which the hand or fingers can move. **(C) Momentum Constraint.** On the assumption that subjects can not accelerate instantaneously, a smoothing parameter α constrains Δ_t .

range. This is because the score is maximised when a subject reports the objective uncertainty (as described in Performance Feedback). For more detail, see Appendix A. Maximum likelihood provides a principled description of optimal behaviour that has been observed in a number of studies.

4.2.3.2 Sensorimotor Delay Model

The ideal observer can perform instantaneous computations and act on sensory information immediately. Human beings, on the other hand, can not. In the presence of inevitable sensory, processing and motor delays and noise how would the ideal observer now perform? Let us define an ideal-observer model constrained by the three global parameters, δ , α and β , capturing natural kinematic constraints on hand motion.

Suppose the observer has witnessed k cues by time $t + \delta$. Modified estimates of mean and variance are derived from equations 4.10 and 4.11:

$$\hat{\mu}_{t+\delta} = \frac{1}{k} \sum_{i=1}^k x_i \quad (4.13)$$

$$\hat{\sigma}_{t+\delta}^2 = \frac{1}{k-1} \sum_{i=1}^k (x_i - \hat{\mu}_{t+\delta})^2 \quad (4.14)$$

In the mean estimation task subjects can compute $\hat{\mu}_t$ from equation 4.13 to form their time-delayed internal estimate of the mean.

In the confidence estimation task subjects are expected to estimate their objective uncertainty. From equation 4.14 the observer can calculate the time-delayed variance estimate $\hat{\sigma}_t^2$, but they need to have learned how to relate this to the objective error range d_{target} (equation 4.4) to achieve optimal performance in the task. This is accomplished by performing a linear regression (using data from the mean estimation task) to compute m_σ and c_σ in the relationship

$$d_{target} = m_\sigma \cdot \hat{\sigma}_t + c_\sigma \quad (4.15)$$

allowing the observer to choose the optimal confidence window from stimuli observed within a trial.

In addition to sensory delays I introduce two motion constraints. At time t let the *reported estimate* (i.e. the position of the cursor) be x_t , and the *perceived estimate* (i.e. our time-delayed internal estimate of the mean) be y_t . Let the observer make discrete steps of size Δ_t so that the reported estimate smoothly converges on the perceived estimate. The model constrains motion using two parameters: a maximum speed parameter, β , constrains the maximum displacement made by the observer in a given time-step; and a momentum parameter, α , prevents sudden speed changes by smoothing these displacements over time. i.e.

$$x_t = x_{t-1} + \Delta_t \quad (4.16)$$

$$\Delta_t = (1 - \alpha) \cdot f(y_t - x_{t-1}) + \alpha \cdot \Delta_{t-1} \quad (4.17)$$

$$f(z) = \begin{cases} z & \text{if } |z| < \beta \\ +\beta & \text{if } z \geq \beta \\ -\beta & \text{if } z \leq -\beta \end{cases} \quad (4.18)$$

Note that the model applies to both mean and confidence judgements: For the mean estimation task, I set $y_t = \hat{\mu}_t$, and for the confidence estimation task I replace x_t with w_t (the width of the cursor at time t) and set $y_t = \sqrt{\frac{15}{k}} \cdot d_{target}$.

One additional parameter was added to the confidence estimation model: a *bias* term, y_0 . In equation 4.17 this replaces the term y_t with $y_t + y_0$. This can be thought of as a safety margin or constant systematic error. This is considered a suboptimal component of the model, while the other parameters capture natural kinematic limitations.

Fig. 4.3 illustrates the effect of each of these parameters on model trajectories.

4.2.3.3 Weight Regression

To compute the contribution of each cue in the temporal sequence to the empirical trajectories observed, a multiple linear regression is performed at each time-step.

For the mean estimation task the non-negative weight least-squares algorithm described in [Lawson and Hanson \(1974\)](#) is used at each time-step to regress all of the cues for a trial (including those not yet seen), plus an additional constant, to the position of the cursor at that time. On trial n let the sequence of cues x_1^n, \dots, x_{15}^n result in the trajectory $Y_n = [y_1^n, \dots, y_T^n]^\dagger$ taken by the subject. To compute the weights assigned to the cues over all such trajectories a matrix, C , is formed, which contains columns for each of the N trials. Each column contains a constant term and the K visual cues for the corresponding trial:

$$C = \begin{bmatrix} 1, & \dots & 1 \\ c_1^1, & \dots & c_1^N \\ \vdots & \ddots & \vdots \\ c_K^1, & \dots & c_K^N \end{bmatrix}$$

A trajectory matrix Y , is also formed, containing columns for each of the N trials. Each column contains the recorded trajectory for the corresponding trial:

$$Y = [Y_1, \dots, Y_N] = \begin{bmatrix} y^1(1), & \dots & y^N(1) \\ \vdots & \ddots & \vdots \\ y^1(T), & \dots & y^N(T) \end{bmatrix}$$

The purpose of the regression is to compute a weight matrix W that minimises the error in the mapping $Y = WC$, where

$$W = \begin{bmatrix} s_1, & w_1(1), & \dots & w_K(1) \\ \vdots & \vdots & \ddots & \vdots \\ s_T, & w_1(T), & \dots & w_K(T) \end{bmatrix}$$

The regression method described in [Lawson and Hanson \(1974\)](#) is applied in a row-wise manner, i.e. for each time-step t . The resulting weight matrix W can be decomposed into a systematic trajectory $s_{1:T}$ which captures systematic bias not explained by

the cues, and a time-series of cue weights indicating the contribution of each cue over time to the trajectory.

For the mean estimation task the cue matrix C is initialised with pixel value of the cue relative to the target location, i.e.

$$c_k^n = x_k^n - \frac{1}{K} \sum_{i=1}^K x_i^n \quad (4.19)$$

Similarly Y is initialised with the pixel value of the subject's estimate of the mean centred on the target location.

For the uncertainty estimation task C is initialised with the *absolute deviation* of the cue from the mean of the cues seen so far, i.e.

$$c_k^n = \left| x_k^n - \frac{1}{k} \sum_{i=1}^k x_i^n \right| \quad (4.20)$$

and Y is initialised with the pixel value of the width of the subject's confidence window.

In performing the regression the systematic component is allowed to take any value, but the cue weights are restricted to be strictly greater than zero. Since weighting a cue is equivalent to negatively weighting all other cues (due to correlations between cues), this makes the algorithm more stable.

4.2.3.4 Model Parameter Learning

Our model (see section Sensorimotor Delay Model) has relatively few parameters. The parameters are optimised to achieve the best fit to the data, but note that this process does not confound the validity of our approach. The global model does not modify the magnitude of weights assigned to each cue, it merely constrains the trajectory through which the decision manifests itself.

To optimise the parameters the regression method discussed previously (section Weight Regression) is used to generate weights for the parametrised model trajectory:

$$\hat{W}(\delta, \alpha, \beta, y_0) = \begin{bmatrix} s_1, & w_1(1), & \dots & w_K(1) \\ \vdots & \vdots & \ddots & \vdots \\ s_T, & w_1(T), & \dots & x_K(T) \end{bmatrix}$$

The square of the difference between \hat{W} and the empirical W is minimised with respect to the model parameters using the constrained interior-reflective Newton minimisation method (described in Coleman and Li, 1994, 1996), implemented in Matlab

(Mathworks Inc., USA). To improve the rate of convergence we normalise the systematic weight terms s_t prior to minimisation, to compensate for their excessive magnitude relative to the cue weights.

For the mean estimation model we set $y_0 = 0$ and do not allow for its optimisation. This sub-optimal term is not necessary to explain the gross features of the data.

4.3 Results

4.3.1 Mean estimation performance

In this experiment I demonstrate the stereotypical trajectories and time-evolving cue weights that characterise subject's ability in the butterfly catching paradigm (see *Methods*). Visual uncertainty is introduced in the form of spatio-temporally distributed stimuli, and subjects are asked to continuously report (i) their estimate of the cue mean over time; and (ii) their confidence window around this estimate, in two separate phases of the experiment.

It was found that subjects were equally good at mean estimation in both the mean estimation task (phase *1B*) and the confidence estimation task (phase *2B*), shown in Fig. 4.4. To compare the two tasks (excluding trials with perturbations) I conducted a within-subjects analysis of variance (ANOVA) on the endpoint error (the absolute deviation from the target), with a two-level factor of task (*1B* and *2B*) and three-level factor of σ (low, medium, high). This revealed a significant main effect of σ ($F(2, 12) = 270, p < 0.001$) but no effect of task ($F(2, 12) = 0.022, p = .86$) and no interaction ($F(4, 12) = 0.11, p = .90$). The significant effect of σ indicates that the uncertainty manipulation increases the task difficulty as expected. I posit that the confidence estimation data reliably captures mean estimation ability, and that the confidence estimation process adds no significant difficulties. Thus, phase *2B* captures both mean estimation and confidence estimation, so in all subsequent analyses I present data from phase *2B* unless otherwise stated.

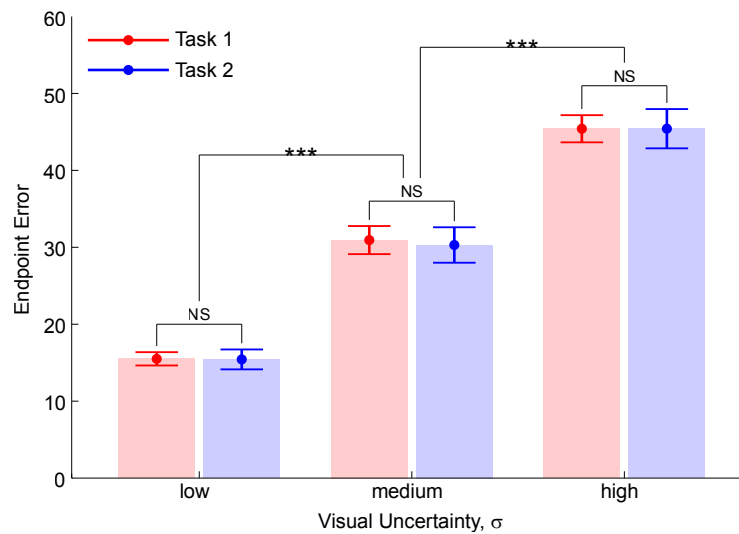


Figure 4.4: **Overall Task Performance.** This figure shows the absolute deviation from the target location for different levels of uncertainty in the two tasks of the experiment. Trials with perturbations are excluded. Note that the mean estimation task (Task 1) and confidence estimation task (Task 2) give indistinguishable mean-estimation performance, indicating that ability at Task 2 is not compromised by the additional demands of the task. This argument justifies the use of Task 2 data to explain mean estimation ability.

Given the results of the ANOVA it is clear that the endpoint error is a reliable measure of *objective performance*. From the mean-estimation data (phase 1B) a linear mapping from σ to endpoint error was established (equation 4.15). This mapping was devised to enable a mapping from σ to the *objective performance* for the provision of performance feedback that encourages subjects to report their objective uncertainty (see Performance Feedback). This mapping also allows the optimal performance for the confidence estimation model to be computed (as the ideal observer should also aim to represent the objective error).

4.3.2 The effect of perturbations on mean estimation trajectories

In the confidence estimation task the timing and direction of perturbations were modulated from trial-to-trial. During these perturbations a subset of the cues we shifted (in the early, middle or late third) by a fraction of σ (see *Methods*). In Fig. 4.5 the resulting trajectories for a single subject are shown. Fig. 4.5A shows four example trajectories which illustrate the consequence of early, middle and late-onset perturbations on decisions. Fig. 4.5B combines these individual trajectories to show the global effect of perturbations across cues. As expected, early-onset perturbations cause a greater deviation from the target, but these deviations are soon corrected as more evidence

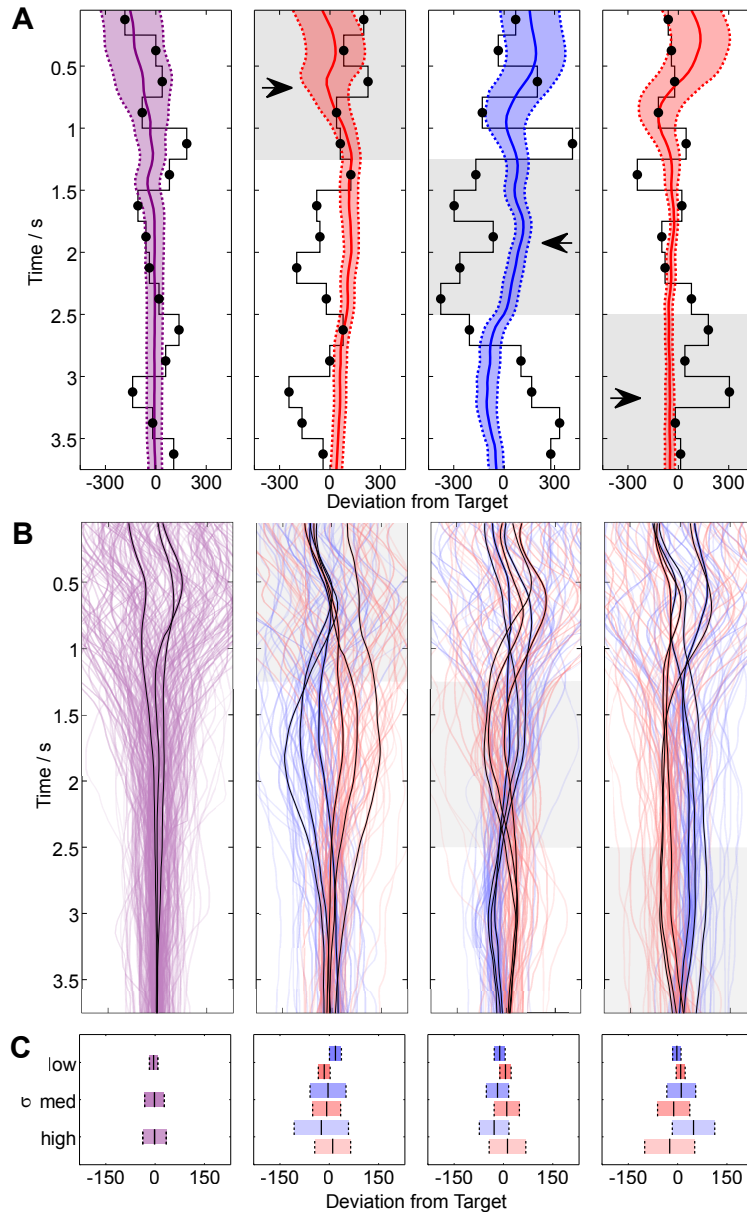


Figure 4.5: **Data for a single subject.** **(A) Typical trajectories** for four experimental conditions, showing typical trajectory deviations as a results of perturbations (shaded region and dark arrows). From left to right the no perturbation, early, middle and late-onset perturbation conditions are plotted. **(B) Average trajectories for one subject.** A plot of the average trajectories for one subject over all experimental conditions. Leftward and rightward perturbations are plotted in blue and red respectively. Note that the average trajectories for the subjects behave as described in A. **(C) Endpoint Variability.** Note that although there is a high level of variability in the trajectories in B, much of this variability is explained by the uncertainty, σ , and the onset and direction of the perturbation added to the cues. I plot the mean (solid line) \pm the variance (dotted line) of the *endpoint of the trajectory* for each experimental condition.

arrives. Middle-onset perturbations result in a meandering trajectory, and late-onset perturbations are similar to early-onset albeit of lesser magnitude and for a sustained duration. This is also expected, since a rightward perturbation of the final third is equivalent to a leftward perturbation of the first and second thirds. In addition to plotting the trajectories, in Fig. 4.5C the mean and variance of the endpoint of the trajectory are shown. Leftward perturbations (red) typically result in means that are left of the target, especially for larger σ or late-onset perturbation. Likewise for rightward perturbations (blue). Larger values of σ result in correspondingly larger endpoint variability. The observed increase in objective variability as a function of σ was previously discussed.

Late-onset rightward perturbations increased the probability of rightward errors and late-onset leftward perturbations increased the probability of leftward errors. From the trajectories it is clear that for this subject there is a latency of almost 1 second between the onset of a perturbation and a resulting change of decision. This of course is due to the gradual accumulation of evidence as well as sensory and motor delays, and consequently results in the observed errors for late-onset perturbations which were not corrected for in time for the trial's completion.

There is a high level of variability in trajectories, shown in Fig. 4.5B. Target locations are randomised, and hence one would expect much variability at the beginning of the trajectories. The later variability might be explained by the uncertainty, σ , and the onset and direction of the perturbations added to the cues. However, it is also possible that this variability reflects *sub-optimality*.

4.3.3 Mean estimation performance across subjects

Trajectories are averaged over all subjects. This reveals that the anecdotal observations for a single subject in Fig. 4.5 are consistent across subjects. Fig. 4.6A presents the average across-subject trajectories as the standard error of the mean (SEM). In all conditions, including the zero perturbation condition, there is initial variability (arrow *a*). This is due to the random target locations on each trial. After about 1 second this variability subsides, indicating that subjects have navigated to the target by this time. In all other conditions one can observe inflexions shortly after the onset of the perturbation (arrows *b*, *d* and *g*). These represent the decision to change the current estimate based on the arrival of new evidence. The trajectories are smooth, indicating that the decisions reflect the gradual accumulation of sensory information, but may also be explained by smoothness constraints on motion. A secondary observed effect is *changes of mind* (arrows *c* and *e*). These, too, are gradual and continuous unlike discrete processes previously reported in the literature Resulaj et al. (2009). These magnitude of

deviations induced by these two effects vary with σ and perturbation onset. It seems highly likely that the cues within a trial directly contribute to the final decision.

4.3.4 Optimal mean estimation model

We devised a model of motor behaviour to account for the latencies observed in decisions (see *Methods* and Fig. 4.3). For mean estimation performance we introduce three parameters, namely motor latency, δ , maximum speed, β and momentum α . Subject only to these kinematic constraints the modelled observer integrates cues in a statistically optimal fashion. This a model accounts both qualitatively and quantitatively for key features of the empirical data, such as the magnitude and timing of inflexions, and the magnitude of endpoint deviation and endpoint error (Fig. 4.6C and 4.6D). The model parameters were fine-tuned to ensure the best possible fit to the data (see *Methods*), but nevertheless have no capacity to explain the effects of cues perturbations or the effect of sensory variance σ — the effect of these manipulations depends solely on how the specific cues observed within a trial are combined to form the decision. Given that in the model the cues are computed in a statistically optimal fashion we conclude that subjects also combine the cues in a statistically optimal fashion.

From the interval of the standard error around each trajectory it is apparent that this phenomenon is robust across subjects. It is interesting that even though subjects show deviations from the target (figures 4.6B, 4.6C and 4.6D) the model also makes similar errors, in both direction and magnitude. We conclude that this does not reflect sub-optimality but is in fact just a consequence of sensory and motor limitations. The qualitative and quantitative nature of the fit is clear from the figures, although there is one notable asymmetry. In Fig. 4.6C we see that the empirical data is slightly biased in the positive direction. This is clearest for the unperturbed condition (purple) where the model predicts an average deviation of zero, but the empirical data shows a +6 pixel deviation. We feel it unlikely that the deviations are due to an alignment issue between the visual stimuli and the hand as the apparatus was calibrated. Anyway, visual-spatial mismatch should have minimal impact on task performance Helbig and Ernst (2007). It is possible that subjects were less good at localising more distal stimuli, presumably as they were further away, which may be an explanation for this small systematic error. Another possible explanation comes from observing the trajectories in Fig. 4.6A. The rightward bias is evident throughout the trajectory, in particular for large leftward deviations, suggesting that perhaps certain limb configurations may be unpreferable for subjects. Nevertheless, we consider such deviations minor in comparison to the predictable gross features of the trajectory.

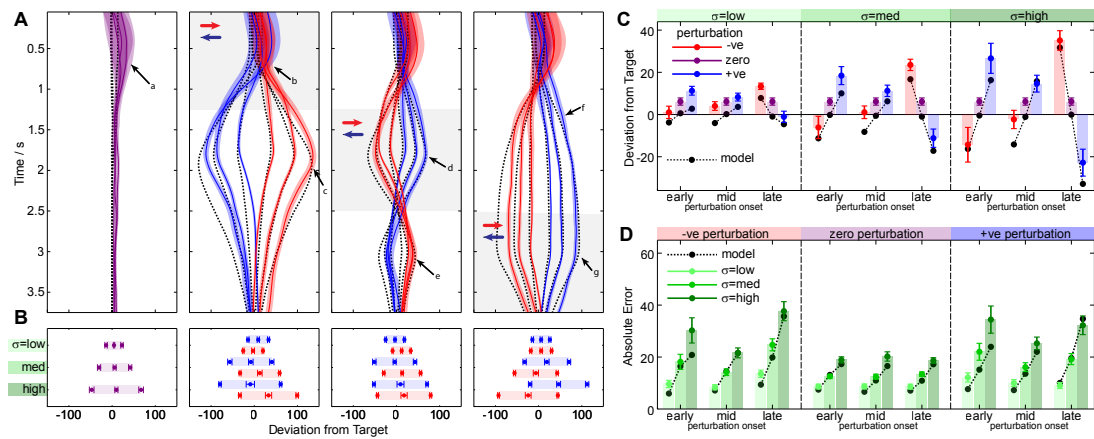


Figure 4.6: **Mean estimation data grouped across subjects.** This figure illustrates the close quantitative match between the model and the data. **(A) Average Trajectories.** In this figure the average empirical trajectories across subjects are compared to model predictions. Trajectories are computed for each subject by averaging over the trials for each condition. From left to right are plotted the no perturbation, early, middle and late-onset perturbation conditions (indicated by shaded region). Negative (blue), Zero (purple) and Positive (red) perturbations are shown. Each trajectory shows the mean across subjects \pm the standard error of the mean (SEM). The across subjects data reflect the trends observed for the per-subject trajectories in Fig. 4.5, in particular the cue-induced inflexions (arrows b, d and g) and subsequent corrections as further evidence arrives (arrows c and e). Note the qualitative and quantitative nature of the model fit to the data (dashed line). **(B) Endpoint mean and variability.** At the end of each trial (after 3.75s) the final decision of the subject determines whether they succeeded or failed. For each of the experimental conditions the figure shows (from left to right) the left confidence bound, the mean decision and the right confidence bound, comparable to Fig. 4.5C. Subjects show increasing confidence windows for larger values of σ , and show deviations from the target as a result of the perturbations. **(C) Endpoint Error.** For each of the experiment conditions the endpoint deviation is a predictable function of σ , perturbation onset and direction. The model makes a reasonable quantitative fit for all conditions, though note that it does not capture the asymmetry in the empirical data (which is slightly positively biased) **(D) Absolute Endpoint Error.** The absolute deviation from the target captures the average error in the task. This increases with σ and with perturbations, the magnitude of which are well explained by the model

4.3.5 Optimal weight evolution for mean estimation

The observed trajectories align closely with the optimal model, warranting further analysis. The close match between the magnitude of inflexions, deviations and errors (figures 4.6A, 4.6C and 4.6D respectively) can not be explained by the model parameters, suggesting that subjects are, in fact, optimally integrating cues over time to form their decision. To verify this we computed the evolving weights assigned to the visual cues over time. This involved performing a linear regression from the cues locations to the decision at each time-step (for full details see *Methods*).

Figure 4.7 shows the resultant cue weights for the empirical trajectories (figures 4.7A-4.7D) and the model trajectories (4.7E-4.7H). Our regression method assigns a weight to each cue (including cues that have not yet been observed), quantifying its contribution to the decision at each time step. The weight assigned to future cues provides useful validation that the regression method is successfully discriminating the contributions of each cue and not fitting noise. During the initial 0.5s of the trajectory we see that causality can *not* be reliably discerned, and therefore all cues (including future ones) are equally weighted (figure 4.7C). However, after this brief initial stage we see that the weight assigned to future cues declines, indicating that empirical decisions are correctly attributed to only the observed cues.

In figure 4.7A we plot the “integration window” at different times within the trial - this illustrates the weights assigned to all of the the observed cues at each time-step. We notice that each line is approximately horizontal, indicating that each cue contributes equal weight to the decision at each time step. . In figure 4.7B we plot a curve for each cue to show how each cue’s weight rises after it has been seen, then gradually decays as more evidence arrives to share equal weight with the other cues. This phenomenon is more obvious in the video included on the CD.

Finally I consider the systematic component of the weight matrix, shown in Fig. 4.7D. Initially there is a systematic error of +20 pixels, but this soon subsides after around 1 second. This error could simply be due to the randomised target locations, which subjects quickly navigate towards. A slight positive systematic component of around +6 pixels remains for the entire trajectory. This was previously observed in the average trajectories (see Fig. 4.3), and the weight regression confirms that this is not a cue-driven error but indeed a systematic bias.

The same regression method is used to plot the weight matrix \hat{W} for an ideal-observer model subject to kinematic constraints (see *Methods*). W and \hat{W} are qualitatively similar (Fig. 4.7C and 4.7G), and a quantitative match is confirmed between figures 4.7A and 4.7E, and between figures 4.7B and 4.7F. The model does not reveal an overall systematic bias, but there is an initial systematic error that subsides after around 1

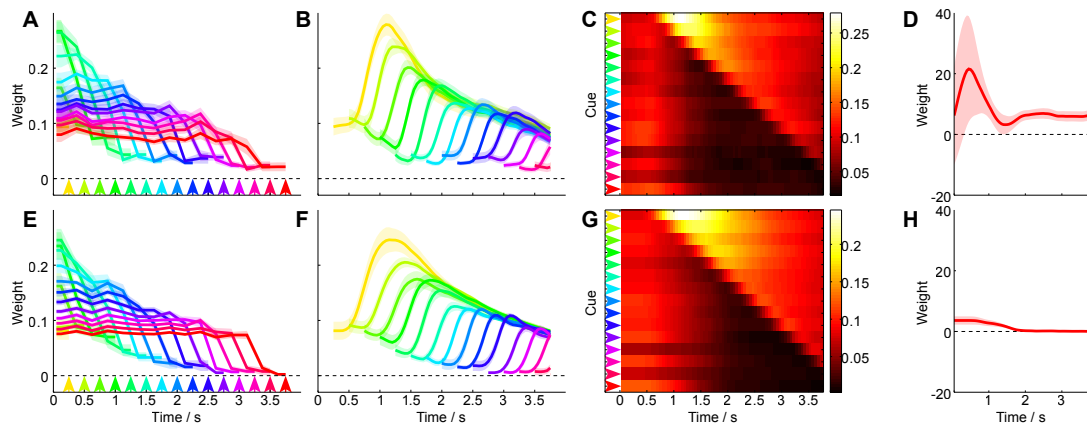


Figure 4.7: **Mean-Estimation Model Weights.** To measure the evolution of cue weights I perform a linear regression of the position of each cue in the sequence to the current trajectory position, using data over all trajectories (see *Methods*). This figure illustrates the very close match between the empirically observed weights and the model predictions. **(A) Empirical Data ‘Moving Average’.** At different time-steps in the trial (indicated by coloured arrows) the weights allocated to all cues in the sequence (coloured curves) \pm the SEM across subjects are plotted. The weights assigned to future cues are not shown. This plot reveals that the decision at each time step is due to a weighted average of the cues seen up until that point. In fact, at all time steps we can see that all cues have approximately *equal* weight, with the exception of a 0.5s window immediately preceding the time step, presumably due to sensorimotor latency. This weight equality is indicative of optimal integration (as shown in E) **(B) Empirical Data Cue Evolution.** An alternative visualisation of cue weight evolution shows how the weight allocated to the cue at each of the time steps indicated in A, evolves over the time-course of a trial. We do not show the weight allocated to the cue prior to it being seen. This plot reveals that shortly after being seen, each cue’s weight suddenly increases as it contributes to the estimate, settling at a weight that is the same across all cues. These weight profiles are indicative of optimal integration (as shown in F). **(C) Empirical Weights.** The weight matrix W , excluding the systematic component, captures the evolution of cue weights over time (see *Methods*). When visualised in this way, using colour to represent cue weight, we can see the initial response delay and the evolution of cue combination, as summarised in A and B. This weight matrix is indicative of optimal integration (as shown for the optimal matrix \hat{W} in G) **(D) Empirical Systematic Bias.** The regression of cue to decision allows for a systematic component to capture the variability in the trajectory that is not explained by the cue weights. We observe empirically a non-zero systematic bias in the positive direction, especially for early time steps. Our optimal model predicts an initial bias (as shown in H), but the overall bias is sub-optimal. I believe this to be an unavoidable consequence of the configuration of the experiment (see text) **(E-F) Model Predictions** for comparison, with three parameters (α , β and δ) optimised to minimise the difference between W and \hat{W} (plots C and G).

second, confirming that the distribution of the randomised target locations could be the cause of initial positive errors observed empirically.

4.3.6 Uncertainty estimation performance

The above analyses were repeated for confidence estimation to establish whether or not subjects were optimally estimating confidence just as they were optimally estimating the mean. Firstly, it was established statistically that subjects were able to distinguish the sensory uncertainty present in the stimuli. Fig. 4.8 shows these results.

Fig. 4.8A shows the mean error range, equal to twice the mean absolute error (equation 4.3). This is equal to the *optimal* confidence window, since maximum expected reward is achieved when subjects report a confidence window of one standard deviation of the objective uncertainty either side of the sample mean (see *Methods*). Fig. 4.8B shows the reported (subjective) confidence window, the width in pixels of the confidence decision on the final time-step of the trial, averaged within conditions and then across subjects. In each plot the slope of the objective and subjective confidence window is shown for *each subject*. The perturbed trials and unperturbed trials are plotted separately to show the effect of perturbations on objective and subjective uncertainty. Note the distinct clusters of lines in the objective uncertainty plot, indicating that inter-subject variability was low, in contrast to the overlapping lines for subjective uncertainty indicating widely differing perceptions of confidence across subjects.

An ANOVA was conducted on the mean error range, with within-subject factors of perturbation (*unperturbed vs perturbed*, grouping over the perturbation conditions) and σ (*low, medium and high*). This revealed a significant main effect of σ ($F(2, 12) = 261$, $p < .001$), a significant main effect of perturbation ($F(2, 12) = 110$, $p < .001$), as well as a significant interaction between σ and perturbation ($F(4, 12) = 30.7$, $p < .001$). The interaction was expected since the perturbation magnitude is a fraction of σ .

An ANOVA was also conducted on the confidence window range, with within-subject factors of perturbation (*unperturbed vs perturbed*, grouping over the perturbation conditions) and σ (*low, medium and high*). This revealed a significant main effect of σ ($F(2, 12) = 29.5$, $p < .001$), a significant main effect of perturbation ($F(2, 12) = 37.6$, $p < .001$), as well as an interaction between σ and perturbation ($F(4, 12) = 3.26$, $p = .074$). The magnitude of the interaction was less than expected.

The ANOVA results indicate that the task manipulations has significant behavioural consequences. Firstly, they significantly modulated the objective uncertainty. Secondly, they significantly modulated *perception* of this uncertainty, i.e. the subjective uncertainty. For the mean error range I conducted t-tests to compute the differences between conditions, and found that unperturbed trials were significantly easier than perturbed

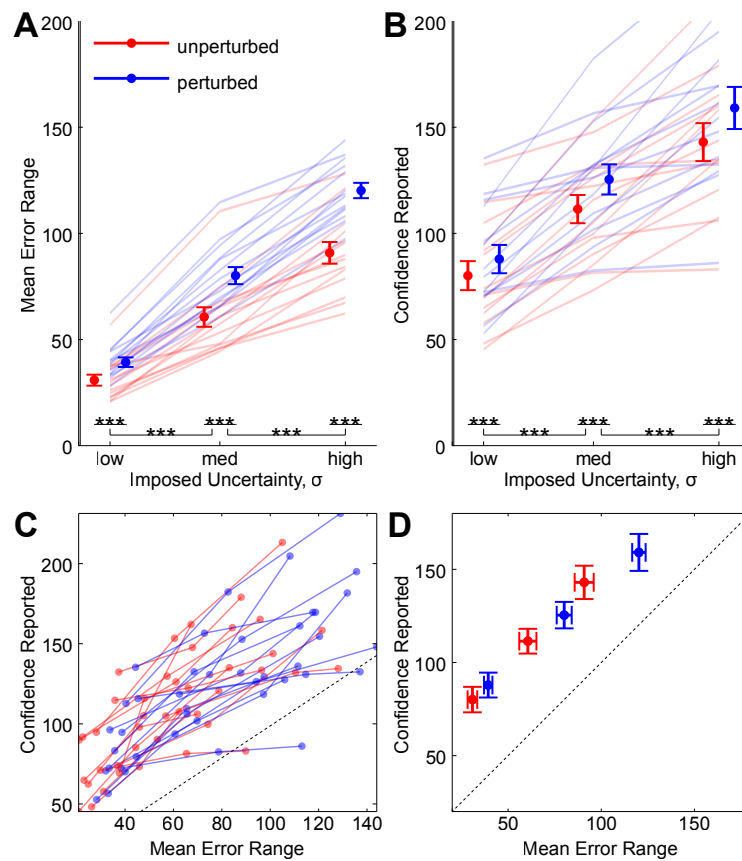


Figure 4.8: **Uncertainty Estimation Performance.** Subjects are able to discern different levels of uncertainty added to the cues. Individual subject errors are plotted for unperturbed (red) and perturbed (blue) trials, shown by the lines. In addition the average and standard error across subjects are plotted, indicated by the error bars. **(A) Objective Uncertainty.** The mean error range (twice the mean absolute error) \pm SEM, for different levels of σ (solid blobs and error bars) are plotted for perturbed (red) and unperturbed (blue) trials. Overlaid are the average results for each subject (faded lines). Subjects show statistically significantly increased errors as a result of both cue uncertainty and the presence of perturbations. Between-subject variability is low, as indicated by the distinct separation between red and blue lines and the consistency of the gradient. **(B) Subjective Uncertainty.** The average width of subject's confidence window at the end of the trial for each σ and perturbation is plotted, similar to A. Subjects show a statistically significantly increased confidence window as a result of both cue uncertainty and the presence of perturbations, mimicking the objective uncertainty. However, between-subject variability is high, indicating that different subjects have widely differing abilities at estimating uncertainty. **(C) Subjective-Objective Mapping.** Per-subject data from A and B are combined, plotting the mean error for each condition versus the confidence reported. The ideal mapping is shown with a dotted line. Subjects consistently over-estimate the objective uncertainty. **(D) Grouped Subjective-Objective Mapping.** The average mapping across subjects \pm the SEM in each direction. Although between-subject variability appears high in (C) it is clear that subjects consistently over-estimate their objective uncertainty.

trials (measure: *mean error range*, $p < .001$ for all σ). They were also perceived as easier (measure: *confidence window*, $p < .001$ for all σ). Likewise, the increase in difficulty between low, medium and high σ was significant for each comparison (measure: *mean error range*, $p < .001$ for both perturbation conditions), and were also perceived as such (measure: *confidence window*, $p < .001$ for both perturbation conditions). Figures 4.8A and 4.8B provide a graphical representation of these findings.

I am interested in the question of how subjects represent objective uncertainty, so figures 4.8A and 4.8B were combined to examine their relationship. In Fig. 4.8C these results are shown per-subject by plotting the mean error range for each condition versus the confidence reported for each condition, separated into unperturbed (red) and perturbed (blue) trials. The positive slope of each line indicates that all subjects were able to discriminate uncertainty, though there is some variability in the slopes indicating different levels of ability at discriminating uncertainty. 96% of the data lies above the line $y = x$, indicating that although subjects are able to discriminate uncertainty they consistently over-estimate it. In Fig. 4.8D the combined data across subjects are shown. Each point in the figure shows the relationship between mean error range and the reported confidence, with error bars to show the standard error across subjects in either direction, revealing a consistent effect of over-estimation of confidence across subjects. However, it is noted that the points fall on a straight line parallel to the line $y = x$, indicating that subjective uncertainty is linearly related to the objective uncertainty. Most subjects were capable of estimating the uncertainty of stimuli in all of the experimental conditions, but this uncertainty was uniformly over-estimated by a constant amount. The variability between subjects could indicate differences in subjective perception of of uncertainty, or simply that some subjects found it difficult to accurately report this quantity. We return to this in the discussion.

4.3.7 Near-optimal model for uncertainty estimation

In this final analysis I consider the evolution of confidence estimates over the course of a trial. Previously it was shown that endpoint confidence (*subjective uncertainty*) reliably discriminates perturbation-induced and σ -induced *objective uncertainty*. Here I show that this behaviour not only holds for binary decisions but also for continuous confidence estimation. In Fig. 4.9A I plot the average trajectories across subjects. subjects can differentiate levels of σ by reporting different levels of confidence — after about 1 second the trajectories diverge to reflect the added uncertainty. It should also be noted that there are changes in perceived uncertainty as a result of the perturbations. These effects are more subtle but one can see a delayed inflexion as a result of early-onset perturbation (arrow *b*), and inflexions as a direct result of middle- and late-onset

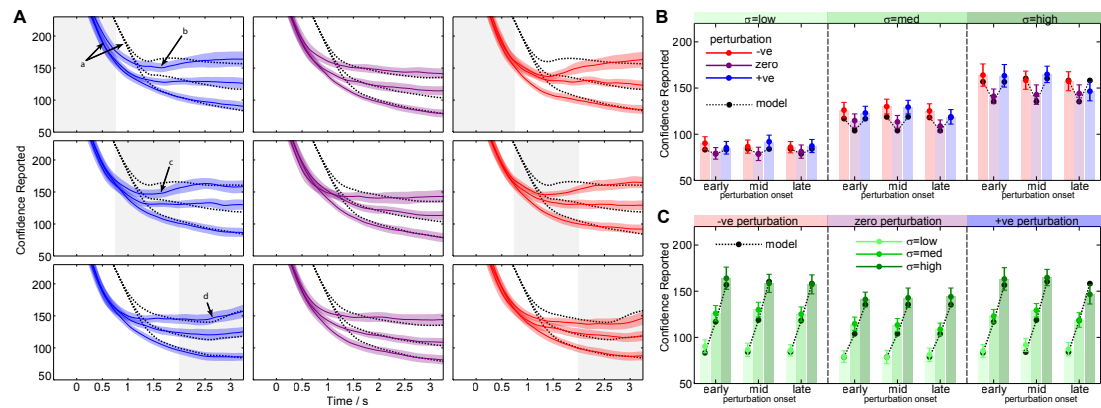


Figure 4.9: **Uncertainty estimation data grouped across subjects.** This figure illustrates the close quantitative match between the model and the data. **(A) Average Trajectories.** In this figure the average empirical trajectories across subjects are compared to model predictions. Trajectories are computed for each subject by averaging over the trials for each condition. From top-to-bottom are the no perturbation, early, middle and late-onset perturbation conditions (indicated by shaded region), and from left-to-right I plot negative (blue), zero (purple) and positive (red) perturbation directions. Each trajectory shows the mean across subjects \pm the standard error of the mean (SEM). The model fit to the data is shown using a dashed line. Note that the model does not explain the initial part of the trajectory (arrow *a*), but does reasonably well at explaining inflexions in uncertainty that arise as a consequence of perturbations (arrows *b*, *c* and *d*) **(B and C) Confidence Reported.** For each of the experiment conditions the final reported uncertainty is a predictable function of σ , perturbation onset and direction. Plots B and C present the same results grouped in different ways. The model makes a good quantitative fit for all conditions, but note that the model contains a systematic ‘safety margin’ parameter y_0 which may explain some aspects of the data fit (see text)

perturbations (arrows *c* and *d*).

Similar to the analysis for mean estimation, I devised a kinematic model to capture inevitable sensory and motor latencies on task performance (see *Methods* and Fig. 4.3). For confidence estimation performance the models maintain the three parameters of motor latency, δ , maximum speed, β and momentum α , and has an additional parameter of safety margin y_0 . Subject only to these constraints the modelled observer integrates the *deviations* of cues from the current mean estimate so as to maximise the expected reward (which is achieved when the confidence window equals one standard deviation of the objective uncertainty either side of the sample mean, see *Methods*).

This a model accounts both qualitatively and quantitatively for some key features of the empirical data, such as the magnitude and shape of σ -induced differences, the

magnitude and timing of perturbation-induced inflexions, and the magnitude of the final decision (Fig. 4.9B and 4.9C). The model parameters were fine-tuned to ensure the best possible fit to the data, but nevertheless have no capacity to explain the effects of cue perturbations or the effect of sensory variance σ — the effect of these manipulations depends solely on how the specific cues observed within a trial are combined to form the decision. While the safety margin parameter y_0 does have the capacity to explain the overall magnitude of decisions, it is simply a per-subject constant and can not explain the differences between the trajectories. Given that in the model the cues are computed in a statistically optimal fashion it is concluded that subjects also combine cues in a near-optimal fashion, with the exception of a safety-margin.

The model fails to capture one key aspect of the data: the initial slope and delay (Fig. 4.9A, arrow *a*). This reflects an inadequacy of the model which we attempt to explain here. The mean estimation and uncertainty estimation tasks are coupled, yet our models treat mean estimation and uncertainty estimation as separate tasks. For example, cue perturbations result in an increase in perceived uncertainty (Fig. 4.9A, arrows *b*, *c* and *d*), which occur at the same time as mean estimation ‘changes of mind’ (Fig. 4.6A arrows *c*, *d* and *g*). An alternative model may consider coupled mean estimation and confidence estimation processes operating simultaneously, where subjects may perhaps choose to first estimate the mean before correcting the confidence window. Therefore, the initial variability for the first second of the mean estimation trajectories (Fig. 4.6A arrow *a*) is due to subjects localising the randomly located target, and may be the cause of our inability to explain the first second of the confidence trajectory. Apart from this one discrepancy, the model does appear to fit the remainder of the trajectory both qualitatively and quantitatively.

Finally, the weight matrix W is computed to explain the evolution of cue weights (see Fig. 4.10). This was only roughly in agreement with the model. Empirically it is observed that each cue deviation does not contribute equally to the final decision as one would expect, indicating that subjects are, in fact, sub-optimal at estimating uncertainty from time-evolving visual cues. However, this may not be conclusive as the experiment involves mean perturbations rather than variance perturbations, and so the contribution of individual cues is harder to discern. There is also a much higher level of noise in the confidence estimation weight matrices for each subject, leaving the possibility that the parameters chosen reflect local minima. Finally there was a high level of variability between subjects, and so average performance may not reflect the true nature of decision-making. It can not conclusively be claimed that subjects were sub-optimal at computing the uncertainty, but the presence of a conservative safety margin and an inability to fit the model weights indicates that uncertainty estimation is a

complex task that can not be explained with a straightforward model of cue integration.

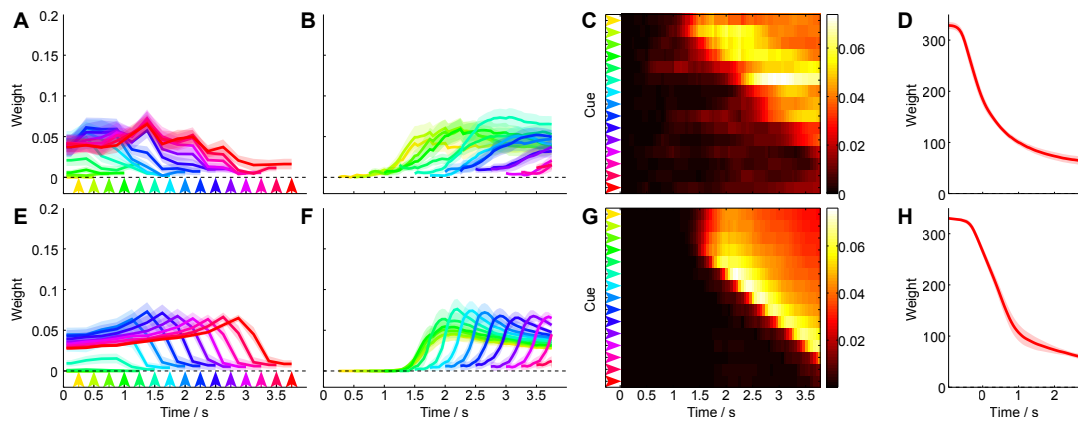


Figure 4.10: **Confidence-Estimation Model Weights.** To measure the evolution of cue weights a linear regression is computed of the deviation of each cue in the sequence from the current mean estimate to the confidence window width, using data over all trajectories (see *Methods*). This figure illustrates the poor match between the empirically observed weights and the model predictions. **(A) Empirical Data Integration Windows.** At different time-steps in the trial (indicated by coloured arrows) the weight allocated to all cues in the sequence (coloured curves) \pm the SEM across subjects is computed. The weights assigned to future cues are not shown. This plot reveals that the decision at each time step is due to a weighted average of the cues deviations observed until that point. These weight profiles do not match the model (as shown in E) **(B) Empirical Data Cue Evolution.** An alternative visualisation of cue weight evolution shows how the weight allocated to the cues at each of the time steps indicated in A, evolves over the time-course of a trial. The weight allocated to the cue prior to it being seen is not shown. This plot reveals that shortly after being seen, each cue's weight increases as it contributes to the estimate, then gradually decays. These weight profiles do not match the model (as shown in F). **(C) Empirical Weights.** The weight matrix W , excluding the systematic component, captures the evolution of cue weights over time (see *Methods*). When visualised in this way, using colour to represent cue weight, one can see an initial response delay and the evolution of cue combination, as summarised in A and B. This weight matrix roughly matches the model (as shown in the plot of \hat{W} in G), but is very noisy, making it unsuitable to draw any conclusive conclusions. **(D) Empirical Systematic Bias.** In computing the regression of cue to decision a systematic component captures the variability in the trajectory that is not explained by the cue weights. The model roughly predicts the shape of the systematic component **(E-F) Model Predictions** for comparison, with four parameters (α , β , δ and y_0) optimised to minimise the difference between W and \hat{W} (plots C and G).

4.4 Discussion

4.4.1 Overview

In this chapter I have shown that subjects estimate the mean of time-varying stimuli in a predictable manner. By manipulating the variance as well as the onset and direction of perturbations I have shown that this estimate is computed in a statistically-principled way that assigns equal weight to all observed cues to form a final estimate. Our model constrains only kinematic parameters, and is otherwise statistically-optimal. A very close match between empirical data and the model is observed, suggesting that subjects can accumulate evidence over time to form *optimal continuous estimates* of the mean of noisy visual stimuli.

By manipulating the variance of the underlying stimuli I examined the relationship between *objective uncertainty* and *subjective uncertainty*, showing that the two are closely, but not directly coupled. By manipulating subsets of the cues through perturbations I also evaluated the respective weighting given to each cue for confidence estimation, and showed that with the addition of a conservative *safety-margin*, the responses to cue variance and perturbations can be reliably predicted. While the evolution of cue weights was not well explained by the model, possibly indicative of sub-optimal integration, subjects were clearly capable of accumulating evidence over time to *continuously discriminate* the objective uncertainty present in noisy visual stimuli.

4.4.2 Implications

4.4.2.1 Objective Uncertainty Acquisition

In making decisions, subjects must make a trade-off between allocating time to perception, and time to action Faisal and Wolpert (2009). Since there is a considerable time delay between sensing the world and initiating motor actions, subjects often make decisions while sensory information is arriving, and it has been shown that certain decisions made under these conditions, in particular *changes of mind*, reflect the properties of this processing pipeline (Resulaj et al., 2009). In a vision-based reaching task Resulaj et al. (2009) are able to predict discrete events (subjects changing their mind) based on the time-delayed accumulation of evidence. In this chapter I have shown how subjects form decisions based on visual cues and correct their estimate when their estimate changes, as indicated by the trajectories under different levels of perturbation. In our continuous task these ‘changes of mind’ are not discrete events but in fact evolving decisions related to our perception of uncertainty. There exists a large temporal window for estimating uncertainty (Graf et al., 2005), and our results confirm that subjects can accumulate and integrate evidence over this time to report continuous statistical estimates.

Our use of a continuous time-varying task provides the first direct explanation of the process of objective-uncertainty acquisition. It was recently argued that forced-choice paradigms may induce apprehension, especially with increased uncertainty (Helbig and Ernst, 2007), and this apprehension may indirectly provide a measure of stimulus uncertainty that does not require an explicit conscious representation (Helbig and Ernst, 2007). Experimental manipulations to increase uncertainty, such as decreasing stimulus contrast or adding uncorrelated noise, may increase the latency with which subjects can react to stimuli, further confounding the interpretation of explicit awareness of uncertainty. Even our method of time-varying jittering cues may trigger unconscious neural mechanisms that could indirectly account for uncertainty judgements. Much research on statistical optimality includes situations in which an *implicit* internal representation of uncertainty may explain task performance (e.g. Alais and Burr, 2004, Ernst and Banks, 2002, Gepshtein and Banks, 2003, Gepshtein et al., 2005, Hillis et al., 2004, Knill and Saunders, 2003 and more). By asking subjects to report their sensory uncertainty I directly tackle the question of whether subjects can *explicitly* acquire representations of sensory uncertainty in order to make optimal decisions (Barthelmé and Mamassian, 2009).

4.4.2.2 Optimal Perception

To what extent are the observed continuous trajectories optimal? The global parameters of the model are optimised to achieve the best fit for each subject, but as these parameters are fixed across all trials they can not explain the differences in the trajectories observed for each condition - these can only be explained by the contribution of individual cues to the decisions (although the parameters can explain the general shape of the trajectories and the latency after which cues contribute to the trajectories). In the mean estimation model the cue contributions are chosen optimally (i.e. according to the ML estimate of the mean). The resultant close match between the empirical and observed trajectories for each of the conditions indicates optimal cue weighting. In contrast, in the confidence estimation model a suboptimal “safety margin” is used to explain the magnitude of the estimate and thus a match between empirical and model trajectories does not indicate optimality. This safety margin causes subjects to significantly over-estimate uncertainty, resulting in less than optimal performance in the task.

Could the finding of optimal mean estimation and suboptimal confidence estimation be explained by subjects relying on a simpler heuristic? For example, subjects may position their thumb and forefinger on the extremes of the cues seen so far, or choose an aperture size proportional to this range. This was our primary motivation

for computing the weights assigned to each cue in the sequence, which revealed that each cue was approximately equally weighted for the mean-estimation task. This would not be the case for subjects relying on subsets of the cues: as the mean of the cues is not equal to the median due to perturbations, the suboptimal heuristic strategies would result in different endpoint decisions, different trajectories and different weight profiles. We therefore posit that mean estimation trajectories are indeed based on optimal cue weighting. In contrast, uncertainty estimation empirical weights do not match the optimal model weights. The presence of a consistent overestimation of uncertainty indicates that subjects may be relying on a subset of the observed cues to form their estimate. Nonetheless, subjects still increase their aperture in response to uncertainty increases and perturbations, indicating that subjects do have access to some measure of their objective uncertainty.

It is certainly a possibility that subjects are, rather than expressing a measure of their internal belief about the uncertainty of the stimuli, reporting a learned quantity. However, I do not believe this poses a confounding factor in the conclusions drawn. Whether or not subjects are (a) expressing a quantity which is represented internally, (b) an arbitrary quantity which correlates with an internal measure, or even (c) an arbitrary quantity which they learn to represent over the time-course of the experiment, it should be noted that that they are able to do this in a manner that: (i) reflects the uncertainty, σ^2 , imposed on a given trial; (ii) captures increases in uncertainty which arise as a result of cue perturbations; and (iii) evolves over time in a way that appears to reflect the accumulation of information over the course of the trial. Regardless of the quantity subjects are expressing, the fact that they are able to do this indicates that they are able to compute and express a measure of cue uncertainty, based on the information acquired within a single trial. Nonetheless, the reported quantity is far from that required to maximise the expected score.

Our finding that subjective perception of uncertainty over-estimates objective uncertainty is consistent with the experimental finding of underconfidence in forced-choice tasks (e.g. see [Barthelmé and Mamassian \(2009\)](#)). From the present results it appears that subjects are relying on a (suboptimal) uncertainty estimate rather than the maximum likelihood estimate, though there are a number of alternative potential causes of over-estimated uncertainty: (i) It is not known if subjects fixate on the jittering stimuli or on the cursor, which may effect their ability to accurately judge (or anticipate) the stimulus location; (ii) Subjects may not have been able to maximise their expected gain (in contrast to [Trommershäuser et al. \(2003\)](#)), due to differences in experimental design; (iii) The kinematic model fit to the data may be insufficient to describe behaviour; (iv) The data collected may have been too noisy for reliable model fitting. To address points

(i) and (ii) further research is needed to decouple the factors that determine objective variability and performance maximisation. For example, subjects were not aware of the exact functional form of the score function (in contrast to Trommershäuser et al. (2003)), and were required to report a quantity which may have differed from their true internal measure of uncertainty, adding additional learning demands. Whilst the effects of learning were not observed in the data these potential limitations of the scoring system should be noted. To address points (iii) and (iv) we must evaluate the viability of our kinematic model (See *Materials and Methods*, and figure 4.3). In our model the delay parameter captures the combined effect of sensory and motor latency and motor kinematic limitations are captured by speed and momentum parameters, which affect the overall shape of the trajectories. It was found that these three parameters were sufficient to explain the average empirical data for mean estimation. Alternative models may introduce additional parameters to explain different aspects of the data, such as the addition of sensory and motor noise or separate sensory and motor delays. Further experiments would be required to test such models.

Our experiment design utilised a grasping task within a fixed plane. As the task does not abstract the cursor or targets to a computer screen, it maintains many aspects of ordinary grasping (visual feedback, proprioceptive feedback, feedforward control etc.), keeping the task as natural as possible. As detailed in the methods, feedback of the fingers was aligned with the true finger locations (see Gepshtein and Banks (2003)). The design relied on the fact that subjects could independently control their grasp aperture and hand position, which we felt was likely (although see Schot et al. (2011); independent finger and thumb control has not been conclusively demonstrated). Target stimuli were presented along the line of the left forearm, though it could also have been achieved by presenting stimuli along any fixed line in the plane. We chose to use the arm as a reference because (i) this design lends itself to a number of follow-up experiments in which the cues may be tactile rather than visual; and (ii) it allows subjects to position both the target line (with their left arm) and the cursor (with their right arm) in any comfortable configuration of their choosing.

Our results are consistent with a number of studies that report optimal multisensory integration, (e.g. audio-visual Alais and Burr (2004), Heron et al. (2004), visuo-haptic Ernst and Banks (2002), Gepshtein and Banks (2003), Helbig and Ernst (2007) visuo-proprioceptive van Beers et al. (1999) and visual Jacobs (1999), Oruç et al. (2003) integration). However, these results provide *indirect* evidence of subjective representation of objective uncertainty Barthelmé and Mamassian (2009). In the present study we find that subjects are able to form an optimal estimate of the mean and an overestimate of the uncertainty, providing *direct* evidence of continuous mean- and confidence-

estimation mechanisms that may underlie the observation of optimal integration. In contrast, there are a number of studies in which optimal behaviour was not observed. Multisensory integration studies have demonstrated a significant under-weighting of sensory uncertainty for texture information Knill and Saunders (2003) and auditory information Burr et al. (2009) and in a third study it was found that visuo-haptic integration performance was inconsistent with maximum likelihood estimation in more than 80% of the data Rosas et al. (2005). However, the authors conceded that subjects may have attempted to combine cues optimally but did not have an accurate estimate of the variance of the individual cues. Consistent with this finding, in the present study we have observed a suboptimal *safety-margin* in subjects estimating their uncertainty. By extending our experimental paradigm to multiple sensory modalities we would predict different integration weights for subjects using either *subjective* or *objective* uncertainty to form multimodal estimates. By allowing for simultaneous measurement of mean and confidence our experimental paradigm readily lends itself to the testing of such hypotheses.

4.4.2.3 Cognitive Mechanisms

There is a growing body of research which aims to understand the neural substrate of uncertainty representation. For example, neural firing activity in orbitofrontal cortex in rats is an accurate predictor of olfactory discrimination uncertainty (Kepecs et al., 2008), and neurons in parietal cortex encode information about the degree of decision-making uncertainty in monkeys (Kiani and Shadlen, 2009). The presence of confidence-estimation mechanisms in the brain is supported by biologically plausible computational models (such as reviewed in Pouget et al., 2000) in which neural populations readily encode sensory uncertainty and allow networks to compute posterior probability distributions. The results presented in this paper provide direct evidence that humans have rapid and reliable access to some measure of this statistical information, which could presumably be attained from such neural representations.

While it is certainly possible that uncertainty may be represented neurally, the present results of suboptimal acquisition indicate that to understand these processes one needs to examine the processes on an even finer temporal granularity than presented here. This could possibly be achieved in the present paradigm by slowing down the arrival of sensory evidence, reducing the effects of motor noise and allowing responses to *each cue* to be measured.

4.4.3 Conclusion

My quantitative paradigm allows for the simultaneous measurement of both mean and confidence estimation. It allows this process to be observed over time as the arrival of evidence is controlled. From this I am able to make qualitative and quantitative predictions of the performance of subjects based on a statistically optimal model constrained only by elementary kinematic limitations, exposing the fundamental mechanisms of mean and uncertainty estimation over time. The paradigm naturally lends itself to a wide variety of future experimental manipulations, for example in understanding the methods deployed when integrating cues from multiple modalities, for understanding the time-courses of decisions, and for decoupling the roles of objective and subjective uncertainty perception for decision-making.

Chapter 5

Optimal Multisensory Integration

The degree of integration of an artificial feedback system with existing sensory channels is potentially a good indicator of perceptual rehabilitation. If this is achieved in the context of a sensorimotor task this may be also be a valuable indicator of sensorimotor rehabilitation. In this chapter I test the vibrotactile feedback channel developed in chapter 3 in a novel multisensory cursor tracking task. Subjects are able to perform the task using either visual or vibrotactile feedback, suggesting that *sensory substitution* has been achieved. It is also found that subjects make active use of the artificial sense when they have a choice between vision and vibrotactile feedback. Performance in a multimodal condition is greater than that for each modality presented alone, suggesting *sensory integration*. When vision and vibrotactile feedback are corrupted by uncertainty, objective uncertainty increases. Subjects choose to integrate the two percepts as a function of the objective uncertainty, resulting in a performance stereotypical of Bayes-optimal multisensory integration.

Relevant Publications

- Ian Saunders, Sethu Vijayakumar. (2009b). **A Closed-Loop Prosthetic Hand as a Model Sensorimotor Circuit.** *Proc. International Workshop on Computational Principles of Sensorimotor Learning.*

5.1 Motivation

In developing an artificial sensory channel, it is an important question to ask whether or not it will integrate with our existing senses so that it can complement and, where necessary, substitute for our existing senses. This chapter attempts to quantify the degree to which the artificial vibrotactile feedback channel developed in Chapter 3 integrates with visual feedback. This is achieved by means of continuous cursor-tracking tasks, motivated in Chapter 2 as valuable for evaluating sensorimotor function and by analogy to prosthesis control.

A number of multisensory integration studies in the literature have reported that the weight attributed to different sensory modalities is a function of their respective sensory uncertainty. This has been shown for vision and proprioception (van Beers et al., 1999) for audio-visual integration (Battaglia et al., 2003) and visual and haptic integration (Ernst and Banks, 2002) and is often consistent with an optimal “Bayesian” weighting strategy (but see Chapter 2 for further detail).

These results suggest the presence of statistically-principled mechanisms in the brain. However, Ernst and Banks (2002) acknowledge that “although explicit calculation or learning may occur, there are plausible schemes in which explicit calculation of variances or weights is unnecessary”. To further understand the mechanisms of integration it is desirable to distinguish *explicit* and *implicit* integration schemes (see Chapter 2).

Further, it is not yet known whether statistically optimal multisensory integration extends to a “new” (artificial) sense. When the amputee uses the sensorised prosthetic hand introduced in Chapter 3, although exploiting residual nerves and latent plasticity, feedback from sensors will be issued at a different *location* (e.g. the arm), in a different *modality* (e.g. vibration), and with a different *encoding* (e.g. a spatial code) to that of natural sensation of this information. To this extent we have created an *artificial sensory channel*.

Ernst and Banks (2002) raise the question “Does the nervous system need to calculate or learn the variances associated with the visual and haptic estimators for each property and situation to implement MLE integration?” The experiments presented in this chapter use an artificial modality allow us to answer the question: is this weighting learned or calculated? An artificial modality has no pre-learned component and so can be used to test this hypothesis.

5.1.1 Pilot Experiment

In understanding the limitations of present prostheses it is important to understand both the sensory and motor components of rehabilitation. Much research in the literature has examined a variety of feedback codes. However, a less explored question is the choice of prosthesis kinematic controller. In the pilot experiment I chose to compare a differential (velocity-control) prosthesis controller to an absolute (position-control) prosthesis controller, in the presence of visual and tactile feedback. The experiment aims to provide a quantitative comparison of the benefits of (uncertain) sensory feedback under each of these control methods.

To achieve these aims, I have developed a multimodal pursuit tracking task. This task was developed with the following considerations in mind:

- (i) the task should be considered analogous to prosthesis control (insofar as the dynamics of the cursor correspond to the output of a prosthesis); and
- (ii) the visual and tactile modalities may be identically manipulated to induce uncertainty.

The iLIMB hand deploys a differential controller, as discussed in Chapter 3. In such a controller, hand velocity is directly proportional to muscle activity and therefore the efferent copy of motor commands and muscle proprioception provide feedback of grasp *speed*. To estimate grasp position from this quantity one would need to integrate the signal over time. Under this additional difficulty I hypothesised that an artificial channel would have a beneficial effect on grasp position estimation. An alternative prosthesis controller could adopt an absolute control strategy. In this configuration grasp size is directly proportional to muscle activity and therefore the motor efferent copy and muscle proprioception provide direct feedback of grasp size. I therefore hypothesised that the benefits of tactile feedback may be less pronounced in the presence of these extra sensory signals.

5.1.2 Main Experiment

To determine the strategy deployed by subjects to perform multisensory integration I conducted an experiment to quantify the degree of multisensory integration. Similar to the paradigm developed for the pilot experiment I examined target acquisition ability under uncertain visual and tactile feedback. Extending the paradigm I added two additional considerations:

- (iii) The task should impose minimal bias to either modality.

- (iv) The visual and tactile modalities should be matched in terms of utility, to allow their integration to be measured;

To address point (iii), task bias was reduced by limiting the number of “target locations” to 1. The advantage of having a single fixed target is that neither the visual nor tactile modality are inherently favoured.

In the main experiment it was decided that a differential controller would be more relevant for generalisability of results to control of the iLIMB hand and to prosthesis control in general, with which

To address point (iv), the major difference between the main experiment and the pilot was that that tactile and visual performance were adjusted so that the magnitude of error in each condition overlapped. Running a larger cohort of subjects, with increased tactile training and an improved vibrotactile feedback code it was hoped that sufficient data could be attained in which the utility of visual and tactile feedback were comparable in terms of the objective performance of subjects using each modality alone.

The feedback system was improved by increasing the number of tactors and using an interpolated duty-cycle code (see Chapter 3). This meant that a spatially-continuous tactile display could be simulated by co-activating neighbouring tactors. This increased the number of distinct perceptual sensations achievable from the tactile display. In addition, the visual feedback uncertainty was adjusted on a per-subject basis to ensure that overlap was achieved.

Finally, to distinguish explicit (active) uncertainty perception from implicit (passive) perception, a conflict (or offset) was added between the modalities (see *methods*).

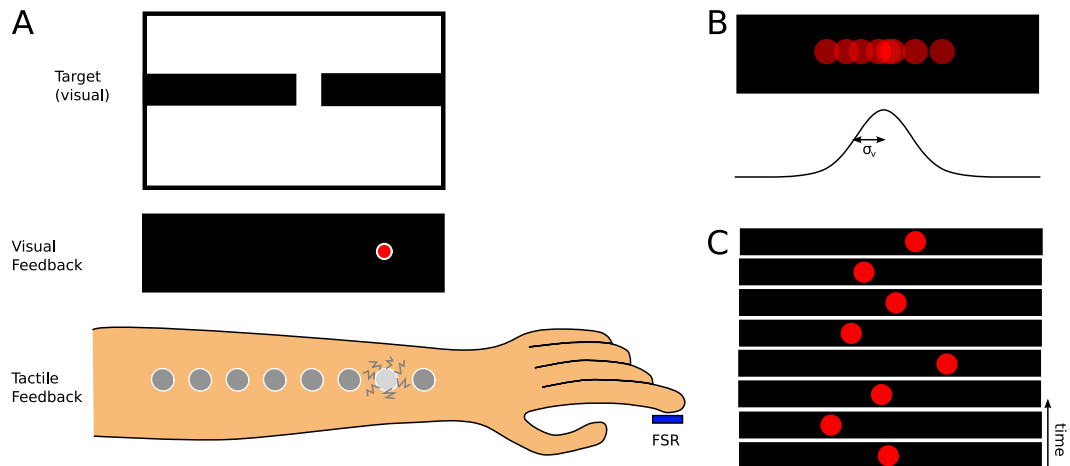


Figure 5.1: **Pilot Target Localisation Task 2.** (A), Schematic of the tracking task. Subjects are required to move a cursor to a target position using visual and/or tactile feedback of cursor position, presented on screen and/or to the forearm respectively (B), In previous multisensory integration studies, spatial uncertainty has been applied to visual feedback resulting in a cloud of blobs (e.g. Tassinari et al. 2006, Körding and Wolpert 2004a). This could be presented as pictured, distributed with variance σ_v (C), In the present experiment uncertain cues are presented as a sequence, resulting in a cursor which ‘jitters’ over time. This manipulation is applied to feedback in both the visual and tactile modalities, to modulate the uncertainty of each.

5.2 Methods

5.2.1 Pilot Experiment

5.2.1.1 Overview

Subjects were required to move a cursor to a target location. On each trial the target location was presented in the visual modality and appeared in one of 8 locations corresponding to the eight vibrating motors on the arm. Fig. 5.1 illustrates the task.

5.2.1.2 Stimuli

On each trial, subjects were presented with a stream of feedback of the current cursor position in both visual and tactile modalities. The feedback was perturbed by independent sequences of samples from a Normal distribution with mean 0 and variance σ_v^2 and σ_t^2 in the visual and tactile modalities respectively. On each trial 20 samples were presented in each modality, spaced by 200ms.

In blocks of 5 trials, each of σ_v and σ_t were chosen randomly in the range $\{0, 0.5, 1, 1.5, \infty\}$ factors. This quantity is given in ‘factor space’ defined as ranging from from

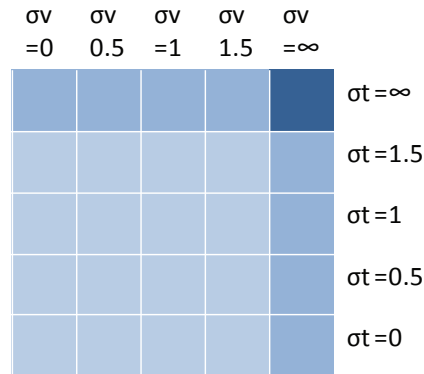


Figure 5.2: **Matrix of Stimulus Uncertainty** To examine the interaction between five values of stimulus uncertainty in each modality, 25 trial configurations are required. This figure illustrates the conditions considered, and highlights the first row and final column to indicate unimodal trials ($\sigma = \infty$ conditions).

0 to 7, corresponding to each of the 8 vibrating tactors. In trials with infinite variance, no feedback signal is given. Fig. 5.2 illustrates the 25 conditions enumerated by the combinations of $\sigma_v \times \sigma_t$.

Stimuli were recorded and presented in ‘pixel space’, corresponding to the width of the visual display which spanned 1024 pixels. Tactors were spaced by 114 pixels, so that tactor $i \in \{0, \dots, 7\}$ appeared at pixel location $114 + 114i$. The ranges of each of σ_v and σ_t is equivalently given by $\{0, 57, 114, 171, \infty\}$ pixels. Visual stimuli were presented horizontally, as shown in Fig. 5.1A, and projected onto a large visual display at eye-level. Tactile stimuli are presented via a custom built vibrotactile array, featuring 8 tactors spaced by 4cm in a linear array along the arm. Feedback was encoded using the duty-cycle method (as discussed in Chapter 3), and between-tactor interpolation was not used in the pilot experiment.

The visual and tactile cues were presented as a “jittering” sequence (as introduced in Chapter 4). Fig. 5.3 illustrates the effect of this jitter applied to the tactile modality (discretised in each motor). Unlike other methods such as blur (e.g. Helbig and Ernst 2007) and spatial scattering (e.g. Körding and Wolpert, 2004a), this method can be applied to both visual and tactile channels, allowing modulation of the uncertainty of both.

Each trial lasted approximately 5 seconds. On completion of the trial, subjects were alerted of success or failure by the target turning green (success) or red (failure). Each subject completed 125 trials in a 10-minute run, with randomly located targets presented on each trial, drawn Uniformly over all tactor locations $\{0, \dots, 7\}$, i.e. pixel locations $\{114, \dots, 910\}$. The jitter in the visual and tactile channels, σ_v and σ_t respectively, was varied at random every 5 trials throughout the run. Subjects performed three such

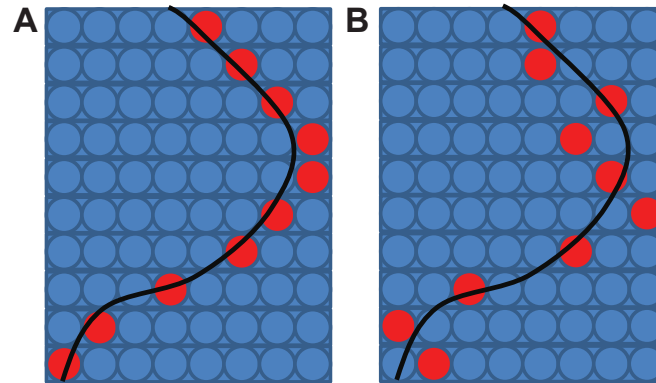


Figure 5.3: **Spatio-temporal Jitter.** This illustration shows how spatio-temporal jitter is applied to a discretised modality, i.e. in the tactile channel. **(A)** A nearest-neighbour approach was used to choose the appropriate factor to stimulate in the no-noise condition ($\sigma_t = 0$). The figure shows a trajectory over time (black line) and with which the corresponding stimulated factor (red dot). **(B)** Under a moderate amount of tactile noise ($\sigma_t = 1$) the trajectory at each time step is perturbed by a sample from a Gaussian distribution before the nearest neighbour method is applied.

runs, separated by brief rests.

5.2.1.3 Control

The cursor was controlled in one of two ways for two separate groups of subjects.

In the **position control** group the cursor was controlled by a single FSR. The position of the cursor was set to 0 pixels for a force of $\leq 0.2\text{N}$ to a maximum 1024 pixels for 2N of force. These values were chosen due to the linear range available from the force sensors used, which were low-cost force-sensing resistors (FSR). As the FSR was linear in this range this control algorithm produced a cursor position directly proportional to force.

In the **velocity control** group the cursor was controlled by two FSRs, one to control leftward motion and the other to control rightward motion of the cursor. The initial position of the cursor was randomised on each trial. The magnitude of the cursor's displacement per time frame (200ms) was set to 0 pixels for a force of $\leq 0.2\text{N}$ to a maximum of 200 pixels for 2N of force. As the FSR was linear in this range this control algorithm produced a cursor velocity directly proportional to force.

5.2.1.4 Analysis

The following quantities were measured for each trial:

- Success / failure;
- The distance of the cursor from the target at the end of the run;
- The trajectory taken to reach the target;

5.2.1.5 Training

Prior to experimentation, subjects were trained in four conditions: (i) Perfect visual and tactile f/b; (ii) Just tactile f/b; (iii) Just visual f/b; and (iv) Perfect visual and tactile f/b.

The order of (ii) and (iii) were counterbalanced across subjects so that if the order of training imposed biases these biases should be eliminated in the average overall behaviour.

5.2.1.6 Hypotheses

In the pilot experiment four hypotheses were considered. Fig. 5.4 highlights these strategies.

- **(A) Multimodal Integration:** Modalities are combined in proportion to their reliabilities (see Chapter 2); The mean distance of the cursor from the target (*mean error*) with two modalities will be less than (or equal to) the mean error for each modality alone.
- **(B) Unimodal:** One modality is rejected irrespective of its reliability.
- **(C) Winner takes all:** The more reliable modality is used and the other modality is rejected. (This is not the same as **(A)** which may exploit the redundancy between the modalities).
- **(D) Interference:** It is possible that the presence of an additional modality causes confusion, especially if the noise in the modalities causes a noticeable discrepancy between the cues (see Gepshtein and Banks, 2003, Spence et al., 2004, Gepshtein et al., 2005, but also see Welch et al., 1979, Warren et al., 1983 and discussion in Chapter 2). Subjects may show reduced mean error in the unimodal condition than in a multimodal condition where one modality is particularly noisy.

5.2.2 Main Experiment

5.2.2.1 Task

A variant of the cursor navigation task from the pilot experiment was developed (Fig. 5.5). Similar to the pilot experiment, feedback of the cursor was presented in two

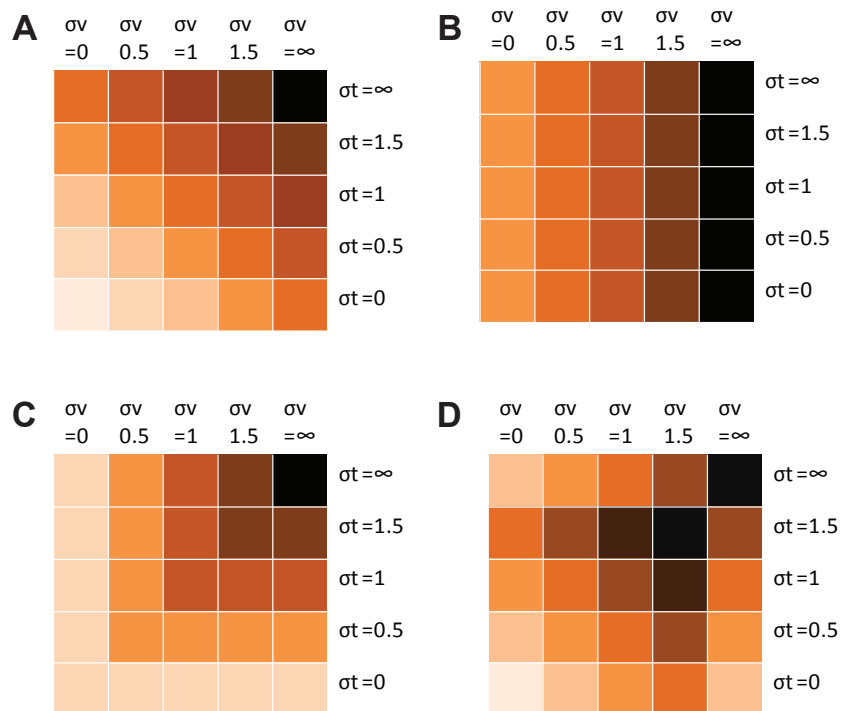


Figure 5.4: **Integration Hypotheses.** Predicted performance under four integration conditions are plotted. Darker tones indicate worse performance. **(A)** Multimodal **(B)** Unimodal; **(C)** Winner takes all. **(D)** Cross-modal Interference. See text for description of these hypotheses.

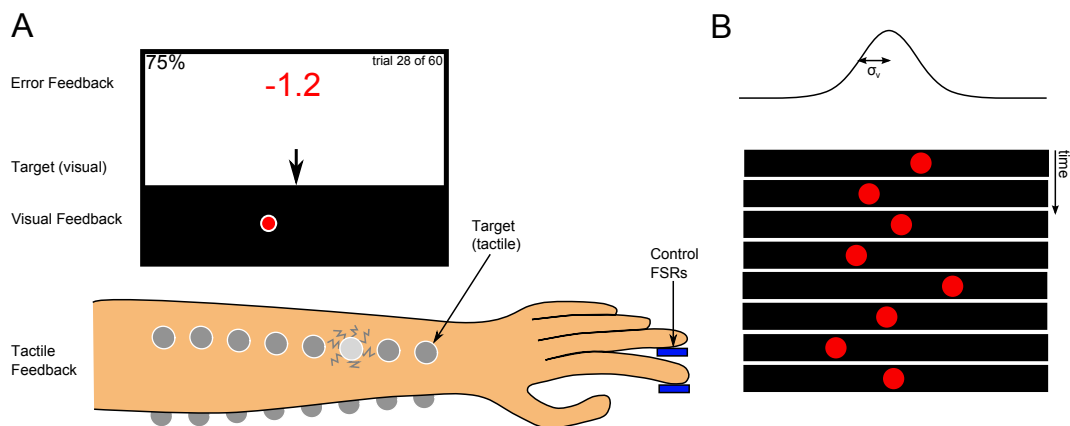


Figure 5.5: **Cursor Navigation Task.** **(A)**, Schematic of the task. Subjects are required to track a cursor to a fixed target position using visual and tactile feedback of cursor position. The target is fixed to the centre of the screen (visual target) and a single factor (tactile target). On-screen feedback is given at the end of each trial. **(B)** Spatial uncertainty of variance σ_v (noise) is applied to the visual modality to create spatiotemporally modulated cue sequence (jitter).

modalities, with “jitter” added to each modality to vary the underlying uncertainty of each. In contrast to the pilot experiment, subjects were required to navigate a cursor to a *fixed* multimodal target location. Each trial duration was 4.5-seconds, and visual and tactile uncertainty were varied randomly *from trial-to-trial*.

5.2.2.2 Experiment Structure

Instructions Prior to the experiment, subjects were told that the cursor would be presented both on-screen as a blob and on their arm as a vibratory sensation. The experimenter pointed at a particular vibrating motor and a particular location on the screen so that subjects were aware of the target location in both modalities. Subjects were then informed that the task would be made more difficult by adding noise to either the visual information, the tactile information, or both sources of information. The noise would be random from trial to trial.

Unimodal Training Phases Following these instructions, the experiment comprised four phases. In the first training phase, **V**, subjects were told that visual feedback would be the dominant modality, and to rely on visual cues to complete the task. In the second training phase, **T**, subjects were told that tactile feedback would be the dominant modality, and to rely on tactile cues to complete the task. The order these two training phases was counterbalanced across subjects. The training required subjects to navigate the cursor to the target for three different values of jitter in the dominant modality (with jitter ranging from ± 20 to ± 200 pixels). The non-dominant modality was given a much larger range of jitter (± 400 pixels). There were no biases imposed on either modality in the training. 4 blocks of trials were performed. Within each block, each value of jitter was tested 5 times (but not in sequence) so that in each training phase 60 trials were performed. This resulted in approximately 4 minutes of training for each condition.

Multimodal Training Phase In the third training phase, subjects were exposed to a sample of the full task, with two values of tactile jitter (the ranges ± 20 and ± 100 pixels) and two of visual jitter (the ranges were chosen based on the earlier training trials, **T** and **V**, such that the mean error for each of the visual conditions would match the mean error for the corresponding tactile conditions). On each trial the amount of jitter in each modality was chosen in a randomised full factorial design to avoid any biases being induced at this stage. After 20 training trials it was assumed that subjects were familiar with the idea of having to choose to use vision or tactile feedback on each trial.

Following training, subjects were asked to comment on their performance. If they

reported that they struggled to use a given modality they were given the opportunity to repeat the training. If necessary, the range of variances was modified by the experimenter so that the range of errors in the tactile training would continue to overlap with those in the visual training.

Test Phase After training, subjects performed 4 blocks of a full factorial test phase, whereby three values of visual and tactile jitter were combined to create 9 conditions in total. with which

In the test phase a deliberate discrepancy (or *offset*) was imposed between the modalities. The magnitude of the offset was varied from trial to trial, but was at most half of the standard deviation of the jitter in each modality, ensuring that the discrepancy was not noticed by subjects. Each experimental condition was tested for 5 different values of modality offset so that in total 180 trials were run. The test phase lasted approximately 15 minutes.

5.2.2.3 Cursor Control

The true cursor at time t (denoted x_t) was controlled by two FSRs, one to control leftward motion and the other to control rightward motion. The initial position of the cursor, x_0 , was randomised on each trial. The magnitude of the cursor's displacement per time frame (125ms) was set to 0 pixels for a force of $\leq 0.2\text{N}$ to a maximum of 200 pixels for 2N of force. As the FSR was roughly linear in this range this control algorithm produced a cursor velocity proportional to force.

5.2.2.4 Success/Failure Feedback

Subjects received feedback at the end of each trial in the form of a number on screen, with a negative number to indicate that the final cursor location was left of the target, and positive for right of the target. The magnitude of the error was a decimal value representing the number of vibrotactors between the target and the subject's final estimate, given to 1 decimal place. If the magnitude of this value was less than 0.5 vibrotactors (32 pixels) a 'success' sound effect was played, and if unsuccessful a different 'disappointment' sound effect was played. Furthermore, at the end of the trial the true location of the underlying cursor was presented to both the visual and tactile modalities for a duration of 300ms.

5.2.2.5 Subjects

The task was performed by 12 subjects. One subject's data was discarded as their mean error in the visual and tactile training phases did not overlap for the range of

uncertainties available.

Subjects were recruited and tested by Eduardo Moraud, an M.Sc. student under my supervision. However, all aspects of the experiment were designed by myself, and all analyses presented here were conducted independently of Moraud (2009).

5.2.2.6 Stimuli

Manipulations Across trials two factors were modulated: (i) the amount of ‘jitter’ in each modality; and (ii) the ‘offset’ between modalities. At a particular time t , let the underlying cursor be at position x_t . The visual v_t and tactile (haptic) h_t cues at time t were samples from uniform distributions, given by:

$$h_t \sim \text{Uniform}(x_t - (1 + b)a_h, x_t + (1 - b)a_h) \quad (5.1)$$

$$v_t \sim \text{Uniform}(x_t - (1 - b)a_v, x_t + (1 + b)a_v) \quad (5.2)$$

where $\pm a_h$ and $\pm a_v$ define the range of the tactile and visual distributions, and the offset term b separates the distributions by a fraction of their width.

The magnitude of $b \in \{-0.5, 0, 0.5\}$ was varied randomly from trial to trial, so that the visual and tactile distributions still overlapped but their means were slightly different.

a_h and a_v were initially chosen $\in \{20, 100, 200\}$. After training these values were adjusted (per subject) to achieve overlap between visual and tactile unimodal performance.

Feedback was temporally quantised so that visual feedback samples were received every 250ms and tactile feedback samples every 125ms. Since visual feedback has a better spatial resolution this allowed it to be penalised temporally. Thus, in a complete trial, subjects received 36 samples of tactile information and 18 samples of visual information.

Over the course of a single trial, subjects perceived quantised visual and vibrotactile cues. Feedback was spatially quantised into the range $(0, 1024]$ in pixel space, with the target location at position 512 (the centre of the screen and factor 8). Tactors were spaced by 64 pixels. Tactor 1 appeared at pixel location 64, and tactor 16 at pixel location 1024.

5.2.2.7 Analysis

Quantities are expressed in pixel coordinates. Let v_t and h_t be noisy cues in the visual and tactile modalities respectively, at a particular time t . The cues are centred around x_t , the underlying cursor trajectory, as defined in equations 5.1 and 5.2. Visual samples

are spaced by $\delta_v = 250\text{ms}$, and tactile samples are spaced by $\delta_h = 125\text{ms}$. The total trial duration $T = 4500\text{ms}$. The target location on each trial is 512 pixels.

On each trial I calculate the *absolute endpoint error*, the absolute distance between the target location and the value of the underlying cursor at the end of the trial, defined in equation 5.3:

$$\text{Error} = |x_T - 512| \quad (5.3)$$

At each time-step in the trial, t , we measure (i) the location of the visual and tactile cues relative to the true cursor; and (ii) the variance of the cues around the true cursor. These quantities may relate to the decision made by subjects at each time step.

$$[\mu_v]_t = \frac{\delta_v}{t} \sum_{s \in \{\delta_v: \delta_v:t\}} (v_s - x_s) \quad (5.4)$$

$$[\sigma_v^2]_t = \frac{\delta_v}{t-1} \sum_{s \in \{\delta_v: \delta_v:t\}} (v_s - x_s - [\mu_v]_s)^2 \quad (5.5)$$

Similar calculations are made for $[\mu_h]_t$ and $[\sigma_h^2]_t$ for the tactile modality.

As previously discussed, a random offset, b , between visual and tactile distributions is introduced so that the modalities are slightly (but not detectably) discrepant. For positive offsets, $[\mu_v]_T < [\mu_h]_T$ and for negative offsets $[\mu_v]_T > [\mu_h]_T$. In these cases, if the subject was relying on just vision, or just tactile feedback, one should see an effect of this in their decision, x_T . This allows for per-trial visual and tactile *weights* to be computed:

$$w_h = \frac{[\mu_v]_T - x_T}{[\mu_v]_T - [\mu_h]_T} \quad (5.6)$$

$$w_v = \frac{[\mu_h]_T - x_T}{[\mu_h]_T - [\mu_v]_T} \quad (5.7)$$

Note that these values are scaled with respect to the separation of the means. Each weight will range from 0 to 1 if x_T lies between $[\mu_v]_T$ and $[\mu_h]_T$. Also, note that $w_h = 1 - w_v$. To quantify the bias towards one modality or the other we use a measure in which -1 represents a tactile bias, and +1 represents a visual bias:

$$\text{Bias} = w_v - w_h \quad (5.8)$$

This Bias quantity disproportionately amplifies decisions when the visual and tactile means are close or indistinguishable. To avoid noisy terms dominating statistical computations Tukey's range test, (also Tukey's HSD equation 5.9) allows trials to be discarded where the means are indistinguishable (in which case we can assume that the data offers little discriminative power). In practice this corresponds mainly to data

from the condition where the offset is 0, though also arises by chance in the other offset conditions. Equation 5.10 allows such trials to be removed from the Bias measure.

$$Q = \frac{|\mu_1 - \mu_2|}{\sqrt{\frac{1}{N}MSE}} \quad (5.9)$$

$$= \frac{|[\mu_v]_T - [\mu_h]_T|}{\sqrt{\frac{1}{2}([\sigma_v^2]_T + [\sigma_h^2]_T)}} \quad (5.10)$$

Using the two measures, Error and Bias, the “hallmarks” of multisensory integration (see Angelaki et al., 2009 and others) can be evaluated by comparing the metrics for different experimental conditions:

- (i) **Sensory Substitution.** In both of the dominant-modality conditions, i.e. ($a_h = \text{low}$, $a_v = \text{high}$) and ($a_h = \text{high}$, $a_v = \text{low}$), if the Error measure is lower than in the high uncertainty condition ($a_h = \text{high}$, $a_v = \text{high}$), then *either* modality can be used to complete the task. Hence, the modalities can *substitute* for one another.
- (ii) **Multisensory Integration.** A larger Error measure in the dominant-modality condition ($\sigma_x = \text{low}$, $\sigma_y = \text{high}$) compared to the multi-modal condition ($\sigma_x = \text{low}$, $\sigma_y = \text{low}$) indicates that *both* modalities have been used to complete the task. Hence, the modalities have been *integrated*. A Bias measure of zero would reinforce this.
- (iv) **Optimal Multisensory Integration.** The Bias measure indicates the relative weight allocated to each modality. If each modality is weighted by its *objective reliability*, this is indicative of optimal integration.

5.2.2.8 Simulation

To aid interpretation of results, five hypotheses were simulated, termed *unimodal visual*, *even weights*, *random weights*, *winner-takes-all* and *Bayes-optimal* (see Chapter 2), defined below.

Integration Hypotheses The present task requires subjects to navigate a noisy cursor to a target location. To achieve this successfully an *ideal observer* would estimate the mean and uncertainty of the cues in each modality to reliably compute the cursor location (as a weighted sum of the unimodal estimates, see 2). Let us define the *true* cursor location as μ . The simulated observer needs to form an estimate of the cursor location (denoted $\hat{\mu}$) to succeed at the task. We can ignore (for now) how the cursor is moved by the subject.

Now, consider a random variable V as the source of evidence in the visual modality. Let us assume that each sample of V , denoted v_t , is drawn from an underlying distribution with unknown mean μ , and unknown variance. At time t we can form an estimate, μ_v , of the underlying mean, based on the samples seen so far, and likewise an estimate, σ_v^2 , of the underlying variance (given previously by equations 5.4 and 5.5, but with the time indices removed for convenience). Now, consider a second random variable H as the source of tactile evidence. Again, samples are drawn from an underlying distribution with unknown mean μ and unknown variance. Likewise we may choose to compute μ_h and σ_h^2 .

If one uses only μ_v and μ_h to compute an *uncertainty-independent* estimate of the mean of the underlying distribution the following three integration hypotheses may be considered:

$$\begin{aligned}
 \text{Unimodal Visual} \quad \hat{\mu} &= \mu_v \\
 \text{Even Weights} \quad \hat{\mu} &= \frac{1}{2}(\mu_v + \mu_h) \\
 \text{Random Weights} \quad \hat{\mu} &= q\mu_v + (1 - q)\mu_h
 \end{aligned} \tag{5.11}$$

Where q is a random number generated from trial-to-trial, drawn from $\text{Uniform}(0, 1)$.

If one uses μ_v , μ_h , σ_v^2 and σ_h^2 to compute an *uncertainty-weighted* estimate of the mean of the underlying distribution, the following two hypotheses may also be considered:

$$\begin{aligned}
 \text{Winner Takes All} \quad \hat{\mu} &= \begin{cases} \mu_v & \text{if } \sigma_v^2 < \sigma_h^2 \\ \mu_h & \text{otherwise} \end{cases} \\
 \text{Bayes Optimal} \quad \hat{\mu} &= \frac{\mu_h \sigma_v^2 + \mu_v \sigma_h^2}{\sigma_v^2 + \sigma_h^2}
 \end{aligned} \tag{5.12}$$

These hypotheses were introduced in Chapter 2.

Kinematic Constraints The above definitions allow for the cursor position to be calculated, but another important aspect of the task is that the cursor can be moved. In simulation, time is discretised into steps of size 125ms. At each time step the underlying cursor, $x_{1:T}$, is updated according to the following difference equation:

$$x_{t+1} = (1 - \alpha) \cdot x_t + \alpha \cdot (\hat{\mu} - x_t + \epsilon) \tag{5.13}$$

Where ϵ is a Gaussian-distributed noise term and α is a smoothing parameter set to 0.1. Hence the trajectory eventually converges on the estimate ($\hat{\mu}$), constrained by motion smoothing (α) and perturbed by motor noise (ϵ). As the purpose of the simulation is simply for comparison with endpoint Error and Bias measures it was not necessary to use the more detailed kinematic model introduced in Chapter 4.

Uncertain Uncertainty The ideal observer requires an accurate measure of their objective variability (*viz.* the reliability of the sensory information in each modality) to determine the optimal integration weights. This is not the same as simply the variance of the cues, as there are also uncontrolled sources of uncertainty ranging from low-level noise (e.g. sensory, neural, processing and motor uncertainty) as well as high-level variability (e.g. distraction, inattention, forgetting). To compare empirical to simulated behaviour, the unimodal objective variability can be determined during the unimodal *training* phases. this is then used to predict the multimodal objective variability in the test phase. We define the *objective variability* during the training phase as the variance of the endpoint decision across training trials, i.e.

$$\tau^2 = \frac{1}{K} \sum_k (x_T^{(k)} - 512)^2 \quad (5.14)$$

Where $x_t^{(k)}$ denotes the position of the cursor at time t on trial k . Therefore let τ_v^2 denote the variability of the endpoint decision across all K trials for each subject in the visual training phase, and similarly let τ_h^2 denote the variability in the tactile training phase. τ_v^2 and τ_h^2 replace σ_v^2 and σ_h^2 in equation 5.12. Each of the strategies is simulated using the data for each subject, then averaged across all subjects to enable quantitative comparison of empirical and simulation results.

5.3 Results

5.3.1 Notation

In the test phase of the pilot experiment, and in the unimodal training phases of the main experiment, three baseline experimental conditions are discriminated:

- **Vision-only.** $\mathbf{V} = (\sigma_v = low, \sigma_t = \infty)$
- **Tactile-only.** $\mathbf{T} = (\sigma_v = \infty, \sigma_t = low)$
- **No feedback.** $\mathbf{X} = (\sigma_v = \infty, \sigma_t = \infty)$.

In the multimodal test phase of each experiment, four experimental conditions are discriminated:

- **Vision-dominant.** $\mathbf{VT} = (\sigma_v = low, \sigma_t = high)$
- **Tactile-dominant.** $\mathbf{VT} = (\sigma_v = high, \sigma_t = low)$
- **Multimodal.** $\mathbf{VT} = (\sigma_v = low, \sigma_t = low)$
- **No dominant feedback.** $\mathbf{VT} = (\sigma_v = high, \sigma_t = high)$.

These conditions allow for the discrimination of the different integration hypotheses (see *methods*).

5.3.2 Pilot Results

In the pilot experiment I examined multisensory target localisation performance in subjects controlling either a *position-controlled* or *velocity-controlled* noisy cursor (see *methods*).

5.3.2.1 Position Control Group

Within-trial performance can be visualised via the trajectories observed in achieving different target locations. Fig. 5.6 illustrates the within-trial trajectories for a single subject controlling the cursor with position (proportional) control. For this subject the smoothest and most reliable trajectories occur with either reliable visual feedback (bottom panels) and tactile feedback (left panels), but noise and errors increase for increasing uncertainty. The subject in Fig. 5.6 was also moderately accurate in the presence of no feedback (top right panel).

Fig. 5.7 illustrates these trajectories normalised into the range $[0,1]$, with 0 corresponding to the start location and 1 corresponding to the target location, for the same subject as above. For this subject the fastest convergence occurs with reliable visual

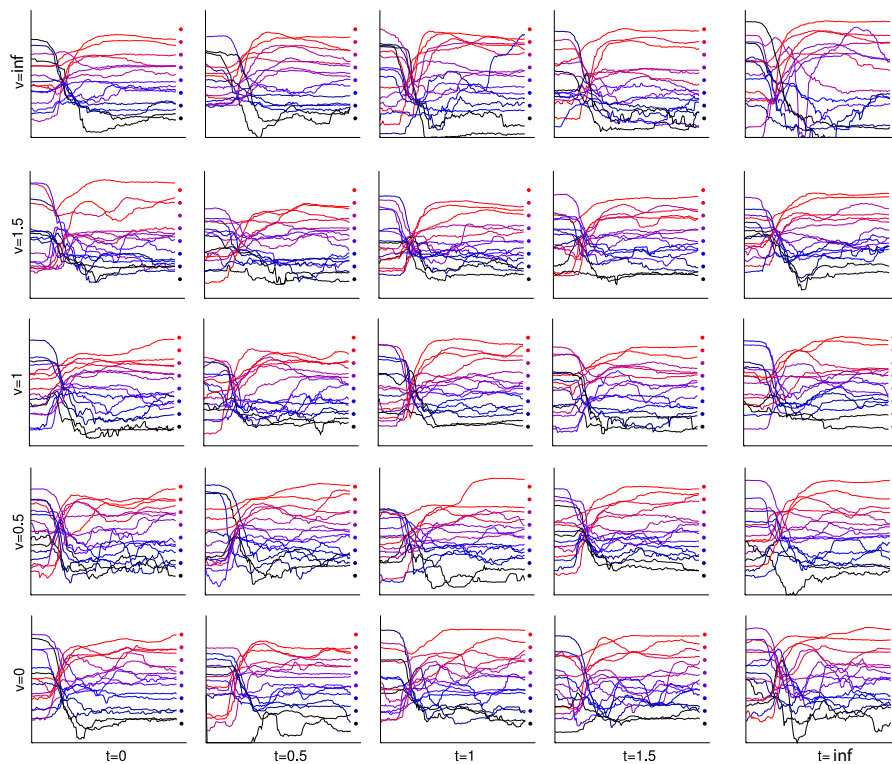


Figure 5.6: **Position Control Trajectories.** Sub-plots show cursor trajectories over time for all 25 conditions of visual (v) and tactile (t) jitter, for a single subject in the proportional control condition. The x-axis of each plot represents time (from left to right) for the 5s duration of the trial. The y-axis corresponds to the horizontal position of the cursor recorded over the time course of the trial. Trajectories are colour coded with respect to the target location (coloured blobs).

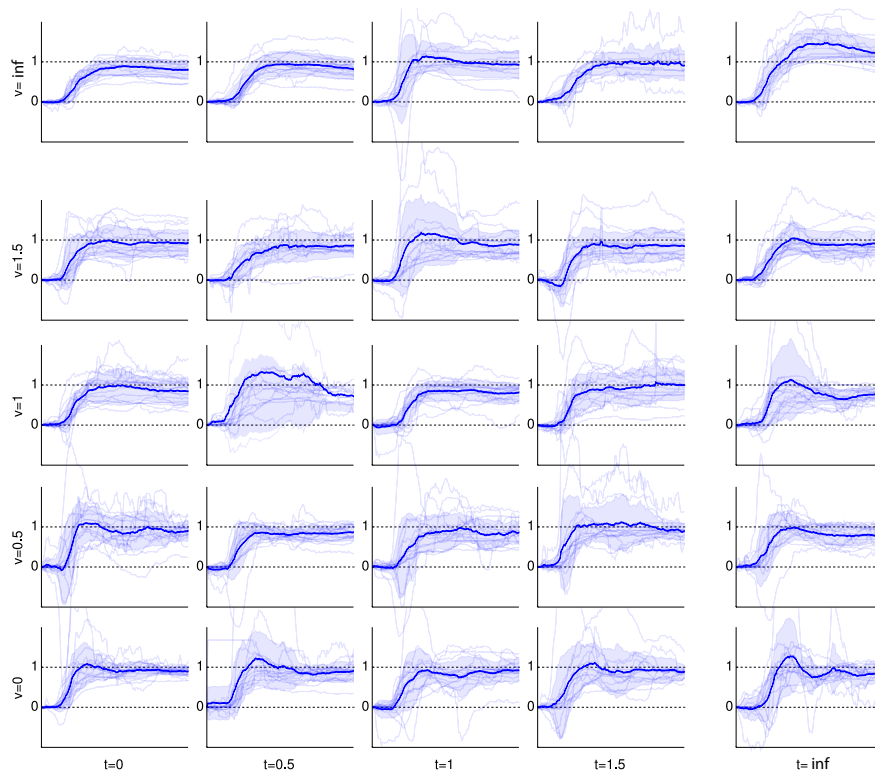


Figure 5.7: **Normalised Position Control Trajectories.** Normalised cursor trajectories over time for all 25 conditions for a single subject in the proportional control condition. The x-axis of each plot represents time (from left to right) for the 5s duration of the trial. The y-axis corresponds to the normalised horizontal position of the cursor ranging from the start position (0) to the target location (1). For each condition the normalised trajectories (faded lines) are plotted with the overall mean (solid line) and standard error across trajectories (shaded region).

feedback (bottom panels), less erratic trajectories occur with reliable tactile feedback (left panels) and performance worsens for higher levels of uncertainty (top right panel).

Fig. 5.8 illustrates the use of mean endpoint error to characterise performance, for the same subject as above. For this subject the best performance is observed for low visual and tactile uncertainty (towards the bottom left) and worst performance is observed for high visual and tactile uncertainty (towards the top right), as expected.

The grouped data across 5 subjects using the position control strategy is illustrated in a normalised surface plot (Fig. 5.9, see caption for details). Note that the surface slope varies as a function of visual jitter, but not as a function of tactile jitter, except in the absence of visual feedback (**VT** and **VT** conditions). This suggests (qualitatively) that sensory substitution was achieved but not necessarily sensory integration (see *methods*).

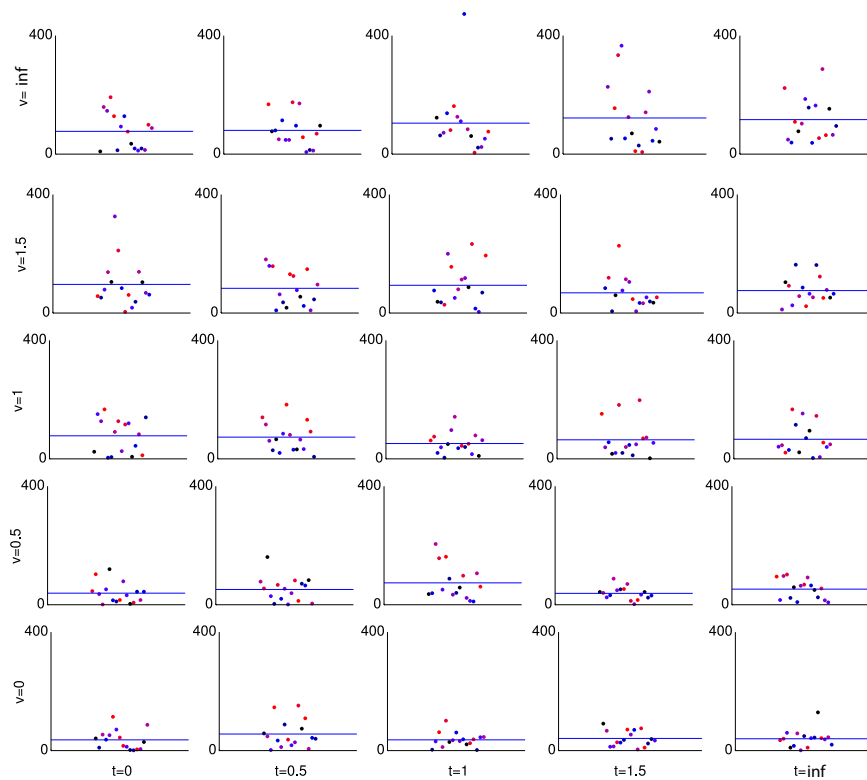


Figure 5.8: **Position Control Endpoint Errors.** Mean endpoint error (pixels) for all 25 conditions for a single subject in the proportional control condition. The x-axis of each plot represents the trial number (from left to right), revealing no obvious effect of learning or fatigue across trials. The y-axis corresponds to the mean endpoint error between the cursor position and the target. Coloured blobs represent the result of each trajectory, and are colour coded according to the target locations in 5.6. Horizontal lines capture the mean endpoint error for each condition.

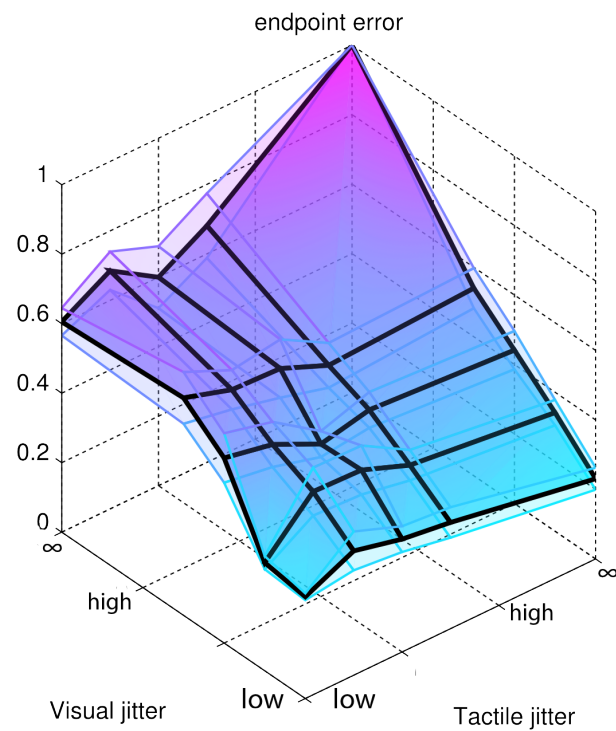


Figure 5.9: **Position Control normalised endpoint error (N=5)**. Mean endpoint errors for all 25 conditions (emboldened grid) \pm standard error across subjects (transparent grid). Before averaging across subjects, error data are scaled for each subject so that the no-feedback trial ($\sigma_v = \infty$, $\sigma_t = \infty$) has an error of 1. This reduces between-subject variability when averaging across subjects.

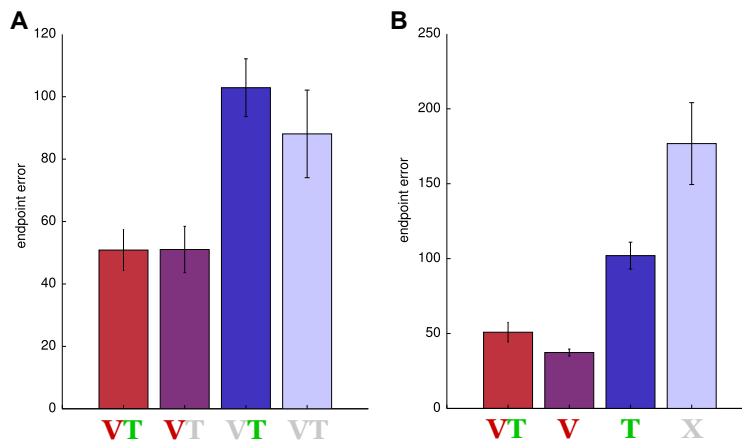


Figure 5.10: **Position Control comparison (N=5)**. (See text for description of shorthand notation used) **(A)** Comparison of low uncertainty to high uncertainty: There was no observed difference due to tactile feedback uncertainty in the presence of vision ($\mathbf{VT} \approx \mathbf{V}$ and $\mathbf{T} \approx \mathbf{VT}$). In contrast, a more pronounced effect of visual feedback uncertainty was observed in presence of tactile feedback ($\mathbf{VT} > \mathbf{T}$, and $\mathbf{V} > \mathbf{VT}$). These differences may or may not be significant, as statistical tests were not performed. **(B)** Comparison between conditions with presence/absence of feedback: Multimodal performance was worse than unimodal visual performance ($\mathbf{VT} < \mathbf{VT}$) but multimodal performance appeared better than unimodal tactile performance. Performance was worse with neither source of feedback ($\mathbf{VT} > \mathbf{VT}$, $\mathbf{VT} > \mathbf{VT}$ and $\mathbf{VT} > \mathbf{VT}$). These differences may or may not be significant, as statistical tests were not performed.

Fig. 5.10A illustrates the role of *uncertainty* on performance (endpoint error) by comparing the low uncertainty conditions to the high uncertainty conditions. Low visual uncertainty (\mathbf{VT} and \mathbf{VT}) produces lowest errors, and high visual uncertainty (\mathbf{VT} and \mathbf{VT}) produces highest errors. A benefit of low tactile uncertainty is not observed. Owing to the small number of subjects, statistical tests were not performed, and so these conclusions may not be significant.

Fig. 5.10B illustrates the role of the *presence of feedback* on performance (endpoint error). \mathbf{VT} results in slightly greater error compared to \mathbf{V} , indicating that tactile feedback may add an additional burden to the task. However, \mathbf{VT} results in *reduced* error compared to \mathbf{VT} . Performance is worst in the absence of both sources of feedback.

5.11 illustrates the interaction between the modalities. In unimodal trials there was no observed effect of tactile feedback uncertainty on Error (Fig. 5.11A, zero slope), but increasing visual feedback uncertainty increased Error (Fig. 5.11B, non-zero slope). However, the magnitude of error between the two modalities does not overlap and therefore (consistent with the prediction of a Bayesian model of integration) there is

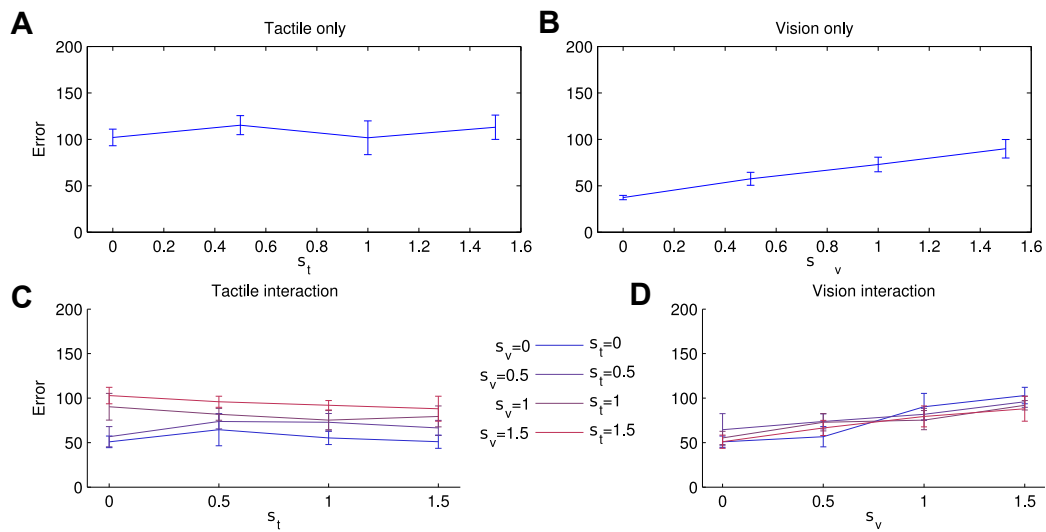


Figure 5.11: **Position Control Integration (N=5)**. Mean endpoint errors are shown for unimodal and multimodal conditions. **(A)** unimodal tactile condition ($\sigma_v = \infty$) **(B)** Unimodal visual condition ($\sigma_t = \infty$) **(C)** Multimodal conditions. Each line corresponds to different σ_v . x-axis corresponds to σ_t **(D)** Multimodal conditions. Each line corresponds to different σ_t . x-axis corresponds to σ_v . Key is shared between C and D.

no observed effect of tactile feedback uncertainty in the multimodal conditions (Fig. 5.11C, zero slope). These differences may or may not be significant, as statistical tests were not performed.

5.3.2.2 Velocity Control Group

The grouped data across 5 subjects using the *velocity* control strategy are illustrated in a normalised surface plot in Fig. 5.12. Note that the surface slope varies as a function of both visual jitter and tactile jitter. In contrast to the position control group this suggests that sensory substitution was achieved as well as some degree of sensory integration (see *methods*).

Fig. 5.13A illustrates the role of *uncertainty* on performance by comparing the low uncertainty conditions to the high uncertainty conditions. Low visual uncertainty (**VT** and **V**T) produces lowest errors, and high visual uncertainty (**V**T and **VT**) produces highest errors. Under high visual uncertainty, tactile feedback reduces errors (**V**T shows reduced errors compared to **VT**). Owing to the small number of subjects, statistical tests were not performed, and so these conclusions may not be significant.

Fig. 5.13B illustrates the role of the *presence of feedback* on performance. Error in **V**T is again greater than **V**, suggesting that tactile feedback may add an additional burden to the task. In contrast, **V**T shows reduced errors compared to **T**. In the no-

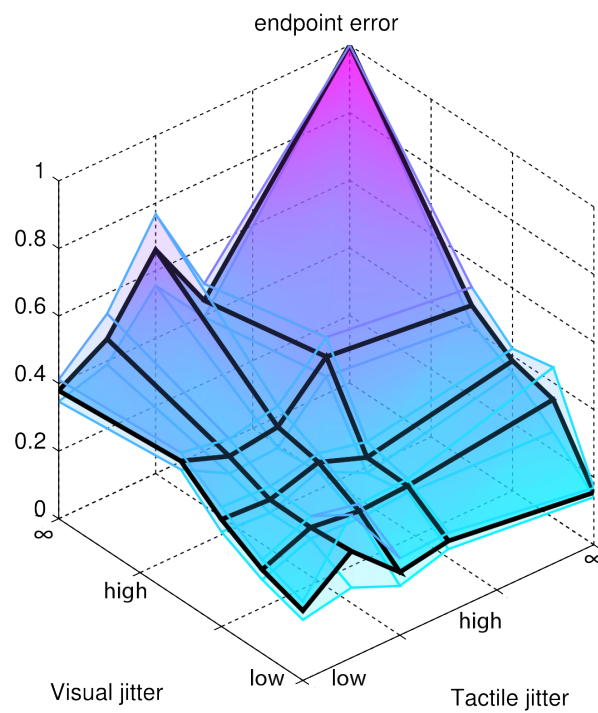


Figure 5.12: **Velocity Control normalised endpoint error (N=5)**. Mean endpoint errors for all 25 conditions (emboldened grid) \pm standard error across subjects (transparent grid). Before averaging across subjects, error data are scaled for each subject so that the no-feedback trial ($\sigma_v = \infty, \sigma_t = \infty$) has an error of 1. This reduces between-subject variability.

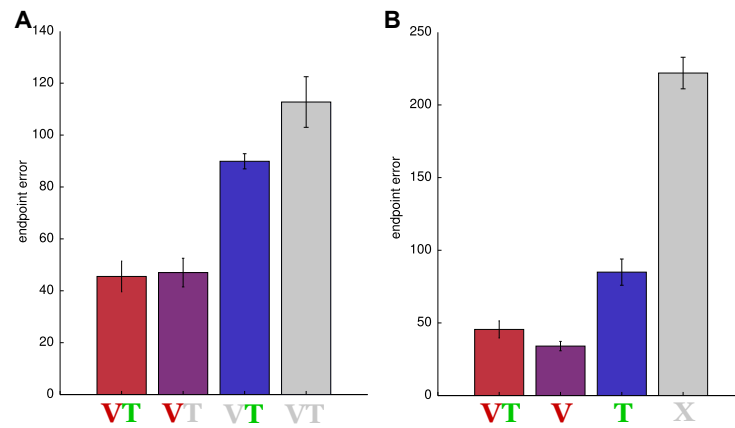


Figure 5.13: **Velocity Control comparison (N=5)**. (See text for description of short-hand notation used) **(A)** Comparison of low uncertainty to high uncertainty: Weak effect of tactile feedback uncertainty in presence of vision ($VT \approx V$) but in absence of vision the effect is observed ($T > VT$). There is an effect of visual feedback uncertainty in the presence of tactile feedback ($VT > T$, and $V > VT$). These differences may or may not be significant, as statistical tests were not performed. **(B)** Comparison between conditions with presence/absence of feedback. Multimodal visual worse than unimodal visual ($VT < VT$), Multimodal tactile better than unimodal tactile ($VT < VT$), performance much worse with neither ($VT > VT$, $VT > VT$ and $VT > VT$). These differences may or may not be significant, as statistical tests were not performed.

feedback condition performance is considerably worse than for position control (see Fig. 5.10). These differences may or may not be significant, as statistical tests were not performed.

5.14 illustrates the interaction between the modalities. In contrast to position control the range of Error in the unimodal tactile trials overlaps the range of Error in the unimodal visual trials. Moreover, both tactile and visual uncertainty appear to affect the Error (Fig. 5.14A and 5.14B, non-zero slope). Consequently, in the multimodal conditions a slight positive slope due to tactile uncertainty is seen as visual uncertainty is degraded past $\sigma_v = 0.5$. A positive slope is also seen due to visual uncertainty for all multimodal conditions. However, these differences may not be significant, as statistical tests were not performed.

5.3.3 Main Experiment Results

5.3.3.1 Sensory Substitution

Unimodal performance was compared for the vision-alone condition (V) and vibrotactile-alone condition (T). Of the 12 subjects, 3 performed considerably better with visual

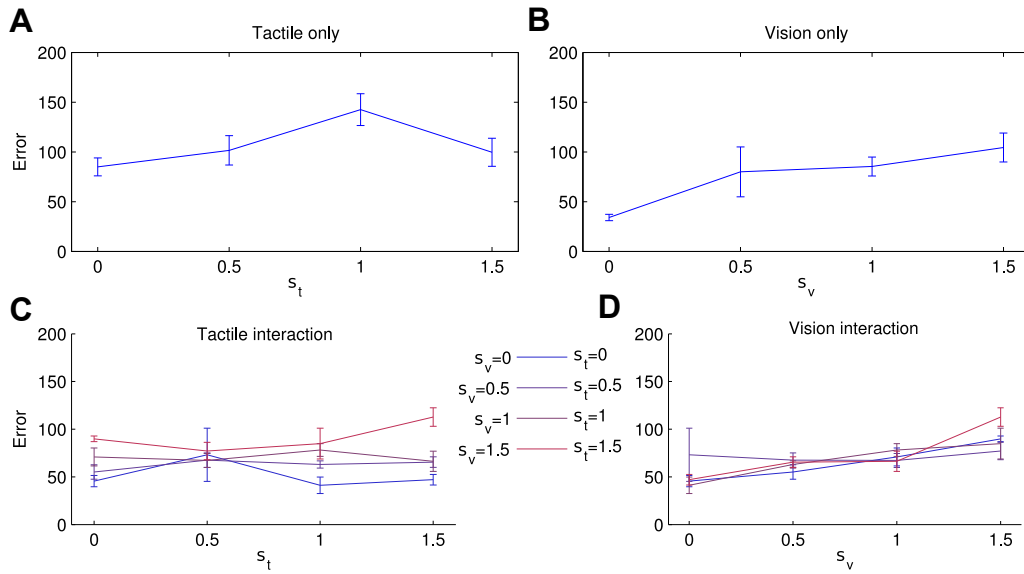


Figure 5.14: **Velocity Control Integration (N=5)**. Mean endpoint errors are shown for unimodal and multimodal conditions. **(A)** unimodal tactile condition ($\sigma_v = \infty$) **(B)** Unimodal visual condition ($\sigma_t = \infty$) **(C)** Multimodal conditions. Each line corresponds to different σ_v . x-axis corresponds to σ_t **(D)** Multimodal conditions. Each line corresponds to different σ_t . x-axis corresponds to σ_v

feedback alone than with tactile feedback alone, to the extent that their Error in the high visual uncertainty condition was greater than in the low tactile uncertainty condition in training. These subjects were retrained with compromised vision (as detailed in *methods*), and two showed sufficient overlap in the ranges of Errors for each modality, whereas one did not. This subject was discarded from further analyses. Fig. 5.15 presents these findings.

5.3.3.2 Sensory Integration

I introduce a shorthand notation for describing relative performance in different conditions. The default measure of performance is endpoint error. For example, **VT** < **VT**, indicates that the **VT** trials have a smaller endpoint error than the **VT** trials. Using this notation:

- *Sensory substitution* is achieved if both **VT** < **VT** and **VT** < **VT**, i.e. each of tactile and visual feedback improve task performance over no feedback at all (see *methods*).
- *Multisensory integration* is achieved if both **VT** < **VT** and **VT** < **VT**, i.e. two modalities together improves task performance over each alone (see *methods*).

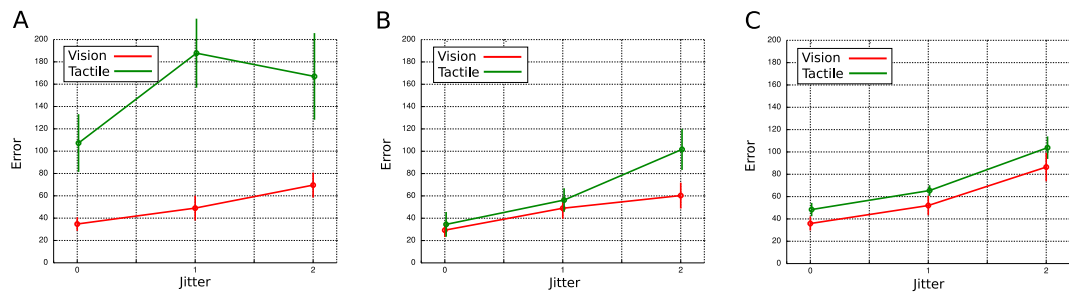


Figure 5.15: **Unimodal Performance.** (A) Mean endpoint error \pm SEM across trials for a single subject in the unimodal training trials (visual feedback only, red, and tactile feedback only, green). The x-axis marks three levels of jitter (from low to high uncertainty, left to right). This subject was discarded from further analysis as it was expected that they would show no interaction between visual and tactile feedback in the multimodal trials. (B) Mean endpoint error \pm SEM across trials for a typical subject. This subject showed comparable performance with both visual and tactile feedback. (C) Mean endpoint error \pm SEM across 11 subjects (for the final training trial in each modality). Note that the magnitude of errors in the two conditions overlap.

Fig. 5.16 presents the resulting trajectories for a typical subject. Note that the ability to quickly and accurately navigate the cursor to the target increases with jitter in both modalities. Fig. 5.17 presents the endpoint error for the same subject to support this observation.

Simulation results Endpoint error can distinguish between different multisensory integration hypotheses discussed previously. Figures 5.18 and 5.19 show simulated plots for these different hypotheses (using a kinematically constrained model, see *methods*).

Empirical results Plotting the empirical data in a similar way (Fig. 5.20) shows that $\mathbf{VT} < \mathbf{VT}$, $\mathbf{VT} < \mathbf{VT}$, and $\mathbf{VT} < \mathbf{VT}$ and $\mathbf{VT} < \mathbf{VT}$ (t-test, $p < 0.001$ for all conditions), and therefore the suboptimal strategies of *unimodal visual*, *unimodal tactile*, *even weights* and *winner takes all* (see above) can be discounted.

An ANOVA was conducted on the measure of mean endpoint error with between-subjects factors of tactile feedback uncertainty $\in \{\text{low, med, high}\}$ and visual feedback uncertainty $\in \{\text{low, med, high}\}$. This revealed a significant main effect of tactile feedback uncertainty $F(2, 10) = 18.0$, $p < .001$, a significant effect of visual feedback uncertainty $F(2, 10) = 49.495$, $p < .001$ and a significant interaction $F(4, 10) = 3.041$, $p = .016$. The interaction was expected as the uncertainties were not predicted to combine additively. Post-hoc two-tailed t-tests were used to compare individual conditions. The results are summarised in Fig. 5.21.

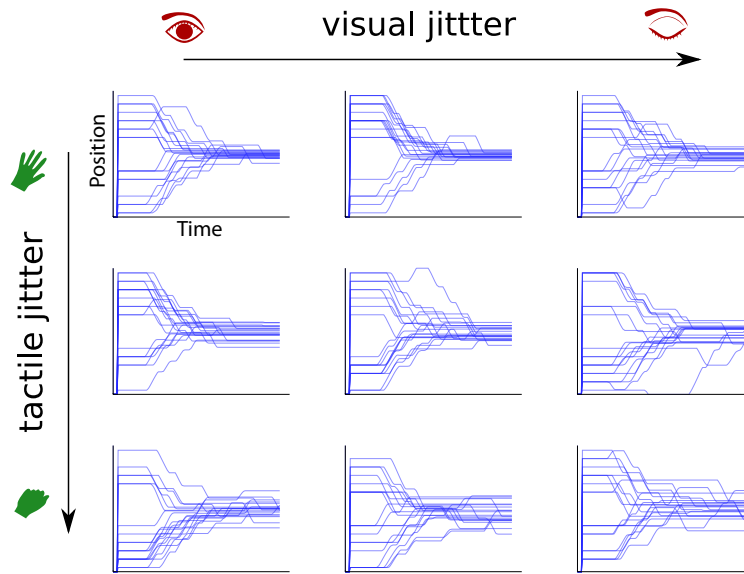


Figure 5.16: **Typical Trajectories (N=1)**. Plot of trajectories for a single subject, for different values of visual and tactile jitter. Each plot presents time on the x-axis and horizontal cursor position on the y axis.

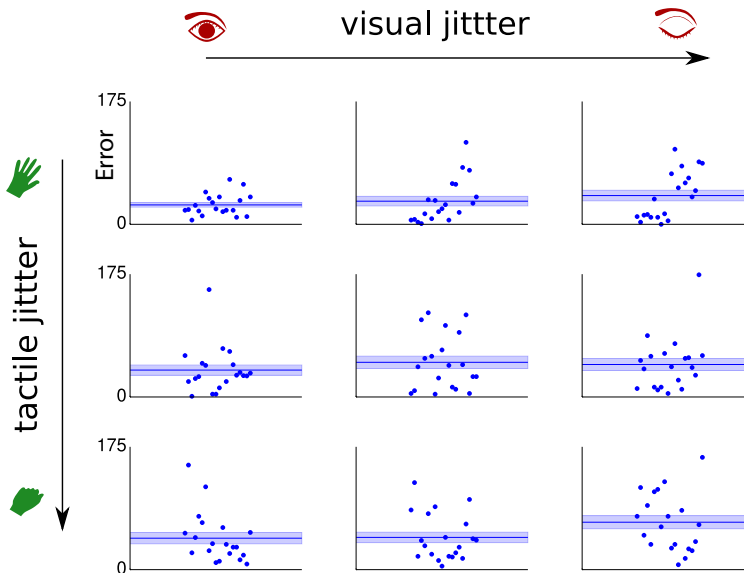


Figure 5.17: **Endpoint Error (N=1)**. Plot of endpoint errors for a single subject, for different values of visual and tactile jitter. Each plot shows the endpoint error for each trial (blobs), from left to right in the order that they were completed. The mean absolute error is on the y axis. The mean and standard error across trials are also shown (line and shaded region respectively).

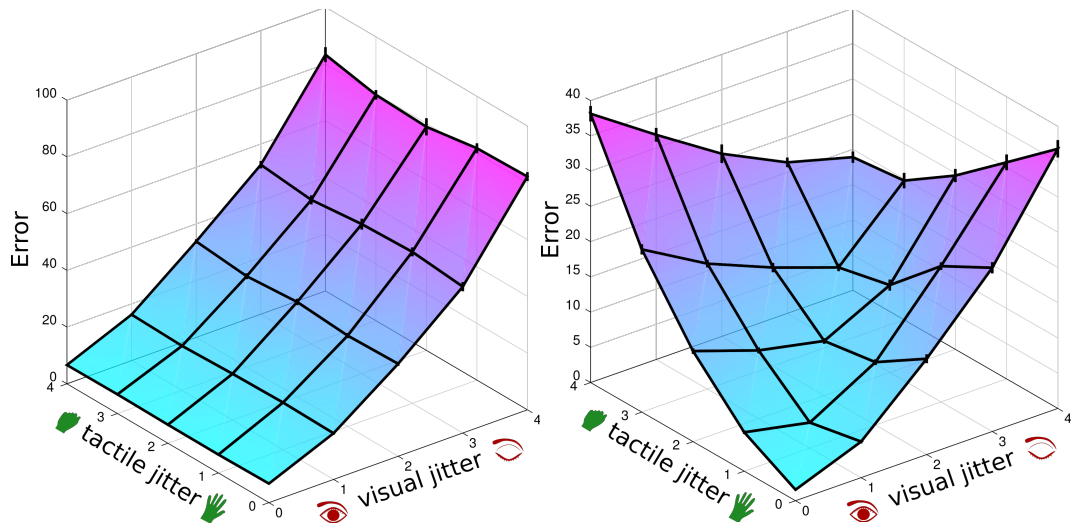


Figure 5.18: **Integration Hypotheses 1.** (left) Simulated data for a subject relying on a single modality (*unimodal visual*). Note that $V_T < V_T$ and $V_T < V_T$ but $V_T = V_T$ and $V_T = V_T$; (right) Simulated data for a subject integrating vision and tactile information, but not based on sensory uncertainty (*even weights*). Note that while $V_T < V_T$ and $V_T < V_T$, $V_T > V_T$ and $V_T > V_T$

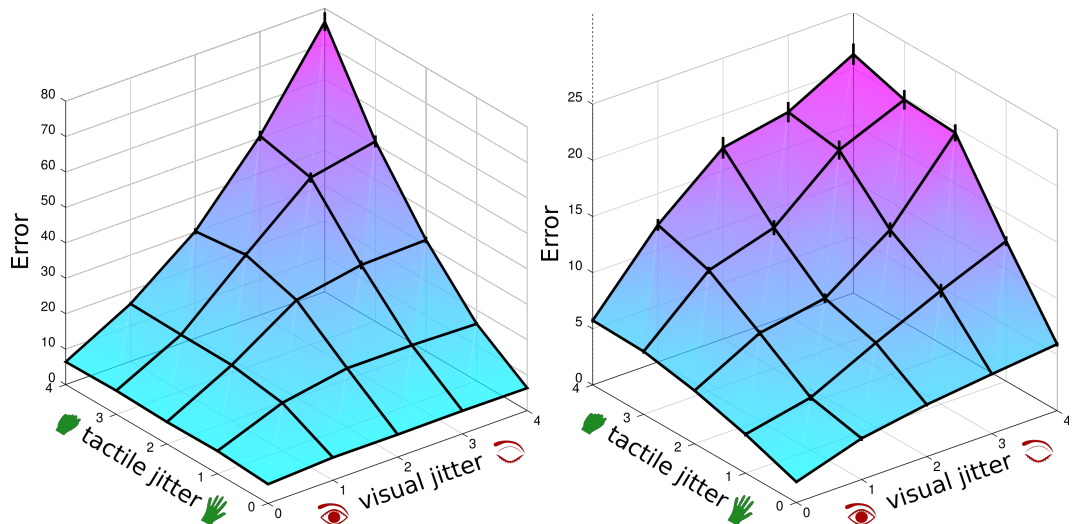


Figure 5.19: **Integration Hypotheses 2.** (left) Simulated data for a subject using a multimodal strategy (*winner takes all*). Note that $V_T < V_T$, $V_T < V_T$, but $V_T = V_T$ and $V_T = V_T$; (right) Simulated data for a subject optimally integrating vision and tactile information (*bayes-optimal*). Note that $V_T < V_T$, $V_T < V_T$, and $V_T < V_T$ and $V_T < V_T$

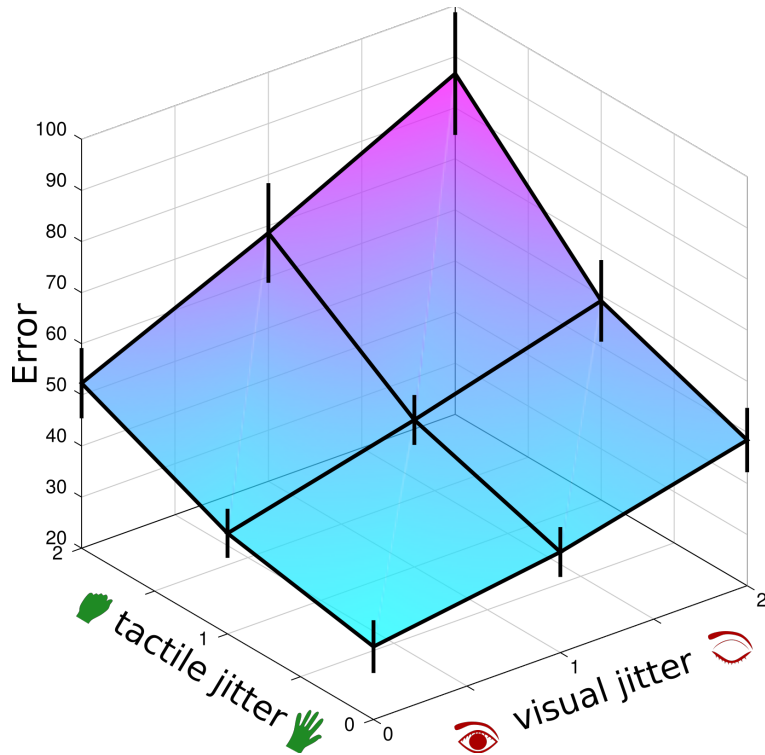


Figure 5.20: **Sensory Integration (N=12)**. Empirical results, suggesting that subjects perform multimodal integration. $V_T < V_T$, $V_T < V_T$, and $V_T < V_T$ and $V_T < V_T$ (t-test, $p < 0.00001$ for all conditions). Error bars denote standard error. There is a significant effect of visual jitter (ANOVA, $p < 0.001$) and tactile jitter (ANOVA, $p < 0.001$)

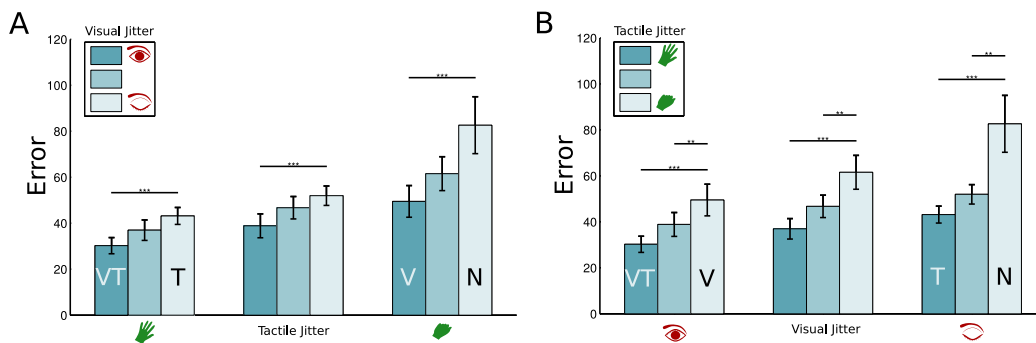


Figure 5.21: **Endpoint error comparison**. (A) Endpoint error \pm SEM as a function of visual jitter and tactile jitter; (B) The same data from (A) plotted with the visual and tactile groups swapped for convenience; Conditions are compared by two-tailed t-tests, with stars to denote significance level ($* = p < 0.05$, $** = p < 0.001$ and $*** = p < 0.00001$)

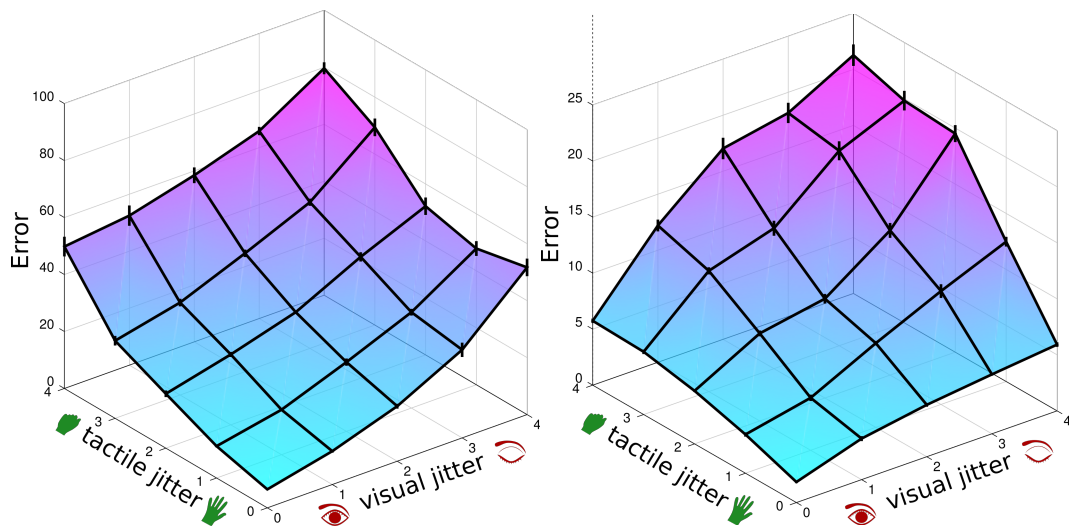


Figure 5.22: **Integration Hypotheses 3.** (*left*) Simulated data for a subject ignoring visual and tactile uncertainty, but randomly weighting either modality (*random weights*). While the magnitude of errors are greater in this suboptimal condition, note that $\mathbf{VT} < \mathbf{VT}$, $\mathbf{VT} < \mathbf{VT}$, and $\mathbf{VT} < \mathbf{VT}$ and $\mathbf{VT} < \mathbf{VT}$; (*right*) The optimal performance plot, for comparison. Apart from the magnitude of the errors, it is not obvious how one could distinguish the surfaces. [Note that the convexity and concavity of these plots depends on the range of variances used, and is not a reliable comparator, especially given the magnitude of noise in the empirical data].

It was observed that $\mathbf{VT} < \mathbf{VT}$, $\mathbf{VT} < \mathbf{VT}$ (sensory substitution) and $\mathbf{VT} < \mathbf{VT}$, $\mathbf{VT} < \mathbf{VT}$ (sensory integration). This suggests that a multimodal integration strategy is being used. Moreover, error in the unimodal training phase conditions (Fig. 5.15) reveals that $\mathbf{VT} < \mathbf{V}$ and $\mathbf{VT} < \mathbf{T}$. This decrease in error is characteristic of optimal behaviour.

However, an alternative multimodal strategy may also explain the above findings. If a subject picks an arbitrary (random) weighting of the modalities on each trial, when data is averaged across trials the resulting plot demonstrates that the *random-weights* hypothesis also satisfies the conditions of optimality discussed above (Fig. 5.22).

The random weights hypothesis captures the uncertainty of the sensory modalities *passively*, or *implicitly*. To distinguish actively optimal behaviour from a passive interpretation requires the Bias measure (see *methods*).

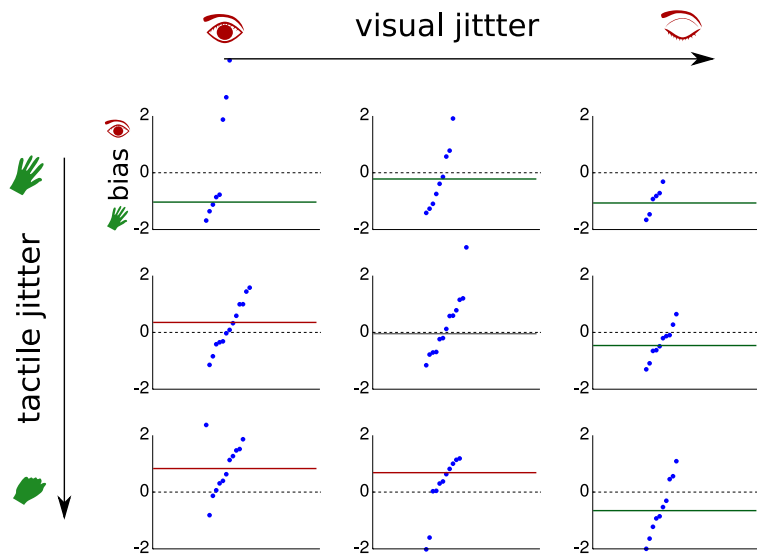


Figure 5.23: **Bias Measurement (N=1)**. Biases of a single subject for the different tactile and visual jitter conditions. In the **VT** condition, the bias is towards vision, whereas in the **TVT** condition the bias is towards the vibrotactile modality. Blobs represent trials and lines represent mean across trials. Trials are sorted from negative to positive bias to illustrate the clustering of behavioural patterns.

5.3.3.3 Optimal multisensory integration

The passive policy (*random weights*) and active policy (*bayes optimal*) are qualitatively indistinguishable using the mean endpoint error metric. Even if it is argued that the magnitude of errors discriminates the two cases, this does not control for the possibility of subjects combining multiple passive strategies, e.g. *random weights* and *mean weight*, to reduce errors. However, active decisions may be distinguished from passive effects by computing a decision ‘bias’ (see *methods*).

Biases for a single subject, for different values of tactile and visual jitter, are shown in Fig. 5.23. In the **VT** condition, the bias is towards vision, whereas in the **TVT** condition the bias is towards the vibrotactile modality. In this framework, the hallmark of optimal integration is when **VT** $_{bias} > 0$, **TVT** $_{bias} < 0$, as the subject makes an active decision to choose one modality over the other.

The average results across all subjects are summarised in Fig. 5.24.

An ANOVA on the measure of mean endpoint error with between-subjects factors of tactile feedback uncertainty $\in \{\text{low, med, high}\}$ and visual feedback uncertainty $\in \{\text{low, med, high}\}$ revealed a significant main effect of tactile feedback uncertainty ($F(2, 10) = 18.0$, $p < .001$) a significant effect of visual feedback uncertainty ($F(2, 10) = 14.8$, $p < .001$) and no significant interaction ($F(4, 10) = 0.57$, $p = .684$). Post-hoc two-tailed t-tests were used to compare individual conditions. Visual feedback incurred a visual bias (t-test:

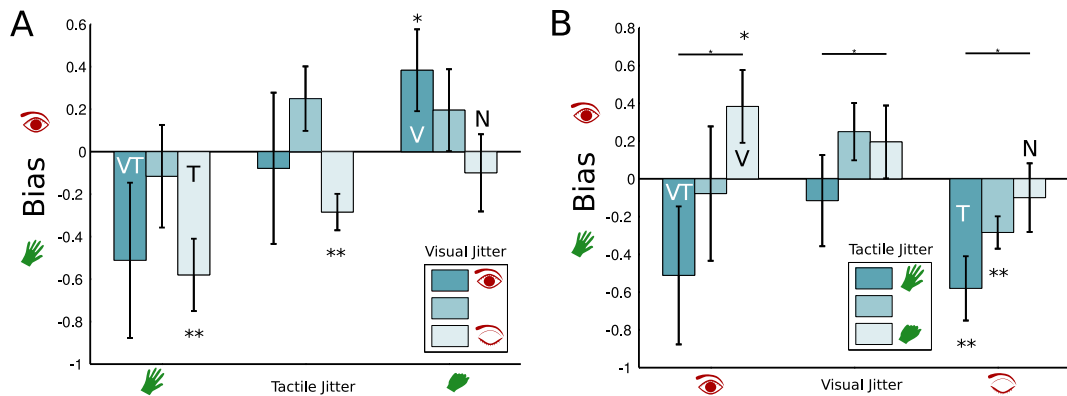


Figure 5.24: **Bias Measure Comparison.** (A) Modality Bias \pm SEM as a function of visual jitter and tactile jitter; (B) The data from (A) plotted with the visual and tactile groups swapped for convenience; SConditions are compared by two-tailed t-tests, with stars to denote significance level ($* = p < 0.05$ and $** = p < 0.001$)

$\mathbf{VT}_{bias} > 0, p < 0.05$) and tactile feedback incurred a tactile bias (t-test: $\mathbf{VT}_{bias} < 0, p < 0.001$).

It is interesting to note that when both vision and tactile are reliable there is a tactile bias. This apparent preference is not significant. (t-test: $\mathbf{VT} < 0, p > 0.1$), however subjective reports suggested that subjects did prefer to rely on the vibrotactile feedback whenever possible.

Quantitative match between Empirical data and Simulation To illustrate the quantitative match between the empirical and optimal simulated data, Fig. 5.25 plots the Bias measure for the empirical data alongside the simulated *Bayes-optimal* (active) strategy and the *Random-Weights* (passive) strategy. In the Bayes-optimal simulation the objective variability for each subject in the training trials is used to compute the modality weighting in the multimodal simulation for each subject (see *methods*). Note that the active strategy results in a non-zero slope of the Bias measure, whilst the passive strategy results in a slope of approximately zero. There is a close quantitative match between empirical data and the Bayes-optimal observer.

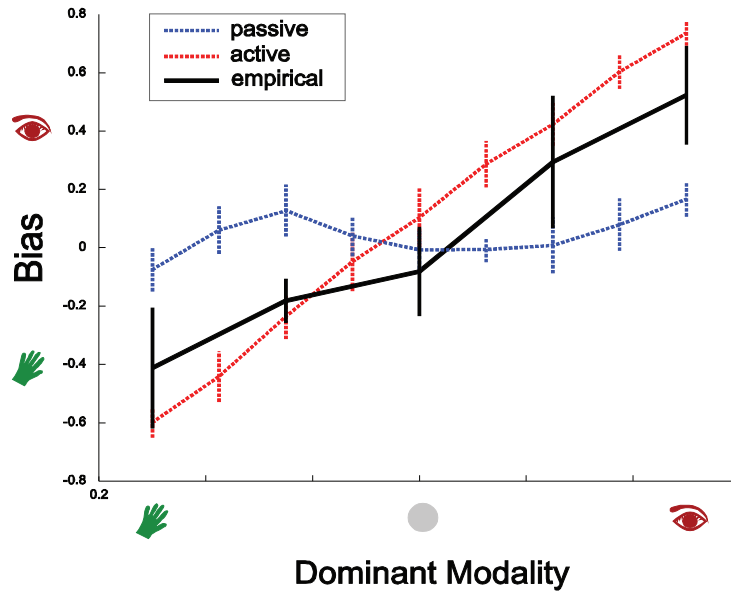


Figure 5.25: **Weighting Indistinguishable from Optimal.** We plot the bias for five of the experimental conditions spanning tactile-dominant (**VT**), no feedback (**VT**), and vision-dominant (**VT**) cases. Empirical data are shown in black, with the *bayes-optimal* (active) strategy in red and the *random weights* (passive) strategy shown in blue. As can be seen, the empirical data are indistinguishable from the ideal-observer data.

5.4 Discussion

5.4.1 Pilot Experiment

The pilot experiment aimed to provide a comparison of the benefits of (uncertain) sensory feedback two different control methods, *position-control* and *velocity-control*, using a multimodal pursuit tracking task. I hypothesised that tactile feedback would show more pronounced benefits in the velocity-control condition.

Owing to the small number of subjects and the absence of statistical tests it is difficult to draw strong conclusions. However, the qualitative findings hinted at differences due to the control method. For example, for subjects using the absolute or position-controlled cursor, tactile feedback reduced task errors compared to no feedback at all. However, there was limited interaction between visual and tactile feedback and in the presence of visual feedback the artificial modality did not improve performance. It was found that across subjects there was no overlap in performance between the sensory modalities, i.e. performance with *unreliable* visual feedback alone was superior to performance with *reliable* tactile feedback alone.

A possible explanation for not observing a benefit of tactile feedback in the presence of visual feedback is that tactile feedback was not needed for success at the task.

Together, the fingertip force feedback, proprioceptive cues of the force applied, and the efferent copy of the feedforward control command may have been sufficiently reliable *internal signals* which could be combined with visual feedback (and even unreliable visual feedback) in order to compute the cursor position.

For subjects using the relative or velocity-controlled cursor the benefits of feedback were more evident. Although there was no reduction in error for reduced tactile feedback uncertainty when visual feedback was reliable, there was a reduction in error for reduced tactile feedback uncertainty when vision was unreliable. Task performance in the absence of all feedback indicated that feedforward control ability was poorer for the velocity-control group, presumably owing to the absence of internal feedback signals (as provided by force feedback, proprioceptive feedback and efferent copy feedback in the position control group).

It seems, then, that under conditions of feedforward uncertainty the benefits of feedback become more apparent. Feedforward uncertainty will naturally arise in many ADLs for amputees, such as (i) situations of unpredictable hand motion, such as with noisy EMG control; (ii) under visual or attentional distraction, such as during more complex tasks; and (iii) when grasping unknown objects, such as of different size, shape and softness. I return to test this hypothesis in Chapter 6. The state-of-the-art open-loop iLIMB hand deploys a velocity control strategy, and would presumably also benefit from the presence of tactile feedback.

5.4.2 Main Experiment

It was an intention of the pilot experiment design that both modalities had the same range of noise variation, to ensure that there was minimal bias towards either modality. In the main experiment, to more directly assess the degree of multimodal interaction, the modalities were adjusted so that both had the same range of *objective variability*. Tactile spatial uncertainty may arise due to: (i) cross-talk between vibrating motors, owing to vibration of the cuff and of the whole arm (Kaczmarek et al., 1991); and (ii) difficulty in precisely localising tactile stimuli due to the large receptive fields of the deep SA-II and RA-II nerves which likely mediate vibration perception (reviewed in Johnson, 2001). The per-subject adjustment of visual uncertainty ensured that these subjective differences were accounted for.

In the main experiment it was found that multisensory localisation performance improves in the presence of redundant sensory information: subjects showed reduced error in the multimodal condition compared to unimodal conditions. Ernst and Bühlhoff (2004) argue that this reduction variance is a good indicator of multisensory integration that rules out suboptimal 'cue switching' hypotheses.

To more reliably distinguish passive (uncertainty-independent) integration hypotheses from active (uncertainty-dependent) hypotheses, a random offset between sensory modalities allowed measurement of decision bias on each trial (i.e. the weight attributed to each modality, see *methods*). These results were compared to simulations (based on unimodal empirical behaviour), revealing that the empirical *bias* (a measure of the weight attributed to each modality) was indiscriminable from an optimal integration strategy (with added kinematic constraints), but clearly discriminated from passive integration hypotheses.

These results suggest that subjects have access to a measure of their objective uncertainty in both visual and tactile modalities. In Chapter 4 it was found that, although subjects could discriminate different levels of sensory uncertainty, they over-estimated the overall level of sensory uncertainty in visual stimuli. However, this apparent suboptimality (if consistent across modalities) may not affect a subject's ability to assign a weight to each modality in accordance with its objective uncertainty in a manner indistinguishable from the ideal-observer: the results presented here require only that subjects have access to a reliable measure of the *relative* uncertainty of the two modalities.

Empirical data were compared to simulation results. The simulation was constrained by two kinematic parameters, a smoothing parameter, α , and a noise parameter, ϵ , which were chosen arbitrarily. Further simulations revealed that the effects of these parameters had limited effect on the gross aspects of the data: whilst modulating the magnitude and variance of endpoint errors, they had no effect on the qualitative trends of the trajectories under both the mean endpoint error and bias metrics, and no overall quantitative effect on the endpoint error and bias measures when averaged over all trials (data not shown). Importantly, the parameters are global constants, and therefore have the same influence on the trajectory for different values of uncertainty and offset. The parameters therefore have no power to explain or influence the differences found between the experimental conditions (for a more detailed discussion, see Chapter 4). However, a more complex model would be needed to explain the distinguishing features of the empirical trajectories, such as reaction-time, sensory and motor noise and realistic smoothing parameter, such as that presented in Chapter 4; such a model could be fit to empirical trajectories to provide quantitative evaluation of trajectories and behaviour. The present data set was not suitable for fitting such a model (as within-trial perturbations would be needed to establish cue weighting, as per Chapter 4). Nevertheless, the simpler model presented here is sufficient to support the observations made.

In this chapter subjects were given the abstract task of cursor navigation, but this may be considered analogous to differential position control of a prosthesis. Feedback

was issued at a different location (the arm), in a different modality (vibration) and encoded differently (spatial code) to that of natural proprioceptive sensation. Moreover, the uncertainty of the tactile modality was modulated in a way that has no natural analogue: spatio-temporal jitter. Nevertheless, multisensory integration was observed despite the unnatural nature of the feedback and feedback uncertainty. It seems improbable that the relationship between the jittering tactile cursor and the objective uncertainty of the modality was known by subjects prior to the experiment, yet 11 of the 12 subjects were able to acquire this mapping over the 20 minute duration of the experiment to form a multisensory estimate of stimulus location that weighted each modality in proportion to its objective uncertainty. Ernst and Banks (2002) ask whether optimal multisensory weighting is learned or if it is an intrinsic feature of the central nervous system. The results presented here show that subjects are able to quickly learn the novel relationship between artificial sensory information and their objective uncertainty, suggesting that learning plays a crucial role in multisensory phenomena.

Overall, it appears that people exhibit optimal decision-making processes in this continuous estimation task, consistent with binary decision tasks (e.g. Ernst and Banks, 2002, Hillis et al., 2004). The paradigm is useful for understanding the mechanisms of multisensory integration and as a sensorimotor task it is more directly relevant to the design and evaluation of prosthesis feedback systems.

5.4.3 Conclusion

In this chapter I have explored the phenomenon of multisensory integration in a sensorimotor tracking paradigm. This was motivated by a need to understand the fundamental mechanisms of sensory integration: (i) in a closed-loop context relevant to prosthesis control; and (ii) using an artificial sensory modality.

In a pilot experiment the selective benefits of feedback as a function of control strategy were observed. In particular, for a velocity-controlled cursor (in which feedforward control performance was lower) tactile feedback was beneficial when visual feedback uncertainty was increased, whereas for a position-controlled cursor tactile feedback was only beneficial in the complete absence of visual feedback. In the following chapter I will explore this finding further by examining the role of feedforward influences in a real-world sensorimotor task.

In the main experiment the tracking task from the pilot experiment was modified to allow quantitative evaluation of the the degree of multisensory integration. It was found that subjects were indeed capable of integrating multiple modalities, measured both by performance (mean endpoint error) and by modality *bias* (the weight allocated to each modality), consistent with an active optimal integration strategy.

The paradigm of visuomotor tracking is useful for quantifying sensorimotor impairment in numerous neurological disorders, and the novel experiments presented here demonstrate its utility for explaining multisensory integration in a sensorimotor context.

Chapter 6

Feedforward and Feedback processes during Closed-Loop Prosthesis Control

Using the closed-loop prosthetic hand as a manipulandum, this chapter addresses the interplay between feed-forward and feed-back mechanisms for grasping and lifting. It is found that subjects form economical grasps in controlled conditions, and this ability is preserved even when visual, tactile and both sources of feedback are removed. However, when uncertainty is introduced into the hand controller performance degrades significantly in the absence of visual or tactile feedback. Greatest performance is achieved when both sources of feedback are present, supporting the idea of complementary roles for feed-forward and feed-back mechanisms. I show quantitatively that tactile feedback can significantly improve performance in the presence of feed-forward uncertainty, and conclude that in designing closed-loop prostheses we should deploy feedback systems that enable users to correct for the inevitable uncertainty in feed-forward control.

Relevant Publications

- Ian Saunders, Sethu Vijayakumar. (2011). **The Role of Feed-forward and Feedback Processes for Closed-Loop Prosthesis Control.** *Journal of Neuroengineering and Rehabilitation*

6.1 Motivation

For many decades researchers have considered the possibility of ‘closing the loop’ for upper-limb prosthesis wearers. Historically, feedback has been added to increase patient confidence (Shannon, 1979b) and to improve object grasping and lifting (Scott et al., 1980, Riso et al., 1991). In the future we may see prosthetic hands that integrate directly with the amputee’s nervous system, utilising state-of-the-art sensor technology (Edin et al., 2008, Ascari et al., 2009) and relying on pioneering medical procedures (Kuiken et al., 2004, Dhillon and Horch, 2005, Miller et al., 2008). Nevertheless, state-of-the-art upper limb prostheses are still open-loop devices with limited degrees of control, described as “clumsy” (see Zhou et al., 2007) and requiring considerable mental effort (Carrozza et al., 2006). As technology continues to advance it is more important than ever that we find effective ways of delivering feedback to amputees.

Artificial feedback systems can exploit the idea of *sensory substitution*: feedback delivered in a different modality or to a different location on the body in an attempt to exploit the latent plasticity of the nervous system. For example, Multiple Sclerosis patients significantly over-grip objects (Iyengar et al., 2009), but when sufferers receive vibratory feedback of their grip force (displaced to their less-affected hand) these forces reduce (Jiang et al., 2009). In a similar way, prosthesis fingertip forces have been transferred to the stump (Cipriani et al., 2009) or even the toes of amputees (Panarese et al., 2009) to create appropriate and useful sensations. Successful substitution is achieved when subjects no longer perceive the stimulation as an abstract signal but instead as an extension of their sense of touch. Achieving ‘embodiment’ in this sense depends critically on the presence of feedback (Marasco et al., 2011).

Despite these promising results, few studies have attempted to objectively quantify the benefits of artificial tactile feedback, and feedback has not yet made it into commercially available prostheses. It is important to ask why this is the case. One must not only question the efficacy of the feedback method (e.g. its resolution and latency) but also identify what feedback information should be provided, and observe how well it integrates with our existing senses (i.e. whether their presence obviates its utility, Zafar and Doren, 2000).

In this chapter I use the behavioural phenomenon of *economical grasping and lifting* to understand the role of feedback for prosthesis wearers. Economical grasping, the stereotypical human behaviour in which grip forces scale appropriately with objects of different loads (minimising effort yet avoiding slip), is well-characterised for both healthy (Johansson and Westling, 1984) and sensory-impaired subjects (Augurelle et al., 2003, Hermsdörfer et al., 2004). In this chapter, healthy subjects are augmented with an artificial extension to their nervous system (Fig. 6.1) and the effects of artificial sensory

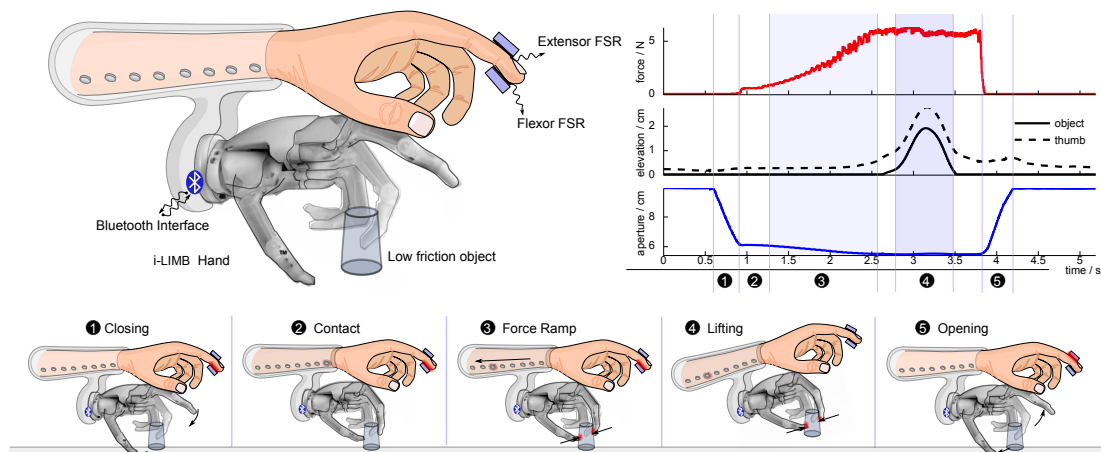


Figure 6.1: The ‘Grasp and Lift’ paradigm with our Closed-Loop prosthetic hand. Healthy subjects are fitted with a modified iLIMB Pulse prosthetic hand, and force feedback is delivered to their arm using a vibrotactile feedback array. They are instructed to grasp, lift and replace a low-friction object using a differential force-ramp controller (inset 1-5). A typical trajectory (showing grip force, object and thumb elevation, and grasp aperture) is also shown.

impairments on grasp and lift performance are observed. The attached closed-loop prosthetic hand serves as a model system in which one can readily manipulate the control interface, the robotic controller, on-board sensors, and feedback transduction. Different instantiations of the hardware allow us to decouple the role of sensory and motor processes in grasping and lifting objects.

I conduct three experiments designed to examine the interaction between feed-forward and feed-back uncertainty. In the first experiment I create an idealised scenario in which sensory and motor uncertainty are minimised. In the second experiment I deprive subjects of visual, tactile and all sources of feedback in order to quantify the resulting performance deficit. In the third experiment I induce random variability to the controller in order to manipulate feed-forward uncertainty, and again quantify the utility of different sources of feedback. Together these experiments provide a window into the role of feed-forward and feed-back processes for prosthesis control.

Research in intact and deafferented humans has suggested that both feed-back and feed-forward mechanisms are required for successful object manipulation, with a marked disassociation between these aspects of control (Hermsdörfer et al., 2008). The difference between feed-forward and feed-back processes is of fundamental importance to our understanding of human sensori-motor behaviour (Flanagan and Wing, 1997), and likewise should be considered crucial in designing a prosthesis to improve the quality of life for amputees. Feed-forward anticipatory grip forces precede load changes due to accel-

eration, a phenomenon not impaired by digital anaesthesia (Augurelle et al., 2003) nor long-term peripheral sensory neuropathy (Hermsdörfer et al., 2004). In contrast, the scaling of grip force magnitude is not preserved under anaesthesia, resulting in over-grip and unstable forces (Augurelle et al., 2003), suggesting that cutaneous cues are required to allow us to maintain our forward model of grip force. These studies indicate a vital role of tactile feedback for both learning and maintenance of internal models.

In this chapter I aim to explore a well characterised behavioural phenomenon using a novel sensori-motor platform, open to arbitrary manipulation. The results confirm differential roles for feed-forward and feed-back processes, and reveals their complementary nature.

6.2 Methods

6.2.1 Subjects

Subjects were healthy males and females, aged between 21 and 30 years old, sampled from the academic institute. They had both upper limbs intact, and had normal or corrected-to-normal eyesight. None of the subjects had previous experience controlling a prosthesis.

6.2.2 Hardware Setup

6.2.2.1 Closed Loop Hand

Healthy subjects were fitted with a modified Touch Bionics iLIMB Pulse prosthetic hand, using a custom-built ‘socket’ (Fig. 6.1). This state-of-the-art, commercially available prosthesis has a differential controller, driven by two surface electromyography (EMG) electrodes. The hand has 5 individually-powered digits, and a bluetooth interface to allow real-time streaming of data to a PC for data logging. It has scored highly in terms of patient satisfaction (Otr et al., 2010) and is an open-loop hand, making it an ideal candidate for developing a feedback system. See Chapter 3 for more details.

The firmware of the hand was modified to enable differential force control, and used an object-mounted force sensing resistor (FSR) to signal force feedback to subjects.

6.2.2.2 Vibrotactile Feedback Array

The feedback system was a ‘vibrotactile feedback array’ comprising eight vibration motors, as described in Chapter 3, controlled by a PIC18F4550 microcontroller. The microcontroller was running custom firmware, including a universal serial bus (USB) module that enabled a personal computer (PC) to control the vibrotactile stimulation. The hardware was running a spatial tactile encoding, with between-tactor sensations achieved by co-stimulation of neighbouring motors (see Chapter 3).

Subjects were fitted with a socket containing the vibrating motors (shown in Fig. 6.1). The eight motors spanned the full length of the palmar-side of the forearm. The grip force on the object was translated into a stimulation location: light forces were perceived near the wrist and heavy forces near the elbow.

6.2.2.3 Differential Force Control

A variety of different control algorithms can be found across commercially available prostheses, trading-off low power consumption, stable grasp formation, or bio-inspired strategies that feel more ‘natural’ to the user. Traditional shoulder-position controlled

prostheses have the advantage of ‘extended physiological proprioception’ (Doubler and Childress, 1984), whereby the shoulder position itself is a source of feedback to the patient. All ‘proportional’ controllers have this advantage. Differential controllers, however, are often more practical, especially given the noisy and unreliable nature of EMG signals used to control the hands.

In this study I used a ‘gated ramp’ controller, for two-channel differential position and force control (Humbert et al., 2002). This controller was chosen because it was comparable to state-of-the-art hands such as the iLIMB and because I have previously found benefits of feedback for differential controllers (see Chapter 5). Subjects controlled the hand using extensor and flexor signals detected at the fingertip. For simplicity of operation, the signals operated as binary switches. The flexor signal closed the hand at a constant speed of 0.12m/s, and when contact was made the force ramped up at approximately 5N/s. The extensor signal opened the hand at a constant speed of 0.12m/s. This simple controller allowed subjects to control the force they exerted, in the range 0-15N, by modulating the duration of the signal. This method was chosen as it is similar to the existing controller on the iLIMB pulse hand.

6.2.2.4 Sensor Recording Equipment

A large FSR (5cm square) was attached to the object being lifted. This was done for practical reasons as embedding a sensor into the digits of the prosthesis would have posed additional technological challenges outwith the scope of the study. A number of studies in the literature have focused on embedded tactile sensors apparatus (see Edin et al. 2006, 2008). Given that the task involved grasping the object in the same location each time we achieved an entirely equivalent result by mounting the sensor on the object. I do not believe that this caused any confounding effects. The sensor was calibrated using high precision digital scales, so that the force output could be accurately recorded at 1kHz in the range 0N to 10N, using a 10-bit analogue-to-digital converter (ADC) on the the microcontroller. Data were logged by PC software to ensure accurate temporal calibration of sensor data, then streamed back to the microcontroller for provision of vibrotactile feedback. Position sensors were attached to the thumb and forefinger, the wrist and the base of the object, to enable accurate three dimensional tracking using a Polhemus Liberty 240Hz 8-sensor motion tracking system (POLHEMUS, USA), and logged by PC software. The iLIMB hand was configured to stream state information, such as control signals from the EMG inputs to the hand, via bluetooth to the PC software.

Figures 6.2 and 6.3 illustrate two typical trajectories recorded from a subject instructed to grasp, lift and translate an object.

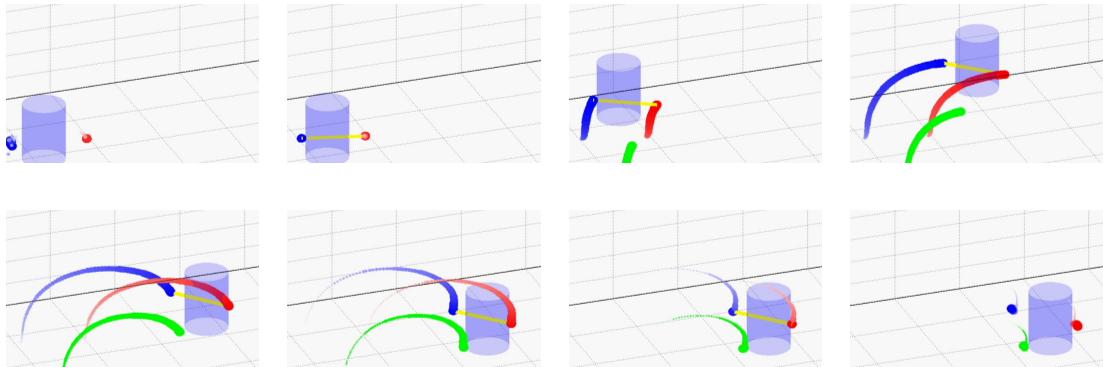


Figure 6.2: **A Successful Translation.** Force and position trajectories are recorded in real time from subjects fitted with the manipulandum. The plots above show a sample of fingertip trajectories recorded when grasping and moving object. A typical recorded trajectory showing the motion of the thumb (blue), forefinger (red) and wrist (green). 3D marker trails reduce in size over time. Object contact is indicated by a yellow bar. Note, the motion sensors are on the volar finger surface and thus not exactly aligned with the object surface (cylinder).

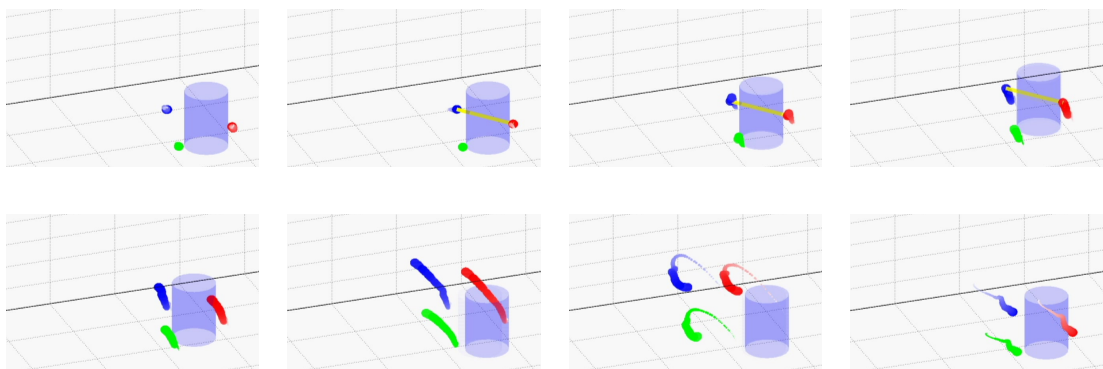


Figure 6.3: **An Unsuccessful Translation.** Force and position trajectories are recorded in real time from subjects fitted with the manipulandum. The plots above show a typical recorded trajectory showing the motion of the thumb (blue), forefinger (red) and wrist (green). Object contact is indicated by a yellow bar. In this example the object is lifted with insufficient force and so the finger and thumb slip from the objects. The subject then returns to re-initiate a lift.

6.2.3 Experiments

6.2.3.1 Preliminary Experiment: ‘Just noticeable difference’ measurement

To establish the efficacy of the feedback system, I ran an adaptive-staircase design two-interval-forced-choice (2-IFC) just-noticeable-difference (JND) protocol. Subjects ($N=6$) participated in this study. Detailed methods and results have been presented already in Chapter 3.

6.2.3.2 Overview: Economical Grasping Paradigm




Healthy individuals exhibit stereotypical and repeatable grasping profiles (Johansson and Westling, 1984, Westling and Johansson, 1984) and the term ‘economical grasp’ describes this ability to minimise grip force while avoiding slip. This phenomenon has proven useful for studying both closed- and open-loop human behaviour, comparing healthy patients to deafferented (Hermsdörfer et al., 2004, 2008) or anaesthetised (Augurelle et al., 2003) subjects. Healthy people predictively accommodate arbitrary loads with just enough force to avoid slip, taking into account size, shape and frictional properties of objects and it is believed that this behaviour relies on both feed-forward and feed-back mechanisms (see Chapter 2). Economical grasping provides an ideal paradigm for studying human sensorimotor processes.

In our experiments, subjects were given on-screen instructions to grasp and lift objects with sufficient force, and to avoid dropping or over-gripping the object. Two objects were used, one ‘heavy’, (300g) and one ‘lightweight’ (150g). The objects were upward-tapered identical rigid beakers, 55mm diameter at the point of contact, covered with a low-friction cellulose film. Since I was primarily interested in establishing whether or not subjects were able to differentially control their grip force, an economical grasp is defined as occurring when subjects are able to appropriately assign different grip forces to the two objects. Note that this is a sufficiently difficult task when the properties of the object are unknown such as is the case in the absence of sensory feedback. In the third experiment, just the heavy object is used to reduce the experiment complexity, and so ability at this task is judged by the difference in measured performance magnitude between the feedback conditions.




6.2.3.3 Experiment 1: Grasp, lift and move task

In the first experiment *idealised conditions* were created. The iLIMB hand was controlled using force-sensing resistors, so that it would respond immediately and predictably to control signals. Subjects were allowed to use visual feedback throughout, and performed repeated trials with each object weight. Subjects also received vibrotactile feedback on

A Experiment 1

	no fb		fb		no fb		fb	
	✓		✓		✓		✓	
	x	↔	✓		x	↔	✓	
	H	L	H	L	H	L	H	L

B Experiment 2

	group one			group two		
	✓	✓	x	✓	✓	x
		x			✓	
	H	L	H	L	H	L

C Experiment 3



		phase one			phase two		
	✓	✓	↔	x	✓	↔	x
	✓	✓	↔	x	✓	↔	x

Figure 6.4: **Experiment Overview.** Three behavioural experiments were conducted to examine the role of feedback. **(A)** In Experiment 1 subjects were allowed to use visual feedback throughout, and alternated the presence of vibrotactile feedback and object weights (Heavy and Lightweight) from trial to trial as shown. The order of presentation of feedback was counterbalanced (indicated by the double-headed arrow). **(B)** In Experiment 2 two groups of subjects were used, one with vibrotactile feedback and one without. Subjects performed two blocks in the light, and a third in the dark, with different object weights. **(C)** In Experiment 3 subjects had an initial training phase, then had two phases of trials in all four feedback configurations (visual, tactile, neither and both), counterbalanced as shown.

half of the trials. For healthy individuals, digital anaesthesia does not impair anticipatory behaviour but does impair maintenance of forces (Augurelle et al., 2003). I therefore hypothesised that, under ‘simulated anaesthesia’, subjects would be able to grip economically, albeit with larger variability.

Subjects (N=6) were fitted with the iLIMB socket with vibrotactile motors along the palmar forearm. On a given *trial* subjects were instructed to grasp, lift and transfer an object between two locations, spaced 20cm apart. Subjects performed four *blocks* of trials, each of which included 20 trials with the heavy object and 20 trials with the lightweight object.

In a given block, each subject was exposed to one of two counterbalanced experimental conditions: either *with* or *without* vibrotactile feedback of grasp force (see Fig. 6.4).

The effects of *tactile feedback condition* and *object weight* on performance were analysed.

6.2.3.4 Experiment 2: Grasp and lift task with feed-back deprivation

In the second experiment I examined performance when subjects were deprived of all useful sources of feedback as much as was possible: visual, auditory and additional tactile cues were eliminated or masked. Two groups were compared in these sensory deprivation conditions so as to observe the sole benefits of tactile feedback on performance. A study comparing the effects of deafferentation on anticipatory grip force (Hermsdörfer et al., 2008) suggests that intermittent sensory feedback is necessary to update and maintain internal models of object dynamics. In addition, tactile feedback has been shown to be beneficial under partial sensory deprivation (Zafar and Doren, 2000). I therefore hypothesised that under complete sensory deprivation economical grasping ability would decline, but in the presence of vibrotactile feedback it would not.

Twelve subjects were split into two groups for *vibrotactile feedback condition*. One group (N=6) had vibrotactile feedback for the duration of the experiment, and the other group (N=6) received random (uncorrelated) tactile stimuli.

On a given *trial*, subjects were instructed to grasp and lift an object in a fixed location, then return it to the same location. Subjects experienced three *blocks* of trials, two in the light, and one in the dark. Each block included 12 trials with a heavy object, and 12 trials with a lightweight object.

Visual feedback was removed by immersing subjects in darkness. The robotic hand and the object were covered in dark materials so that the hand and its movements were not visible at any time. Subjects were also instructed to look at a screen throughout each the trial, though they were able to see if the object had been successfully lifted

by observing the movement of a phosphorescent strip attached to the top of the object. Auditory feedback was removed by playing white noise through earphones, and separately through a speaker. Additional sources of tactile feedback, such as vibrations when contact is made or during force ramping, were removed by the use of random (uncorrelated) vibrotactile stimuli. These stimuli appeared at random locations on the arm, vibrating with randomised frequencies and for unpredictable durations. All subjects in the control group reported that they were unable to see, hear or feel when contact was made with the object, although they were able to detect a successful grasp from movement of the object observed in their peripheral vision and through the additional torque experienced in their arm. Although these subjective reports do not rule out unconscious perception, a pilot experiment (see results) indicated that untrained subjects had significant difficulty learning to lift the object, suggesting that these feedback deprivation conditions were sufficient for the purpose of the task.

The effects of *tactile feedback condition*, *visual feedback condition* (block 2 versus 3) and *object weight* on task performance were analysed.

6.2.3.5 Experiment 3: Grasp and lift task with feed-back deprivation and feed-forward deprivation

In the third main experiment I introduced *feed-forward uncertainty*, by inducing random unpredictable delays to the hand controller. In contrast to experiments 1 and 2, where the control of the hand was repeatable and predictable, this experiment was designed to examine the role of feedback under motor uncertainty, such as is more typical in real-world situations. Random delays were added to the hand motion before the onset of movement and before the onset of the force ramp. Delays were drawn uniformly from the interval 0s to 1.5s, the duration to fully close the hand, simulating the grasping of an unknown-size object (see *discussion* for a detailed justification). By adding this temporal unpredictability to the hand, I hypothesised that subjects would experience reduced utility of feed-forward control, which should increase their dependency on vibrotactile feedback. I was interested in characterising the selective benefits of visual and tactile feedback on grasp economy under this added uncertainty.

Each subject (N=12) was exposed to four different feedback conditions, by varying *visual feedback condition* (light versus dark) and *tactile feedback condition* (vibrotactile feedback versus no feedback). For each condition subjects performed a block of 12 trials. In a given trial, subjects were instructed to grasp and lift an object in a fixed location, then return it to the same location, as per experiment 2.

A within-subjects design was used to reduce inter-subject variability. Since using a within-subjects design it was important to minimise interaction between the order of

blocks and subjects' ability to control the hand. Therefore subjects were mixed into four between-subject *groups*. Each group had a different configuration of the *visual feedback order* and the *tactile feedback order*, to ensure any learning effects were counterbalanced. This enabled for the control of carry-over effects within-subjects. Furthermore, subjects were trained briefly before the start of the first trial, with full feedback sensibility, so that they could get used to the control mechanism of the hand.

Subjects performed the four blocks of the experiment over two separate *phases* to detect any effects of learning. The same (heavy) object was used for all trials.

The effects of *tactile feedback condition*, *visual feedback condition* and the *phase* of the experiment were analysed. It was also ensured that there were no effects of *visual feedback order* or *tactile feedback order* which might confound the results. One subject was discarded from these analyses as he admitted to 'cheating' when deprived of all sensory feedback.

6.2.4 Performance measures and statistical analysis

6.2.4.1 Automatic Segmentation

Data from each trial were automatically segmented into phases based on the configuration of the hand and object. Data were annotated to mark occasions where the object slipped or was dropped (see Fig. 6.5) The start and end of the force ramp were located, and the period for which the object was elevated. Fig. 6.1 shows a typical recorded trajectory, and illustrates segmentation features. Phases 3 and 4, highlighted, are the 'force ramp' and 'lifting phase' respectively This temporal segmentation allows one to automatically compute the duration of the motion, count the number of errors made, and compute the grasp force during object lift.

6.2.4.2 Grasp Force

A key indicator of economical grasping is avoidance of over-grip. Lightweight objects should be gripped with less force than heavier objects. For a given trial i the grasp force, f_i , is defined as the average grip force (in Newtons) applied the object for the duration of its elevation.

6.2.4.3 Ramp Duration

The duration of the control signal is directly related to the subjects intended grasp force. This is a more reliable indicator of force than the FSR reading, as subjects might make imperfect contact with the sensor. For a given trial i the ramp duration, r_i , is

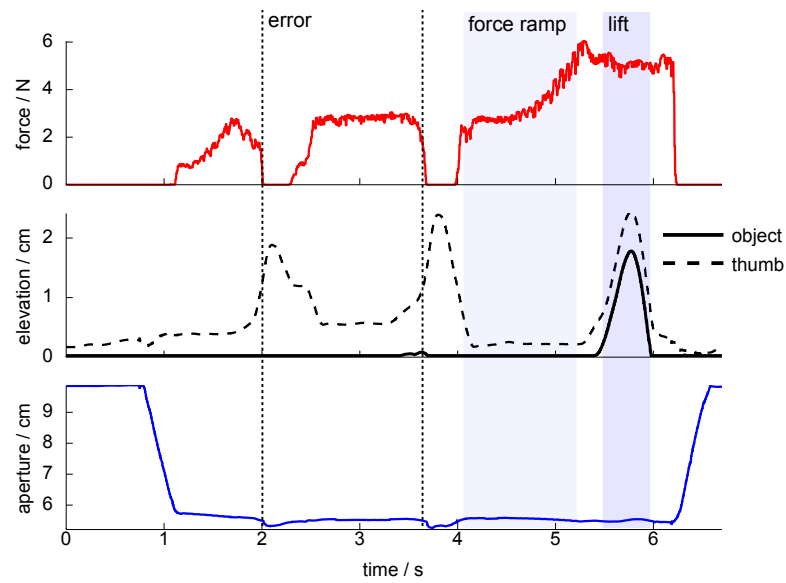


Figure 6.5: **Trajectory segmentation.** During the force ramp phase (shaded region 1) the force exerted on the object slowly ramps up. Once a suitable force is attained, the subject lifts the object (shaded region 2). If the subject attempts to lift too early, the thumb moves but the object does not, resulting in a failed attempt (dotted lines).

defined as the duration in milliseconds of the force ramp phase, excluding any random delays induced in experiment 3.

6.2.4.4 Trial Duration

For a given trial i the trial duration, d_i , is defined as the duration in milliseconds of the entire trial, excluding any random delays induced in experiment 3.

6.2.4.5 Number of errors

For a given trial i the number of errors, e_i , is defined as the sum of ‘drops’, ‘slips’ and ‘failed lifts’. A drop occurs when the object is in a stable grasp (between the thumb and forefinger with grip force $> 1\text{N}$), and the downward acceleration of the object is 5m/s^2 greater than the downward acceleration of the thumb. A slip occurs when the object is in a stable grasp, and the upward velocity measured at the tip of the thumb is greater than the upward velocity measured at the base of the object by more than 0.1m/s . A failed lift occurs when the object is not in a stable grasp (grip force $< 1\text{N}$) and the upward velocity measured at the tip of the thumb is greater than the upward velocity measured at the base of the object by 0.1m/s . If two errors are detected in a given 60ms period this is counted as just one error. These thresholds were chosen as a

result of pilot experiments (data not shown), prior to the experiments detailed in this chapter.

6.2.4.6 Grasp Score

In pilot studies it was found that different subjects prioritised different aspects of the task — some aimed to reduce errors while others focused on speed and others used lower grip forces. A compound metric was devised to handle inter-subject variability: a per-trial grasp score s_i , rates each trajectory, i , in terms of both speed and accuracy. A higher grasp score indicates worse performance. This metric is comprised of four terms, to capture the grasp force, f , the ramp duration, r , the trial duration d , and the number of errors, e , defined as follows:

$$s_i = \text{norm}(f, i) + \text{norm}(r, i) + \text{norm}(d, i) + e_i \quad (6.1)$$

$$\text{norm}(x, i) = \frac{x_i - \text{target}(x)}{\text{peak}(x) - \text{target}(x)} \quad (6.2)$$

$$\text{target}(x) = \min_j (x_j | e_j = 0) \quad (6.3)$$

$$\text{peak}(x) = \max_j (x_j) \quad (6.4)$$

target computes the best performance from a given subject's successful trials (i.e. only using trials in which there were no errors, denoted by the conditional term). This is therefore a measure of the subjects target performance. **peak**, is a measure of the subject's worst performance over all trials. **norm** uses the **target** and **peak** functions to normalise each trajectory into a *per-subject* range, where $s_i = 0$ indicates good performance on trial i , and $s_i \geq 1$ indicates bad performance on trial i .

6.2.4.7 Analyses

In the subsequent data analyses the *grasp force*, *duration of ramp* and the *grasp score* measures are used to compare performance unless otherwise stated. We consider these to be the most relevant measures of a successful grasp. I correct for the use of repeated measures when reporting statistics (except where univariate results are explicitly reported).

6.3 Results

6.3.1 Preliminary Experiment: Grasp forces are effectively communicated to patients using artificial feedback

The efficacy of the tactile feedback interface was established prior to experimentation. The just-noticeable-difference (JND) threshold of the stimuli were computed for each subject (see Chapter 3), revealing a satisfactory communication bandwidth for the provision of feedback. Moreover, the feedback interface has previously been shown to be effective in the presence of a differential controller, achieving optimal sensory integration when combined with visual feedback.

6.3.2 Experiment 1: In ideal conditions, ‘simulated amputees’ perform economical grasps regardless of feedback

Economical grasping is achieved when subjects appropriately assign different grip forces to objects of different weight. This indicator of grasp economy is known to depend on feed-back and feed-forward predictions (see *introduction*), making it a highly applicable method to measure performance.

In this experiment the robotic prosthesis was controlled in ‘ideal conditions’. The robot hand, attached to healthy individuals, was controlled with a noise-free, predictable and responsive differential force-control algorithm. Spatial trajectories, force profiles and control signals were logged during object grasping, lifting and moving to measure control performance as a function of different levels of feedback (see *methods*).

The force trajectories for one subject are shown in Fig. 6.6A. The data indicates that, for this subject, while there is more variability when feedback is not available, economical grasps are formed *regardless* of feedback condition: the lightweight object is grasped with less force, and the heavier object with greater force. A compound metric of grasp score was devised to reduce inter-subject variability by scoring various features of the observed trajectories (see *methods*). In order to evaluate this observation statistically, the recorded data were analysed in terms of three measures of performance: *grasp force*, *duration of force ramp* and *grasp score* (see *methods*). Fig. 6.6B shows the data grouped across subjects..

A within-subjects ANOVA, with factors of *object weight* (heavy / lightweight) and *tactile feedback condition* (with vibrotactile feedback / without vibrotactile feedback) revealed a significant main effect of *object weight* ($F(3, 3) = 659$, $p < .001$), but no significant effect of *tactile feedback condition* ($F(3, 3) = 2.61$, $p = .226$), and no interaction ($F(3, 3) = 1.42$, $p = .390$) The main effect of *object weight* was significant on all measures ($F(1, 5) \geq 92.9$, $p \leq .001$). However, no significant effect of *tactile feedback*

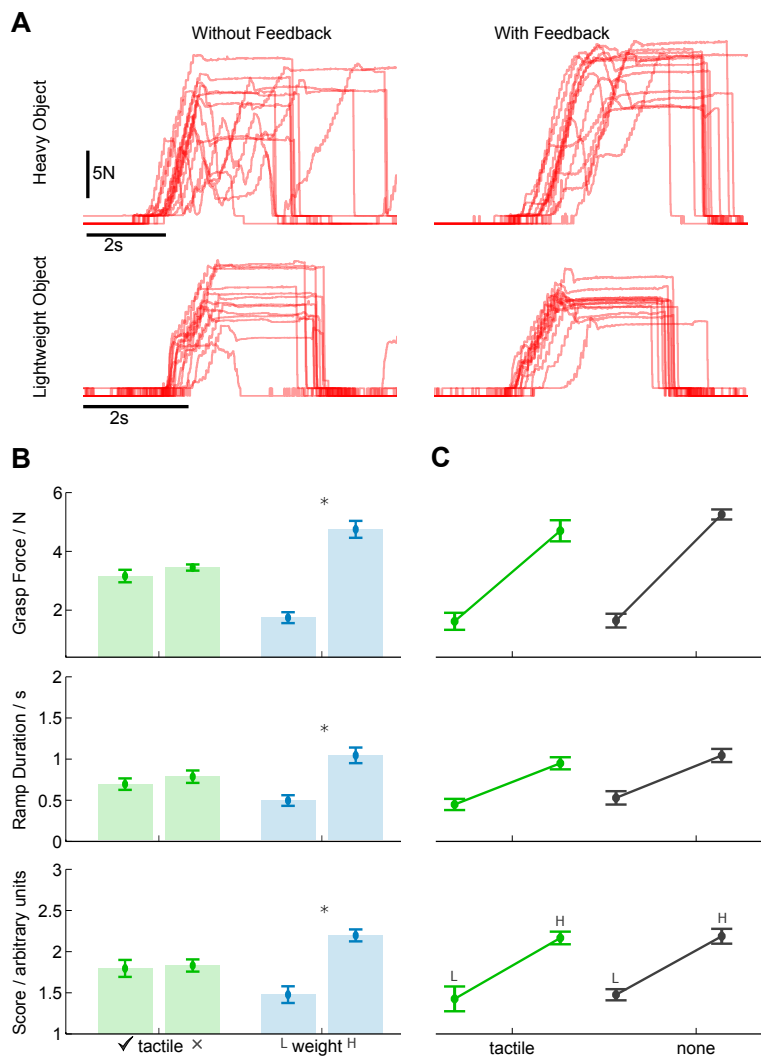


Figure 6.6: **(A) Sample grasp-force trajectories from Experiment 1**, from a single subject. In each plot the x-axis denotes time in seconds, and the y-axis the force in Newtons. The plots show four different experimental conditions: lifting a heavy object without (*top left*), and with vibrotactile feedback (*top right*); lifting a lightweight object without (*bottom left*), and with vibrotactile feedback (*bottom right*). For this subject, tactile feedback offers little utility in reducing grasp force, only in reducing variability. Object weight, on the other hand, has a clear effect on grasp forces. **(B) Data from Experiment 1, grouped by factor**, using three metrics to compare performance. Error bars denote standard error. $N=6$. Comparison of within-subject factors of tactile feedback condition (*green bars*) and object weight (*blue bars*). Weight is split into lightweight ('L') and heavy ('H'). ANOVA results revealed a significant main effect of object weight, but not of tactile feedback condition, denoted by the stars. **(C) Data from Experiment 1, grouped by feedback condition**, using three metrics. Error bars denote standard error. $N=6$. Comparison of subjects' ability to discriminate object weight as a function of feedback condition. Feedback conditions were (*left to right*): no feedback; vibrotactile feedback only; visual feedback only; and both sources of feedback. The two bars per condition indicate performance with the lightweight object (*left*) and heavy object (*right*). Successful discrimination is indicated by a positive slope. Subjects were able to discriminate equally as well in either feedback condition.

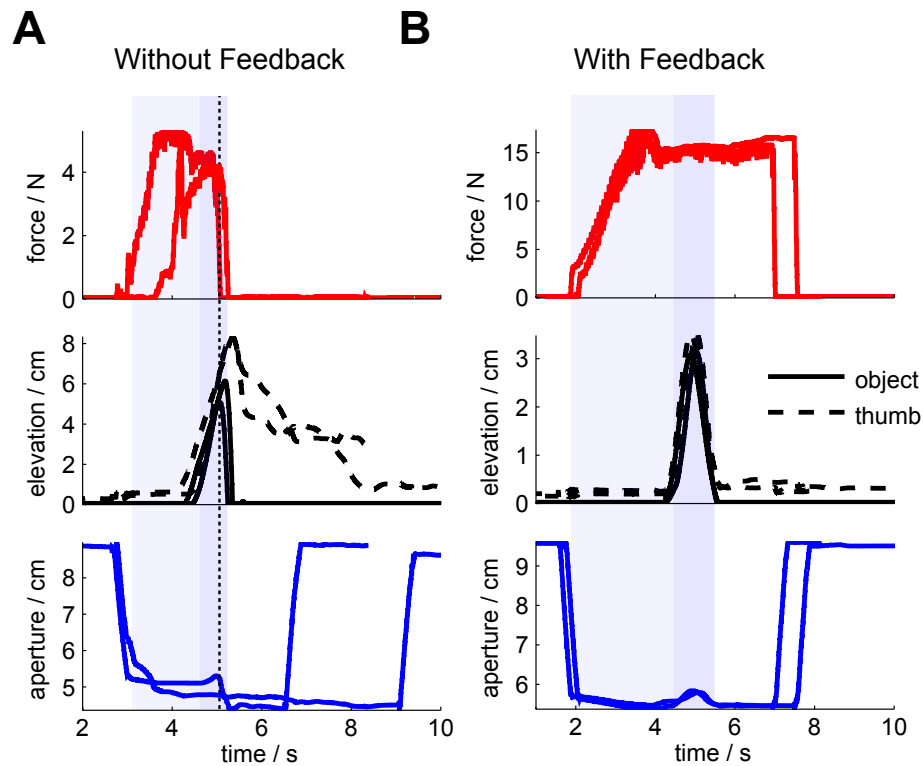


Figure 6.7: **Visual Training on Task Performance.** Typical trajectories for a subject in the dark. **(top)** Without training. **(bottom)** Following vision-assisted training.

condition was found for any of the three measures ($F(1, 5) \leq 2.74$, $p \geq .159$).

Though there were no performance benefits as a result of the feedback in the first experiment, all subjects reported that they found the task easier with feedback. Together with the preliminary experiment which established the efficacy of the feedback, this suggests not that the feedback system was poor but instead that abundant sensory cues from other sources were sufficient to succeed at the task.

6.3.3 Experiment 2: When deprived of additional sensory cues, trained subjects still show no significant deficit in grasp economy

With all additional sensory cues removed (visual, tactile and auditory, see *methods*), it was hypothesised that subjects would show marked deficits in grip force control in the absence of vibrotactile feedback.

As a preliminary experiment a single naive subject was observed for ten trials in the dark. It was found that performance was very poor in the initial dark block, and over all trials the subject failed to supply enough force to lift the object. However, the same subject completed the task with ease in a second dark block after 10 trials of vision-assisted training. Fig. 6.7 illustrates typical trajectories for this subject.

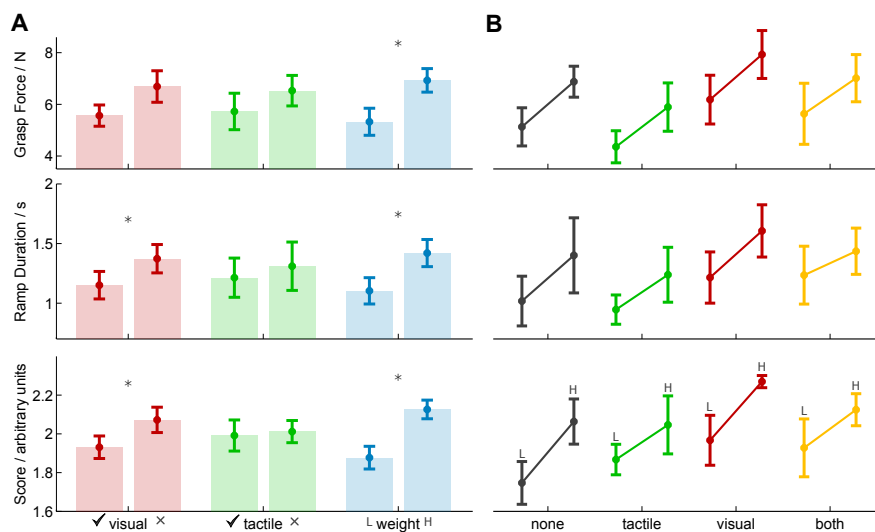


Figure 6.8: **Grouped data from Experiment 2**, using three metrics to compare performance. Error bars denote standard error. Data are from two groups of subjects, one with vibrotactile feedback ($N=6$), one without vibrotactile feedback ($N=6$). **(A)** Comparison of within-subject factors of visual feedback condition (*red bars*), tactile feedback condition (*green bars*), and object weight (*blue bars*). There was a significant within-subjects effect of both object weight and visual feedback condition, but not tactile feedback condition. Post-hoc results confirmed these differences (denoted by stars, significance at the $p = .05$ level.) **(B)** Comparison of subject's ability to discriminate object weight as a function of feedback condition. Feedback conditions were (*left to right*): no feedback; vibrotactile feedback only; visual feedback only; and both visual and tactile feedback. The two bars per condition indicate performance with the lightweight object (*left*) and heavy object (*right*). Successful discrimination is indicated by a positive slope. Subjects discriminated well in all feedback conditions, including in the absence of any feedback.

In the second experiment the performance with and without tactile feedback was compared between two distinct groups. To assess if feedback aided maintenance of anticipatory grip force, as has been suggested in the literature (Hermsdörfer et al., 2008), subjects were exposed to three blocks of trials, the first two in the light and the third in the dark. The grouped data are shown in Fig. 6.8.

A between-subjects ANOVA, with factors of *object weight* (heavy object / lightweight object), *visual feedback condition* (light block / dark block) and *tactile feedback condition* (with vibrotactile feedback / without vibrotactile feedback) revealed a significant main effect of *visual feedback condition* ($F(3, 8) = 4.68$, $p = .036$). While no significant main effect was found for *object weight* ($F(3, 8) = 2.1$, $p = .179$), univariate tests did reveal a significant effect of *object weight*, on all three measures: *grasp force* ($F(1, 10) = 7.84$, $p = .019$), *ramp duration* ($F(1, 10) = 5.01$, $p = .049$) and *grasp score*

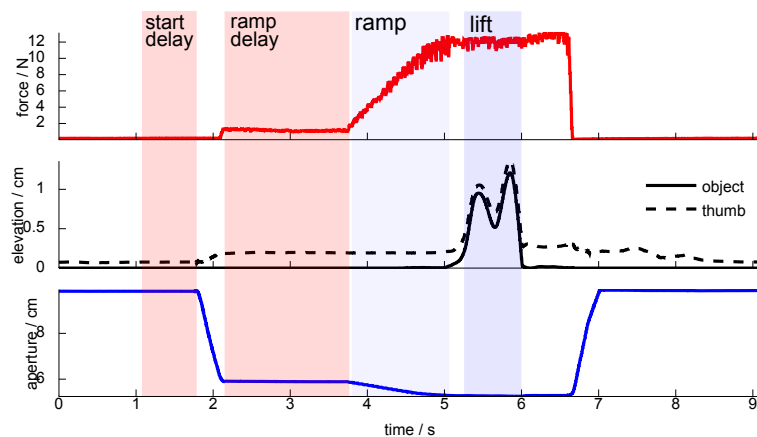


Figure 6.9: **Adding Controller Delays to increase Uncertainty.**

($F(1, 10) = 6.58$, $p = .028$). Univariate tests also confirmed the main effect of *visual feedback condition* ($F(1, 10) \geq 7.62$, $p \leq .020$, all measures). There was no significant between-groups main effect of *tactile feedback condition* ($F(3, 8) = 0.218$, $p = .881$) and univariate tests also revealed no significant effect on any measure of performance of *tactile feedback condition* ($F(1, 10) \leq 0.764$, $p \geq .402$).

These comparisons imply that subjects were able to grasp economically in the dark, albeit with an increase in the base level of force. Interestingly, as observed for an individual subject, vibrotactile feedback had no effect on the grip force. The effect of *object weight*, and no interaction with *tactile feedback condition* or *visual feedback condition*, implies that that grip force control is indeed *maintained* when in the dark with no feedback. This argues that *feed-forward control* mechanisms can be formed in the absence of tactile feedback, and maintained (across multiple trials) in the absence of all feedback.

6.3.4 Experiment 3: When feed-forward uncertainty is increased, trained subjects show significant performance deficits when deprived of either visual or tactile feedback

Experiments 1 and 2 indicate that tactile feedback may offer limited practical utility for grasp force control if the hand controller is predictable. To test this, uncertainty to the hand controller in Experiment 3, in the form of brief randomised delays (see *methods* and *discussion*). This unpredictability was used to reduce subjects' ability to form an accurate feed-forward prediction. Fig. 6.9 illustrates the effect of controller delay on the force profile and movement trajectory.

When controller delays were added, subjects found the task more difficult (indicated

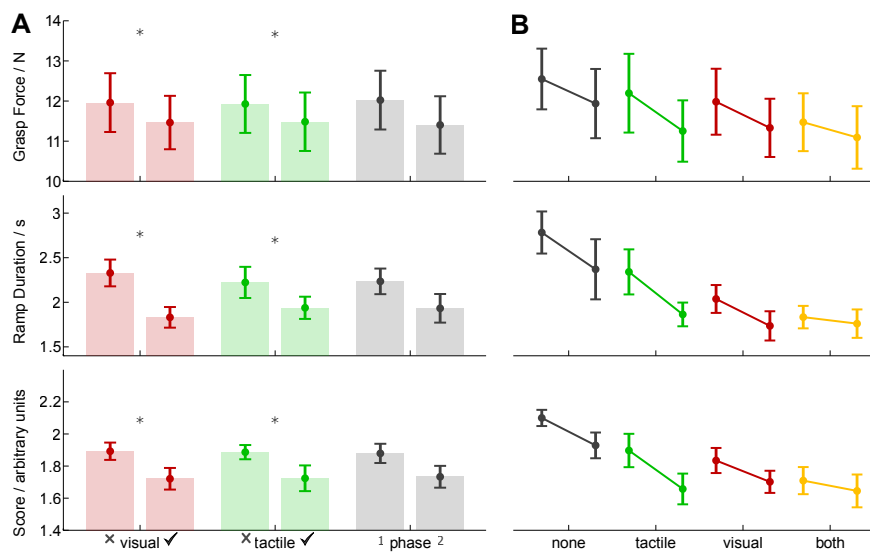


Figure 6.10: **Grouped results from Experiment 3**, using two metrics to compare performance. Error bars denote standard error. Data are from one cohort of subjects ($N=11$). **(A)** Comparison of within-subject factors of visual feedback condition (*red* bars), tactile feedback condition (*green* bars), and trial phase (*grey* bars). Within-subjects ANOVA revealed significant main effects of visual feedback condition and tactile feedback condition, but not phase, indicated by stars. For detailed statistics see text. **(B)** Comparison of subjects' performance as a function of feedback condition: (*left to right*) no feedback; vibrotactile feedback only; visual feedback only; both visual and tactile feedback. The two bars per condition indicate performance in the first (*left*) and second (*right*) phases of training. Subjects performed significantly worse in the absence of either source of feedback.

by a higher *grasp score* compared to experiment 2). Under this increased difficulty, subjects' grasp forces were much higher (and outside the anticipated linear range of our force sensor). For consistency this measure was retained in our analyses. Nevertheless, the remaining metrics were sufficient to show a significant main effect of *tactile feedback*. The grouped data are shown in Fig. 6.10.

A within-subjects ANOVA, with factors of *visual feedback condition* (light block / dark block), *tactile feedback condition* (with vibrotactile feedback / without vibrotactile feedback) and *phase* (phase one / phase two) revealed a significant main effect of *visual feedback condition* ($F(3, 8) = 6.91$, $p = .013$) and a significant main effect of *tactile feedback condition* ($F(3, 8) = 7.51$, $p = .010$). There was no significant main effect of *phase* ($F(3, 8) = 1.56$, $p = .274$), and there were no significant interactions ($F(3, 8) \leq 2.17$, $p \geq .169$).

Post-hoc comparisons revealed that the cause of the effects was best explained with the *grasp score* measure (see Fig. 6.10) As an additional analysis, I compared the *grasp*

score measure for the various feedback conditions in the second phase of trials. In trials without visual feedback a significant effect of tactile feedback was found ($F(1, 11) = 6.4, p = .028$), but with visual feedback there was no significant effect of tactile feedback ($F(1, 11) = 0.405, p = .538$). It was also found that without tactile feedback there was a significant effect of visual feedback ($F(1, 11) = 9.27, p = .011$), but with tactile feedback there was no significant effect of visual feedback ($F(1, 11) = 0.231, p = .640$). This suggests that, after training, either modality was sufficient to enable task performance (see *discussion*).

6.4 Discussion

6.4.1 Overview

The purpose of the first experiment was to quantify the benefits of tactile feedback in an idealised grasping and lifting task. *Grasp economy* was chosen as our measure of performance, a phenomenon known to depend on feedback and feedforward predictions. It has previously been shown that two chronically deafferented patients were not significantly different from healthy matched controls at scaling grip force to different object weights (Hermsdörfer et al., 2008). A study to quantify the benefits of artificial feedback for force control also found no significant difference between feedback and no-feedback groups (Chatterjee et al., 2008). Consistent with these studies, there was no effect of tactile feedback condition, yet there was a highly significant effect of object weight, indicating economical grasps regardless of tactile feedback. Previous results have confirmed that our feedback system offers adequate bandwidth to subjects. It was therefore suspected that, under the ideal conditions of experiment 1, subjects' ability to grasp economically was due to abundant sensory cues (from visual and auditory modalities).

Contrary to our hypothesis, in the second experiment subjects were still capable of differentiating object weights and applying appropriately economical grip forces when deprived of all sources of sensory feedback. No significant difference was found in grasp economy between two groups, one with vibrotactile feedback and one without, nor was there a significant difference between the light and dark conditions. It has been previously shown in healthy humans that cutaneous feedback enables maintenance of the anticipatory components of grasping (Hermsdörfer et al., 2008), but our results suggest that, under the idealised control conditions, force feedback was not necessary for this purpose. However, there was a higher overall grip force in the absence of visual feedback, consistent with an increased safety-margin observed in feedback-deprived individuals (Augurelle et al., 2003). Nevertheless, subjects still differentiated the two objects, which requires precise signal timing in order to set appropriate grasp forces. Since the objects were lifted multiple times, it was concluded that subjects were able to learn an internal model in the absence of within-trial feedback. It is likely that a *feedforward process* was playing a crucial role in the observed behaviour.

The results of the third experiment showed that when feedforward predictability was degraded, performance degraded too. However, with the addition of either visual or tactile feedback, performance was restored, providing evidence that feedback is required in the presence of feedforward uncertainty. Best performance was achieved in the presence of both sources of feedback, suggesting that visual and tactile cues play complementary roles in facilitating successful grasps in the presence of uncertainty.

6.4.2 Justification of Methods

6.4.2.1 Feedback Choice

In this study I used a vibrotactile feedback interface. Direct pressure-feedback devices (Patterson and Katz, 1992) may offer a more natural sensation, and electrotactile feedback might provide greater spatial resolution (Kaczmarek et al., 1991) at the expense of safety. However, vibrotactile feedback systems are given credit for their low cost, size and weight and the simplicity and flexibility with which they can be used in sensory substitution applications (Alahakone and Senanayake, 2009). For these practical reasons it was felt that the spatially-encoded vibrotactile feedback interface (similar to Cholewiak and Collins, 2000) discussed in Chapters 2 and 3 was more than suitable for the present experiments. In pilot studies it was found that this method affords greater stimulus bandwidth than a single factor providing frequency- or amplitude-encoded feedback, as well as the observation of reduced adaptation. In previous experiments it has been shown that subjects are immediately able to discriminate tactile stimuli, rapidly learning to use the artificial modality in a sensory integration task. JND experiments demonstrated that the vibrotactile channel offered a sufficient perceptual range. Furthermore, in the present study subjects were clearly able to utilise vibrotactile feedback to their advantage (in the third experiment). For these reasons I argue that the feedback interface was at least sufficient to enable successful performance. I concede that it is possible that with considerably more training there may have been a measurable difference in performance between the vibrotactile group and non-vibrotactile group in experiment 2. However, this does not invalidate the finding that subjects could form economical grasps *regardless* of feedback under ideal experimental conditions.

6.4.2.2 “Ideal” Conditions

Zafar and Doren (2000) found that using a video-based simulated amputation, feedback offered quantifiable improvements in grasping performance. It would be interesting to know how subjects would perform in their task completely in the dark (i.e. with the screen turned off), as this would indicate their ability to perform repeatable shoulder control movements (i.e. the efficacy of subjects’ feed-forward strategy). One might argue that the 2D (on-screen) cues presented to subjects offered insufficient feedback, or the observed benefits were due to lack of other sources of feedback - auditory and tactile for example. However, since subjects were deprived of all feedback sources, it seems more likely that that the limb controller used by Zafar and Doren (2000) was insufficiently predictable to control.

It is likely that our observations were a result of the ideal control conditions created.

Since blocks of trials were in a predictable order and subjects performed multiple repeated trials per object, subjects could learn by trial-and-error. Furthermore, subjects were aware of a successful lift via feedback from their arm muscles as well as on-screen feedback at the end of each trial, allowing them to refine their judgements. Our work assumes that, by these processes, subjects can establish a feedforward prediction. This is defined as the ability to anticipate the forces they are exerting in the absence of *externally-arising* cues to that fact (see *introduction*). It is important to note that proprioceptive and tactile cues of the control signal are considered to be *internal* cues — they provide no feedback of how the robotic hand is interacting with the environment. However, it should also be noted that, in contrast to our ideal controller, commercially available prostheses are typically controlled by noisy EMG signals and that prosthesis control methods often do not provide predictable force control. Our results indicate that predictable control can obviate the practical benefits of feedback. However, in the presence of unavoidable feedforward uncertainty the benefits of feedback are apparent.

6.4.2.3 Temporal Delays

In this study I induced random temporal delays when simulating feedforward uncertainty in experiment 3. Temporal uncertainty and temporal judgement impact many dexterous tasks, in both healthy humans and prosthesis wears. At the task-level one can expect unpredictable sensory and motor delays (Kennedy et al., 2009), such as when grasping objects of unknown size or shape, or when not paying full visual attention. Every motor action is undertaken in the presence of uncertainty (Bays and Wolpert, 2007), resulting in some degree of temporal error. Temporal uncertainty is also a considerable concern for prosthesis designers. Since EMG signals used to initiate and control prosthesis movement fluctuate as a function of sweat, movement, muscle fatigue and skin-conductivity (Duchêne and Goubel, 1993) the most reliable EMG classifiers require 250-300ms of sampling time before accurate classification can be made (Lorrain et al., 2010). In the interest of responsiveness, controllability and expense, many commercially available prostheses use differential (“open/close”) controllers to defer the problem of EMG signal reliability to the temporal domain. Our results reveal that temporal uncertainty can significantly impair performance, but these effects are reduced with appropriate feedback.

To our knowledge this research provides first demonstration of the existence of feedforward and feedback processes for an artificial limb. Our results support, and perhaps provide an explanation for, similar studies in the literature. A study that showed no significant prosthesis control improvements with vibrotactile feedback (Chatterjee et al., 2008) could be explained by our finding of a strong feedforward contribution. The be-

nefit of feedback in the presence of partial sensory deprivation (Zafar and Doren, 2000) or with visual distractions (Cincotti et al., 2007) is supported by the present finding of the role of feedback in the presence of uncertainty.

6.4.2.4 Task and performance measurement

The task was designed to be simple for subjects to perform, and success was characterised by measuring performance differences for subjects lifting objects of different weights in different feedback conditions. In an abstract view of the task we could describe it simply as that of choosing an appropriate grasp duration to match the object weight, which could be learned by subjects over repeated lifts and over the course of the trial. It was, of course, our intention to make it as easy as possible for subjects to learn their feedforward model (to create idealised conditions, as discussed in section 6.4.2.2). Such conditions helped to show that feedforward uncertainty is an important aspect of control. Further research is necessary to quantify the degree of feedforward uncertainty in non-ideal (real-world) conditions. Minimising this uncertainty remains a challenge for future research.

In pilot studies it was observed that different subjects prioritised different aspects of the task. For example, one subject attempted to complete the task as quickly as possible, while another was more cautious and aimed to minimise errors. Consequently, no single basic measure of performance was suitable to quantify the relative merits of feedback across all subject. A score measure was used in all analyses in this chapter to provide a single, unified numerical quantity for the purpose of statistical comparison. This does not diminish the statistical power of the ANOVA which was completed with all available measures. It may have been preferable to provide stricter task demands, or provide further training to subjects, so as to constrain the inter-subject variability. However, this would have been at the expense of increased fatigue for subjects as the attached prosthesis was found to be heavy.

6.4.3 Implications

6.4.3.1 Recommendations

I have shown quantitatively that tactile feedback can significantly improve performance in the presence of feedforward uncertainty. These results have important implications for the prosthetics field, and consequently three recommendations can be made: (i) Prostheses should be designed to make control as predictable and repeatable as possible, to minimise feedforward uncertainty; (ii) Feedback should be provided to handle the inevitable uncertainty that will arise, and should be chosen to enable better feedforward

learning (such as error-corrective feedback, or force-derivative feedback, described in Engeberg and Meek (2008)); and (iii) We should aim to exploit the different sources of noise between robotic and human systems: trade-offs in design, for example, allow temporal uncertainty to be transformed into spatial uncertainty. If we can minimise uncertainty in task-specific domains we may increase control reliability and considerably improve hand functionality.

6.4.3.2 Reactive behaviour

How may feedback be utilised in *reactive* and even *reflexive* ways? During our experiments it was observed that some subjects could react to insufficient grip force feedback to avoid slip. Of course, considerable training would be needed to establish reflexive behaviour. However, reflexes could easily be programmed into hardware, alleviating the user of these demands, and by handling the uncertainty in this way the uncertainty exposed to the human user is decreased.

6.4.3.3 Control Strategy

In this study we have only considered a differential controller. Based on the present findings, in designing a prosthesis we may consider a proportional controller in which force output is proportional to the control signal. This would reduce the demand for accurate timing, and would be a useful method of delivering feedback. This would require further research in order to improve both control (more reliable EMG recording) and actuation (to reduce power consumption), but may see more direct benefits.

6.4.3.4 Generalisability

This study raises a number of interesting possibilities for future work. I have presented here a robotic system that replaces the healthy sensorimotor system for the elementary task of object lifting, but what are the limits of this analogy? Amputees fitted with prostheses such as the one presented in this paper will not have the benefit of ‘idealised control’: real-world prostheses are controlled by EMG electrodes which, as previously discussed, add control uncertainty. Our results suggest that EMG control will result in diminished grasp economy that can be remedied either by improving the reliability of EMG measurement (reducing feedforward uncertainty) or through provision of a reliable limb-state feedback. Our robotic manipulandum also provides a viable platform to test this hypothesis. Multifunction prostheses of the future offer increased dexterity and functionality at the expense of additional feedforward and feedback demands (as discussed in Dosen et al. (2010)). Tasks involving dynamic or unstable loads, such as handwriting, or tying shoelaces, require the learning of much more complex internal

models. It is not obvious how these models are acquired, nor how they depend on motor control or available feedback, yet they are key to the design of a system that needs to mimic human behaviour. I argue that this novel manipulandum is an ideal platform to study human sensorimotor processes as it allows the experimenter to access sensory and motor components that, in intact individuals, is either unethical or practically impossible.

6.4.3.5 Closing Remarks

The results in this chapter suggest that feedback should be chosen to complement the uncertainty in the control system. This does not mean, however, that by removing all uncertainty from the controller removes the necessity for feedback: a device which acts automatically and intelligently will surely reduce the number of grasping errors, but may not be accepted by the amputee as a natural extension of their nervous system. Vivid sensations of *embodiment* and prosthesis *ownership* can only be achieved through physiologically appropriate cutaneous feedback (Marasco et al., 2011).

Chapter 7

General Discussion

7.1 Summary of Results

The scientific and technological achievements chronicled in this thesis are, in part, due to considerable hardware, firmware and software engineering (Chapter 3). After creating numerous designs I developed and refined a **vibrotactile feedback system** to communicate feedback to the amputee. My design comprised low-cost components and was optimised to maximise bandwidth, minimise latency and avoid adaptation hypo-sensitivity. Working alongside Touch Bionics, an award-winning prosthetics company, I also developed several **prosthesis control algorithms**. My hardware, firmware and software have been licensed to the company and I am the primary inventor on a patent application (Saunders et al., 2011a)

At the time of writing, feedback is not a standard feature of state-of-the-art prostheses. A key aim of this thesis was to characterise the **role of feedback** to understand the limitations of sensory plasticity and sensorimotor rehabilitation. I aimed not only to satisfy indirect functionality measures with my feedback system (bandwidth, latency, etc.) but also to maximise the end-goal of increased functionality of the complete closed-loop system. However, unlike studies which designed a specific plant and aimed to quantify the benefits of feedback on performance, an approach which I felt lacked generality, I aimed instead to characterise the role of feedback in idealised, generalisable and controlled conditions. Such experimental scenarios ranged from (i) **Healthy Hand Scenarios**: A cue-tracking experiment using the healthy hand to localise noisy visual stimuli (Chapter 4); (ii) **Simulation Scenarios**: navigating a computer-controlled cursor (analogous to prosthesis control) with feedback presented in both visual and tactile modalities (Chapter 5); and (iii) **Real-World Scenarios**: grasping objects with a robotic hand (Chapter 6). Each of these required the development of original experimental methods, building on existing tracking protocols in the scientific literature combined with new insights. It was intended that experimentation at multiple levels of abstraction would inform the transition from theoretical concept to practical application, as well as providing findings of significant scientific merit at each stage.

In Chapter 4 I presented a novel visual tracking task, developed to ask the fundamental question of **how** estimates of statistical information (mean and uncertainty) are **acquired** and utilised by subjects. I showed that subjects estimate the **mean** of time-varying stimuli in a predictable manner: this estimate is computed in a **statistically-principled** way that assigns equal weight to cues observed over time to form an accurate final estimate. Using an optimal model with **kinematic constraints** I showed that subjects can accumulate evidence over time to form an **optimal continuous estimate** of the mean of noisy visual stimuli.

Moreover, using a novel variant of the paradigm, where subjects indicate the **range** in which they believe the target to lie (a direct measure of their **confidence**), I showed that subjects' perception of the variability of noise-perturbed time-varying stimuli (**subjective uncertainty**) is closely, but not directly, coupled with the underlying variability in performance of the task (**objective uncertainty**). By manipulating subsets of the cues through perturbations I evaluated the respective weighting given to each cue over time, suggesting that cue weighting was suboptimal due to a conservative **safety-margin**. I conclude that subjects are capable of accumulating evidence over time to **continuously discriminate** (albeit overestimate) the objective uncertainty present in noisy visual stimuli.

In Chapter 5 I presented the task of tracking a target with a **multimodal** cursor, under a variety of different control and feedback configurations. It was found that vibrotactile feedback could serve as a viable method of conveying task information, serving a similar function to the visual modality (a phenomenon termed **sensory augmentation** or **substitution**). Moreover, it was found that vibrotactile feedback was used in conjunction with visual information (termed **sensory integration**, Chapter 5, Pilot), but this effect depended on the influence of feed-forward control method as well as the quality of feedback.

In a modified task where the quality of visual and tactile feedback were equally matched, subjects were asked to localise a fixed target with a differentially-controlled noisy cursor. Vibrotactile feedback was combined with visual feedback in a near-statistically optimal manner (termed **optimal multisensory integration**, Chapter 5, Main Experiment). This process is based entirely on **sensory evidence** gained within a 5-second trial, and each modality is **optimally weighted** according to its **objectively-determined** variability. This result is consistent with discrete forced-choice studies, and provides the first evidence of the phenomenon for a **continuous** decision-making task.

These above results indicate the presence of optimal sensory processes extending to an "**artificial modality**". This is of relevance to prosthesis wearers who could directly benefit from an artificial sense of touch. I tested this hypothesis using an idealised "simulated amputation" scenario in Chapter 6. I completed three behavioural experiments to quantify the role of grip force feedback on economical grasping with a prosthesis. Feedback (visual or tactile) resulted in significant performance benefits in the presence of **feed-forward uncertainty** (control noise), but when "ideal" feed-forward control was enabled subjects could operate the limb and grasp economically in the absence of all feedback (both visual and tactile).

These results paint a picture of decision-making under uncertainty, showing the

transition of statistically-principled processes from the theoretical level to practical application. These results can inform our choices in designing state-of-the-art prostheses **optimised to the residual capabilities of the amputee** (in particular by exploiting residual feed-forward control ability, and/or through the provision of appropriate task-level feedback).

7.2 Critical Evaluation

7.2.1 High Dimensionality

In Chapter 3 I discussed a large number of different dimensions relevant to prosthesis design (see Fig. 3.1). These many dimensions result in a combinatorial explosion of possible closed-loop configurations. As such, it is impossible to consider all of these dimensions together, and instead the present approach has been to evaluate their contributions independently of one another. This approach has obvious practical advantages, but it overlooks the possibility of an interaction between design dimensions.

In this thesis it was assumed that a modular system design was appropriate and that the respective roles of control, actuation, sensation and feedback could be decoupled. This approach is shared by studies focusing on each of these specific areas, such as studies into vibrotactile hardware (Mortimer et al., 2007), vibrotactile perception (Cholewiak and Collins, 2003, Soto-Faraco and Deco, 2009), prosthesis control (Cipriani et al., 2008, Dosen et al., 2010) and sensor research (Edin et al., 2006).

However, an important difference in the approach taken this thesis is that the main experiments require subjects to perform closed-loop tasks. Continuous uncertainty estimation is reported in a novel visuomotor paradigm, multisensory integration is reported in a novel multisensory sensorimotor paradigm, and feedforward and feedback processes are decoupled in a real-world ‘grasp and lift’ sensorimotor paradigm. Hence, although a limited number of system configurations are considered here, these tasks are in the relevant context for understanding closed-loop behaviour and thus the present approach lends itself readily to the full dimensionality of the problem.

7.2.2 Feedback Encoding

In this thesis I have presented several results specifically related to a spatial encoding of vibrotactile feedback. For practical reasons I have not explored the wide range of possible encoding strategies (see Chapter 3 and Fig. 3.1). For example, Kadkade et al. (2003) demonstrate the utility of differential error signals over absolute error feedback, Engeberg and Meek (2008) demonstrate the utility of force-derivative feedback to aid a prosthesis controller, and Kohli et al. (2006) use stimulus motion to convey information.

It is possible that such alternative feedback encodings may provide improved utility or alternative integration effects.

In this thesis I have presented a feedback system that provides an immediate and intuitive signal (reasonable JND-thresholds were computed in a task of ~ 4 minutes duration and multisensory integration measured in a task of ~ 20 minutes duration, in contrast to the intensive electrotactile training protocol devised by Szeto and Chung, 1986). It has previously been argued that having control of the feedback signal (such as control of the camera in TVS studies by Rita et al., 1969) is crucial for task success. The optimal multisensory integration result in this thesis may reflect the utility of the sensorimotor paradigm for the assessment of feedback integration in a closed-loop context.

It was found that with spatial feedback it was easy to discriminate different stimuli but precise localisation was more difficult (see JND experiments, Chapter 3). Perhaps localisation ability would improve with training (learning to associate stimuli with locations), but it also seems likely that discrimination and localisation are fundamentally different tasks, not least because the former relies on short-term tactile memory and the latter on long-term tactile memory. Hence, it may be a preferable approach to ask subjects to perform an absolute recall task over a discrimination task in calculating the ‘quality’ of sensory feedback, as alternative to classical JND threshold calculation. However, even this may be insufficient to capture the full range of desirable feedback properties. For example, some encodings may have greater bandwidth at the expense of increased mental effort, latency to decode, or rate of desensitisation. These individual parameters may be investigated by specific experimental study, but testing them in a sensorimotor task such as the tracking paradigm developed in this thesis may provide a more valuable means of assessing the overall utility of the feedback system.

7.2.3 Sensorimotor Task Design

In this thesis I have presented a range of variants of the classic tracking paradigm. In developing the tasks used in Chapter 5, multiple variants were considered. In the main experiment it was found that subjects optimally integrated information from multiple sensory modalities. It is important to ask why this effect was less evident in the pilot experiment and earlier experiments (data not shown).

One obvious reason is that the main experiment was designed to ensure that visual and tactile performance overlap across the range of uncertainties tested. This was achieved by adjusting the baseline visual feedback reliability to cover the same range as the tactile feedback reliability, to ensure that the effects of interaction were measurable. Moreover, the main experiment removed visual biases by having a fixed multimodal

target, simplifying the task demands. It should be acknowledged that the scalability of multisensory optimality to more complex sensorimotor tasks and modality-biased sensorimotor tasks is not yet known.

Finally, it is worth considering that, owing to the observed dominance of the visual modality on performance, visual feedback appears to be a significantly more reliable source of sensory feedback than artificial tactile feedback. However, it should be noted that it is impractical and undesirable to rely heavily on a single modality, especially for more complex tasks involving visual distraction (Cincotti et al., 2007), occlusion Zafar and Doren (2000), and attention modulation (Spence et al., 2004). Tactile feedback provides a valuable channel, although admittedly its full exploitation may require further development of more reliable tactile interfaces.

7.2.4 The Benefits of Feedback

In Chapter 6, three experiments were presented to quantify the benefits of feedback on grasping performance. Under ideal conditions it was found that feedback had no effect on economical grasping, even in the complete absence of visual and auditory feedback. This is in contrast to Zafar and Doren (2000), Pylatiuk et al. (2004).

The key difference between these studies was our use of an ‘idealised’ controller. Such a controller had predictable feed-forward nature which presumably obviated the need for feedback once the control was learned. These ideal control conditions may not presently be available to amputees (owing to the unreliability of real-world tasks as well as the high level of variability in sEMG recordings and the use of differential-control algorithms. See Chapter 6 for further discussion). A natural follow-up to the experiments presented in this thesis would be to quantify the level of feedforward control for a range of typical EMG classification algorithms, and quantify the benefits of feedback in these realistic cases.

The study presented in Chapter 6 only considers the task of grasping and lifting. I have previously discussed the relevance and applicability of this task but it is obviously limited in its ability to explain the full range of human hand dexterity. Even within the task of grasping, a number of important variables were omitted. In particular, all objects were the same size and shape and has the same smooth surfaces. It would be interesting to investigate the role of feedback in handling these properties, as feedforward control may become increasingly unreliable in the presence of more complex task demands.

7.2.5 Uncertain Uncertainty

In Chapter 4 it was found that uncertainty estimation trajectories could be reliably modelled by an optimal estimator with kinematic constraints — with the addition of

conservative error margin. When evaluating the weights allocated to individual cues the model and empirical data did not match. It is important to address the question of whether this reflects: (i) a failure of the model to capture the factors influencing movement; (ii) inadequacy of the model fitting procedure; or (iii) suboptimality of human uncertainty estimation. All three are plausible explanations for the observation.

The present work can not fully resolve this debate, but there are a number of potential methods to distinguish the causes of uncertainty overestimation. Firstly, it is possible that cues were arriving far quicker than they could be processed. One could slow down the arrival of cues so that the contributions of each cue could be more reliably distinguished behaviourally. Secondly, perturbations were added to the mean of the stimulus but not to the uncertainty. A more direct approach would be to adjust the uncertainty and observe the impulse response to this change. Thirdly it is acknowledged that the high levels of noise in the uncertainty estimation data made it difficult to reliably fit the model parameters to the data using the least-squares approach. Either a more robust fitting procedure could be used, or further data collected to reduce the effect of noise. Only when these aspects are corrected should the model be revised to explain the empirical observations.

7.2.6 Healthy grasping

In Chapter 6 it was shown that an overall increase in grip force occurred in the absence of visual feedback. This could be interpreted as evidence that vision is required to modulate or maintain the absolute level of grip force of the prosthesis in the absence of feedback. This has been shown in healthy individuals with digital anaesthesia (Jenmalm and Johansson, 1997, Jenmalm et al., 2000). However, an alternative interpretation is that vision provides a *context switch* (see Chapter 2 section 2.3.3.1, and Buckingham et al., 2011) which modulates the background level of force used by subjects. The use of vision for activation of internal models has also been demonstrated for object shape (Jenmalm and Johansson, 1997) and prediction of object weight based on object size (Gordon et al., 1991). Augurelle et al. (2003) provided evidence that the background level of force is also modulated by digital anaesthesia in healthy individuals, but this was not shown for prosthesis wearers in the present study.

Therefore it seems that the manipulandum developed here captures only a subset of healthy human phenomena. This could be attributed to a number of possibilities, such as: (i) the degree of sensorimotor restoration (limited degrees of control and feedback); (ii) due to fundamental differences in the way the device is controlled compared to a healthy hand; (iii) due to the fundamental differences in the way the feedback is provided compared to a healthy hand (i.e. its source, location and encoding); or (iv) the fact that

the prosthesis has not been connected to the wearer's nervous system for much longer than 30 minutes in any of the experiments presented in this thesis. Of these possibilities, (i) and (iv) could be addressed by training the subject with the limb for a longer period, or by using existing amputees. Points (ii) and (iii) are more difficult to address directly due to the limitations of prosthesis hardware. As posited in Chapter 3, these variables could be explored by starting with the healthy human hand and gradually stripping it of different control and feedback capabilities. Obviously this is impractical with healthy individuals, which was a primary motivation of the manipulandum developed in this thesis. Another potential approach may be to revert to *virtual-reality*, wherein the control of the hand could be achieved using any range of control algorithms based on natural hand control.

7.2.7 Achievement of Aims

With respect to the aims reported in section 1.2, the present thesis addressed all themes under consideration. In this section I discuss the degree to which the aims were achieved.

- **1: Sensory Communication:** Can I establish a high-bandwidth sensory feedback channel that people are able to detect and decode?

In Chapter 3 I present a vibrotactile sensory communication interface. As previously discussed, direct pressure-feedback devices may offer a more natural sensation (Patterson and Katz, 1992), and electro tactile feedback might provide greater spatial resolution (Kaczmarek et al., 1991). A more thorough evaluation of alternative feedback systems in a closed-loop context is needed to decide the most appropriate feedback system for amputees. The feedback system presented here can be learned quickly and has a good bandwidth (Chapter 3), but spatial localisation accuracy is particularly poor and greater bandwidth may be achieved by other encoding methods. Nevertheless, I argue that the system presented here provides a sufficient communication channel for the purposes of this research, and is useful at least for providing a single dimension of feedback.

- **2: Sensory Augmentation:** If I can establish a sensory feedback channel with sufficient bandwidth, will a person be able to use it to do a task, such as estimating forces, or positions? Can it adequately *augment* or *substitute* for information presented in another modality, such as vision?

In Chapter 5 it was found that the vibrotactile feedback system designed allowed for sensory substitution. In the absence of (or under degraded) visual feedback, the feedback system could be used for navigating a cursor to a target in a number of tracking tasks, though the tactile feedback baseline performance was poorer than visual feedback. In

Chapter 6 it was found that vibrotactile feedback could substitute for visual feedback in the presence of feedforward uncertainty, enabling economical grasps albeit with a higher overall level of grip force.

- **3: Sensory Integration:** If I can establish a sensory feedback channel with sufficient bandwidth, and the person can use it, will a person also *integrate* this information with their existing senses? Will it *complement* existing modalities, and add additional benefits?

In Chapter 5, sensory integration was observed. This was defined as the selective use of both visual and vibrotactile feedback in relation to their respective reliability. It was found that, when visual and tactile feedback were equally reliable (in terms of objective variability) there was a reduction in variability (improvement in performance) compared to when each modality was presented alone. In contrast, this reduction in variance was not observed for absolute cursor control (Pilot experiment). This may be partly due to the limited degree of overlap in objective variability of each of the modalities in the pilot experiment, but also implies that multisensory integration does not depend on just the reliability of the cues but also the reliability of the efferent copy for control.

- **4: Optimal Sensory Integration:** Will a successfully integrated artificial modality be combined with existing senses in a manner which is *optimal* with respect to the reliability of the sensory information it provides? Are optimal weights *learned* or *innate*?

In Chapter 5, cue weighting was governed by the *objective* uncertainty (the empirically observed variability of localisation performance), indicative of **Optimal Sensory Integration**. This was measured both by observing a reduction in variance in the multimodal condition as well as by computing the weight attributed to each modality. The per-modality weightings were indistinguishable from a simulated Bayes-optimal ideal-observer. Subjects are able to learn to discriminate different levels of uncertainty of visual stimuli over the time-course of an experiment (Chapter 4). As the vibrotactile feedback system is, in many regards, an artificial sense (issued at a different *location*, in a different *modality*, and with a different *encoding* to that of natural sensation), it may also be argued that the mapping between sensory signals and the task-level uncertainty required for optimal integration is also learned over the time-course of the experiment (Chapter 5).

- **5: Sensory Uncertainty Acquisition:** Optimal sensory integration assumes an ability of subjects to *acquire* statistical information from the world. How is such information (such as the mean and uncertainty of sensory evidence) computed? To what extent can this explain multisensory perception?

Chapter 4 revealed that subjects have access to a measure of the mean and uncertainty of sensory cues, which evolves continuously as evidence arrives. The results provide a strong indication that cues throughout the trial are combined optimally to form reliable estimate of the mean, but uncertainty estimation appears less than optimal, involving overestimation of the uncertainty required to achieve the maximum score. The mechanisms of sensory uncertainty acquisition remain elusive, though I feel that the paradigm I have developed offers a valuable tool to further instigate this problem. Multisensory perception of uncertainty is still an open question which can also be addressed using this paradigm.

- **6: Sensorimotor Integration:** If I can establish an optimally integrated sensory feedback channel, does this scale to real world sensorimotor tasks such as grasping and lifting objects? To what extent is present prosthesis-control suboptimality governed by sensory uncertainty versus motor uncertainty?

In Chapter 6 I investigated sensorimotor integration for the real-world task of grasping and lifting objects. Using an idealised prosthesis control system I found that, comparable to healthy human studies, prosthesis-control depended on *both* feedforward and feedback influences. It is important to also consider the generalisability of the idealised system to EMG control and more complex task demands. These aspects were not tested in this thesis and further work is required to fully appreciate the full dimensionality of closed-loop prosthesis design.

Overall the work presented in this thesis satisfies the aims in section 1.2. However, the greater goal and underlying motivation of the research is a more complex problem of high dimensionality. To restore a replacement sense of touch to amputees will require advances in robotic technology, sensor design and new and improved interfaces with the nervous system. By further understanding the limits of sensory plasticity it may be possible to exploit the residual capabilities of the amputee.

7.3 Future Perspectives

7.3.1 Multisensory Confidence Estimation

In Chapter 4 I presented a *confidence estimation* task for visual uncertainty estimation. The task naturally lends itself to multimodal confidence estimation as illustrated in Fig. 7.1. I hypothesised that, given subjects integrate sensory information in a statistically optimal fashion (weighting each modality in accordance with its objective reliability, Chapter 5) and subjects can form a subjective estimate of their objective uncertainty (although suboptimally, Chapter 4) then their multimodal confidence should be a function of their unimodal confidence. Combining Chapters 4 and 5 into a new multimodal

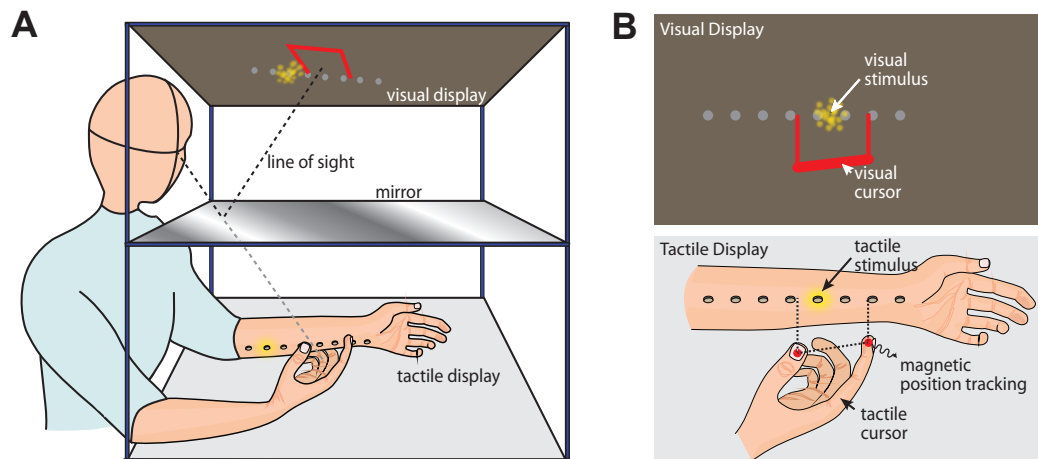


Figure 7.1: **Multisensory Confidence Estimation Task.** (A) Consider a variant of uncertainty estimation paradigm in which subjects are presented with both visual and tactile jittering stimuli. (B) Subjects are required to localise the mean of the *multisensory* stimuli using the grasping technique previously described .

confidence estimation paradigm I conducted a preliminary investigation with subjects reaching for multimodal targets. The modalities were offset on some trials to enable discrimination of weights.

The preliminary results are presented in Fig. 7.2. Unfortunately, in this experiment there was insufficient interaction between visual and tactile feedback due to their non-overlapping nature (7.2A). However, interesting observations can be made nonetheless. In the absence of modality offset, performance followed the qualitative predictions of optimal multimodal integration, with multimodal variance smaller than unimodal variances (Fig. 7.2B). However, confidence estimation did not appear to follow these same trends. While the multimodal confidence window is generally smaller than the unimodal visual confidence window, it is strangely larger than the unimodal tactile confidence window in some cases (Fig. 7.2C and 7.2D). This peculiar behaviour suggests that subjective perception of multisensory confidence is not optimal, and that subjective perception does not govern optimal integration as observed in Fig. 7.2B. Plausible explanations may be: (i) the presence of visual and tactile feedback provide a context switch that additionally modulates perception of uncertainty (Chapter 6); (ii) inherent biases towards one modality may result in a mismatch between perception of uncertainty and objective uncertainty; and (iii) the contrasting suboptimality of uncertainty perception (Chapter 4) and optimality of multisensory integration (Chapter 5) may indicate that two separate processes mediate these phenomena. These theories warrant further investigation.

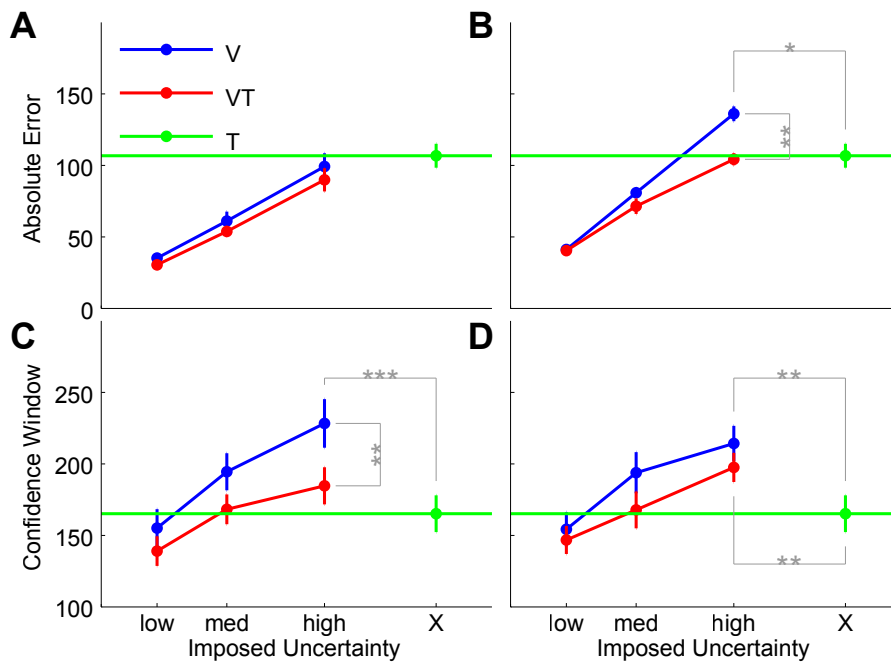


Figure 7.2: **Multisensory Confidence Estimation Preliminary Results (N=8)**. Vision-only trials (V, blue), Tactile-only trials (T, green) and Multimodal trials (VT, red) are distinguished. Results for low, medium and high visual uncertainty are plotted. Data for 8 subjects are shown, with 3 further subjects discarded from analysis due to inadequate performance. **(A)** Mean absolute error \pm SEM for trials **without** an offset between modalities. Owing to the superiority of visual feedback there is little interaction between vision and tactile. **(B)** Mean absolute error \pm SEM for trials **with** an offset between modalities. Multimodal performance is superior to unimodal performance. **(C)** Mean confidence estimate \pm SEM for trials **without** an offset between modalities. The multimodal confidence window is generally smaller than the unimodal visual confidence window, but strangely larger than the unimodal tactile confidence window in some cases. **(D)** Mean confidence estimate \pm SEM for trials **without** an offset between modalities. Similar results to C.

7.3.2 Remaining Dimensions

In this thesis I have aimed to tackle a subset design dimensions in order to understand the limitations of sensory feedback for restoring healthy performance to prosthesis wearers. The same general approach could enable further sensory dimensions to be introduced, such as additional sources of sensory feedback, additional control methods and additional tasks. One may consider: (i) human discrimination of object softness; (ii) assessment of surface frictional properties; and (iii) detection (and reaction to) object slip. These can presumably not adequately be restored through grip force feedback alone. Advances in these directions will be limited by sensor technology though simulation may allow for these aspects of prosthesis design to be evaluated prior to an investment in this direction. Open questions such as the number of sensory “channels” that can maximally be restored, and the degree of improvement restored by the additional sensory burden, are yet to be answered. However, they may both be addressed by building on the methods presented in this thesis.

At the time of writing the mobile phone industry is driving miniaturisation of portable batteries and electronic components, whilst the computer gaming industry is exploring novel sensory devices. Due to reducing component costs it seems highly likely that the next generation of prostheses will be fitted with sensor arrays and powerful microprocessors. It will be exciting to see improvements to state-of-the art prostheses incorporating the capabilities of these technologies. However, before this can be fully exploited it is imperative that we continue to address the basic research question of how best to communicate with the user via the peripheral nervous system.

Appendix A

Uncertainty in Sample Standard Deviation

In chapter 4 I introduced a novel visual tracking experiment which required subjects to maximise their expected reward in order to achieve optimum uncertainty-estimation performance. In this appendix I provide further detail to support this approach, including a derivation of ideal-observer behaviour and the choice score function which rewards success in the task.

Relevant Publications

- Ian Saunders, Sethu Vijayakumar. (2012). **Continuous Evolution of Statistical Estimators for Optimal Decision-Making.** *PLoS ONE*
- Ian Saunders, Sethu Vijayakumar, (2011b) **Continuous Estimation of Mean and Uncertainty,** *Proc. The 21st Annual Conference of the Japanese Neural Network Society.*

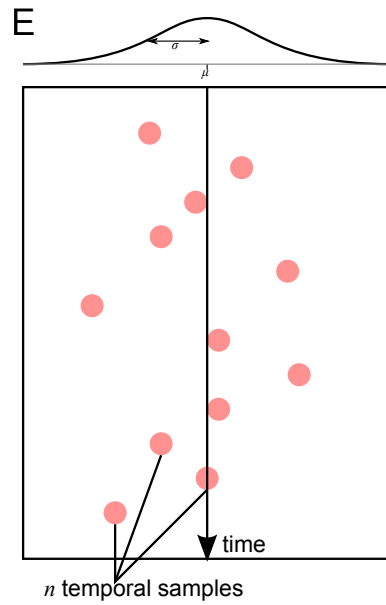


Figure A.1: The butterfly-catching paradigm presents subjects with a sequence of jittering samples.

A.0.3 Computing the uncertainty in our estimate of the mean

A.0.3.1 Butterfly Catching

In the butterfly catching paradigm (chapter 4), subjects witness a sequence of n samples, X_1, \dots, X_n , each assumed to be drawn from an underlying Normal distribution with unknown mean μ and variance σ^2 . Figure A.1 illustrates this.

In any given trial, their task is to demonstrate their estimate of the true mean by indicating a *confidence window* around this estimate. Subjects are awarded more points for smaller confidence windows, and so must trade-off the probability of being correct versus the reward attained i.e. they must maximise the expected reward. To do this they need to acquire and utilise the statistical information present in the samples. To define *ideal observer* or *optimal* behaviour we must characterise the probability distributions with which these statistical inferences can be made.

From the samples one can easily state the maximum-likelihood unbiased estimates of the mean and variance:

$$\hat{\mu} = \frac{1}{n} \sum_i X_i \quad (\text{A.1})$$

$$\hat{\sigma}^2 = \frac{1}{n-1} \sum_i (X_i - \hat{\mu})^2 \quad (\text{A.2})$$

We will show that the ideal observer can use these estimators to compute the probability of success at the task, and complete the task with a given accuracy, allowing the

ideal observer to maximise expected reward. In this section we derive these quantities from basic probability theory.

A.0.3.2 Cochran's Theorem

Cochran's Theorem states that:

For U_1, \dots, U_n , where each $U_i \sim \mathcal{N}(0, 1)$ we can rearrange the sum of squares of U_i into a linear sum of random variables, $\sum_{i=1}^n U_i^2 = Q_1 + \dots + Q_k$.
 If $r_1 + \dots + r_k = n$, where r_i is the rank of Q_i , then it follows that:

- (a) the Q_i are independent, and
- (b) each Q_i has a Chi-square distribution with r_i degrees of freedom: $Q_i \sim \chi^2(r_i)$.

A.0.3.3 Derivation of deviate distributions

Given our X_i described above, then let

$$U_i = \frac{X_i - \mu}{\sigma} \sim \mathcal{N}(0, 1)$$

Rearranging the sum of squares we find that

$$\begin{aligned} \sum_i U_i^2 &= \sum_i \left(\frac{X_i - \mu}{\sigma} \right)^2 \\ &= \frac{1}{\sigma^2} \sum_i (X_i^2 - 2\mu X_i + \mu^2) \\ &= \frac{1}{\sigma^2} \sum_i (X_i^2 - 2\mu X_i + \mu^2 - 2\hat{\mu}^2 + 2\hat{\mu}^2) \\ &= \frac{1}{\sigma^2} (\sum_i X_i^2 - 2\mu \sum_i X_i + \sum_i \mu^2 - 2\hat{\mu} \sum_i \hat{\mu} + \sum_i \hat{\mu}^2 + \sum_i \hat{\mu}^2) \\ &= \frac{1}{\sigma^2} (\sum_i X_i^2 - 2\mu \sum_i X_i + \sum_i \mu^2 - 2\hat{\mu} \sum_i X_i + \sum_i \hat{\mu}^2 + \sum_i \hat{\mu}^2) \\ &= \frac{1}{\sigma^2} (\sum_i X_i^2 - 2\hat{\mu} \sum_i X_i + \sum_i \hat{\mu}^2 + \sum_i \mu^2 - 2\mu \sum_i X_i + \sum_i \mu^2) \\ &= \frac{1}{\sigma^2} \left(\sum_i (X_i^2 - 2\hat{\mu} X_i + \hat{\mu}^2) + (n\hat{\mu}^2 - 2n\mu\hat{\mu} + n\mu^2) \right) \\ &= \sum_i \left(\frac{X_i - \hat{\mu}}{\sigma} \right)^2 + n \left(\frac{\hat{\mu} - \mu}{\sigma} \right)^2 = Q_1 + Q_2 \end{aligned}$$

Thus, we can express it as the sum of two terms, which we call Q_1 and Q_2 :

$$\sum_i \left(\frac{X_i - \mu}{\sigma} \right)^2 = \underbrace{\sum_i \left(\frac{X_i - \hat{\mu}}{\sigma} \right)^2}_{Q_1} + \underbrace{n \left(\frac{\hat{\mu} - \mu}{\sigma} \right)^2}_{Q_2} \quad (\text{A.3})$$

The rank of Q_2 is clearly 1 (it is the square of just one linear combination of Normal random variables). The rank of Q_1 is $n - 1$ (it is sum of squares of n linear combinations of Normal random variables, but they are not independent; $\hat{\mu}$ removes a degree of freedom).

Therefore, by Cochran's theorem,

$$Q_1 \text{ and } Q_2 \text{ are independent} \quad (\text{A.4})$$

$$\sum_i \left(\frac{X_i - \hat{\mu}}{\sigma} \right)^2 \sim \chi^2(n - 1), \text{ and} \quad (\text{A.5})$$

$$n \left(\frac{\hat{\mu} - \mu}{\sigma} \right)^2 \sim \chi^2(1). \quad (\text{A.6})$$

Substituting equation A.2 in equation A.3, we find that:

$$\sum_i \left(\frac{X_i - \mu}{\sigma} \right)^2 = \underbrace{(n - 1) \frac{\hat{\sigma}^2}{\sigma^2}}_V + \underbrace{\left((\hat{\mu} - \mu) \frac{\sqrt{n}}{\sigma} \right)^2}_{Z^2}$$

For later convenience we have labeled the terms V and Z^2 . Thus, it follows that

$$V \text{ and } Z \text{ are independent} \quad (\text{A.7})$$

$$Q_1 = V \sim \chi^2(n - 1) \quad (\text{A.8})$$

$$Q_2 = Z^2 \sim \chi^2(1) \quad (\text{A.9})$$

And from the definition of the Chi-square distribution

$$Z \sim \mathcal{N}(0, 1) \quad (\text{A.10})$$

A.0.3.4 The distribution of mean estimator

Since

$$Z = (\hat{\mu} - \mu) \frac{\sqrt{n}}{\sigma} \sim \mathcal{N}(0, 1)$$

We can compute the probability that an observer is successful for a chosen confidence interval

$$\begin{aligned}\Pr(-\alpha \leq Z \leq \alpha) &= \int_{-\alpha}^{+\alpha} \mathcal{N}(x; 0, 1) dx \\ \Pr\left(-\alpha \leq (\hat{\mu} - \mu) \frac{\sqrt{n}}{\sigma} \leq \alpha\right) &= \int_{-\alpha}^{+\alpha} \mathcal{N}(x; 0, 1) dx \\ \Pr\left(\mu - \frac{\alpha\sigma}{\sqrt{n}} \leq \hat{\mu} \leq \mu + \frac{\alpha\sigma}{\sqrt{n}}\right) &= \int_{-\alpha}^{+\alpha} \mathcal{N}(x; 0, 1) dx\end{aligned}$$

Letting

$$\alpha = \frac{d\sqrt{n}}{2\sigma}$$

We see that

$$\begin{aligned}\Pr\left(\mu - \frac{d}{2} \leq \hat{\mu} \leq \mu + \frac{d}{2}\right) &= \int_{-\frac{d\sqrt{n}}{2\sigma}}^{+\frac{d\sqrt{n}}{2\sigma}} \mathcal{N}(x; 0, 1) dx \\ &= \int_{-\frac{d}{2}}^{+\frac{d}{2}} \mathcal{N}\left(x; 0, \frac{\sigma}{\sqrt{n}}\right) dx\end{aligned}\tag{A.11}$$

That is, we can compute the probability of the sample mean falling in a confidence interval of width d around the true mean (equation A.11).

A.0.3.5 Student's t distribution

The butterfly cating paradigm requires not only that we estimate the mean, but also that we report a confidence interval around it. Unfortunately the *ideal observer* can not utilise equation A.11 as this would require knoweldge of the *true* variance σ^2 . In order to substitute the sample variance $\hat{\sigma}^2$ we rely on the definition of Student's t distribution.

For independent Z and V , where $Z \sim \mathcal{N}(0, 1)$ and $V \sim \chi^2(\nu)$,

We can form the ratio:

$$Y = \frac{Z}{\sqrt{V/\nu}} \quad (\text{A.12})$$

$Y \sim \mathcal{T}(\nu)$, i.e. the probability distribution of the ratio is Student's t-distribution with ν degrees of freedom Johnson et al. (1995)

Where we use the standard definitions:

$$\begin{aligned} \mathcal{T}(t; \nu) &= \frac{\Gamma(\frac{\nu+1}{2})}{\sqrt{\nu\pi} \Gamma(\frac{\nu}{2})} \left(1 + \frac{t^2}{\nu}\right)^{-\frac{\nu+1}{2}}, \text{ and} \\ \Gamma(t; z) &= \int_0^\infty t^{z-1} e^{-t} dt \end{aligned}$$

A.0.3.6 Estimating the distribution of the mean estimator

We previously introduced V and Z (equations A.8 and A.10), to derive the distribution of the sample mean (equation A.1).

By appropriately setting $\nu = (n - 1)$ in A.12, it follows from the definition of Student's t distribution that

$$\begin{aligned} Y &= \frac{Z}{\sqrt{V/(n-1)}} \\ &\sim \mathcal{T}(n-1) \end{aligned}$$

Substituting equations A.8 and A.10 we see that

$$\begin{aligned} Y &= \frac{Z}{\sqrt{V/(n-1)}} \\ &= \frac{(\hat{\mu} - \mu) \frac{\sqrt{n}}{\sigma}}{\sqrt{\frac{(n-1) \hat{\sigma}^2}{(n-1) \sigma^2}}} \\ &= \sqrt{n} \left(\frac{\hat{\mu} - \mu}{\hat{\sigma}} \right) \end{aligned}$$

Compare this to our definition of Z

$$Z = \sqrt{n} \left(\frac{\hat{\mu} - \mu}{\sigma} \right)$$

Note that Y differs from Z in that the exact standard deviation σ^2 is replaced by the sample standard deviation $\hat{\sigma}^2$.

In an identical manner as before, we can therefore compute probabilities over a given confidence interval

$$\begin{aligned}\Pr(-\alpha \leq Y \leq \alpha) &= \int_{-\alpha}^{+\alpha} \mathcal{T}(x; n-1) dx \\ \Pr\left(-\alpha \leq (\hat{\mu} - \mu) \frac{\sqrt{n}}{\hat{\sigma}} \leq \alpha\right) &= \int_{-\alpha}^{+\alpha} \mathcal{T}(x; n-1) dx \\ \Pr\left(\mu - \frac{\alpha \hat{\sigma}}{\sqrt{n}} \leq \hat{\mu} \leq \mu + \frac{\alpha \hat{\sigma}}{\sqrt{n}}\right) &= \int_{-\alpha}^{+\alpha} \mathcal{T}(x; n-1) dx\end{aligned}\quad (\text{A.13})$$

Again, letting

$$\alpha = \frac{d\sqrt{n}}{2\hat{\sigma}}$$

We see that

$$\begin{aligned}\Pr\left(\mu - \frac{d}{2} \leq \hat{\mu} \leq \mu + \frac{d}{2}\right) &= \int_{-\frac{d\sqrt{n}}{2\hat{\sigma}}}^{+\frac{d\sqrt{n}}{2\hat{\sigma}}} \mathcal{T}(x; n-1) dx \\ &= 2 \int_0^{\frac{d\sqrt{n}}{2\hat{\sigma}}} \mathcal{T}(x; n-1) dx - 1\end{aligned}\quad (\text{A.14})$$

A.0.3.7 Application

Based on equation A.14, the *ideal observer* can determine the optimal confidence interval d , such that for a given probability p ,

$$\Pr\left(\mu - \frac{d}{2} \leq \hat{\mu} \leq \mu + \frac{d}{2}\right) = p$$

Utilising the cumulative t-distribution \mathcal{C} , where

$$\mathcal{C}(a; n) = \int_0^a \mathcal{T}(x; n) dx$$

We can rewrite equation A.14 as

$$p = 2\mathcal{C}\left(\frac{d\sqrt{n}}{2\hat{\sigma}}; n-1\right) - 1$$

Denoting the inverse cumulative t distribution \mathcal{C}^{-1} , we see that

$$d = \frac{2\hat{\sigma}^2 \mathcal{C}^{-1}\left(\frac{p+1}{2}; n-1\right)}{\sqrt{n}}\quad (\text{A.15})$$

For any given n , μ and σ , we can vary p and visualise the optimal d graphically (see figure A.2).

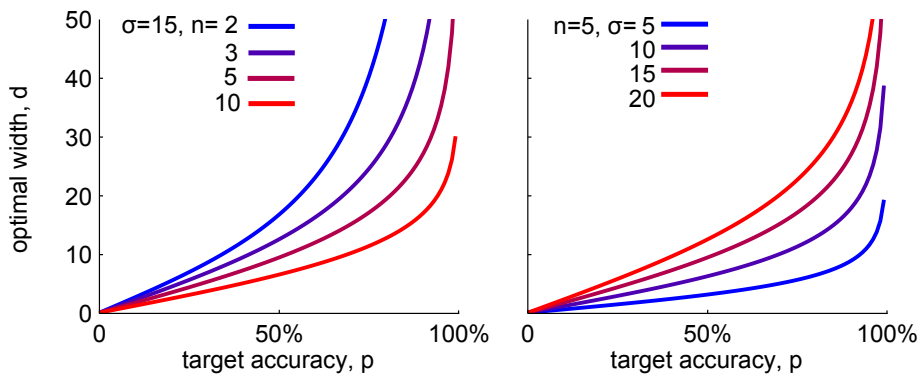


Figure A.2: **Optimal Confidence Window.** The confidence window required to achieve a given target probability, for a number of samples n and underlying variance σ^2 .

A.0.3.8 Conclusion

Equipped with evidence available from a sequence of samples, in particular the sample mean and variance, the ideal observer can calculate the confidence interval around their estimate of the mean. This confidence interval can be chosen to achieve a given probability of success at the task. Since the expected reward in the butterfly-catching task requires the trade-off of between the probability of success and the score obtained for a given confidence interval (see chapter 4 and below), the ideal observer can maximise their expected reward.

A.0.4 Score functions

A.0.4.1 Motivation

In the butterfly-catching paradigm, subjects are rewarded for accuracy in each trial. The purpose of this is to motivate them and maintain their full attention throughout. As we are interested not only in success at the task but also accurate estimation of the uncertainty of the stimuli, we reward this aspect of the task too. We consider two plausible *score functions*, designed to encourage subjects to represent their perceived uncertainty in the stimuli.

A.0.4.2 Score Functions

On a given trial subjects position their fingers to indicate their estimate of the mean, x , and a confidence interval around the mean of width w . We reward them with a score $S(x, w, \mu, \sigma)$, that depends on the true mean of the cues, μ , and the uncertainty variable σ .

$$S(x, w, \mu, \sigma) = \begin{cases} f(w, \sigma) & \text{if } \mu - \frac{w}{2} \leq x \leq \mu + \frac{w}{2} \\ 0 & \text{otherwise} \end{cases}$$

where f is the *score function*.

Note that the uncertainty variable σ is intended to describe the uncertainty in the distribution of the cues.

We consider 2 possibilities for the functional form of the score function f , illustrated in figure A.3. These are:

- Uncertainty-invariant score function (UI);
- Bounded reciprocal square score function (BR);

The expected score can be computed by multiplying the probability of success for a given width w , by the score attained for that width $S(w)$, i.e.

$$\begin{aligned} E(S|w, \sigma) &= \int_{-\infty}^{+\infty} \Pr(\hat{\mu} = x|w, \sigma) \cdot S(x, w, \mu, \sigma) dx \\ &= \Pr\left(\mu - \frac{w}{2} \leq \hat{\mu} \leq \mu + \frac{w}{2}\right) \cdot f(w, d) \\ &= f(w, \sigma) \cdot \int_{-\frac{d}{2}}^{+\frac{d}{2}} \mathcal{N}(x; 0, \frac{\sigma}{\sqrt{n}}) dx \end{aligned}$$

The two score functions can be expressed in their functional form:

$$\begin{aligned} S_{UI} : \quad f(w, \sigma) &= w^{-0.709} \\ S_{BR} : \quad f(w, \sigma) &= \begin{cases} 10 & \text{if } w \leq \sigma \\ 10 \cdot (\frac{\sigma}{w})^2 & \text{otherwise} \end{cases} \end{aligned}$$

In both cases, the peak of the expected reward is achieved when $w = \sigma$. This is achieved by the index -0.709 in the UI method, and by the discontinuity in the BR method. This is illustrated in figure A.3. The advantage of the UI method is that it uses a score function that does not depend on the ideal-observer uncertainty (and so the subject's choice is unbiased by the magnitude of the score). The advantage of the BR method is that the aim of the task is much clearer to subjects - they are to aim to maximise reward, which amounts to estimating σ .

A.0.4.3 Levels of Uncertainty

In using the BR method we must choose an appropriate quantity σ to capture the uncertainty. This can actually describe a number of properties of the system in question:

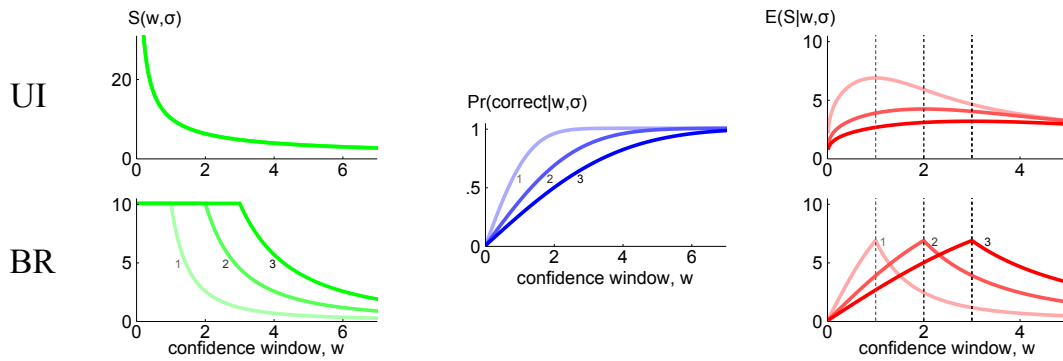


Figure A.3: **Choice of score function.** We consider, from top to bottom, Uncertainty-invariant (UI); and Bounded reciprocal square (BR); score functions (*left*). Note that the UI score function is the same for all values of σ , whereas BR is different (show by separate curves for $\sigma = 1, 2$ and 3 .) Both score functions are designed to result in an expected score, $E(S|w, \sigma)$, that peaks when $w = \sigma$, (*right*) indicated by the dashed lines. The probability of success for a given width is the same regardless of score function (*middle*).

1. The distribution of the deviation of the sample mean of the cues from the true mean (which we will call the *stimulus uncertainty*)
2. The uncertainty of the cues as they are perceived by the subjects (which we will call the *subjective uncertainty*)
3. The distribution of behavioural responses that are exhibited by the subject (which we will call the *objective uncertainty*)

Essentially these can be considered as three steps of the perceptual pipeline: the stimulus, sensory perception of the stimulus and the behavioural response. As each of these stages adds its own level of noise, we are interested to ask: which statistical information is used by subjects to form their estimate of their confidence in their decision? [Obviously they do not have access to the true *stimulus uncertainty*].

In the task our choice of σ determines the target towards which subjects aim. One could argue that this should therefore be set to the stimulus uncertainty, as this captures the best possible performance an ideal-observer might achieve. However, in practice this level of performance is particularly difficult to achieve - especially since this uncertainty approaches zero as the number of cues increases. In the interest of keeping subjects motivated, we decided that the target should be based on the objective uncertainty (obtained during independent training trails, see chapter 4).

Bibliography

- M. M. Adamczyk and P. E. Crago. Input-output nonlinearities and time delays increase tracking errors in hand grasp neuroprostheses. *Rehabilitation Engineering, IEEE Transactions on*, 4(4):271–279, dec 1996. ISSN 1063-6528.
- A. U. Alahakone and S. M. N. A. Senanayake. Vibrotactile feedback systems: Current trends in rehabilitation, sports and information display. In *Proc. IEEE/ASME Int. Conf. Advanced Intelligent Mechatronics AIM 2009*, pages 1148–1153, 2009.
- D. Alais and D. Burr. The ventriloquist effect results from near-optimal bimodal integration. *Curr Biol*, 14(3):257–262, Feb 2004.
- D. P. Allen, J. R. Playfer, N. M. Aly, P. Duffey, A. Heald, S. L. Smith, and D. M. Halliday. On the use of low-cost computer peripherals for the assessment of motor dysfunction in parkinson’s disease - quantification of bradykinesia using target tracking tasks. *Neural Systems and Rehabilitation Engineering, IEEE Transactions on*, 15(2):286–294, june 2007. ISSN 1534-4320.
- C. Almström, A. Anani, P. Herberts, and L. Körner. Electrical stimulation and myoelectric control. a theoretical and applied study relevant to prosthesis sensory feedback. *Med Biol Eng Comput*, 19(5):645–653, Sep 1981.
- T. J. Anastasio, P. E. Patton, and K. Belkacem-Boussaid. Using bayes’ rule to model multisensory enhancement in the superior colliculus. *Neural Comput*, 12(5):1165–1187, May 2000.
- D. E. Angelaki, Yong Gu, and G. C. DeAngelis. Multisensory integration: psychophysics, neurophysiology, and computation. *Curr Opin Neurobiol*, 19(4):452–458, Aug 2009.
- A. H. Arieta, H. Yokoi, T. Arai, and Wenwei Yu. Fes as biofeedback for an emg controlled prosthetic hand. In *Tencon ’05 - IEEE Region 10 Conference*, Melbourne, Australia, November 2005.

- A. H. Arieta, H. Yokoi, T. Ohnishi, and T. Arai. An f-mri study of an emg prosthetic hand biofeedback system. In *IAS*, pages 921–929, 2006.
- L. Ascari, U. Bertocchi, P. Corradi, C. Laschi, and P. Dario. Bio-inspired grasp control in a robotic hand with massive sensorial input. *Biological cybernetics*, 100(2):109–128, February 2009. ISSN 1432-0770.
- F. Asseman, A. M. Bronstein, and M. A. Gresty. Guidance of visual direction by topographical vibrotactile cues on the torso. *Exp Brain Res*, 186(2):283–292, Mar 2008.
- A. S. Augurelle, A. M. Smith, T. Lejeune, and J. L Thonnard. Importance of cutaneous feedback in maintaining a secure grip during manipulation of hand-held objects. *J Neurophysiol*, 89(2):665–671, Feb 2003.
- R. J. Baddeley, H. A. Ingram, and R. C. Miall. System identification applied to a visuo-motor task: near-optimal human performance in a noisy changing task. *J Neurosci*, 23(7):3066–3075, Apr 2003.
- A. M. Bagley, F. Molitor, L. V. Wagner, W. Tomhave, and Michelle A. James. The unilateral below elbow test: a function test for children with unilateral congenital below elbow deficiency. *Dev Med Child Neurol*, 48(7):569–575, Jul 2006.
- M. J. Barber, J. W. Clark, and C. H. Anderson. Neural representation of probabilistic information. *Neural Comput*, 15(8):1843–1864, Aug 2003.
- K. Bark, J. W. Wheeler, S. Premakumar, and M. R. Cutkosky. Comparison of skin stretch and vibrotactile stimulation for feedback of proprioceptive information. In *Proc. symposium on Haptic interfaces for virtual environment and teleoperator systems haptics 2008*, pages 71–78, 2008.
- S. Barthelmé and P. Mamassian. Evaluation of objective uncertainty in the visual system. *PLoS Comput Biol*, 5(9):e1000504, Sep 2009.
- S. Barthelmé and P. Mamassian. Flexible mechanisms underlie the evaluation of visual confidence. *Proc Natl Acad Sci U S A*, 107(48):20834–20839, Nov 2010.
- P. W. Battaglia, R. A. Jacobs, and R. N. Aslin. Bayesian integration of visual and auditory signals for spatial localization. *J Opt Soc Am A Opt Image Sci Vis*, 20(7):1391–1397, Jul 2003.
- P. M. Bays and D. M. Wolpert. Computational principles of sensorimotor control that minimize uncertainty and variability. *J Physiol*, 578(Pt 2):387–396, Jan 2007.

- T. W. Beeker, J. During, and A. Den Hertog. Artificial touch in a hand-prosthesis. *Med Biol Eng*, 5(1):47–49, Jan 1967.
- H. Beppu, M. Suda, and R. Tanaka. Analysis of cerebellar motor disorders by visually-guided elbow tracking movement. *Brain*, 107(3):787–809, 1984.
- H. Beppu, M. Nagaoka, and R. Tanaka. Analysis of cerebellar motor disorders by visually-guided elbow tracking movement. 2. contribution of the visual cues on slow ramp pursuit. *Brain*, 110 (Pt 1):1–18, Feb 1987.
- N. Bhushan and R. Shadmehr. Computational nature of human adaptive control during learning of reaching movements in force fields. *Biol Cybern*, 81(1):39–60, Jul 1999.
- S. Bitzer and P. van der Smagt. Learning emg control of a robotic hand: towards active prostheses. In *Proc. IEEE Int. Conf. Robotics and Automation ICRA 2006*, pages 2819–2823, 2006.
- C. A. Bloxham, T. A. Mindel, and C. D. Frith. Initiation and execution of predictable and unpredictable movements in parkinson’s disease. *Brain*, 107 (Pt 2):371–384, Jun 1984.
- M. Botvinick and J. Cohen. Rubber hands ‘feel’ touch that eyes see. *Nature*, 391(6669):756, Feb 1998.
- P. Boulinguez and J. Rouhana. Flexibility and individual differences in visuo-proprioceptive integration: evidence from the analysis of a morphokinetic control task. *Exp Brain Res*, 185(1):137–149, Feb 2008.
- R. G. Brown and P. Y. C. Hwang. *Introduction to Random Signals and Applied Kalman Filterin*. John Wiley and Sons, Inc., 1992.
- G. Buckingham, N. S. Ranger, and M. A. Goodale. The role of vision in detecting and correcting fingertip force errors during object lifting. *J Vis*, 11(1):4, 2011.
- D. G. Buma, J. R. Buitenweg, and P. H. Veltink. Intermittent stimulation delays adaptation to electrocutaneous sensory feedback. *IEEE Trans Neural Syst Rehabil Eng*, 15(3):435–441, 2007.
- J. Burge, M. O. Ernst, and M. S. Banks. The statistical determinants of adaptation rate in human reaching. *J Vis*, 8(4):20.1–20.19, 2008.
- D. Burr, M. S. Banks, and M. C. Morrone. Auditory dominance over vision in the perception of interval duration. *Exp Brain Res*, 198(1):49–57, Sep 2009.

- M. C. Carrozza, G. Cappiello, S. Micera, B. B. Edin, L. Beccai, and C. Cipriani. Design of a cybernetic hand for perception and action. *Biol Cybern*, 95(6):629–644, Dec 2006.
- C. Castellini, E. Gruppioni, A. Davalli, and G. Sandini. Fine detection of grasp force and posture by amputees via surface electromyography. *J Physiol Paris*, 103(3-5):255–262, 2009.
- Jongeeun Cha, L. Rahal, and A. El Saddik. A pilot study on simulating continuous sensation with two vibrating motors. In *Proc. IEEE International Workshop on Haptic Audio visual Environments and Games HAVE 2008*, pages 143–147, 2008.
- C. E. Chapman, F. Tremblay, W. Jiang, L. Belingard, and E. M. Meftah. Central neural mechanisms contributing to the perception of tactile roughness. *Behav Brain Res*, 135(1-2):225–233, Sep 2002.
- A. Chatterjee, V. Aggarwal, A. Ramos, S. Acharya, and N. V. Thakor. A brain-computer interface with vibrotactile biofeedback for haptic information. *J Neuroeng Rehabil*, 4:40, 2007.
- A. Chatterjee, P. Chaubey, J. Martin, and N. V. Thakor. Quantifying prosthesis control improvements using a vibrotactile representation of grip force. In *Region 5 Conference, 2008 IEEE*, pages 1–5, 2008.
- R. W. Cholewiak. The perception of tactile distance: influences of body site, space, and time. *Perception*, 28(7):851–875, 1999.
- R. W. Cholewiak and A. A. Collins. The generation of vibrotactile patterns on a linear array: influences of body site, time, and presentation mode. *Percept Psychophys*, 62(6):1220–1235, Aug 2000.
- R. W. Cholewiak and A. A. Collins. Vibrotactile localization on the arm: effects of place, space, and age. *Percept Psychophys*, 65(7):1058–1077, Oct 2003.
- R. W. Cholewiak, J. C. Brill, and A. Schwab. Vibrotactile localization on the abdomen: effects of place and space. *Percept Psychophys*, 66(6):970–987, Aug 2004.
- F. Cincotti, L. Kauhanen, F. Aloise, T. Palomäki, N. Caporusso, P. Jylänki, D. Mattia, F. Babiloni, G. Vanacker, M. Nuttin, M. G. Marciani, and J. D. R. Millan. Vibrotactile feedback for brain-computer interface operation. *Comput Intell Neurosci*, page 48937, 2007.
- F. Cincotti, L. Kauhanen, F. Aloise, T. Palomaki, N. Caporusso, P. Jylänki, F. Babiloni, G. Vanacker, M. Nuttin, M. G. Marciani, J. D. R. Millan, and D. Mattia. Preliminary

- experimentation on vibrotactile feedback in the context of mu-rhythm based bci. *Conf Proc IEEE Eng Med Biol Soc*, 2007:4739–4742, 2007a.
- C. Cipriani, F. Zacccone, S. Micera, and M. C. Carrozza. On the shared control of an emg-controlled prosthetic hand: Analysis of user-prosthesis interaction. *IEEE Transactions on Robotics*, 24(1):170–184, 2008. ISSN 1552-3098.
- C. Cipriani, C. Antfolk, C. Balkenius, B. Rosén, G. Lundborg, M. C. Carrozza, and F. Sebelius. A novel concept for a prosthetic hand with a bidirectional interface: a feasibility study. *IEEE Trans Biomed Eng*, 56(11 Pt 2):2739–2743, Nov 2009.
- J. D. Cole and E. M. Sedgwick. The perceptions of force and of movement in a man without large myelinated sensory afferents below the neck. *J Physiol*, 449:503–515, Apr 1992.
- T. F. Coleman and Y. Li. On the convergence of reflective newton methods for large-scale nonlinear minimization subject to bounds. *Mathematical Programming*, 67(2):189–224, 1994.
- T. F. Coleman and Y. Li. An interior, trust region approach for nonlinear minimization subject to bounds. *SIAM Journal on Optimization*, 6:418–445, 1996.
- M. Costantini and P. Haggard. The rubber hand illusion: sensitivity and reference frame for body ownership. *Conscious Cogn*, 16(2):229–240, Jun 2007.
- P. R. Davidson, R. D. Jones, H. R. Sirisena, and J. H. Andrae. Detection of adaptive inverse models in the human motor system. *Human Movement Science*, 19(5):761–795, 2000. ISSN 0167-9457.
- P. R. Davidson, R. D. Jones, J. H. Andrae, and H. R. Sirisena. Simulating closed- and open-loop voluntary movement: a nonlinear control-systems approach. *Biomedical Engineering, IEEE Transactions on*, 49(11):1242–1252, nov. 2002. ISSN 0018-9294.
- B. L. Day, J. P. Dick, and C. D. Marsden. Patients with parkinson’s disease can employ a predictive motor strategy. *J Neurol Neurosurg Psychiatry*, 47(12):1299–1306, Dec 1984.
- S. Deneve and A. Pouget. Bayesian multisensory integration and cross-modal spatial links. *J Physiol Paris*, 98(1-3):249–258, 2004.
- S. Deneve, P. E. Latham, and A. Pouget. Reading population codes: a neural implementation of ideal observers. *Nat Neurosci*, 2(8):740–745, Aug 1999.

- S. Deneve, P. E. Latham, and A. Pouget. Efficient computation and cue integration with noisy population codes. *Nat Neurosci*, 4(8):826–831, Aug 2001.
- Dermatology.co.uk. Keratosis.
- G. S. Dhillon and K. W. Horch. Direct neural sensory feedback and control of a prosthetic arm. *IEEE Trans Neural Syst Rehabil Eng*, 13(4):468–472, Dec 2005.
- S. Dosen, C. Cipriani, M. Kostić, M Controzzi, M C Carrozza, and D B Popović. Cognitive vision system for control of dexterous prosthetic hands: experimental evaluation. *Journal of neuroengineering and rehabilitation*, 7(1):42+, 2010. ISSN 1743-0003.
- H. Dostmohamed and V. Hayward. Trajectory of contact region on the fingerpad gives the illusion of haptic shape. *Exp Brain Res*, 164(3):387–394, Jul 2005.
- J. A. Doubler and D. S. Childress. An analysis of extended physiological proprioception as a prosthesis-control technique. *J Rehabil Res Dev*, 21(1):5–18, May 1984.
- J. Duchêne and F. Goubel. Surface electromyogram during voluntary contraction: processing tools and relation to physiological events. *Crit Rev Biomed Eng*, 21(4):313–397, 1993.
- B. B. Edin, L. Beccai, L. Ascari, S. Roccella, J. J. Cabibihan, and M. C. Carrozza. Bio-inspired approach for the design and characterization of a tactile sensory system for a cybernetic prosthetic hand. In *Robotics and Automation, 2006. ICRA 2006. Proceedings 2006 IEEE International Conference on*, pages 1354–1358, May 2006.
- B. B. Edin, L. Ascari, L. Beccai, S. Roccella, J-J. Cabibihan, and M. C. Carrozza. Bio-inspired sensorization of a biomechatronic robot hand for the grasp-and-lift task. *Brain Res Bull*, 75(6):785–795, Apr 2008.
- H. H. Ehrsson, C. Spence, and R. E. Passingham. That’s my hand! activity in premotor cortex reflects feeling of ownership of a limb. *Science*, 305(5685):875–877, Aug 2004.
- H. H. Ehrsson, B. Rosén, A. Stocksélius, C. Ragnö, P. Köhler, and G. Lundborg. Upper limb amputees can be induced to experience a rubber hand as their own. *Brain*, 131 (Pt 12):3443–3452, Dec 2008.
- E. D. Engeberg and S. Meek. Improved grasp group force sensitivity for prosthetic hands through force derivative feedback. *IEEE transactions on bio-medical engineering*, June 2008. ISSN 1558-2531.
- M. O. Ernst. *A Bayesian view on multimodal cue integration.*, chapter Chapter 6, pages 105–131. Oxford University Press, New York, NY, USA, 2006.

- M. O. Ernst. Multisensory integration: A late bloomer. *Current Biology*, 18(12):R519 – R521, 2008. ISSN 0960-9822.
- M. O. Ernst and M. S. Banks. Humans integrate visual and haptic information in a statistically optimal fashion. *Nature*, 415(6870):429–433, Jan 2002.
- M. O. Ernst and H. H. Bühlhoff. Merging the senses into a robust percept. *Trends Cogn Sci*, 8(4):162–169, Apr 2004.
- A. A. Faisal and D. M. Wolpert. Near optimal combination of sensory and motor uncertainty in time during a naturalistic perception-action task. *J Neurophysiol*, 101(4):1901–1912, Apr 2009.
- J. R. Flanagan and A. M. Wing. The role of internal models in motion planning and control: evidence from grip force adjustments during movements of hand-held loads. *J Neurosci*, 17(4):1519–1528, Feb 1997.
- J. R. Flanagan, S. King, D. M. Wolpert, and R. S. Johansson. Sensorimotor prediction and memory in object manipulation. *Can J Exp Psychol*, 55(2):87–95, Jun 2001.
- J. R. Flanagan, P. Vetter, R. S. Johansson, and Daniel M. Wolpert. Prediction precedes control in motor learning. *Curr Biol*, 13(2):146–150, Jan 2003.
- J. R. Flanagan, J. P. Bittner, and R. S. Johansson. Experience can change distinct size-weight priors engaged in lifting objects and judging their weights. *Curr Biol*, 18(22):1742–1747, Nov 2008.
- A. E. Flatt. Grasp. *Proceedings (Baylor University. Medical Center)*, 13(4):343–8, October 2000. ISSN 0899-8280.
- M. Fleury, C. Bard, N. Teasdale, J. Paillard, J. Cole, Y. Lajoie, and Y. Lamarre. Weight judgment. the discrimination capacity of a deafferented subject. *Brain*, 118 (Pt 5): 1149–1156, Oct 1995.
- H. Flor, T. Elbert, S. Knecht, C. Wienbruch, C. Pantev, N. Birbaumer, W. Larbig, and E. Taub. Phantom-limb pain as a perceptual correlate of cortical reorganization following arm amputation. *Nature*, 375(6531):482–484, Jun 1995.
- A. J. Foulkes and R. C. Miall. Adaptation to visual feedback delays in a human manual tracking task. *Experimental Brain Research*, 131:101–110, 2000. ISSN 0014-4819. 10.1007/s002219900286.
- G. J. Gage, K. A. Ludwig, K. J. Otto, E. L. Ionides, and D. R. Kipke. Naive coadaptive cortical control. *Journal of Neural Engineering*, 2(2):52, 2005.

- Z. Gahahramani, D. M. Wolpert, and M. I. Jordan. *Self Organization, Computational Maps and Motor Control*, chapter Computational models of sensorimotor integration, pages 117–147. 1997.
- M. A. García-Pérez. Forced-choice staircases with fixed step sizes: asymptotic and small-sample properties. *Vision Res*, 38(12):1861–1881, Jun 1998.
- S. Gepshtein and M. S. Banks. Viewing geometry determines how vision and haptics combine in size perception. *Curr Biol*, 13(6):483–488, Mar 2003.
- S. Gepshtein, J. Burge, M. O. Ernst, and M. S. Banks. The combination of vision and touch depends on spatial proximity. *J Vis*, 5(11):1013–1023, 2005.
- J. I. Gold and M. N. Shadlen. The neural basis of decision making. *Annu Rev Neurosci*, 30:535–574, 2007.
- C. Gomersall. Cutaneous vasculitis, February 2008a.
- C. Gomersall. Erythema multiforme, February 2008b.
- A. W. Goodwin and H. E. Wheat. Sensory signals in neural populations underlying tactile perception and manipulation. *Annu Rev Neurosci*, 27:53–77, 2004.
- A. M. Gordon, H. Forssberg, R. S. Johansson, and G. Westling. Visual size cues in the programming of manipulative forces during precision grip. *Exp Brain Res*, 83(3):477–482, 1991.
- M. Gori, M. D. Viva, G. Sandini, and D. C. Burr. Young children do not integrate visual and haptic form information. *Current Biology*, 18(9):694–698, 2008. ISSN 0960-9822.
- E. W. Graf, P. A. Warren, and L. T. Maloney. Explicit estimation of visual uncertainty in human motion processing. *Vision Res*, 45(24):3050–3059, Nov 2005.
- H. B. Helbig and M. O. Ernst. Optimal integration of shape information from vision and touch. *Exp Brain Res*, 179(4):595–606, Jun 2007.
- H. B. Helbig and M. O. Ernst. Visual-haptic cue weighting is independent of modality-specific attention. *J Vis*, 8(1):21.1–2116, 2008.
- J. Hermsdörfer, E. Hagl, and D. A. Nowak. Deficits of anticipatory grip force control after damage to peripheral and central sensorimotor systems. *Hum Mov Sci*, 23(5):643–662, Nov 2004.

- J. Hermsdörfer, Z. Elias, J. D. Cole, B. M. Quaney, and D. A. Nowak. Preserved and impaired aspects of feed-forward grip force control after chronic somatosensory deafferentation. *Neurorehabil Neural Repair*, 22(4):374–384, 2008.
- J. Heron, D. Whitaker, and P. V. McGraw. Sensory uncertainty governs the extent of audio-visual interaction. *Vision Res*, 44(25):2875–2884, Nov 2004.
- J. M. Hillis, M. O. Ernst, M. S. Banks, and M. S. Landy. Combining sensory information: mandatory fusion within, but not between, senses. *Science*, 298(5598):1627–1630, Nov 2002.
- J. M. Hillis, S. J. Watt, M. S. Landy, and M. S. Banks. Slant from texture and disparity cues: optimal cue combination. *J Vis*, 4(12):967–992, Dec 2004.
- A. E. Hines, N. E. Owens, and P. E. Crago. Assessment of input-output properties and control of neuroprosthetic hand grasp. *Biomedical Engineering, IEEE Transactions on*, 39(6):610–623, june 1992. ISSN 0018-9294.
- N. P. Holmes and C. Spence. Multisensory integration: Space, time and superadditivity. *Current Biology*, 15(18):R762 – R764, 2005. ISSN 0960-9822.
- T. Hospedales and S. Vijayakumar. Multisensory oddity detection as bayesian inference. *PLoS One*, 4(1):e4205, 2009.
- R. D. Howe and M. R. Cutkosky. Dynamic tactile sensing: perception of fine surface features with stress rate sensing. *Robotics and Automation, IEEE Transactions on*, 9(2):140–151, 1993.
- P. O. Hoyer and A. Hyvärinen. Interpreting neural response variability as monte carlo sampling of the posterior. In Klaus Obermayer Suzanna Becker, Sebastian Thrun, editor, *Advances in Neural Information Processing Systems 15: Proceedings of the 2002 Neural Information Processing Systems Conference*. The MIT Press, 2002.
- S. S. Hsiao, J. Lane, and P. Fitzgerald. Representation of orientation in the somatosensory system. *Behav Brain Res*, 135(1-2):93–103, Sep 2002.
- S. D. Humbert, S. A. Snyder, and W. M. Grill. Evaluation of command algorithms for control of upper-extremity neural prostheses. *IEEE Trans Neural Syst Rehabil Eng*, 10(2):94–101, Jun 2002.
- V. Iyengar, M. J. Santos, M. Ko, and A. S. Aruin. Grip force control in individuals with multiple sclerosis. *Neurorehabil Neural Repair*, 23(8):855–861, Oct 2009.

- J. Izawa and R. Shadmehr. On-line processing of uncertain information in visuomotor control. *J Neurosci*, 28(44):11360–11368, Oct 2008.
- C. E. Jack and W. R. Thurlow. Effects of degree of visual association and angle of displacement on the "ventriloquism" effect. *Percept Mot Skills*, 37(3):967–979, Dec 1973.
- R. A. Jacobs. Optimal integration of texture and motion cues to depth. *Vision Res*, 39(21):3621–3629, Oct 1999.
- R. A. Jacobs. What determines visual cue reliability? *Trends Cogn Sci*, 6(8):345–350, Aug 2002.
- N. Jain, Hui-Xin Qi, C. E. Collins, and J. H. Kaas. Large-scale reorganization in the somatosensory cortex and thalamus after sensory loss in macaque monkeys. *J Neurosci*, 28(43):11042–11060, Oct 2008.
- P. Jenmalm and R. S. Johansson. Visual and somatosensory information about object shape control manipulative fingertip forces. *J Neurosci*, 17(11):4486–4499, Jun 1997.
- P. Jenmalm, S. Dahlstedt, and R. S. Johansson. Visual and tactile information about object-curvature control fingertip forces and grasp kinematics in human dexterous manipulation. *J Neurophysiol*, 84(6):2984–2997, Dec 2000.
- Li Jiang, M. R. Cutkosky, J. Ruutinen, and R. Raisamo. Using haptic feedback to improve grasp force control in multiple sclerosis patients. *IEEE Transactions on Robotics*, 25(3):593–601, 2009.
- R. S. Johansson. Dynamic use of tactile afferent signals in control of dexterous manipulation. *Adv Exp Med Biol*, 508:397–410, 2002.
- R. S. Johansson and G. Westling. Roles of glabrous skin receptors and sensorimotor memory in automatic control of precision grip when lifting rougher or more slippery objects. *Exp Brain Res*, 56(3):550–564, 1984.
- R. S. Johansson and G. Westling. *Somatosensory Mechanisms*, chapter Influences of Cutaneous Sensory Input on the Motor Coordination During Precision Manipulation, pages 249–258. MacMillan, 1984a.
- K. O. Johnson. The roles and functions of cutaneous mechanoreceptors. *Curr Opin Neurobiol*, 11(4):455–461, Aug 2001.
- N. L. Johnson, S. Kotz, and N. Balakrishnan. *Continuous Univariate Distributions*. New York: J. Wiley, 1995.

- E. B. Johnston, B. G. Cumming, and M. S. Landy. Integration of stereopsis and motion shape cues. *Vision Res*, 34(17):2259–2275, Sep 1994.
- R. D. Jones and I. M. Donaldson. Measurement of sensory-motor integrated function in neurological disorders: three computerised tracking tasks. *Med Biol Eng Comput*, 24(5):536–540, Sep 1986.
- M. I. Jordan and D. M. Wolpert. Computational motor control. *The Cognitive Neurosciences*, 601, 1999.
- V. Jousmäki and R. Hari. Parchment-skin illusion: sound-biased touch. *Curr Biol*, 8(6):R190, Mar 1998.
- K. A. Kaczmarek, J. G. Webster, P. Bach-y Rita, and W. J. Tompkins. Electrotactile and vibrotactile displays for sensory substitution systems. *IEEE Transactions on Biomedical Engineering*, 38(1):1–16, 1991. ISSN 0018-9294.
- K. A. Kaczmarek, K. M. Kramer, J. G. Webster, and R. G. Radwin. A 16-channel 8-parameter waveform electrotactile stimulation system. *IEEE Trans Biomed Eng*, 38(10):933–943, 1991a.
- P. P. Kadhade, B. J. Benda, P. B. Schmidt, and C. Wall. Vibrotactile display coding for a balance prosthesis. *IEEE Trans Neural Syst Rehabil Eng*, 11(4):392–399, Dec 2003.
- R. E. Kalman. A new approach to linear filtering and prediction problems. *Transactions of the ASME—Journal of Basic Engineering*, 82(Series D):35–45, 1960.
- J. S. Kennedy, M. J. Buehner, and S. K. Rushton. Adaptation to sensory-motor temporal misalignment: instrumental or perceptual learning? *Q J Exp Psychol (Colchester)*, 62(3):453–469, Mar 2009.
- A. Kepecs, N. Uchida, H. A. Zariwala, and Z. F. Mainen. Neural correlates, computation and behavioural impact of decision confidence. *Nature*, 455(7210):227–231, Sep 2008.
- R. Kiani and M. N. Shadlen. Representation of confidence associated with a decision by neurons in the parietal cortex. *Science*, 324(5928):759–764, May 2009.
- G. Kim, Y. Asakura, R. Okuno, and K. Akazawa. Tactile substitution system for transmitting a few words to a prosthetic hand user. In *Proc. 27th Annual Int. Conf. of the Engineering in Medicine and Biology Society IEEE-EMBS 2005*, pages 6908–6911, 2005.

- D. C. Knill and J. A. Saunders. Do humans optimally integrate stereo and texture information for judgments of surface slant? *Vision Res*, 43(24):2539–2558, Nov 2003.
- L. Kohli, M. Niwa, H. Noma, K. Susami, Y. Yanagida, R. W. Lindeman, K. Hosaka, and Y. Kume. Towards effective information display using vibrotactile apparent motion. In *Proc. 14th Symp. Haptic Interfaces for Virtual Environment and Teleoperator Systems*, pages 445–451, 2006.
- K. P. Körding and D. M. Wolpert. Bayesian integration in sensorimotor learning. *Nature*, 427(6971):244–7, January 2004a. ISSN 1476-4687.
- K. P. Körding and D. M. Wolpert. The loss function of sensorimotor learning. *Proc Natl Acad Sci U S A*, 101(26):9839–9842, Jun 2004b.
- K. P. Körding and D. M. Wolpert. Bayesian decision theory in sensorimotor control. *Trends Cogn Sci*, 10(7):319–326, Jul 2006.
- K. P. Körding, Shih-pi Ku, and D. M. Wolpert. Bayesian integration in force estimation. *J Neurophysiol*, 92(5):3161–5, November 2004. ISSN 0022-3077.
- K. P. Körding, W. Beierholm, Wei Ji Ma, S. Quartz, J. B. Tenenbaum, and L. Shams. Causal inference in multisensory perception. *PLoS One*, 2(9):e943, 2007.
- T. A. Kuiken, G. A. Dumanian, R. D. Lipschutz, L. A. Miller, and K. A. Stubblefield. The use of targeted muscle reinnervation for improved myoelectric prosthesis control in a bilateral shoulder disarticulation amputee. *Prosthet Orthot Int*, 28(3):245–253, Dec 2004.
- A. D. Kuo. An optimal control model for analyzing human postural balance. *IEEE Trans Biomed Eng*, 42(1):87–101, Jan 1995.
- M. S. Landy and H. Kojima. Ideal cue combination for localizing texture-defined edges. *J Opt Soc Am A Opt Image Sci Vis*, 18(9):2307–2320, Sep 2001.
- M. S. Landy, L. T. Maloney, E. B. Johnston, and M. Young. Measurement and modeling of depth cue combination: in defense of weak fusion. *Vision Res*, 35(3):389–412, Feb 1995.
- C. L. Lawson and R. J. Hanson. *Solving least squares problems*. Prentice-Hall, 1974. ISBN 9780898713565.
- C. M. Light, P. H. Chappell, and P. J. Kyberd. Establishing a standardized clinical assessment tool of pathologic and prosthetic hand function: normative data, reliability, and validity. *Arch Phys Med Rehabil*, 83(6):776–783, Jun 2002.

- C. Long. Intrinsic-extrinsic muscle control of the fingers. electromyographic studies. *J Bone Joint Surg Am*, 50(5):973–984, Jul 1968.
- T. Lorrain, N. Jiang, and D. Farina. Surface emg classification during dynamic contractions for multifunction transradial prostheses. *Conf Proc IEEE Eng Med Biol Soc*, 1: 2766–2769, 2010.
- E. Magosso, C. Cuppini, A. Serino, G. D. Pellegrino, and M. Ursino. A theoretical study of multisensory integration in the superior colliculus by a neural network model. *Neural Networks*, 21(6):817–829, 2008. ISSN 0893-6080. Computational and Biological Inspired Neural Networks, selected papers from ICANN 2007, 17th International Conference on Artificial Neural Networks (ICANN).
- P. D. Marasco, K. Kim, J. E. Colgate, M. A. Peshkin, and T. A. Kuiken. Robotic touch shifts perception of embodiment to a prosthesis in targeted reinnervation amputees. *Brain*, Jan 2011.
- H. McGurk and J. MacDonald. Hearing lips and seeing voices. *Nature*, 264(5588): 746–748, 1976.
- S. G. Meek, S. C. Jacobsen, and P. P. Goulding. Extended physiologic taction: design and evaluation of a proportional force feedback system. *J Rehabil Res Dev*, 26(3): 53–62, 1989.
- M. A. Meredith and B. E. Stein. Interactions among converging sensory inputs in the superior colliculus. *Science*, 221(4608):389–391, Jul 1983.
- D. M. Merfeld, L. Zupan, and R. J. Peterka. Humans use internal models to estimate gravity and linear acceleration. *Nature*, 398(6728):615–618, Apr 1999.
- R. C. Miall and J. K. Jackson. Adaptation to visual feedback delays in manual tracking: evidence against the smith predictor model of human visually guided action. *Exp Brain Res*, 172(1):77–84, June 2006. ISSN 0014-4819.
- R. C. Miall, D. J. Weir, D. M. Wolpert, and J. F. Stein. Is the cerebellum a smith predictor? *J Mot Behav*, 25(3):203–216, Sep 1993.
- L. A. Miller, R. D. Lipschutz, K. A. Stubblefield, B. A. Lock, He Huang, T. W. Williams, R. F. Weir, and T. A. Kuiken. Control of a six degree of freedom prosthetic arm after targeted muscle reinnervation surgery. *Arch Phys Med Rehabil*, 89(11):2057–2065, Nov 2008.
- J. Monzée, Y. Lamarre, and A. M. Smith. The effects of digital anesthesia on force control using a precision grip. *J Neurophysiol*, 89(2):672–683, Feb 2003.

- E. M. Moraud. Statistical modelling of multisensory integration in the context of a prosthetic hand. *MSc Thesis in Artificial Intelligence, School of Informatics, University of Edinburgh*, 2009.
- M. L. Morgan, G. C. Deangelis, and D. E. Angelaki. Multisensory integration in macaque visual cortex depends on cue reliability. *Neuron*, 59(4):662–673, Aug 2008.
- B. J. P. Mortimer, G. A. Zets, and R. W. Cholewiak. Vibrotactile transduction and transducers. *J Acoust Soc Am*, 121(5 Pt1):2970–2977, May 2007.
- G. H. Mulliken, S. Musallam, and R. A. Andersen. Decoding trajectories from posterior parietal cortex ensembles. *J Neurosci*, 28(48):12913–12926, Nov 2008.
- M. R. Mulvey, H. J. Fawkner, H. Radford, and M. I. Johnson. The use of transcutaneous electrical nerve stimulation (tens) to aid perceptual embodiment of prosthetic limbs. *Medical hypotheses*, 72(2):140–142, February 2009. ISSN 0306-9877.
- D. A. Nowak and J. Hermsdörfer. Selective deficits of grip force control during object manipulation in patients with reduced sensibility of the grasping digits. *Neurosci Res*, 47(1):65–72, Sep 2003.
- D. A. Nowak, J. Hermsdörfer, S. Glasauer, J. Philipp, L. Meyer, and N. Mai. The effects of digital anaesthesia on predictive grip force adjustments during vertical movements of a grasped object. *Eur J Neurosci*, 14(4):756–762, Aug 2001.
- K. Okada, Gwan Kim, and Pyong Sik Pak. Sound information notification system by two-channel electrotactile stimulation for hearing impaired persons. In *Proc. 29th Annual Int. Conf. of the IEEE Engineering in Medicine and Biology Society EMBS 2007*, pages 3826–3829, 2007.
- I. Oruç, L. T. Maloney, and M. S. Landy. Weighted linear cue combination with possibly correlated error. *Vision Res*, 43(23):2451–2468, Oct 2003.
- O. V. D. N. V. Otr, H. A. Reinders-Messelink, R. M. Bongers, H. Bouwsema, and C. K. Van Der Sluis. The i-limb hand and the dmc plus hand compared: a case report. *Prosthetics and orthotics international*, 34(2):216–220, June 2010. ISSN 1746-1553.
- A. Panarese, B. B. Edin, F. Vecchi, M. C. Carrozza, and R. S. Johansson. Humans can integrate force feedback to toes in their sensorimotor control of a robotic hand. *IEEE Trans Neural Syst Rehabil Eng*, 17(6):560–567, Dec 2009.
- P. E. Patterson and J. A. Katz. Design and evaluation of a sensory feedback system that provides grasping pressure in a myoelectric hand. *J Rehabil Res Dev*, 29(1):1–8, 1992.

- M. Penta, J. L. Thonnard, and L. Tesio. Abilhand: a rasch-built measure of manual ability. *Arch Phys Med Rehabil*, 79(9):1038–1042, Sep 1998.
- C. A. Perez, C. Salinas, and A. Santibanez. Vibrotactile sensation thresholds related to parameters of a pulse burst stimulus. In *Proc. 22nd Annual International Conference of the IEEE Engineering in Medicine and Biology Society*, volume 2, pages 1570–1572 vol.2, 2000.
- C. Poirier, A. G. D. Volder, and C. Scheiber. What neuroimaging tells us about sensory substitution. *Neurosci Biobehav Rev*, 31(7):1064–1070, 2007.
- C. J. Poletto and C. L. Van Doren. A high voltage, constant current stimulator for electrocutaneous stimulation through small electrodes. *IEEE Trans Biomed Eng*, 46(8):929–936, Aug 1999.
- H. Pongrac. Vibrotactile perception: Differential effects of frequency, amplitude, and acceleration. In *Proc. IEEE Int. Workshop Haptic Audio Visual Environments and their Applications HAVE 2006*, pages 54–59, 2006.
- A. Pouget, P. Dayan, and R. Zemel. Information processing with population codes. *Nat Rev Neurosci*, 1(2):125–132, Nov 2000.
- C. Pylatiuk, S. Mounier, A. Kargov, S. Schulz, and G. Bretthauer. Progress in the development of a multifunctional hand prosthesis. In *Proc. 26th Annual Int. Conf. of the IEEE Engineering in Medicine and Biology Society IEMBS '04*, volume 2, pages 4260–4263, 2004.
- L. Rahal, J. Cha, A. El Saddik, J. Kammerl, and E. Steinbach. Investigating the influence of temporal intensity changes on apparent movement phenomenon. In *Proc. IEEE International Conference on Virtual Environments, Human-Computer Interfaces and Measurements Systems VECIMS '09*, pages 310–313, 2009.
- V. S. Ramachandran, M. Stewart, and D. C. Rogers-Ramachandran. Perceptual correlates of massive cortical reorganization. *Neuroreport*, 3(7):583–586, Jul 1992.
- A. Resulaj, R. Kiani, D. M. Wolpert, and M. N. Shadlen. Changes of mind in decision-making. *Nature*, 461(7261):263–266, Sep 2009.
- R. R. Riso, A. R. Ignagni, and M. W. Keith. Cognitive feedback for use with fes upper extremity neuroprostheses. *IEEE Trans Biomed Eng*, 38(1):29–38, Jan 1991.
- G. Robles-De-La-Torre and V. Hayward. Force can overcome object geometry in the perception of shape through active touch. *Nature*, 412(6845):445–448, Jul 2001.

- I. Rock and J. Victor. Vision and touch: an experimentally created conflict between the two senses. *Science*, 143:594–596, Feb 1964.
- J. M. Romano, S. R. Gray, N. T. Jacobs, and K. J. Kuchenbecker. Toward tactilely transparent gloves: Collocated slip sensing and vibrotactile actuation. In *Proc. and Symposium on Haptic Interfaces for Virtual Environment and Teleoperator Systems EuroHaptics conference World Haptics 2009. Third Joint*, pages 279–284, 2009.
- P. Rosas, J. Wagemans, M. O. Ernst, and F. A. Wichmann. Texture and haptic cues in slant discrimination: reliability-based cue weighting without statistically optimal cue combination. *J Opt Soc Am A Opt Image Sci Vis*, 22(5):801–809, May 2005.
- B. Rosén, H. H. Ehrsson, C. Antfolk, C. Cipriani, F. Sebelius, and G. Lundborg. Referral of sensation to an advanced humanoid robotic hand prosthesis. *Scandinavian journal of plastic and reconstructive surgery and hand surgery / Nordisk plastikkirurgisk forening [and] Nordisk klubb for handkirurgi*, 43(5):260–266, 2009. ISSN 1651-2073.
- D. D. Rossi. Artificial tactile sensing and haptic perception. *Measurement Science and Technology*, 2(11):1003–1016, 1991.
- N. A. Sachs and G. E. Loeb. Development of a bionic muscle spindle for prosthetic proprioception. *IEEE Trans Biomed Eng*, 54(6 Pt 1):1031–1041, Jun 2007.
- D. Säfström and B. B. Edin. Short-term plasticity of the visuomotor map during grasping movements in humans. *Learn Mem*, 12(1):67–74, 2005. ISSN 1072-0502.
- E. Sampaio, S. Maris, and P. Bach y Rita. Brain plasticity: ‘visual’ acuity of blind persons via the tongue. *Brain Res*, 908(2):204–207, Jul 2001.
- I. Saunders and S. Vijayakumar. A closed-loop prosthetic hand: The development of a novel manipulandum for understanding sensorimotor learning. *Technical Report, EDI-INF-RR-1321*, Mar 2009.
- I. Saunders and S. Vijayakumar. A closed-loop prosthetic hand. *Proc. Key Issues in Sensory Augmentation*, 2009a.
- I. Saunders and S. Vijayakumar. A closed-loop prosthetic hand as a model sensorimotor circuit. *Proc. International Workshop on Computational Principles of Sensorimotor Learning*, 2009b.
- I. Saunders and S. Vijayakumar. The role of feed-forward and feedback processes for closed-loop prosthesis control. *Journal of Neuroengineering and Rehabilitation*, 2011.

- I. Saunders and S. Vijayakumar. Continuous estimation of mean and uncertainty. *Proc. The 21st Annual Conference of the Japanese Neural Network Society*, 2011b.
- I. Saunders and S. Vijayakumar. Continuous evolution of statistical estimators for optimal decision-making. *PLoS ONE*, 2012.
- I. Saunders, S. Vijayakumar, Hugh Gill: The University Court of the University of Edinburgh, and Touch Emas Ltd. Improvements in or relating to prosthetics and orthotics. *GB Patent Application - Category P120168.GB.01*, 2011a.
- J. A. Saunders and D. C. Knill. Visual feedback control of hand movements. *J Neurosci*, 24(13):3223–3234, Mar 2004.
- W. D. Schot, E. Brenner, and J. B. J. Smeets. Grasping and hitting moving objects. *Exp Brain Res*, 212(4):487–496, Aug 2011. doi: 10.1007/s00221-011-2756-2.
- R. N. Scott, R. H. Brittain, R. R. Caldwell, A. B. Cameron, and V. A. Dunfield. Sensory-feedback system compatible with myoelectric control. *Med Biol Eng Comput*, 18(1): 65–69, Jan 1980.
- R. Shadmehr and J. W. Krakauer. A computational neuroanatomy for motor control. *Exp Brain Res*, 185(3):359–381, Mar 2008.
- G. F. Shannon. A comparison of alternative means of providing sensory feedback on upper limb prostheses. *Med Biol Eng*, 14(3):289–94, May 1976. ISSN 0025-696X.
- G. F. Shannon. A myoelectrically-controlled prosthesis with sensory feedback. *Med Biol Eng Comput*, 17(1):73–80, Jan 1979b.
- G. F. Shannon and P. J. Agnew. Fitting below-elbow prostheses which convey a sense of touch. *Med J Aust*, 1(6):242–244, Mar 1979.
- S. Shimada, K. Fukuda, and K. Hiraki. Rubber hand illusion under delayed visual feedback. *PLoS One*, 4(7):e6185, 2009.
- K. H. Sienko, M. D. Balkwill, L. I. E. Oddsson, and C. Wall. Effects of multi-directional vibrotactile feedback on vestibular-deficient postural performance during continuous multi-directional support surface perturbations. *J Vestib Res*, 18(5-6):273–285, 2008.
- S. J. Sober and P. N. Sabes. Flexible strategies for sensory integration during motor planning. *Nat Neurosci*, 8(4):490–497, Apr 2005.
- M. Solomonow and J. Lyman. Artificial sensory communications via the tactile sense: space and frequency optimal displays. *Ann Biomed Eng*, 5(3):273–86, September 1977. ISSN 0090-6964.

- S. Soto-Faraco and G. Deco. Multisensory contributions to the perception of vibrotactile events. *Behavioural Brain Research*, 196(2):145–154, 2009. ISSN 0166-4328.
- C. Spence, F. Pavani, and J. Driver. Spatial constraints on visual-tactile cross-modal distractor congruency effects. *Cogn Affect Behav Neurosci*, 4(2):148–169, Jun 2004.
- M. A. Srinivasan and R. H. LaMotte. Tactual discrimination of softness. *J Neurophysiol*, 73(1):88–101, Jan 1995.
- C. E. Stepp and Y. Matsuoka. Relative to direct haptic feedback, remote vibrotactile feedback improves but slows object manipulation. *Conf Proc IEEE Eng Med Biol Soc*, 2010:2089–2092, 2010.
- A. Szeto. Electrocutaneous code pairs for artificial sensory communication systems. *Annals of Biomedical Engineering*, 10:175–192, 1982. ISSN 0090-6964. 10.1007/BF02367389.
- A. Szeto and Yee-Ming Chung. Effects of training on human tracking of electrocutaneous signals. *Annals of Biomedical Engineering*, 14:369–381, 1986. ISSN 0090-6964. 10.1007/BF02367409.
- A. Szeto and J. Lyman. Comparison of codes for sensory feedback using electrocutaneous tracking. *Annals of Biomedical Engineering*, 5:367–383, 1977. ISSN 0090-6964. 10.1007/BF02367316.
- A. Y. Szeto and G. R. Farrenkopf. Optimization of single electrode tactile codes. *Ann Biomed Eng*, 20(6):647–65, 1992. ISSN 0090-6964.
- A. Y. Szeto and R. R. Riso. "Sensory Feedback using Electrical Stimulation of the Tactile Sense" in *Rehabilitation Engineering*, pages 29–78. CRC Press, 1990.
- A. Y. Szeto and F. A. Saunders. Electrocutaneous stimulation for sensory communication in rehabilitation engineering. *IEEE Trans Biomed Eng*, 29(4):300–8, April 1982. ISSN 0018-9294.
- A. Y. J. Szeto, R. E. Prior, and J. Lyman. Electrocutaneous tracking: A methodology for evaluating sensory feedback codes. *Biomedical Engineering, IEEE Transactions on*, BME-26(1):47–49, jan. 1979. ISSN 0018-9294.
- A. Tajadura-Jiménez, N. Kitagawa, A. Väljamäe, M. Zampini, M. M. Murray, and C. Spence. Auditory-somatosensory multisensory interactions are spatially modulated by stimulated body surface and acoustic spectra. *Neuropsychologia*, 47(1):195–203, Jan 2009.

- H. Tassinari, T. E. Hudson, and M. S. Landy. Combining priors and noisy visual cues in a rapid pointing task. *J Neurosci*, 26(40):10154–10163, Oct 2006.
- E. Taub, I. A. Goldberg, and P. Taub. Deafferentation in monkeys: pointing at a target without visual feedback. *Exp Neurol*, 46(1):178–86, January 1975. ISSN 0014-4886.
- F. Tenore, A. Ramos, A. Fahmy, S. Acharya, R. Etienne-Cummings, and N. V. Thakor. Towards the control of individual fingers of a prosthetic hand using surface emg signals. In *Proc. 29th Annual Int. Conf. of the IEEE Engineering in Medicine and Biology Society EMBS 2007*, pages 6145–6148, 2007.
- W. R. Thurlow and T. M. Rosenthal. Further study of existence regions for the "ventriloquism effect". *J Am Audiol Soc*, 1(6):280–286, 1976.
- A. Toney, L. Dunne, B. H. Thomas, and S. P. Ashdown. A shoulder pad insert vibrotactile display. *Wearable Computers, 2003. Proceedings. Seventh IEEE International Symposium on*, pages 35–44, Oct. 2003. ISSN 1530-0811.
- J. Trommershäuser, L. T. Maloney, and M. S. Landy. Statistical decision theory and the selection of rapid, goal-directed movements. *J Opt Soc Am A Opt Image Sci Vis*, 20(7):1419–1433, Jul 2003.
- M. Tyler, Y. Danilov, and P. Bach-Y-Rita. Closing an open-loop control system: vestibular substitution through the tongue. *J Integr Neurosci*, 2(2):159–164, Dec 2003.
- R. J. van Beers, A. C. Sittig, and J. J. Gon. Integration of proprioceptive and visual position-information: An experimentally supported model. *J Neurophysiol*, 81(3):1355–1364, Mar 1999.
- J. B. F. van Erp. Vibrotactile spatial acuity on the torso: effects of location and timing parameters. In *Proc. First Joint Eurohaptics Conf. and Symp. Haptic Interfaces for Virtual Environment and Teleoperator Systems World Haptics 2005*, pages 80–85, 2005.
- M. T. Wallace, G. E. Roberson, W. D. Hairston, B. E. Stein, J. W. Vaughan, and J. A. Schirillo. Unifying multisensory signals across time and space. *Exp Brain Res*, 158(2):252–258, Sep 2004.
- D. H. Warren, T. J. McCarthy, and R. B. Welch. Discrepancy and nondiscrepancy methods of assessing visual-auditory interaction. *Percept Psychophys*, 33(5):413–419, May 1983.

- D. L. Weeks, S. A. Wallace, and J. T. Noteboom. Precision-grip force changes in the anatomical and prosthetic limb during predictable load increases. *Exp Brain Res*, 132(3):404–410, Jun 2000.
- R. B. Welch, M. H. Widawski, J. Harrington, and D. H. Warren. An examination of the relationship between visual capture and prism adaptation. *Percept Psychophys*, 25(2):126–132, Feb 1979.
- R. B. Welch, L. D. DuttonHurt, and D. H. Warren. Contributions of audition and vision to temporal rate perception. *Percept Psychophys*, 39(4):294–300, Apr 1986.
- G. Westling and R. S. Johansson. Factors influencing the force control during precision grip. *Exp Brain Res*, 53(2):277–284, 1984.
- H. E. Wheat and A. W. Goodwin. Tactile discrimination of edge shape: limits on spatial resolution imposed by parameters of the peripheral neural population. *J Neurosci*, 21(19):7751–7763, Oct 2001.
- R. C. White, A. M. Aimola-Davies, T. J. Halleen, and Martin Davies. Tactile expectations and the perception of self-touch: an investigation using the rubber hand paradigm. *Consciousness and cognition*, 19(2):505–519, June 2010. ISSN 1090-2376.
- A. G. Witney, A. Wing, J. L. Thonnard, and A. M. Smith. The cutaneous contribution to adaptive precision grip. *Trends Neurosci*, 27(10):637–643, Oct 2004.
- D. M. Wolpert. Probabilistic models in human sensorimotor control. *Human Movement Science*, 26(4):511–524, 2007. ISSN 0167-9457. European Workshop on Movement Science 2007, European Workshop on Movement Science 2007.
- D. M. Wolpert and M. Kawato. Multiple paired forward and inverse models for motor control. *Neural Netw*, 11(7-8):1317–1329, Oct 1998.
- D. M. Wolpert, Z. Ghahramani, and M. I. Jordan. An internal model for sensorimotor integration. *Science*, 269(5232):1880–1882, Sep 1995.
- F. V. Wright, S. Hubbard, S. Naumann, and J. Jutai. Evaluation of the validity of the prosthetic upper extremity functional index for children. *Arch Phys Med Rehabil*, 84(4):518–527, Apr 2003.
- P. Bach y Rita. Tactile sensory substitution studies. *Ann N Y Acad Sci*, 1013:83–91, May 2004.
- P. Bach y Rita and S. W. Kercel. Sensory substitution and the human-machine interface. *Trends Cogn Sci*, 7(12):541–546, Dec 2003.

- P. Bach y Rita, C. C. Collins, F. A. Saunders, B. White, and L. Scadden. Vision substitution by tactile image projection. *Nature*, 221(5184):963–964, Mar 1969.
- M. J. Yoon and K. H. Yu. Psychophysical experiment of vibrotactile pattern recognition at fingertip. In *Proc. Int SICE-ICASE Joint Conf*, pages 4601–4605, 2006.
- M. J. Yoon and K. H. Yu. Psychophysical experiment of vibrotactile pattern perception by human fingertip. *IEEE Trans Neural Syst Rehabil Eng*, 16(2):171–177, 2008.
- M. J. Young, M. S. Landy, and L. T. Maloney. A perturbation analysis of depth perception from combinations of texture and motion cues. *Vision Res*, 33(18):2685–2696, Dec 1993.
- A. Yuille and H. H. Bulthoff. *Perception as Bayesian Inference*, chapter Bayesian decision theory and psychophysics., pages 123–161. Cambridge University Press, 1996.
- M. Zafar and C. L. Van Doren. Effectiveness of supplemental grasp-force feedback in the presence of vision. *Med Biol Eng Comput*, 38(3):267–74, May 2000. ISSN 0140-0118.
- P. Zhou, M. M. Lowery, K. B. Englehart, H. Huang, G. Li, L. Hargrove, J. P. A. Dewald, and T. A. Kuiken. Decoding a new neural machine interface for control of artificial limbs. *J Neurophysiol*, 98(5):2974–2982, Nov 2007.